

**Cell Cycle Studies on the Human**  
**Nek3, Nek5 and Nek11 Protein Kinases**

Thesis submitted for the degree of  
Doctor of Philosophy  
at the University of Leicester

by

Navdeep Kaur Sahota BSc (Hons) (Leicester)  
Department of Biochemistry  
University of Leicester

December 2010

## DECLARATION

The accompanying thesis submitted for the degree of Doctor of Philosophy, entitled "*Cell Cycle Studies on the Human Nek3, Nek5 and Nek11 Protein Kinases*" is based on work conducted by the author in the Department of Biochemistry at the University of Leicester during the period October 2006 and September 2010. All of the work recorded in this thesis is original unless otherwise acknowledged in the text or by references. None of the work has been submitted for another degree in this or any other University.

Signed:

Date:

Department of Biochemistry  
University of Leicester  
Lancaster Road  
Leicester  
LE1 9HN

# Cell Cycle Studies on the Human

## Nek3, Nek5 and Nek11 Protein Kinases

### ABSTRACT

Navdeep Kaur Sahota

The NIMA-related kinases represent a family of serine/threonine protein kinases implicated in cell cycle control and ciliogenesis. The founding member of this family, the NIMA kinase of *Aspergillus nidulans*, contributes to multiple aspects of mitotic progression including the timing of mitotic entry, chromatin condensation, spindle organisation and mitotic exit. Mammals contain a family of eleven NIMA related kinases, named Nek1 to Nek11. Of these, to date there is substantial evidence that Nek2, Nek6, Nek7 and Nek9 regulate mitotic spindle formation, while Nek1 and Nek8 are implicated in microtubule organisation in non-dividing cells during ciliogenesis. The common underlying theme between spindle formation and ciliogenesis is the role of microtubules and microtubule organising centres. Hence, the emerging hypothesis is that all Neks may play a role in the organisation of microtubules. However, for several Neks, little if any information is available. In this thesis, I therefore began to examine the properties of three less well researched human Neks, Nek3, Nek5 and Nek11. First of all, antibodies against each of these kinases were generated or characterised. This allowed a broad study of the localisation, expression and activity of these kinases. Intriguingly, Nek3, Nek5 and Nek11 were all localised to centrosomes. Based on these results a more detailed study was performed with human Nek5 for which there is currently no published data. Human Nek5 is a nuclear protein that localises to the centrosomes during interphase, spindle poles during early mitosis, and to basal bodies in mono-ciliated cells. Specifically, Nek5 localised at the proximal ends of centrioles peaking in intensity in early mitosis. Importantly, siRNA-mediated depletion of Nek5 results in premature centrosome splitting and loss of centrosomal  $\gamma$ -tubulin. Hence, Nek5 is uncovered as a potential player in the negative regulation of centrosome separation.

## ACKNOWLEDGEMENTS

It is a pleasure to thank all those who made this thesis possible. First and foremost I would like to thank my supervisor Professor Andrew M. Fry for his advice and encouragement when I considered registering for this higher degree, and for giving me the opportunity to take on this project within his laboratory. Andrew, without your support, guidance and enthusiasm, this thesis would not have been possible.

Thank you to my committee members Dr Kayoko Tanaka and Dr Raj Patel for their insightful criticisms throughout the duration of this project. Kayoko, your passion and enthusiasm has been inspirational. I would like to thank Dr. Kees Straatman, Barbara Birch and Liz Barber for their high spirit and jollity; and I greatly appreciate the efficiency with which they have always fulfilled requests.

Thanks are also due to all members of the Fry lab, past and present. I greatly appreciate the support and training provided in the lab by Dr Guojie Mao, Sam Wattam and Dr Laura O'Regan at the beginning of this research project. I would like to especially thank one lab member, Carla Lopes, who started her PhD journey at the same time as me and has been by my side continuously providing support and encouragement. Carla, I found a true friend in you; *obrigado por seres com és*. In addition to those already mentioned, I appreciate the encouragement from Joëlle, Suzy, Jo, Xav, and Magali and would like to thank everyone for making the lab an enjoyable place to work.

Finally I would like to thank my Mum and Dad for their patience, encouragement and unwavering support through the years –

ਮੇਮ - ਡੈਡ ਤੁਹਾਡੇ ਕਰਕੇ ਅਜ ਮੈਂ ਐਥੇ ਤਕ ਪਹੁੰਚ ਸਕੀ ਆ

A special thanks is also due to my Sister for her tolerance and encouragement through my time at university; and many thanks to those close family members who have always inspired me to do my best.

This research has been financially supported by the BBSRC and by AstraZeneca.

# CONTENTS

Declaration	I
Abstract	II
Acknowledgements	III
Table of contents	IV
Abbreviations	X
Tables and figures	XIV
<b>Chapter 1 Introduction</b>	<b>1</b>
<b>1.1 The eukaryotic cell cycle</b>	<b>2</b>
1.1.1 Interphase	2
1.1.2 M-phase: mitosis and cytokinesis	2
1.1.3 Cell cycle regulation	6
1.1.3.1 Cyclins and cyclin-dependent kinases	6
1.1.3.2 Cell cycle checkpoints	7
1.1.3.2.1 G <sub>1</sub> /S regulation	7
1.1.3.2.2 G <sub>2</sub> /M regulation	9
1.1.3.2.3 Metaphase/Anaphase regulation	10
<b>1.2 Microtubule organising centres</b>	<b>11</b>
1.2.1 The centrosome	12
1.2.2 Centrosomes and microtubule organisation	14
1.2.3 Centrosomes in cell cycle regulation	14
1.2.4 The centrosome duplication cycle	15
1.2.5 Centrosomes and ciliogenesis	17
<b>1.3 Mitotic protein kinases</b>	<b>21</b>
1.3.1 Cyclin-dependent kinases	21
1.3.2 Polo-like kinases	23

1.3.2.1	Plk1	23
1.3.2.2	Plk2, Plk3 and Plk4	27
1.3.3	Aurora kinases	28
1.3.3.1	Aurora A	29
1.3.3.2	Aurora B	31
1.3.3.3	Aurora C	32
<b>1.4</b>	<b>NIMA-related kinases</b>	<b>33</b>
1.4.1	NIMA	33
1.4.2	NIMA homologues in lower eukaryotes	34
1.4.3	Mammalian NIMA-related kinases (Neks)	37
1.4.3.1	Mitotic Neks: Nek2, Nek6, Nek7 and Nek9	37
1.4.3.2	DNA damage response Neks: Nek10 and Nek11	40
1.4.3.3	Ciliary Neks: Nek1 and Nek8	42
1.4.3.4	Signal transducing Neks: Nek3	44
<b>1.5</b>	<b>Cell cycle-dependent kinases as targets in cancer</b>	<b>45</b>
<b>1.6</b>	<b>Project aims and objectives</b>	<b>47</b>
<b>Chapter 2</b>	<b>Materials and Methods</b>	<b>53</b>
<b>2.1</b>	<b>Materials</b>	<b>54</b>
2.1.1	Suppliers and manufacturers	54
2.1.2	Radioisotopes	55
2.1.3	Vectors	55
2.1.4	Antibodies	55
2.1.4.1	Primary antibodies	55
2.1.4.2	Secondary antibodies	56
<b>2.2</b>	<b>Molecular biology techniques</b>	<b>57</b>
2.2.1	Cloning	57
2.2.1.1	Oligonucleotide design	57
2.2.1.2	Polymerase chain reaction	57

2.2.1.3	Agarose gel electrophoresis	58
2.2.1.4	Purification of PCR products for cloning	58
2.2.1.5	Restriction enzyme digest and purification	58
2.2.1.6	DNA ligation	59
2.2.1.7	Bacterial transformation	59
2.2.1.8	DNA insert verification	60
2.2.1.9	Isolation of plasmid DNA by DNA miniprep	60
2.2.1.10	DNA sequencing	60
2.2.2	Isolation of plasmid DNA by DNA maxiprep	60
2.2.3	Site-directed mutagenesis	61
2.2.3.1	Oligonucleotide design	61
2.2.3.2	Site-directed mutagenesis reaction	61
2.2.4	RT-PCR	62
<b>2.3</b>	<b>Protein analysis techniques</b>	<b>62</b>
2.3.1	SDS-PAGE	62
2.3.2	Coomassie Blue staining	63
2.3.3	Western blotting	63
2.3.3.1	Quantification of western blot band intensities	64
2.3.4	<i>In vitro</i> translation	64
2.3.5	Immunoprecipitation	65
2.3.6	<i>In vitro</i> kinase assays	65
<b>2.4</b>	<b>Bacterial protein expression and purification</b>	<b>65</b>
2.4.1	Protein expression in <i>E. coli</i>	65
2.4.2	Recombinant protein purification	66
2.4.3	Quantification of protein concentration	67
<b>2.5</b>	<b>Antibody generation and purification</b>	<b>67</b>
2.5.1	Antibody generation	67
2.5.2	Affinity purification of antibodies	68

<b>2.6</b>	<b>Mammalian cell culture techniques</b>	<b>68</b>
2.6.1	Maintenance of human cell lines	68
2.6.2	Storage of human cell lines	69
2.6.3	Transient transfection of mammalian cells	69
2.6.3.1	Lipofectamine 2000	69
2.6.3.2	Fugene HD	70
2.6.4	Nuclear export block	70
2.6.5	Induction of primary cilia formation	70
2.6.6	Preparation of cell lysates	70
2.6.7	Preparation of RNA extracts	71
2.6.8	Cell synchronisation	71
2.6.9	Flow cytometric analysis	71
2.6.10	RNA interference	72
2.6.11	siRNA-plasmid co-transfection	72
<b>2.7</b>	<b>Indirect immunofluorescence microscopy</b>	<b>73</b>
2.7.1	Data analysis and quantification techniques	74
<b>Chapter 3</b>	<b>Generation and characterisation of antibodies against Nek3, Nek5 and Nek11</b>	<b>75</b>
<b>3.1</b>	<b>Introduction</b>	<b>76</b>
<b>3.2</b>	<b>Results</b>	<b>78</b>
3.2.1	Expression of Nek5 and Nek11 antigens in bacteria	78
3.2.2	Immunisation of rabbits for Nek5 and Nek11 antibody generation	81
3.2.3	Affinity purification of human anti-Nek5 and anti-Nek11 antibodies	85
3.2.4	Characterisation of purified anti-Nek5 and anti-Nek11 antibodies	88
3.2.5	Characterisation of a commercially available Nek3 antibody	91
<b>3.3</b>	<b>Discussion</b>	<b>97</b>

<b>Chapter 4</b>	<b>Nek3, Nek5 and Nek11: Subcellular localisation, expression and activity studies</b>	<b>100</b>
<b>4.1</b>	<b>Introduction</b>	<b>101</b>
<b>4.2</b>	<b>Results</b>	<b>103</b>
4.2.1	Subcellular localisation of recombinant Nek3	103
4.2.2	Subcellular localisation of recombinant Nek5	108
4.2.3	Subcellular localisation of recombinant Nek11c	111
4.2.4	Localisation of endogenous Nek11	111
4.2.5	Optimisation of RT-PCR conditions for Nek3, Nek5 and Nek11	116
4.2.6	mRNA expression in human cancer cell lines	121
4.2.7	Analysis of Nek3 and Nek11c kinase activity <i>in vitro</i>	123
4.2.8	Assay for Nek3 activity from transfected cells	129
<b>4.3</b>	<b>Discussion</b>	<b>131</b>
<b>Chapter 5</b>	<b>Subcellular localisation of Nek5</b>	<b>137</b>
<b>5.1</b>	<b>Introduction</b>	<b>138</b>
<b>5.2</b>	<b>Results</b>	<b>140</b>
5.2.1	Cell cycle dependent localisation of endogenous Nek5	140
5.2.2	Nek5 localises to centrosomes and basal bodies in RPE1 cells	146
5.2.3	Nek5 localises towards the proximal ends of centrioles	146
5.2.4	Nek5 accumulates in the nucleus upon inhibition of nuclear export	149
5.2.5	Nek5 nuclear localisation is dependent on residues 380-460	149
<b>5.3</b>	<b>Discussion</b>	<b>156</b>
<b>Chapter 6</b>	<b>An insight into Nek5 function through RNAi-mediated depletion</b>	<b>159</b>
<b>6.1</b>	<b>Introduction</b>	<b>160</b>
<b>6.2</b>	<b>Results</b>	<b>162</b>
6.2.1	Optimisation of RNAi-mediated depletion of Nek5	162

6.2.2	Nek5 depletion or expression of kinase-inactive Nek5 induces centrosome splitting	165
6.2.3	Nek5 depletion leads to loss of $\gamma$ -tubulin from centrosomes	168
6.2.4	Nek5 depletion leads to split centrosomes during cytokinesis	168
6.2.5	Depletion of Nek5 results in a delay in prometaphase	168
<b>6.3</b>	<b>Discussion</b>	<b>173</b>
<b>Chapter 7</b>	<b>Discussion</b>	<b>176</b>
<b>7.1</b>	<b>Nek5 is a nuclear protein</b>	<b>177</b>
<b>7.2</b>	<b>Nek5 localises to the proximal ends of centrioles</b>	<b>178</b>
<b>7.3</b>	<b>Nek5 regulates centrosome cohesion</b>	<b>179</b>
<b>7.4</b>	<b>Nek5 regulates <math>\gamma</math>-tubulin recruitment</b>	<b>181</b>
<b>7.5</b>	<b>Future directions with Nek3 and Nek11</b>	<b>182</b>
<b>7.6</b>	<b>Concluding remarks</b>	<b>184</b>
<b>Chapter 8</b>	<b>Bibliography</b>	<b>185</b>

## ABBREVIATIONS

A	absorbance
aa	amino acid
ADPKD	autosomal dominant polycystic kidney disease
ATP	adenosine triphosphate
APS	ammonium persulphate
APC/C	anaphase-promoting complex/cyclosome
ATM	ataxia telangiectasia mutated
ATR	ataxia telangiectasia and Rad3-related
bp	base pairs
BSA	bovine serum albumin
C-	carboxy
CAK	Cdk-activating kinase
Cdk	Cyclin-dependent kinase
cDNA	complementary deoxyribonucleic acid
Cep55	centrosome protein 55 kDa
Chk1	checkpoint kinase 1
CKI	Cdk inhibitor
C-Nap1	centrosomal Nek2-associated protein 1
DDR	DNA damage response
DMEM	Dulbecco's modified eagle's medium
DMSO	dimethylsulfoxide
DNA	deoxyribonucleic acid
dNTPs	deoxynucleotide triphosphates
DTT	dithiothreitol
ECT2	epithelial cell transforming protein 2
EDTA	ethylene diamine tetraacetic acid

EGTA	ethylene glycol tetraacetic acid
FACS	fluorescence activated chromosome sorter
FBS	foetal bovine serum
FL	full-length
GFP	green fluorescent protein
GL2	firefly luciferase
HEK293	human embryonic kidney
HeLa	human cervical epithloid carcinoma
hTERT-RPE1	telomerase-immortalised human retinal pigment epithelial
hrs	hours
IF	immunofluorescence microscopy
IFT	intraflagellar transport
IPTG	$\beta$ -D-isopropyl-thiogalactopyranoside
INCENP	inner centromere protein
IVT	<i>in vitro</i> translated
kDa	kilodaltons
LB	Luria Broth
LMB	Leptomycin B
MAPK	mitogen activated protein kinase
MBP	myelin basic protein
MCAK	mitotic centromere-associated kinesin
mg	milligram
mM	millimolar
mins	minutes
MPF	M-phase promoting factor
mRNA	messenger ribonucleic acid
MTOC	microtubule organising centre
N-	amino

Nek	NIMA-related kinase
NES	nuclear export sequence
NIMA	never in mitosis A
ng	nanogram
nM	nanomolar
Nlp	ninein-like protein
NLS	nuclear localisation sequence
NP-40	nonidet P-40
NPHP	nephronophthisis
OD	optical density
Pen/Strep	penicillin/streptomycin
PBD	polo-box domain
PBS	phosphate buffered saline
PCR	polymerase chain reaction
PCM	pericentriolar material
Plk	polo-like kinase
PMSF	phenylmethylsulphonyl fluoride
PKD	polycystic kidney disease
PP1	protein phosphatase-1
PRC1	protein regulator of cytokinesis 1
Rb	retinoblastoma protein
rpm	revolutions per minute
RNA	ribonucleic acid
RNAi	RNA interference
SAC	spindle assembly checkpoint
SCF	Skp1-Cullin-Fbox complex
SDS	sodium dodecyl sulphate
SDS PAGE	SDS polyacrylamide gel electrophoresis
siRNA	small interfering RNA

SIN	septum initiation network
secs	seconds
SPB	spindle pole body
TEA	triethylamine
TEMED	N, N, N, N,-tetramethylethylenediamine
TPX2	target protein for <i>Xenopus</i> kinesin-like protein 2
U2OS	human osteosarcoma
μg	microgram
μl	microlitre
μM	micromolar
μm	micrometre
UV	ultraviolet
V	volts
v/v	volume/volume
WT	wild-type
w/v	weight/volume
γ-TuRC	γ-tubulin ring complex
γ-TuSC	γ-tubulin small complex

## TABLES AND FIGURES

### TABLES

4.1	Potential Nek3 variants	134
-----	-------------------------	-----

### FIGURES

1.1	The eukaryotic cell cycle	3
1.2	M-phase: mitosis and cytokinesis	5
1.3	Cell cycle regulation	8
1.4	The structure of the centrosome	13
1.5	The centrosome duplication cycle	18
1.6	Basal bodies template the formation of the primary cilium	20
1.7	Mammalian Polo-like kinases	24
1.8	Mammalian Aurora kinases	30
1.9	The NIMA-related kinases	35
1.10	Structural features of human Nek3	49
1.11	Structural features of human Nek5	50
1.12	Alignment of human Nek11 isoforms	51
1.13	Structural features of human Nek11	52
3.1	Expression of Nek5 protein fragment for antibody production	79
3.2	Expression of Nek11 protein fragment for antibody production	80
3.3	Quantification of Nek5 and Nek11 recombinant protein fragments	82
3.4	Characterisation of rabbit sera prior to immunisation by Western blot	83
3.5	Characterisation of rabbit sera prior to immunisation by IF microscopy	84
3.6	Characterisation of Nek5 antisera by Western blot analysis	86
3.7	Characterisation of Nek11 antisera by Western blot analysis	87
3.8	Affinity purification of anti-Nek5 and anti-Nek11 antibodies	89
3.9	Comparison of different affinity purified anti-Nek5 antibodies	90
3.10	Characterisation of affinity purified anti-Nek5 and anti-Nek11 antibodies	92
3.11	Nek5 and Nek11 affinity purified antibodies do not detect the complementary protein	93
3.12	Expression of TAP-tagged Nek3, Nek5 and Nek11c	95

3.13	Identification of endogenous Nek3 on Western blot using siRNA	96
4.1	Recombinant Nek3, Nek5 and Nek11c constructs	104
4.2	Recombinant Nek3 protein localises to the cytoplasm during interphase	105
4.3	Localisation of recombinant Nek3 to centrosomes during interphase is cell-type dependent	106
4.4	Recombinant Nek3 does not localise to mitotic spindle poles	107
4.5	Recombinant Nek5 protein localises to the nucleus during interphase	109
4.6	Localisation of recombinant Nek5 to interphase centrosomes following methanol fixation is cell-type dependent	110
4.7	Pre-extraction of cells reveals centrosomal localisation of recombinant Nek5 in U2OS cells	112
4.8	Recombinant Nek11c localises to the cytoplasm during interphase	113
4.9	Recombinant Nek11c proteins do not localise to centrosomes during interphase	114
4.10	Endogenous Nek11 localises to the nucleus and to centrosomes during interphase and on spindle poles through mitosis	115
4.11	Expression of Nek3, Nek5 and Nek11 mRNA in human cell lines	117
4.12	Optimisation of Nek3, Nek5 and Nek11 semi-quantitative RT-PCR	119
4.13	Nek5 mRNA levels are cell cycle regulated	120
4.14	Expression of Nek3, Nek5 and Nek11 mRNA in cancer cell lines	122
4.15	Characterisation of commercial recombinant Nek3 and Nek11c proteins	124
4.16	$\beta$ -casein is a good <i>in vitro</i> substrate for the Nek3 kinase	126
4.17	MBP is a good <i>in vitro</i> substrate for the Nek11c kinase	127
4.18	NaCl inhibits Nek3 and Nek11c kinase activity <i>in vitro</i>	128
4.19	Kinase assay of immunoprecipitated Nek3	130
5.1	Comparison of staining patterns with Nek5 antibodies upon different fixation-extraction techniques	141
5.2	Localisation of endogenous Nek5 protein through mitosis	142
5.3	Nek5 localises at centrosomes and spindle poles in a cell cycle-dependent manner	144
5.4	RNAi knockdown of Nek5 leads to loss of centrosome staining	145

5.5	Nek5 localises to centrosomes in cycling RPE1 cells and to basal bodies in ciliated RPE1 cells	147
5.6	Nek5 localises towards the proximal ends of centrioles	148
5.7	Recombinant Nek5 accumulates in the nucleus in response to treatment with the nuclear export inhibitor LMB	150
5.8	The non-catalytic region of Nek5 is required for nuclear localisation	151
5.9	Nuclear localisation of Nek5 is not affected by mutation of a putative nuclear localisation sequence	153
5.10	Nek5 C-terminal truncations generated to identify nuclear targeting region	154
5.11	Residues 380-460 are required for the nuclear localisation of Nek5	155
6.1	Characterising Nek5 siRNA oligos	163
6.2	Optimising RNAi knockdown of Nek5 in U2OS cells	164
6.3	Nek5 depletion induces centrosome splitting	166
6.4	Overexpression of kinase-inactive Nek5 induces split centrosomes	167
6.5	Nek5 depletion causes loss of $\gamma$ -tubulin from centrosomes	169
6.6	Nek5 depletion increases the frequency of split centrosomes during cytokinesis	170
6.7	Depletion of Nek5 results in an early mitotic delay	172
7.1	Putative roles of Nek5 in centrosome disjunction	180

# **Chapter 1**

## **Introduction**

## **1.1 The eukaryotic cell cycle**

In 1858, the statement “*omnis cellula e cellula*” – all cells come from cells, was first presented (Virchow 1858). This idea that new cells arise from the division of pre-existing cells became generally accepted in the late 19<sup>th</sup> century. Since then research over many years has led to a sophisticated understanding of the core mechanisms that drive the eukaryotic cell cycle, a process during which the cell duplicates its contents and then divides into two daughter cells.

### **1.1.1 Interphase**

A core eukaryotic cell cycle comprises four stages. Three of the four eukaryotic cell cycle stages, G<sub>1</sub>, S, and G<sub>2</sub>, are collectively known as interphase. The fourth is M-phase which comprises the interlinked mitosis and cytokinesis. A fifth stage, G<sub>0</sub>, ensues when cells withdraw from the cell cycle, and in this quiescent stage they remain metabolically active but no longer proliferate unless called on to do so by extracellular signals (Figure 1.1). G<sub>1</sub> phase (gap 1) is the period between mitosis and initiation of DNA replication. During G<sub>1</sub>, the cell continuously grows, is metabolically active and begins to synthesise proteins necessary for DNA replication. G<sub>1</sub> is followed by S phase (synthesis), which is characterised by DNA synthesis in which the chromosomes are duplicated in preparation for cell division. The completion of DNA synthesis is then followed by a second gap phase, G<sub>2</sub>, which allows further cell growth and synthesis of all the components necessary for cell division before the cell enters mitosis and divides (Johnson & Walker 1999; Alberts et al. 2002; Salaun et al. 2008).

### **1.1.2 M-phase: mitosis and cytokinesis**

Mitosis comprises many complex events that result in a dramatic rearrangement of the interphase cell in such a way as to allow the duplicated chromosomes to segregate into two genetically identical daughter cells. This process can be divided into 5 distinct stages: prophase, prometaphase, metaphase, anaphase

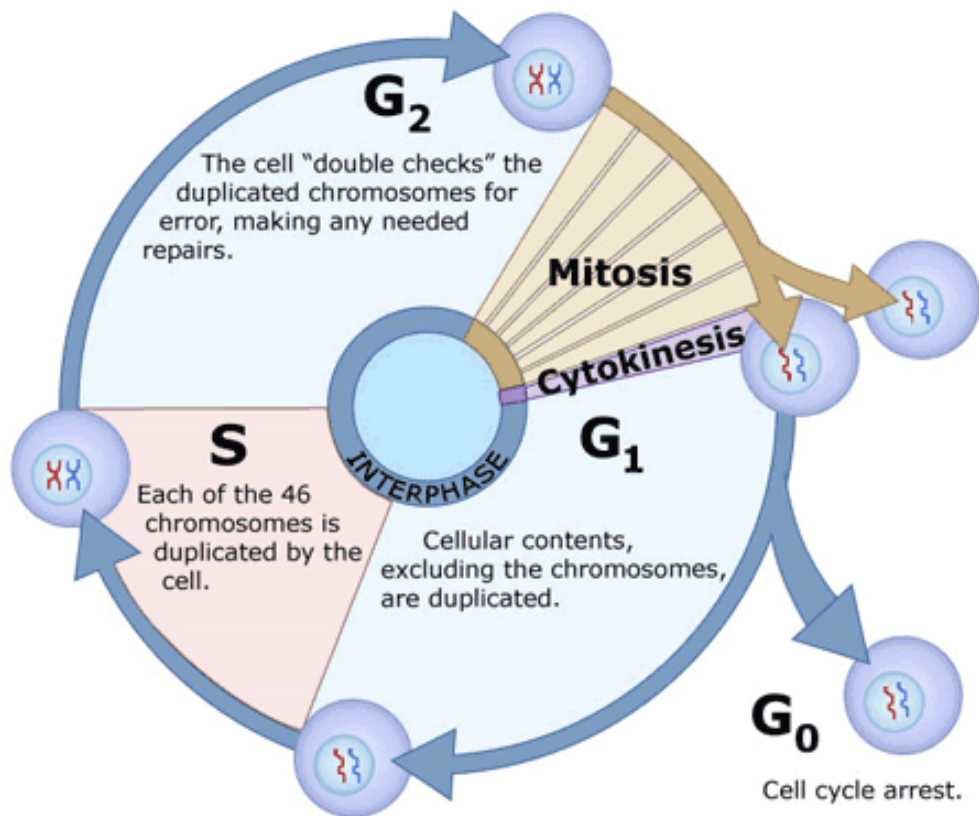


**Figure 1.1 The eukaryotic cell cycle**

The eukaryotic cell cycle is divided into four phases. Three of the four phases G<sub>1</sub>, G<sub>2</sub> (growth phases) and S (DNA synthesis) are collectively known as interphase. The fourth stage, M-phase, is divided into mitosis and cytokinesis. A fifth phase, G<sub>0</sub> or quiescence, ensues when cells receive no stimulus to grow; cells in this phase no longer proliferate until a growth stimulus is restored and then they return to G<sub>1</sub>. Taken from Clinical Tools, Inc via [www.le.ac.uk](http://www.le.ac.uk).

and telophase (Figure 1.2). During prophase, the replicated chromosomes, each consisting of two sister chromatids held together at a constricted region referred to as the centromere, condense becoming densely coiled and folded (Hirano 2000; Shintomi & Hirano 2010). At the same time, the microtubule cytoskeleton undergoes reorganisation as the mitotic spindle begins to assemble. This initially occurs outside the nucleus between the two centrosomes that have been formed by the replication of a single centrosome, or primary microtubule-organising centre, during interphase. With lengthening bundles of microtubules between them, the centrosomes move apart towards opposite ends of the cell (Crasta et al. 2008). The abrupt breakdown of the nuclear envelope then marks the onset of prometaphase. This enables the condensed chromosomes to attach to spindle microtubules via their kinetochores, complex protein machines which form at the centromeres (Kops et al. 2010; Tanaka 2010). Microtubule dynamics push and pull the chromosomes so that at metaphase the chromosomes are aligned at the equator of the spindle, or metaphase plate, midway between the spindle poles (Kops et al. 2010). The sister chromatids attach to opposite poles of the spindle via kinetochore microtubules so that at anaphase they can synchronously separate to form two daughter chromosomes. To enable chromosome separation, the kinetochore microtubules shorten and the spindle poles move further apart pulling the separated daughter chromosomes towards the spindle pole they face (Pines & Rieder 2001; Salaun et al. 2008). Then, during telophase, as the two sets of daughter chromosomes arrive at the spindle poles, they begin to de-condense and a nuclear envelope reassembles around each set. Formation of two nuclei marks the end of mitosis whilst division of the cytoplasm, or cytokinesis, begins with the formation of a cleavage furrow associated with a contractile ring of actin and myosin filaments. These pinch the cell in two to create two daughters, each with one nucleus, indicating that cell division is complete (Figure 1.2) (Sagona & Stenmark 2010; Pines & Rieder 2001; Salaun et al. 2008).

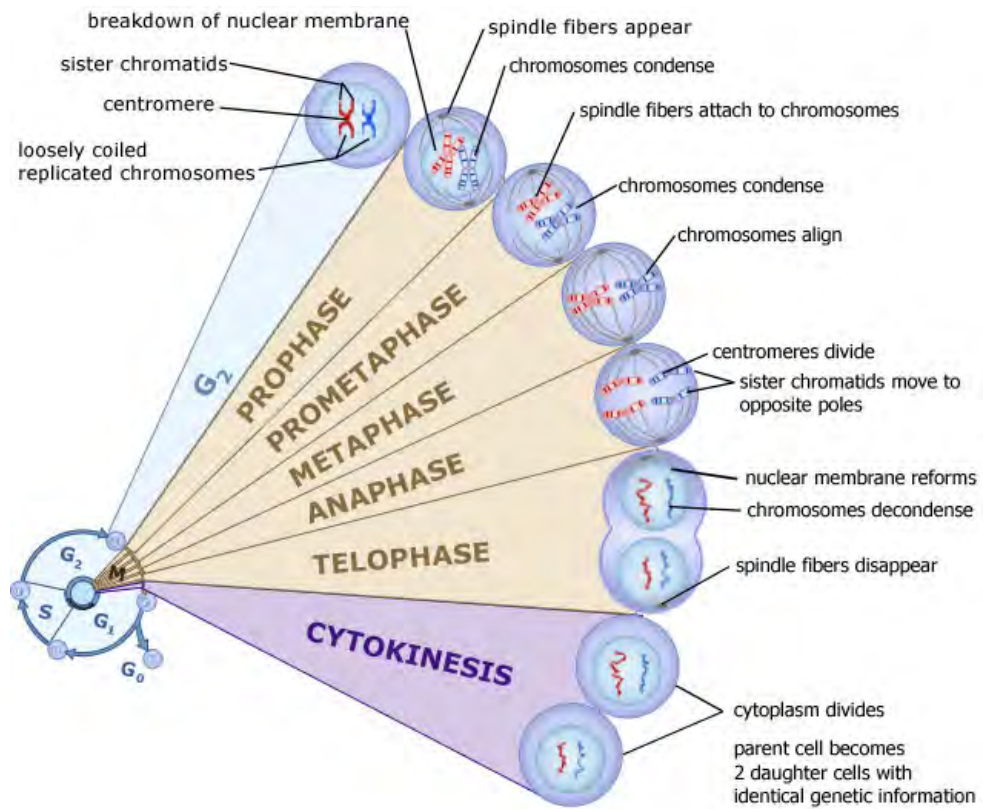


**Figure 1.2 M-phase: mitosis and cytokinesis**

M-phase consists of two interlinked events: mitosis (division of the nucleus) and cytokinesis (division of the cytoplasm). Mitosis is divided up into five distinct stages: prophase, prometaphase, metaphase, anaphase and telophase. Taken from Clinical Tools, Inc via [www.le.ac.uk](http://www.le.ac.uk).

### **1.1.3 Cell cycle regulation**

The timing and rate of cell division is critical with the sequential events of the cell cycle directed by both intracellular and extracellular cues. For this reason, a distinct cell cycle control system involving a complex network of regulatory proteins exists that governs progression through the cell cycle at various checkpoints. At the heart of the cell cycle control system are regulatory proteins whose rhythmic fluctuations in abundance and activity pace the sequential events of the cell cycle. These regulatory proteins are complexes composed of cyclins and cyclin-dependent kinases (Nigg 1995).

#### **1.1.3.1 Cyclins and cyclin-dependent kinases**

Cyclins are regulatory subunits for cyclin-dependent kinases (Cdks), which are core components of the cell cycle control system (Malumbres & Barbacid 2005). Cdks are dependent on cyclins for their kinase activity which rises and falls with changes in the concentration of cyclin partners available in the cell (Morgan 1997). Cyclin levels are regulated at the level of transcription and by specific proteolysis via two ubiquitin-ligase systems: SCF and APC/C (Glotzer et al. 1991; Nakayama & Nakayama 2006). In G<sub>1</sub> and S phase, the SCF (Skp1-Cullin-Fbox complex) recognises cyclins as substrates when they are phosphorylated, whereas in M-phase, the APC/C (anaphase-promoting complex/cyclosome) ubiquitinates cyclins in response to interaction with an activating subunit. Assembled cyclin-Cdk complexes can be modulated by cyclin-dependent kinase inhibitors (INK4 and Cip/Kip proteins) and by inhibitory phosphorylation of tyrosine and threonine residues close to the active site of the Cdk subunit (Morgan 1997; Pavletich 1999). Oscillations in assembly and activation of cyclin-Cdk complexes leads directly to cyclical changes in the phosphorylation of intracellular target proteins that initiate or regulate the major events of the cell cycle. Although human cells contain multiple loci encoding Cdks and cyclins (Malumbres et al. 2009), only a certain subset of cyclin-Cdk complexes is directly involved in driving the cell cycle. These include three interphase Cdks (Cdk2, Cdk4 and Cdk6), a mitotic Cdk (Cdk1), and cyclins that

belong to four different classes (the A-, B-, D- and E-type cyclins) (Malumbres & Barbacid 2009).

### **1.1.3.2 Cell cycle checkpoints**

In 1989 the concept of checkpoints was first introduced. These are critical control points at which the cell cycle can be arrested through inhibitory signals sent by processes which up to that point have not been completed correctly (Hartwell & Weinert 1989). A typical checkpoint pathway consists of three components, the sensor that detects the presence of a defect during the cell division cycle and then sends out a signal, the signal transduction pathway, and the effectors that respond to the signal to trigger a delay in cell cycle progression (Chin & Yeong 2010). The eukaryotic cell cycle is guarded by three main checkpoints that lie at the G<sub>1</sub>/S boundary, the G<sub>2</sub>/M boundary, and the metaphase/anaphase boundary (Figure 1.3).

#### **1.1.3.2.1 G<sub>1</sub>/S regulation**

In G<sub>1</sub> phase of the cell cycle, there is a restriction point where cells check whether their environment favours proliferation or quiescence (Pardee 1974). Activation of cell-surface receptors in response to extracellular mitogens, or growth factors stimulating cell proliferation, leads to increased transcription of genes encoding cyclin D and the proteolysis of Cdk inhibitor proteins (CKIs; Sherr & Roberts 1999; Doonan & Kitsios 2009). This leads to an increase in active cyclin D-Cdk4 or 6 complexes that phosphorylate the retinoblastoma protein (Rb), an inhibitor of cell cycle progression (Lees et al. 1991; Bates et al. 1994; Weinberg 1995). During G<sub>1</sub>, Rb normally binds to a transcription factor, E2F, and blocks transcription of S-phase genes (Chellappan et al. 1991; Kaelin 1999). However, phosphorylation of Rb by active cyclin D-Cdk4 or 6 complexes reduces its affinity for E2F resulting in its dissociation, enabling E2F to then activate expression of genes encoding proteins required for S-phase entry, including cyclin E and A (Harbour et al. 1999; Sherr 2000). Cyclin E binds to and activates Cdk2, and this complex further phosphorylates inhibitors of cell

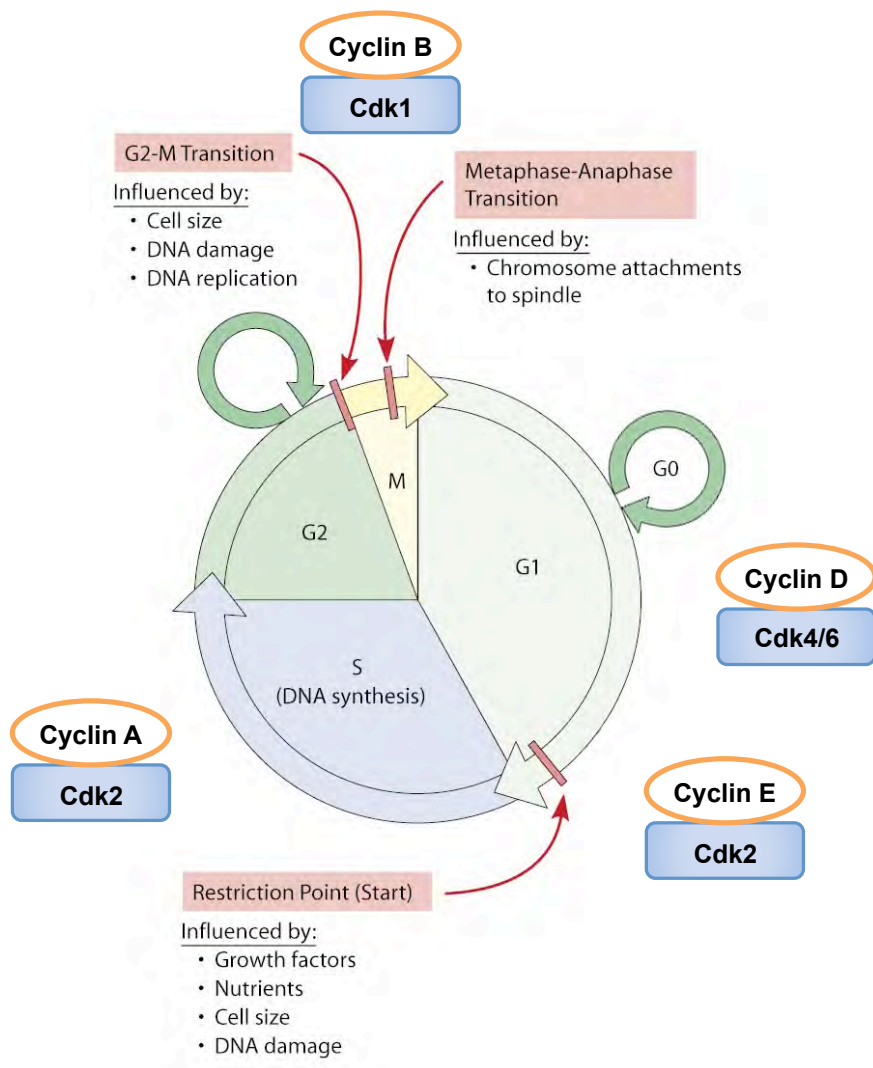


**Figure 1.3 Cell cycle regulation**

The cell cycle is regulated at three prominent checkpoints: at the G<sub>1</sub>/S boundary, the G<sub>2</sub>/M boundary, and the metaphase/anaphase boundary (indicated by the red arrows). Progress through the cell cycle can be halted at these checkpoints if the conditions for successful progression are not met. The key regulatory molecules involved in cell cycle control, the cyclin-dependent kinases (Cdks) associated with their appropriate regulatory cyclin partners, are indicated next to the phases at which they pace the sequential events of the cell cycle. Adapted from Becker et al (2008).

cycle progression leading to their complete inactivation (Koff et al. 1992; Lundberg & Weinberg 1998; Harbour et al. 1999). Cells thus pass the restriction point and reach a state of commitment to DNA replication, mitosis and cell division (Pardee 1989). However, progression into S-phase at this point can be blocked by another checkpoint in response to DNA damage. DNA damage is sensed by two master kinases, ATM and ATR, which then phosphorylate downstream targets in a signal transduction cascade that leads to cell cycle arrest. If DNA is damaged in this cell cycle phase then the p53 transcription factor becomes phosphorylated, blocking interaction with a ubiquitin ligase, Mdm2, which normally targets p53 for degradation. Accumulation of p53 then stimulates transcription of a gene encoding a CKI protein, p21, which binds to assembled cyclin-Cdk complexes, inhibiting their activities and thus arresting cell cycle progression and enabling DNA repair (el-Deiry et al. 1994; Dulić et al. 1994; Bartek & Lukas 2001). Hence, at the G<sub>1</sub>/S boundary, the restriction point and DNA damage checkpoint regulate cell cycle progression via cyclin-Cdk complexes by assessing whether the environment favours proliferation and whether the genome is ready to be replicated (Novak et al. 2001; Doonan & Kitsios 2009; Malumbres & Barbacid 2009).

#### **1.1.3.2.2 G<sub>2</sub>/M regulation**

With cyclin D-Cdk4 or 6 and cyclin E-Cdk2 acting co-operatively to initiate entry into S-phase, cyclin A-Cdk2 then drives the cell cycle through S-phase (Doonan & Kitsios 2009). Together, cyclin E-Cdk2 and cyclin A-Cdk2 phosphorylate substrates that have assembled at the origins of DNA replication as pre-replicative complexes, thus triggering DNA replication once per cell cycle (Mailand & Diffley 2005; Malumbres & Barbacid 2005). Cyclin A-Cdk2 activity remains high during G<sub>2</sub>, preventing re-replication from occurring by blocking assembly of new pre-replicative complexes (Morgan 1997; Sherr & Roberts 2004). During G<sub>2</sub>, an increase in cyclin B transcription leads to an accumulation of cyclin B-Cdk1 complexes, also called M-phase promoting factor (MPF). Although the Cdk in this complex is phosphorylated by Cdk-activating kinase (CAK) at an activating site (Thr161), it is held in an inactive state by inhibitory

phosphorylation at two neighbouring residues close to the ATP binding site (Thr14 and Tyr15) by the Myt1 and Wee1 kinases (Morgan 1995). This ensures that by the end of G<sub>2</sub> there is an abundance of these complexes (preMPF) primed and ready to act, and only upon removal of these inhibitory phosphates by a Plk1-activated protein phosphatase, Cdc25, is the MPF activated triggering entry into mitosis (Schmit & Ahmad 2007). However, before cells can progress into M-phase they must ensure that their DNA is fully replicated and undamaged. These DNA replication and damage checkpoints monitor if incomplete DNA replication or DNA damage is present. If so, then cell cycle arrest is imposed primarily through inhibiting the action of the protein phosphatase, Cdc25, leaving MPF in an inactive state. This enables completion of replication and repair of DNA prior to mitotic entry (Bartek & Lukas 2001; Novak et al. 2001; Doonan & Kitsios 2009; Malumbres & Barbacid 2009).

#### **1.1.3.2.3 Metaphase/Anaphase regulation**

Active MPF triggers complex rearrangements that occur in early mitosis, such as nuclear envelope breakdown and spindle assembly (Nigg 2001). This leads to alignment of the sister chromatids on the metaphase plate, as described earlier. However, the metaphase-to-anaphase transition, when sister chromatid separation is initiated, is regulated by the APC/C (Nakayama & Nakayama 2006). The spindle assembly checkpoint (SAC) ensures that separation of sister chromatids only takes place when all chromosomes are attached in a bi-oriented manner to the bipolar mitotic spindle (Musacchio & Salmon 2007). Until this point, sister chromatids are held together by cohesin proteins (Musacchio & Salmon 2007; Shintomi & Hirano 2010). Cohesins are localised along chromosome arms as well as at the centromeres. Chromosome arm cohesin is released in early mitosis as a result of phosphorylation by Plk1. However, the cohesin at centromeres is only removed by the activity of a protease called separase at the metaphase to anaphase transition (Shintomi & Hirano 2010). Prior to anaphase, separase activity is inhibited by binding of the securin protein and by cyclin B-Cdk1 phosphorylation. When bi-oriented

attachment of all sister kinetochore pairs to microtubules is achieved, the SAC is inactivated releasing the Cdc20 protein, which binds and activates the APC/C leading to the ubiquitylation and degradation of securin. This results in the activation of separase, which targets the cohesin at centromeres (Musacchio & Salmon 2007; Ciliberto & Shah 2009). Cohesin is thought to act as a ring that encompasses the sister chromatids. The action of separase is to cleave the Scc1 subunit of cohesin opening the ring (Uhlmann et al. 1999). This loss of cohesion enables the pulling forces of the mitotic spindle to pull the sister chromatids apart. At this stage, the APC/C also triggers degradation of cyclin B through ubiquitin-dependent proteolysis leading to inactivation of Cdk1 and mitotic exit (Musacchio & Salmon 2007). In the presence of unattached kinetochores, the SAC prevents Cdc20 from activating the APC/C, and hence sister chromatid separation is blocked (Musacchio & Salmon 2007; Malumbres & Barbacid 2009).

An orderly sequence of cell cycle events is therefore maintained by a cell cycle control system, which precisely regulates progression via checkpoints that arrest the cell cycle when extracellular conditions are unfavourable for proliferation, when DNA damage occurs, or when events such as metaphase chromosome alignment are not completed successfully.

## **1.2 Microtubule organising centres**

Microtubules are a component of the cytoskeleton and are required for many cellular processes, including cell division, structural support, cell migration and positioning of membrane bound organelles. Microtubules have a distinctive hollow structure formed by the lateral association of 13 protofilaments – each a polymer of  $\alpha$ - and  $\beta$ -tubulin subunits (Bettencourt-Dias & Glover 2007). To carry out their numerous functions, microtubules are nucleated and assembled into highly ordered arrays by microtubule organising centres (MTOCs) referred to as centrosomes in animal cells.

### 1.2.1 The centrosome

In 1888, Theodor Boveri observed a small focus of dense material within a cell and named this the centrosome (Doxsey 2001). Centrosomes are relatively small (1-2  $\mu\text{m}$  in diameter) but complex non-membranous organelles found in the cytoplasm, usually in the proximity of the nucleus (Doxsey 2001). The centrosome contains a pair of centrioles, referred to as the mother and daughter, that are tethered through their proximal ends by a fibrous, intercentriolar link. They are also surrounded by a matrix of proteins referred to as the pericentriolar material (PCM). Centrioles are short, cylindrical structures that are  $\sim 0.5 \mu\text{m}$  long and  $0.2 \mu\text{m}$  in diameter, and their walls are made of nine triplet microtubules organised in a nine-fold radial symmetry. Both centrioles of the centrosome show a proximo-distal organisation (Doxsey 2001; Bettencourt-Dias & Glover 2007). Mother and daughter centrioles differ from one another in that the mother centriole has two sets of nine appendages close to its distal end that are absent on the daughter centriole; these are referred to as the subdistal appendages, which are required to anchor/dock microtubules, and the distal appendages that participate in the association of the basal body to the plasma membrane in cells undergoing ciliogenesis (Figure 1.4) (Doxsey 2001; Azimzadeh & Bornens 2007; Bettencourt-Dias & Glover 2007; Crasta et al. 2008; Hoyer-Fender 2010). The PCM is a key structure that anchors and nucleates cytoplasmic and spindle microtubules during the cell cycle (Bettencourt-Dias & Glover 2007). It has a lattice-like structure consisting predominantly of coiled-coil proteins, such as pericentrin, that anchor other PCM components that mediate nucleation of microtubules, such as  $\gamma$ -tubulin (Doxsey 2001; Blagden & Glover 2003; Debec et al. 2010). As the centrosome lacks a clear membrane boundary with the cytoplasm, its architecture is maintained through specific protein-protein interactions. Many proteins are therefore able to use the centrosome as a central docking station to perform and co-ordinate multiple cell cycle-specific functions without being true components of the centrosome. Hence, the PCM varies in amount of proteins anchored depending on cell cycle stage (Schatten 2008; Urbani & Stearns 1999).

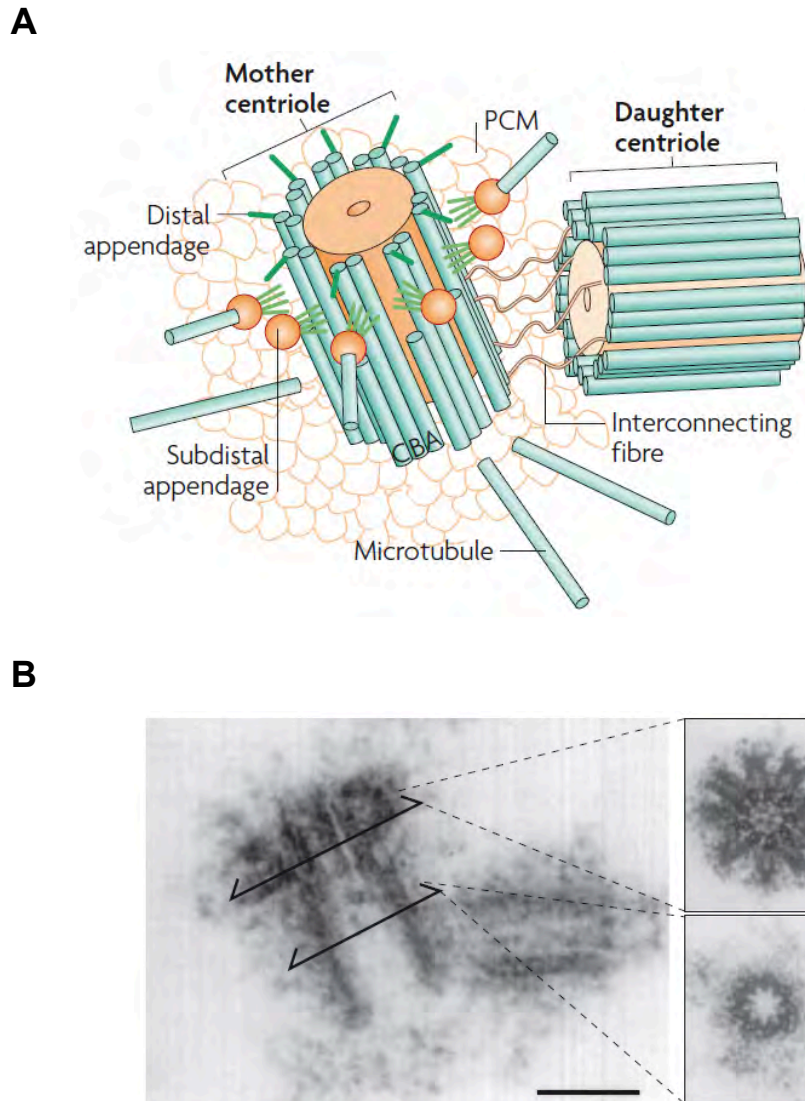


**Figure 1.4 The structure of the centrosome**

**(A)** The centrosome comprises a pair of centrioles that lie in an orthogonal configuration and are surrounded by the proteinaceous pericentriolar material (PCM). Each centriole is made up of nine triplet microtubules that form a barrel-like structure. The pair of centrioles are connected together at their proximal ends by a fibrous, intercentriolar linker. The older, mother, centriole differs from the younger, daughter, centriole in that it has distal and sub-distal appendages. **(B)** Scanning electron micrograph of a mother and daughter centriole pair revealing differences in the structure of the centriole at different cross-sections. Scale bar, 0.2  $\mu\text{m}$ . Taken from Bettencourt-Dias & Glover (2007).

### 1.2.2 Centrosomes and microtubule organisation

The capacity of the centrosome to organise microtubule arrays depends on its ability to nucleate, anchor and release microtubules. The differences between interphase and mitotic microtubule assembly and organisation are thought to be due, at least in part, to the cell cycle-dependent regulation of the  $\gamma$ -tubulin ring complex ( $\gamma$ TuRC) (Schatten 2008). In interphase, the centrosome contains a limited number of  $\gamma$ TuRCs that nucleate fewer but longer microtubules into a radial array. However, in mitosis, centrosomes recruit many more  $\gamma$ TuRCs as the PCM enlarges in a process known as centrosome maturation. These tend to form shorter, larger in number, and highly dynamic microtubules necessary for spindle assembly (Schatten 2008). The  $\gamma$ TuRC itself is a complex structure;  $\gamma$ -tubulin first forms a tetrameric complex with two  $\gamma$ -tubulin molecules binding one copy each of two other proteins (GCP2 and GCP3) to produce a  $\gamma$ -tubulin small complex ( $\gamma$ TuSC) (Bettencourt-Dias & Glover 2007). In *Drosophila melanogaster*, depletion of any  $\gamma$ TuSC subunit orthologue blocks microtubule nucleation (Vérollet et al. 2006). In higher eukaryotes, multiple  $\gamma$ TuSC complexes then assemble into a ring to form the  $\gamma$ TuRC that can cap minus ends of microtubules and facilitate initiation of microtubule protofilaments (Bettencourt-Dias & Glover 2007). Following their nucleation by the  $\gamma$ TuRC, microtubules are either released into the cytoplasm or recaptured and anchored at the centrosome through several different mechanisms that still remain unclear. Ninein, a component of the subdistal appendages of the mother centriole directly interacts with the  $\gamma$ TuRC and is thought to enable these appendages to act as a site for microtubule anchorage at the centrosome (Delgehr et al. 2005). To release microtubules into the cytoplasm, microtubule severing proteins such as katanin are found at the centrosome (Hartman et al. 1998; Ahmad et al. 1999).

### 1.2.3 Centrosomes in cell cycle regulation

Interestingly, although the centrosome is the major microtubule organising centre in most eukaryotes, it is not essential for spindle assembly. Using

*Xenopus* oocytes, it has been shown that in the absence of centrosomes, functional bipolar spindles can form through a pathway in which microtubule motor proteins sort microtubules that are nucleated randomly in the vicinity of the chromosomes (Walczak et al. 1998; Rieder et al. 2001); this has also been shown using mammalian somatic cells (Khodjakov et al. 2000). Furthermore, if the centrosome is removed by microsurgery or laser ablation, then cells are still able to assemble mitotic spindles, although, some acentrosomal cells fail to properly complete cytokinesis (Khodjakov & Rieder 2001), whilst others fail to enter S-phase of the subsequent cell cycle (Hinchcliffe et al. 2001). Hence, in terms of the cell cycle, it is proposed that the centrosome somehow regulates cytokinesis and the G<sub>1</sub>/S transition (Bettencourt-Dias & Glover 2007). In support of a role in cytokinesis, the mother centriole has been observed to move to the intercellular bridge that connects dividing cells, at a time correlating with bridge narrowing and bridge microtubule depolymerisation, and then move away again before cell cleavage (Piel et al. 2001). This suggests that centrosomes might be involved in the activation of the final stages of cytokinesis or in the release of cells from a checkpoint that monitors the completion of mitosis (Doxsey 2001). With regards to regulating G<sub>1</sub>/S transition, loss of centrosome integrity through silencing of centrosome-associated proteins has also been shown to result in a G<sub>1</sub> cell cycle arrest (Mikule et al. 2007). This suggests that an intact centrosome is required for the cell to progress into S phase; however the mechanisms through which the centrosome regulates cell cycle progression remain far from clear.

#### **1.2.4 The centrosome duplication cycle**

As discussed above, the cell cycle entails a recurring sequence of events that include the duplication of cellular contents and subsequent cell division that concludes with the formation of two genetically equivalent daughter cells. Centrosome duplication has to be carefully co-ordinated with the progression of the chromosomal cell cycle to ensure precise partitioning of the genetic material to the daughter cells. The centrosome cycle can be divided into discrete

consecutive steps: centriole disengagement, centriole duplication, centrosome disjunction, and centrosome separation.

Upon exit from M phase, or during early G<sub>1</sub>, the orthogonal association between mother and daughter centrioles is lost – this is referred to as centriole disengagement. However, the two centrioles nevertheless remain tethered by an intercentriolar linkage that assembles between their proximal ends. Centriole disengagement is a prerequisite for the centrosome duplication cycle and is considered to be a licensing event that enables one round of duplication per cell cycle (Lim et al. 2009; Azimzadeh & Bornens 2007). Disengagement requires separase activity, which as mentioned above is also required at the metaphase-to-anaphase transition to facilitate loss of sister chromatid cohesion. However, to prevent premature centriolar disengagement, centriole cohesion is protected by a shugoshin protein splice variant, sSgo1 (Wang et al. 2008; Lim et al. 2009). Duplication of the centrosome is semi-conservative, with each new centrosome receiving one old centriole and one new centriole. Morphologically, centriole duplication is first visualised around the same time as the initiation of DNA synthesis at the G<sub>1</sub>/S transition. Procentrioles begin to assemble orthogonally at a single site next to the proximal wall of each parental centriole (Blagden & Glover 2003; Azimzadeh & Bornens 2007). Procentriole elongation occurs in a proximal to distal direction throughout S and G<sub>2</sub> phases resulting in two pairs of centrioles that constitute a total of two centrosomes; these function as one until the onset of mitosis.

During late G<sub>2</sub>/M, the centrosomes increase in size as the PCM expands through recruitment of additional components that enable nucleation of sufficient numbers of mitotic microtubules; this is referred to as centrosome maturation as indicated above (Sankaran & Parvin 2006). At the onset of mitosis, centrosome disjunction is initiated with the disassembly of the intercentriolar linker that connected the parental centrioles. This enables the duplicated centrosomes to separate and migrate to opposite ends of the cell as the bipolar spindle assembles. The centriole pairs remain in an engaged

configuration throughout these events; only at late mitosis does disengagement occur, thus licensing centriole duplication in the following cell cycle (Figure 1.5). Upon cell division, each daughter cell then inherits one centrosome containing two centrioles and the cycle is complete (Azimzadeh & Bornens 2007; Blagden & Glover 2003; Lim et al. 2009; Sankaran & Parvin 2006; Fry et al. 1998b).

### **1.2.5 Centrosomes and ciliogenesis**

Cilia are hair-like projections extending from the cell surface that are found on virtually all cells in the body (Dawe et al. 2007). The most common type found on the surface of mammalian cells is the single, non-motile, sensory primary cilium (Wheatley et al. 1996). Primary cilia contain a ring of nine peripheral doublet microtubules held together by nexin linkages, that together is referred to as the axoneme (Dawe et al. 2007; Hoyer-Fender 2010; Abou Alaiwi et al. 2009). The ciliary axoneme is enclosed by a ciliary membrane that is structurally and functionally distinct from the cell membrane enabling the specific sensory functions of the cilia (Abou Alaiwi et al. 2009). The space between the ciliary membrane and the axoneme is referred to as the cilioplasm and this is where the intraflagellar transport (IFT) machinery is located that controls the bi-directional movement of cargo along the doublet microtubules to assemble and maintain the cilia (Abou Alaiwi et al. 2009; Dawe et al. 2007).

Primary cilia can form in quiescent cells or during interphase,  $G_1$ , in proliferating cells (Dawe et al. 2007; Hoyer-Fender 2010). All cilia extend from the distal end of a basal body (Figure 1.6) (Dawe et al. 2007). In animal cells, the mother centrioles retain the ability to act as basal bodies templating the assembly of cilia during ciliogenesis. At specific cell cycle or developmental stages, centrioles give rise to basal bodies and vice versa - the older centriole of the pair in a centrosome becomes a basal body to form a primary cilium, and conversely, the basal body that anchors a cilium in interphase can revert into a mother centriole prior to mitosis (Hoyer-Fender 2010). Indeed, it is hypothesised that the disassembly of cilia prior to mitosis may constitute a

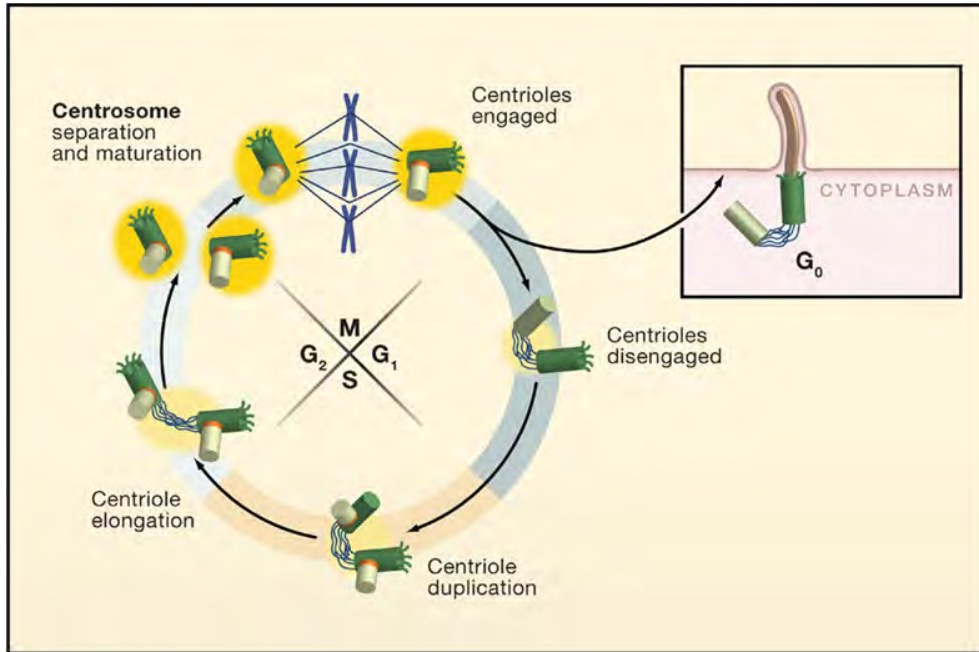


**Figure 1.5 The centrosome duplication cycle**

The centrosome cycle can be divided into discrete consecutive steps. At the end of cell division, each daughter cell inherits a single centrosome comprising two disengaged centrioles that are held together at their proximal ends by a fibrous intercentriolar linker. In S phase, centriole duplication occurs with new procentrioles assembling next to the proximal wall of each parental centriole. These elongate throughout S and G<sub>2</sub> phase. In late G<sub>2</sub>, the centrosome undergoes a process of maturation, involving the recruitment of additional PCM components. Then at the onset of mitosis, the intercentriolar linker is disassembled resulting in separation, or disjunction, of the centrosomes, thus enabling them to move apart to form the poles of the bipolar spindle. The centriole pairs then remain in an engaged configuration preventing re-duplication within the same cycle until late mitosis or early G<sub>1</sub>, when centrosome duplication is licensed to take place in the following cell cycle as a result of centriole disengagement. Taken from Nigg & Raff (2009).

checkpoint that cells must pass to enter division (Abou Alaiwi et al. 2009). The basic structure of both centrioles and basal bodies is highly conserved with both comprising a symmetrical array of nine triplet microtubules in most studied organisms (Hoyer-Fender 2010). Centrioles are referred to as basal bodies once they have migrated to the apical surface, acquired accessory structures and docked with the cell membrane (Dawe et al. 2007). At the base of a primary cilium, the basal body remains associated with its daughter centriole through filamentous bundles, called the striated connector. Accessory structures acquired by the basal body to aid its anchorage include (i) transitional fibres (originating at the distal appendages of the mother centriole) that may also provide a filter at the distal end of the basal body to regulate which molecules can pass into the cilium; (ii) basal feet (modified centriolar subdistal appendages) that directly contact cytoplasmic microtubules and thus link the primary cilium to the microtubule cytoskeleton; and (iii) striated rootlets emanating from the proximal end towards the interior of the cell that help to position and orient the basal body (Hoyer-Fender 2010; Debec et al. 2010; Anderson et al. 2008).

Little detail is known about the early stages of cilia formation, such as how centrioles migrate to the cell surface, and the timing of acquisition of the additional accessory structures required for anchoring the centrioles to the cell membrane (Dawe et al. 2007; Bettencourt-Dias & Glover 2007). However, the primary cilium is thought to originate through three distinct stages (Sorokin 1962). Firstly, a golgi-derived vesicle encapsulates the distal end of the mother centriole, and at the point of encapsulation a necklace region develops that is postulated to serve as a selective barrier at the cilium entrance. In the second stage, accumulation and fusion of additional vesicles form a sheath around the axonemal shaft, which elongates through microtubule assembly. Then in the third stage, the elongating axoneme surrounded by the ciliary-membrane fuses with the cell membrane resulting in the exposition of the primary cilium (Sorokin 1962; Abou Alaiwi et al. 2009; Hoyer-Fender 2010). Further assembly and maintenance of the ciliary axoneme is then mediated by IFT particles that first assemble at the transitional fibres extending from the basal body (Figure 1.6)

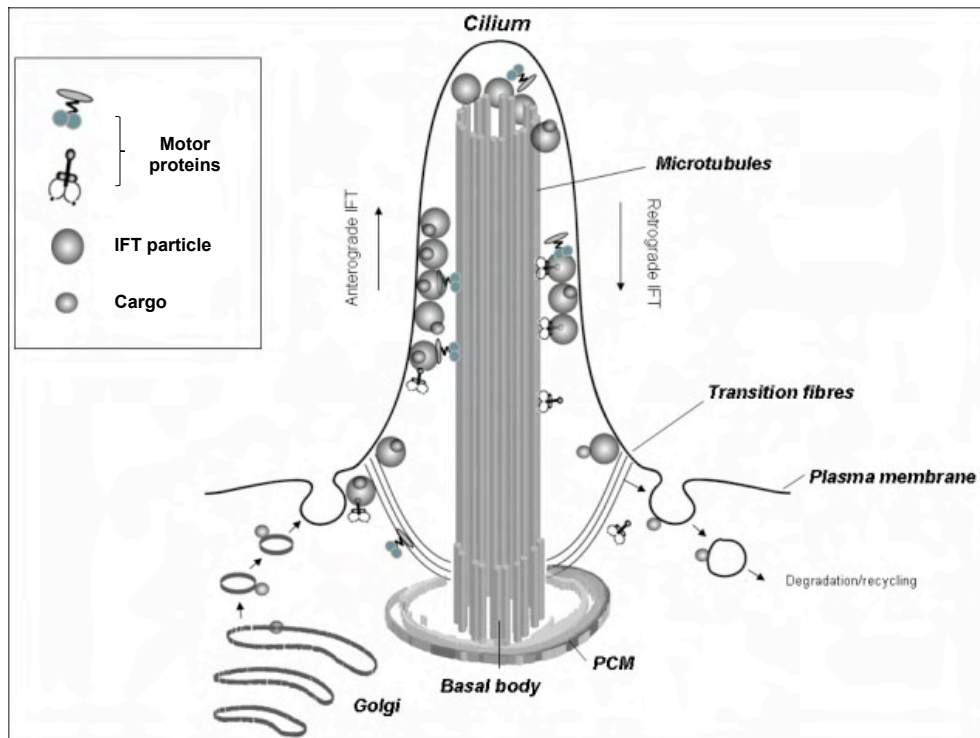


**Figure 1.6 Basal bodies template the formation of the primary cilium**

Schematic diagram of the primary cilium. The ciliary axoneme is nucleated from and anchored by the basal body. Basal bodies are structurally related to centrioles being comprised of a nine-fold symmetrical array of triplet microtubules. The concept of intraflagellar transport (IFT) used to assemble and maintain the ciliary axoneme is illustrated, wherein protein cargo is docked onto IFT particles at the transition zone of fibres emanating from the basal body, and then under the influence of motor proteins, the IFT/cargo assembly is transported along the microtubular axoneme. After unloading the cargo, the IFT can load further cargo and transport it in a motor protein-dependent manner back to the cell cytoplasm. Taken from Waters & Beales (2010).

(Abou Alaiwi et al. 2009; Hoyer-Fender 2010; Nigg & Raff 2009). However, how cilia are then re-absorbed upon cell cycle re-entry is still unclear although a role has been proposed for the mitotic kinase, Aurora A (Pugacheva et al. 2007; Nigg & Raff 2009).

### **1.3 Mitotic protein kinases**

The human genome encodes over 500 protein kinases, which constitute one of the largest human gene families. A substantial number of these act as key regulators of the cell cycle (Manning et al. 2002; Hanks 2003). For example, temporal and spatial regulation of the mitotic machinery is critical to ensuring the accuracy and fidelity of mitosis and protein phosphorylation is a key post-translational mechanism used for this purpose. The reversible covalent addition of a phosphate group to a substrate protein on a serine, threonine or tyrosine residue in a spatiotemporal specific manner by a protein kinase can induce several changes in its physicochemical properties, including charge and conformation. These can result in activation or inactivation of the target protein or changes in protein-protein interactions and complex formation. A number of different protein kinase families are involved in the regulation of M-phase progression including the cyclin-dependent kinases, the Polo-like kinases and the Aurora kinases, which are discussed below, and the NIMA-related kinases as described in section 1.4.

#### **1.3.1 Cyclin-dependent kinases**

As described earlier, cyclin-dependent kinases (Cdks) are serine/threonine protein kinases with a well established role in regulation of the eukaryotic cell cycle. The defining feature for this family of kinases is a requirement for an activating subunit called cyclin (Malumbres & Barbacid 2005). As discussed, cyclins are synthesised and destroyed at specific times during the cell cycle, thus regulating kinase activity in a timely manner. The founding members of the Cdk family were first identified in budding yeast, *S. cerevisiae* (CDC28) and fission yeast, *S. pombe* (Cdc2) through genetic screens of mutants with cell

cycle progression defects (Russell & Nurse 1986; Malumbres & Barbacid 2005). Of the 20 mammalian Cdks that have now been identified, only Cdk1, 2, 4 and 6 have been directly implicated in regulating cell cycle progression and, of these, only Cdk1 is generally considered to be a mitotic kinase (Malumbres et al. 2009b; Malumbres & Barbacid 2007). Moreover, mouse knockout studies have shown that Cdk1 alone is sufficient to drive cell cycle progression, compensating for the loss of Cdk2, 4, and 6, and hence is the only essential Cdk in mammalian cells (Santamaría et al. 2007).

Cdk1 activation is controlled by the balance between Wee1/Myt1 kinases and Cdc25 phosphatases. During G<sub>2</sub>, concomitantly with centrosome maturation, cyclin B-Cdk1 accumulates at the centrosomes; however, association of cyclin B to Cdk1 is not sufficient to form an active complex (Lindqvist et al. 2009). Although the Cdk in the complex is phosphorylated by CAK at an activating site (Thr161) that opens up the catalytic region, it is held in an inactive state by inhibitory phosphorylation on Thr14 and Tyr15 by Myt1 and Wee1 kinases (Morgan 1995). Plk1 phosphorylates Cdc25 (Roshak et al. 2000; Toyoshima-Morimoto et al. 2002), allowing it to then dephosphorylate Thr14 and Tyr15 on Cdk1 (Schmit & Ahmad 2007; Lindqvist et al. 2009). Active cyclin B-Cdk1 can further stimulate its own activation by also activating Cdc25. Meanwhile, both Cdk1 and Plk1 phosphorylate Wee1 leading to its proteasomal degradation, and both Cdk1 and Plk1 also phosphorylate Myt1 inhibiting its kinase activity (Lindqvist et al. 2009; Nigg 2001). As a result, rapid activation of cyclin B-Cdk1 then triggers entry into mitosis.

Upon entry into M-phase, active cyclin B-Cdk1, as well as cyclin A-Cdk1, phosphorylates many targets to promote different mitotic events. For example, phosphorylation of the kinesin motor protein, Eg5, facilitates its recruitment to microtubules stimulating centrosome separation and spindle assembly (Nigg 2001; Blangy et al. 1995; Malumbres & Barbacid 2005); phosphorylation of nuclear lamins reduces nuclear lamina stability triggering nuclear envelope breakdown (Dorée & Galas 1994; Nigg 2001; Malumbres & Barbacid 2005); and

phosphorylation of Histone H1 catalyses chromatin condensation by reducing H1-DNA interaction and thus potentially allowing access to chromosome condensing factors (Dorée & Galas 1994; Hochegger et al. 2008). Once chromosomes are condensed and aligned at the metaphase plate, Cdk1 activity is inactivated as a result of cyclin B degradation by the APC/C, thus enabling mitotic exit and cytokinesis.

### **1.3.2 Polo-like kinases**

Polo-like kinases (Plks) are a conserved family of serine/threonine kinases that regulate cell cycle events (Archambault & Glover 2009). The founding member of the Plk family, Polo, was first identified in *Drosophila melanogaster* as the product of the *polo* gene whose mutation resulted in multiple mitotic defects. These included centrosome separation and spindle formation defects that resulted in abnormal chromosome congression and segregation (Sunkel & Glover 1988; Llamazares et al. 1991). Subsequently, Plks have been identified in many eukaryotes from yeasts to humans: *cdc5* and *Plo1* in budding yeast and fission yeast, respectively, and Plk1-4 in mammals (Figure 1.7A) (Kitada et al. 1993; Ohkura et al. 1995; Hamanaka et al. 1994; Liby et al. 2001; Li et al. 1996; Fode et al. 1994). In all Plks, an amino-terminal serine/threonine kinase domain precedes a carboxy-terminal regulatory domain containing highly conserved polo-box motifs. Polo-box motifs, or domains (PBDs) are important regulatory domains for targeting Plks to specific substrates and subcellular locations by facilitating binding to phosphoepitopes on targets already phosphorylated by a priming kinase (Elia et al. 2003a; Elia et al. 2003b). Here, the roles of human Plks as mitotic kinases are described.

#### **1.3.2.1 *Plk1***

The best characterised member of the human Plk family is Plk1. Like Cdk1, this protein kinase controls many critical events during M-phase of the cell cycle with roles at mitotic entry, the metaphase-to-anaphase transition and mitotic exit (Schöffski 2009). Firstly, Plk1 regulates activation of Cdk1 through controlling

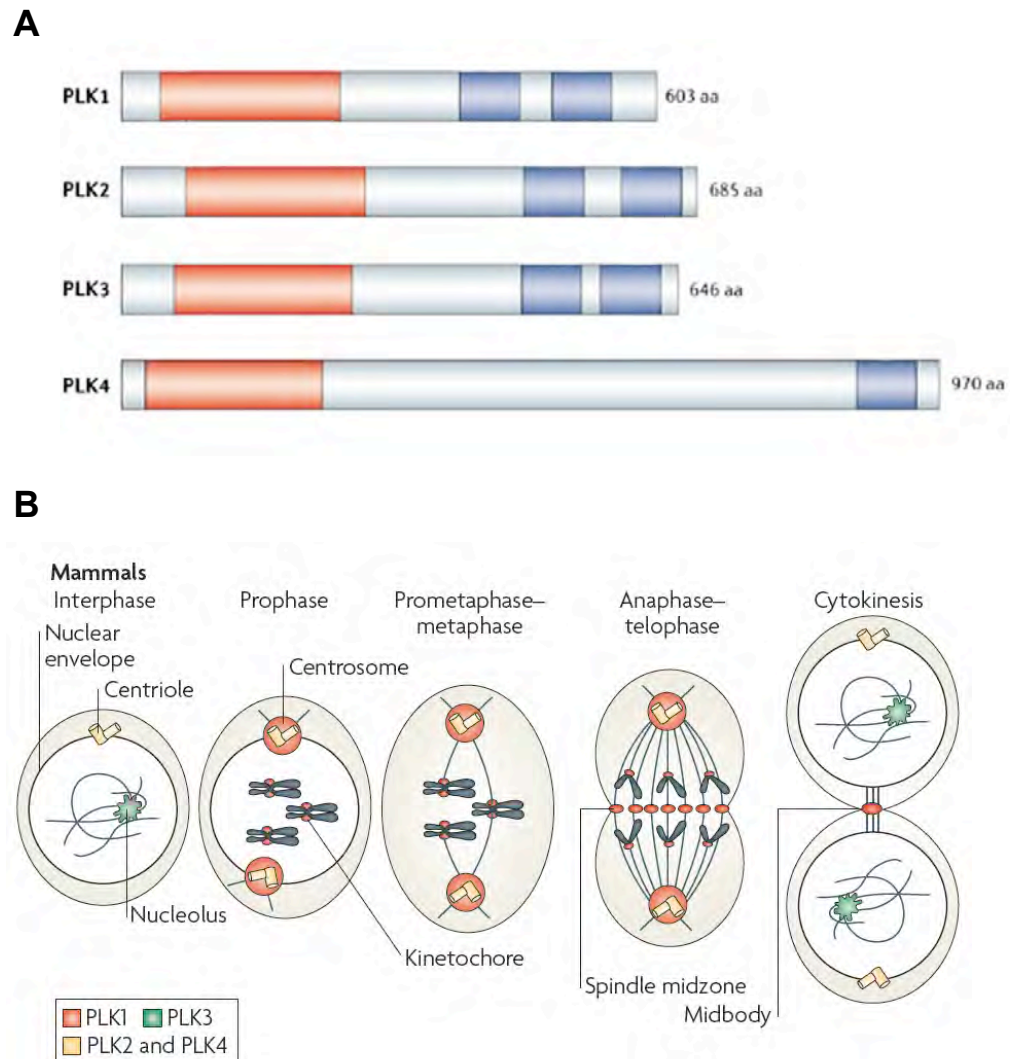


**Figure 1.7 Mammalian Polo-like kinases**

**(A)** Schematic representation of the different members of the mammalian Polo-like kinase family. The kinase domains are highlighted in red and the polo-box domains in blue. The length of each protein in amino acids is indicated. Adapted from Strebhardt & Ullrich (2006). **(B)** Schematic representation of the dynamic cell-cycle dependent localisation of PLK1 and localisation of the other three members of the human Polo-like kinase family. PLK1 associates with centrosomes at prophase, then becomes enriched at kinetochores in prometaphase-metaphase, before being recruited to the spindle midzone in anaphase and midbody during cytokinesis. Taken from Archambault & Glover (2009).

Cdc25 activation as described above. In prophase, Plk1 phosphorylates an inhibitor of the APC/C, early mitotic inhibitor (Emi1), leading to its ubiquitylation and degradation. However, at this point inhibition of the APC/C is taken over by components of the SAC (Hansen et al. 2004; Archambault & Glover 2009). Plk1 also contributes in prophase to sister chromatid separation by phosphorylating cohesin subunits on chromosome arms (Shintomi & Hirano 2010; Sumara et al. 2002; Hauf et al. 2005). However, centromeric cohesin is protected by Shugoshin-dependent recruitment of the phosphatase, PP1, until activation of separase at the metaphase-anaphase transition (McGuinness et al. 2005; Hauf et al. 2005).

In mitosis, Plk1 also plays a number of major roles at centrosomes. For example, it contributes to the process of centrosome maturation. Insight into this function came from a study in which Plk1 antibodies were microinjected into mammalian cells; this led to the formation of reduced microtubule arrays nucleating from small, duplicated but unseparated, centrosomes (Lane & Nigg 1996; Archambault & Glover 2009). Plk1 has since been found to phosphorylate a structural component of the centrosome, Nlp, and as a result, Nlp becomes displaced from the centrosome. This may be necessary to allow the recruitment of mitosis-specific components that increase the capacity of the centrosome to nucleate microtubules (Casenghi et al. 2003; Casenghi et al. 2005). Plk1 has also been shown to regulate the recruitment of Aurora A, another kinase important for centrosome maturation and function (section 1.3.3), to the centrosomes. These data indicate that Plk1 plays both direct and indirect roles in centrosome maturation (Hanisch et al. 2006; De Luca et al. 2006). In addition, Plk1 phosphorylates the centrosomal protein kizuna. This acts to ensure the integrity of spindle poles in response to the severe pulling forces that are exerted by the microtubules during spindle formation and chromosome congression (Oshimori et al. 2006; Fry & Baxter 2006).

At prometaphase, Plk1 also localises to kinetochores where its activity is required for the stable attachment of kinetochores to microtubules. This

supports the establishment of tension that contributes to bipolar spindle assembly and progression through the SAC (section 1.1.3.2) (Sumara et al. 2004; Lénárt et al. 2007). Evidence suggests that interactions of Plk1 with several kinetochore substrates, including Bub1, INCENP and NudC, may contribute to its recruitment to kinetochores. Subsequently, phosphorylation of a checkpoint component, BubR1, by Plk1 might then promote the establishment of stable kinetochore-microtubule interactions and chromosome congression (Qi et al. 2006; Goto et al. 2006; Nishino et al. 2006; Lénárt et al. 2007; Elowe et al. 2007; Matsumura et al. 2007).

Lastly, Plk1 plays important roles in mitotic exit and cytokinesis. In late mitosis, Plk1 moves to the central spindle and midbody through association with protein regulator of cytokinesis 1 (PRC1) and mitotic kinesin-like protein-1 and -2 (Mklp1/2) (Lee et al. 1995; Neef et al. 2003; Liu et al. 2004; Neef et al. 2007). In terms of cytokinesis, Plk1 has been found to promote the recruitment of RhoA guanine nucleotide-exchange factor ECT2 to the central spindle by phosphorylating its anchor protein Cyk4. This then results in the activation of RhoA GTPase, an activator of the cytokinetic acto-myosin ring. Hence, cytokinesis initiates with assembly of the contractile ring and ingression of the cleavage furrow (Petronczki et al. 2008; Archambault & Glover 2009). The APC/C-mediated degradation of Plk1 during mitotic exit has recently been shown to enable an adaptor protein, Cep55, to be recruited to the midbody, in order to promote membrane-remodelling, abscission and the completion of cytokinesis (Bastos & Barr 2010). Plk1 regulates the timing of this process, by phosphorylating Cep55 during cleavage furrow formation. This prevents the premature recruitment of Cep55 to the midbody. Thus, only when Plk1 levels decrease Cep55 interacts with Mklp1 at the midbody leading to the onset of membrane-remodelling events required for the termination of cytokinesis (Bastos & Barr 2010).

Thus, Plk1 changes localisation through mitosis, associating with centrosomes in prophase, then becoming enriched at kinetochores in prometaphase and

metaphase, before being recruited to the central spindle in anaphase (Figure 1.7B). These changes in localisation are regulated spatially and temporally via the PBD thereby allowing Plk1 to perform its diverse mitotic functions (Petronczki et al. 2008).

### **1.3.2.2 *Plk2, Plk3 and Plk4***

Whilst the roles of Plk1 in cell division are well established, the remaining members of the Plk family, Plk2, Plk3 and Plk4, have been less well studied and the roles of these kinases therefore remain to be characterised in detail. Plk2 is expressed maximally in G<sub>1</sub> and early S-phase with kinase activity peaking at the G<sub>1</sub>/S transition (Simmons et al. 1992; Ma et al. 2003b; Warnke et al. 2004; Cizmecioglu et al. 2008). Plk2 has been found to localise to the centrosome and is thought to be involved in centriole duplication (Warnke et al. 2004; Cizmecioglu et al. 2008; Krause & Hoffmann 2010). By interfering with Plk2 function through RNAi-mediated depletion or overexpression of kinase-inactive Plk2, centriole duplication was blocked suggesting that Plk2 regulates this process (Warnke et al. 2004). However, Plk2<sup>-/-</sup> embryos are viable and whilst Plk2<sup>-/-</sup> mouse embryo fibroblasts (MEFs) grow more slowly they do still divide. Furthermore, Plk2 depletion in HeLa and U2OS cells does not prevent cell cycle progression (Ma et al. 2003a; Burns et al. 2003). Hence, it would appear that Plk2 is not essential for centrosome duplication. Plk2 may also play a role in the DNA damage response, as its expression is induced by DNA-damaging agents (Shimizu-Yoshida et al. 2001). It has even been suggested to play a role in the response to spindle damage as significant cell death is induced if Plk2 depleted cells are treated with a microtubule destabilising agent (Burns et al. 2003).

Plk3 may also be required at the G<sub>1</sub>/S transition as it promotes accumulation of cyclin E, which can then bind Cdk2 leading to activation of DNA replication (Zimmerman & Erikson 2007). Plk3 also stimulates Cdc25A phosphatase activity leading to removal of inhibitory phosphorylation on Cdk2 (Myer et al.

2005). However, in addition, Plk3 is activated in response to DNA damage at the G<sub>2</sub>/M transition; here it may phosphorylate Cdc25C in such a way as to cause the nuclear exclusion of this phosphatase. This prevents cyclin B-Cdk1 activation and progression into mitosis is halted (Schmit & Ahmad 2007; Archambault & Glover 2009).

Finally, recent studies have revealed that Plk4 is a key regulator of centriole duplication. Plk4 has been shown to localise to the proximal ends of centrioles, which is consistent with its role in centriole duplication (Kleylein-Sohn et al. 2007). Overexpression of Plk4, or its *Drosophila* homologue Sak, drives centriole amplification, whereas its inhibition, depletion or mutation reduces centriole number (Habedanck et al. 2005; Bettencourt-Dias et al. 2005). Insufficient Plk4 expression has also been observed to lead to the formation of abnormal centrioles lacking key centrosomal proteins required to nucleate microtubules (Kuriyama et al. 2009). Plk4 abundance and kinase activity has been found to fluctuate at the centrosome, being low in G<sub>1</sub> and increasing in S-phase to reach a maximum in mitosis (Sillibourne et al. 2010). Studies carried out in knockout mice have provided further support that Plk4 is essential for mitotic progression (Hudson et al. 2001; Ko et al. 2005).

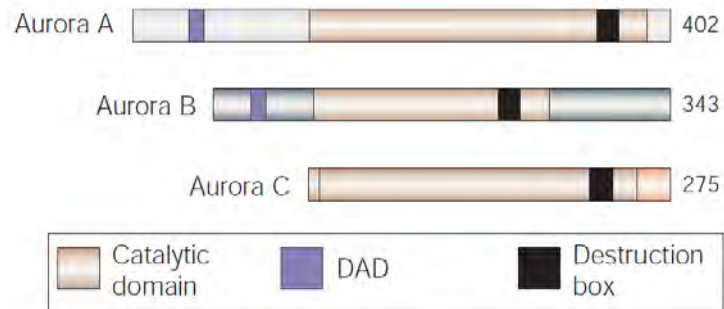
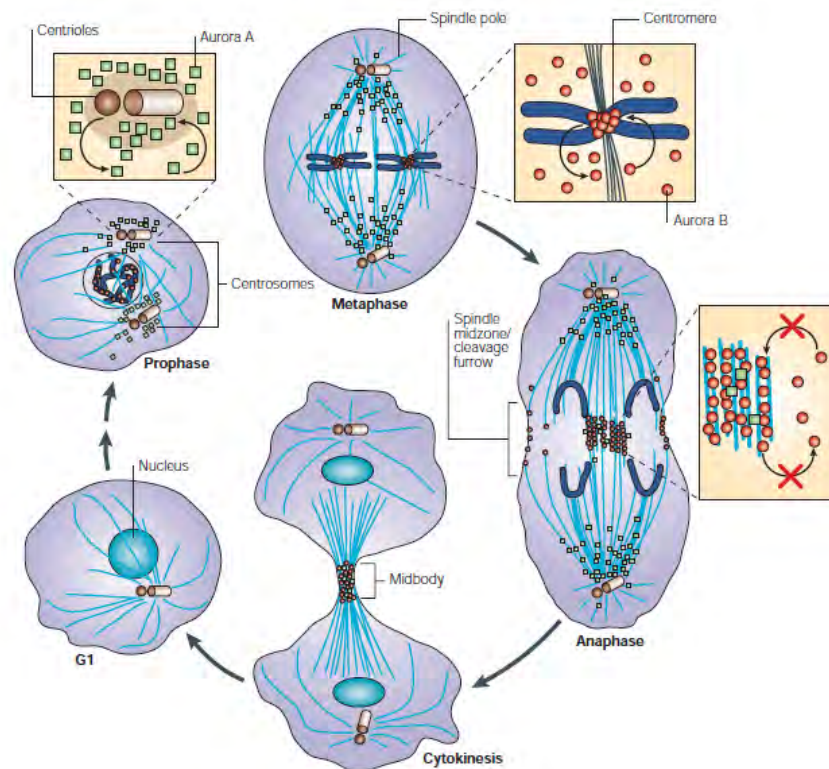
### 1.3.3 Aurora kinases

Aurora kinases are another family of serine/threonine protein kinases that control several aspects of cell division (Vader & Lens 2008). The founding member of the Aurora family, Ipl1, was initially described in the budding yeast, *S. cerevisiae*, after a screen for temperature sensitive mutants that were defective in chromosome segregation; this identified a series of genes designated increase in ploidy (Ipl) (Chan & Botstein 1993). Subsequently, *S. cerevisiae* Ipl1 was found to be homologous to the *Drosophila melanogaster* Aurora kinase, which when mutated resulted in monopolar spindle formation as a result of centrosome separation failure (Glover et al. 1995). The human family of Aurora kinases has three members: Aurora A, B and C, which are

similar in sequence within the C-terminal catalytic domains, but show variability in their N-terminal regulatory regions (Figure 1.8A) (Carmena & Earnshaw 2003). Here, the roles of these human Auroras as mitotic kinases are described.

### **1.3.3.1 Aurora A**

Aurora A is associated with the centrosome from the time of centrosome duplication through to mitotic exit, while it also associates with regions of microtubules proximal to centrosomes in mitosis (Figure 1.8B) (Carmena & Earnshaw 2003). At the centrosomes, Aurora A first contributes to activation of Plk1. During G<sub>2</sub>, Aurora A in complex with its cofactor Aurora Borealis (Bora) (Hutterer et al. 2006), phosphorylates Plk1 at its activating site Thr210 (Macůrek et al. 2008; Seki et al. 2008b). Activated Plk1 then phosphorylates Cdc25 and Wee1 to induce activation of cyclin B-Cdk1 promoting mitotic entry. During mitosis, active Cdk1 then phosphorylates and primes Bora for interaction with and phosphorylation by Plk1 (Chan et al. 2008), which, in turn, leads to the proteasomal degradation of Bora (Chan et al. 2008; Seki et al. 2008a). Degradation of Bora enables free Aurora A to interact with TPX2, a complex necessary for bipolar spindle assembly (Macurek et al. 2009). Whilst Aurora A is required for the correct localisation of centrosomal components that drive centrosome maturation in G<sub>2</sub>, Aurora A function is subsequently required for bipolar mitotic spindle assembly (Vader & Lens 2008). To facilitate spindle assembly, a small GTPase Ran is converted to Ran-GTP in the vicinity of chromosomes. This then releases TPX2 from importin- $\alpha$  allowing TPX2 to bind Aurora A and stimulate its kinase activity (Bayliss et al. 2003). This interaction enables Aurora A to promote chromatin-driven bipolar spindle assembly (Carmena & Earnshaw 2003; Carvajal et al. 2006; Schmit & Ahmad 2007; Vader & Lens 2008). In support of a role for Aurora A and TPX2 in spindle assembly, experiments in *Xenopus* egg extracts revealed that Aurora A coated beads were able to act as MTOCs and promote microtubule assembly even in the absence of both centrosomes and chromatin (Tsai et al. 2003; Tsai & Zheng

**A****B****Figure 1.8 Mammalian Aurora kinases**

**(A)** Schematic representation of the different members of the mammalian Aurora kinase family. The length of each protein in amino acids is indicated; DAD, D-box activating domain. Adapted from Carmena & Earnshaw (2003). **(B)** Schematic representation of the dynamic cell-cycle dependent localisation of Aurora A and Aurora B. Aurora A (green squares) localises to centrosomes from the time of centrosome duplication through to mitotic exit, and from metaphase, associates with microtubules near the spindle poles until mitotic exit. Whilst, Aurora B (red circles) is nuclear during prophase, then locates to the inner centromeres of sister chromatids, before concentrating on the spindle midzone in anaphase and in the midbody during cytokinesis. Taken from Carmena & Earnshaw (2003).

2005). However, the substrates of Aurora A that regulate spindle assembly remain to be clearly defined.

### **1.3.3.2 Aurora B**

Aurora B is a chromosome passenger protein critical for chromosome condensation, correct kinetochore-microtubule attachments, accurate chromosome segregation and cytokinesis (Carvajal et al. 2006; Adams et al. 2001). Upon entry into mitosis, Aurora B is thought to promote chromosome condensation through recruitment and phosphorylation of condensin subunits that bind chromatin (Lipp et al. 2007), and through phosphorylation of Histone H3 (Giet & Glover 2001; Adams et al. 2001; Goto et al. 2002; Vader & Lens 2008). During prometaphase and metaphase, Aurora B localises to the centromeres of sister chromatids (Figure 1.8B), where it is responsible for the correct localisation and stabilisation of centromeric proteins including the inner centromeric protein (INCENP), Borealin and survivin (Carvajal et al. 2006; Ditchfield et al. 2003; Honda et al. 2003). Association of Aurora B with these proteins forms the chromosome passenger complex in which Aurora B becomes activated through INCENP binding and autophosphorylation (Honda et al. 2003). Aurora B is then targeted to different substrates through movement of the whole complex from centromeres in metaphase to the central spindle in anaphase and midbody in cytokinesis (Figure 1.8B) (Carmena & Earnshaw 2003).

At the centromeres, Aurora B plays a central role in the correction of inappropriate kinetochore-microtubule attachments (Hauf et al. 2003; Knowlton et al. 2006). This is a key step in chromosome biorientation and inactivation of the spindle assembly checkpoint (Carvajal et al. 2006). Incorrect attachments are frequently formed during normal mitotic progression. These include syntelic attachments where both sister chromatids are attached to the same pole, and merotelic attachments where individual kinetochores are attached to both poles (Carvajal et al. 2006). Hence it is proposed, that Aurora B promotes disruption

of these incorrect kinetochore-microtubule attachments until the bi-oriented chromosome comes under tension (Tanaka et al. 2002; Liu et al. 2009). Aurora B functions to destabilise these incorrect attachments through regulating the activity of the microtubule depolymerase, MCAK (Andrews et al. 2004; Lan et al. 2004; Knowlton et al. 2006), and the affinity of the Hec1 kinetochore protein for microtubules (DeLuca et al. 2006). These events mediate release of microtubules from kinetochores in the case of inappropriate attachment (Lampson et al. 2004; Vader & Lens 2008). By destabilising incorrect kinetochore-microtubule attachments, Aurora B also plays a role in SAC activation. Aurora B recruits several checkpoint proteins, including BubR1 and Mad2, to unattached kinetochores. These bind Cdc20 and thus activate the SAC by inhibiting activation of the APC/C ubiquitin ligase (Fang 2002; Vader & Lens 2008). Once the SAC is satisfied, Aurora B is thought to regulate the association of separase with mitotic chromosomes to initiate the release of sister chromatid cohesion (Yuan et al. 2009). Finally, Aurora B regulates cytokinesis independently of Plk1 (Petronczki et al. 2007) by phosphorylating components of the centralspindlin complex, such as the Mklp1 kinesin, and proteins in the cleavage furrow, such as the intermediate filament, vimentin (Carmena & Earnshaw 2003; Vader & Lens 2008; Salaun et al. 2008).

### **1.3.3.3 Aurora C**

Aurora C is the least studied member of the Aurora kinase family. Evidence indicates that Aurora C is also a chromosome passenger protein that can bind INCENP but with lower affinity than Aurora B (Sasai et al. 2004). Indeed, overexpression of an inactive mutant of Aurora C has been shown to interfere with Aurora B function by displacing it from its binding partners (Chen et al. 2005). Recently, suppression of Aurora B and its mitotic functions, including the regulation of kinetochore-microtubule attachments and cytokinesis, has been shown to be rescued by overexpression of wild-type but not inactive Aurora C (Slattery et al. 2009). Hence, it seems that Aurora C exhibits similar mitotic functions to those assigned to Aurora B and may have overlapping functions;

however, Aurora C expression appears to be mainly restricted to the testis (Tseng et al. 1998; Kimura et al. 1999).

## **1.4 NIMA-related kinases**

### **1.4.1 NIMA**

NIMA (never in mitosis A) is a serine/threonine protein kinase present in the multicellular filamentous fungus *Aspergillus nidulans*. In the 1970s, Ron Morris identified the gene, *nimA*, as a temperature-sensitive mutant that was never in mitosis (*nim*) when *Aspergillus* cells were incubated at the restrictive temperature (Morris 1975). Approximately a decade later the gene was cloned and the encoded protein was designated NIMA (Osmani et al. 1987; Osmani & Ye 1996; O'Connell et al. 2003). NIMA is a 79 kDa protein with an N-terminal kinase domain and a C-terminal non-catalytic domain rich in regulatory motifs, including a coiled-coil domain required for the formation of NIMA oligomers and two 'PEST' sequences that direct NIMA for degradation (Lu et al. 1994; O'Connell et al. 2003; Fry & Nigg 1995). Activation of this serine/threonine kinase at the G<sub>2</sub>/M transition of the cell cycle was found to be required for entry into mitosis. When the gene encoding NIMA was mutated then cells arrested in G<sub>2</sub>, whereas when the gene was overexpressed the cells were driven into mitosis from any point in the cell cycle (Osmani et al. 1991; Oakley & Morris 1983; Osmani et al. 1988; O'Connell et al. 2003; Fry 2002). On the other hand, degradation of NIMA is absolutely required for mitotic exit and expression of a truncated form of NIMA which lacks the PEST sequences that mediate NIMA proteolysis is highly toxic and results in an arrest in mitosis (Pu & Osmani 1995). Analysis of the expression of NIMA mRNA and protein through the cell cycle demonstrated that, consistent with a role in the regulation of mitotic progression, both mRNA and protein levels increase as cells progress through G<sub>2</sub>, peaking during late G<sub>2</sub> and early mitosis, after which NIMA levels drop as cells progress through mitosis. The kinase activity of NIMA reflects the abundance of the protein with peak levels in late G<sub>2</sub> and early M-phase and this increase in activity is mirrored by the level of NIMA autophosphorylation (Osmani et al. 1987; Osmani et al. 1991; Lu et al. 1993; Ye et al. 1995).

NIMA has been shown to be essential for mitotic entry in *Aspergillus*, which undertakes a closed mitosis in which the nuclear envelope remains intact. More specifically, at the time of mitotic entry, NIMA controls the localisation of cyclin B-Cdc2 to the SPB by promoting the nuclear uptake of cyclin B-Cdc2 (Wu et al. 1998) through interaction with the nuclear pore complex components, SONA and SONB (Wu et al. 1998; De Souza et al. 2003). This enables mitotic entry to be triggered with the initiation of chromosome condensation and spindle formation within the nucleus. NIMA is also proposed to participate in chromosome condensation as it phosphorylates Histone H3 (De Souza et al. 2000), although this role is generally fulfilled by Aurora B in higher eukaryotes.

After the discovery of this mitotic regulator, evidence that NIMA-like kinases may play a role in the mitotic pathway of other eukaryotic cells emerged (Lu & Hunter 1995). For example, ectopic expression of NIMA drives premature chromatin condensation in yeast and human cells (O'Connell et al. 1994). However, it is noteworthy that chromatin condensation by NIMA alone is not a mitosis-promoting function (Ye et al. 1995). Several NIMA-related kinases have since been identified using homology-based screens in different species (Figure 1.9).

#### **1.4.2 NIMA homologues in lower eukaryotes**

The NIM-1 protein from the filamentous fungus, *Neurospora crassa*, has the greatest sequence identity to NIMA, being 75% identical within the kinase domain. More importantly, to date, this is the only true functional homologue of NIMA, as it is able to abolish the late G<sub>2</sub> arrest by restoring normal mitosis in *A. nidulans nimA* temperature sensitive mutants (Pu et al. 1995).

Interestingly, the unicellular alga *Chlamydomonas* has 10 NIMA-related kinases. *Chlamydomonas* is a unicellular green algae that uses two basal bodies to produce two flagella that allow the organism to swim in response to

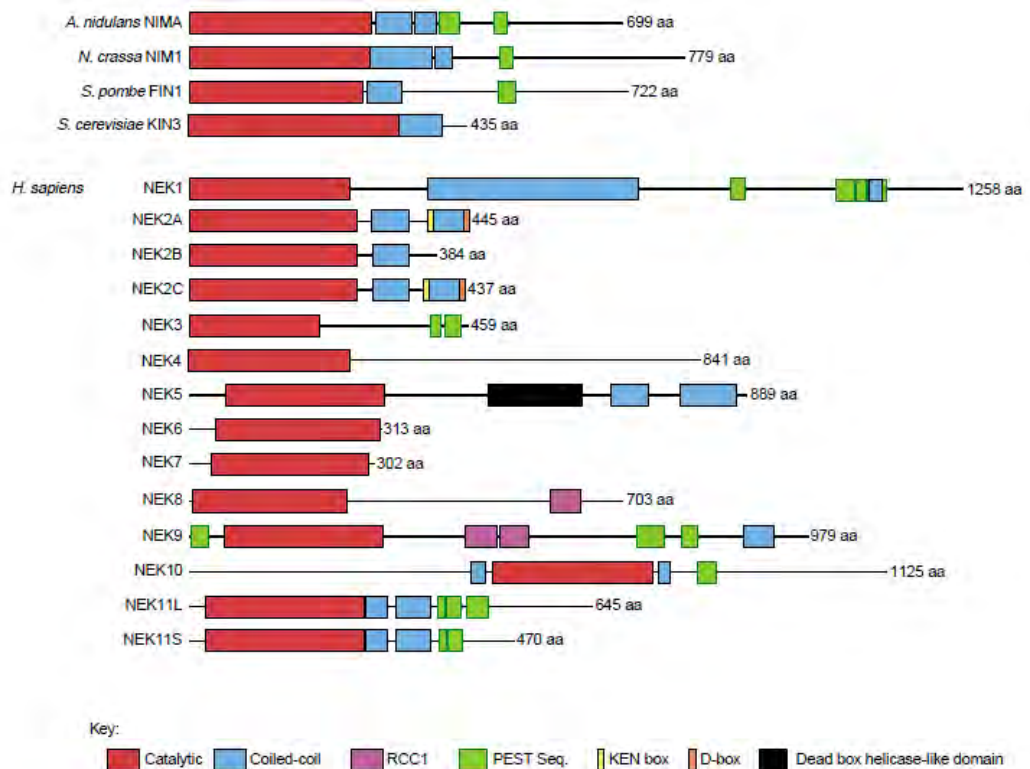


**Figure 1.9 The NIMA-related kinases**

Schematic representation of the NIMA-related kinases. The NIMA kinase family is defined by sequence homology to the *A. nidulans* NIMA kinase domain. The C-terminal regulatory motifs facilitate protein-protein interactions (coiled-coil, RCC1-like domain), or regulate proteolytic degradation (PEST-sequence, KEN-box, D-box). Adapted from O'Connell et al. (2003).

environmental stimuli. As *Chlamydomonas* divides, the flagella retract and the now duplicated basal bodies form the two poles of the mitotic spindle emphasising the interchangeability of basal bodies and centrioles. Fa2p was the first of its NIMA-related kinases to be characterised. Studies of *Fa2* mutants suggested that this kinase has both cell cycle and ciliary functions as *Fa2* mutants failed to deflagellate and also had subtle cell cycle progression defects (Mahjoub et al. 2002). Cnk2p, a second NIMA-related kinase characterised in *Chlamydomonas*, has been shown to localise to the ciliary axoneme and regulate flagellar length and cell size (Bradley & Quarmby 2005). Ectopic expression of Cnk2p resulted in small cells with short flagella whilst RNAi depletion of Cnk2p resulted in large cells with long flagella, thus it is thought that Cnk2p plays a role in cell cycle control by promoting flagellar disassembly and monitoring cell size prior to commitment to mitosis (Bradley & Quarmby 2005). To date, these are the only two NIMA-related kinase genes that have been studied in *Chlamydomonas*, and both affect ciliary disassembly as well as the cell cycle. In comparison to *Chlamydomonas*, another ciliated unicellular eukaryote, *Tetrahymena*, has hundreds of cilia, which fall into different classes depending on their location and length. This organism was found to have 39 Nek genes and all of the encoded proteins studied so far localise to cilia regulating ciliary length (Wloga et al. 2006).

The budding yeast, *S. cerevisiae*, and fission yeast, *S. pombe*, each have one NIMA-related kinase in their genome, Kin3 and Fin1, respectively (Jones & Rosamond 1990; Krien et al. 1998). After NIM-1, Kin3 is the next most similar kinase to NIMA, exhibiting 48% sequence identity; however, *kin3* mutation or overexpression of the protein does not result in an observable phenotype (Barton et al. 1992; Kambouris et al. 1993). However, like NIMA, overexpression of Fin1 induces Cdc2-independent premature chromatin condensation from any point in the cell cycle (Krien et al. 1998); whether this reflects a true physiological function for Fin1 remains unclear as Fin1 kinase activity does not peak until after the metaphase-anaphase transition once chromosome condensation has already occurred (Krien et al. 2002). Although not essential, Fin1 is thought to contribute to the timing of mitotic onset as it is

required to localise the polo-like kinase, Plo1, to the SPB, which potentiates the activation of cyclin B-Cdc2 for mitotic commitment. In addition, mutation of *fin1* has been shown to result in a delay in mitotic entry (Krien et al. 1998; Grallert & Hagan 2002). More specifically, Fin1 has been implicated in regulating mitotic spindle formation as temperature sensitive *fin1* mutants assemble monopolar spindles at the restrictive temperature (Grallert & Hagan 2002). Fin1 also plays a key role regulating mitotic exit by modulating the activity of the septum initiation network (SIN) to prevent premature septation (Grallert et al. 2004). In this regard, Fin1 activity restricts active SIN components to the younger SPB via interaction with SIN inhibitors, thus blocking SIN activation to the older SPB and restraining septation. In the absence of Fin1 function, active SIN components associate with both SPBs and the signal for septation is inappropriately accelerated (Grallert et al. 2004).

### **1.4.3 Mammalian NIMA-related kinases (Neks)**

The Nek family constitutes about 2% of all the human kinases. It contains 11 members (Nek1-Nek11) that have been identified based on similarities with NIMA in the catalytic domain using genomic and biochemical approaches (Manning et al. 2002). The catalytic domains of the human Neks are reasonably well-conserved, being approximately 40% identical to NIMA and approximately 40-85% identical to each other. On the other hand, the non-catalytic C-termini of the human Neks differ from each other in length, sequence and domain organisation. This enables differences in the localisation of the proteins, as well as their expression, regulation, substrates and kinase activity (Quarmby & Mahjoub 2005; O'Connell et al. 2003).

#### **1.4.3.1 Mitotic Neks: Nek2, Nek6, Nek7 and Nek9**

Among the human Nek kinases, Nek2 is the best-characterised and is the most closely related to NIMA, being 44% identical in amino acid sequence across the catalytic domain (O'Connell et al. 2003; Fry 2002). Human Nek2 localises to the centrosome via a motif in the C-terminal domain of the protein (Hames et al.

2005). It maintains this localisation throughout the cell cycle (Fry et al. 1998b; Fry 2002), although its expression and activity are cell cycle regulated with peak levels in S and G<sub>2</sub> (Schultz et al. 1994; Fry et al. 1995; Fry 2002). Nek2 has been shown to exist as two major splice variants, Nek2A and Nek2B (Hames & Fry 2002); however, a third splice variant, Nek2C, was recently identified that preferentially localises to the nucleus (Fardilha et al. 2004; Wu et al. 2007).

Nek2A plays a role in the regulation of centrosome disjunction, which occurs at the start of mitosis and is necessary for the formation of a bipolar spindle (Fry et al. 1998b; Fletcher et al. 2005). Overexpression of active, but not catalytically-inactive, Nek2 stimulates premature centrosome separation in interphase cells (Fry et al. 1998b; Faragher & Fry 2003). Consistent with this, RNAi depletion of Nek2A inhibits centrosome separation (Fletcher et al. 2005; Mardin et al. 2010). Nek2 promotes centrosome separation by interacting with and phosphorylating at least two components of the intercentriolar linkage that holds the centrosomes together in close proximity during interphase. These components are C-Nap1 and rootletin that together form the filamentous intercentriolar linker. Their phosphorylation results in their dissociation from the centrosome leading to loss of centrosome cohesion (Bahe et al. 2005; Fry et al. 1998a). It has recently been reported that the Mst2 protein kinase and hSav1 scaffold protein directly interact with Nek2A and regulate its localisation to centrosomes and phosphorylation of C-Nap1 (Mardin et al. 2010). Nek2 also potentially targets other centrosomal proteins, including Ninein-like protein (Nlp) and centrobilin, which are implicated in nucleation and/or anchoring of microtubules (Rapley et al. 2005; Jeong et al. 2007). Hence, Nek2 is generally implicated in the modification of both centrosome and microtubule organisation at the G<sub>2</sub>/M transition (O'Regan et al. 2007).

Upon expression, Nek2 is thought to constitutively dimerize through an unusual leucine zipper motif (Fry et al. 1999). This facilitates autophosphorylation at key sites within the catalytic domain for kinase activation (Rellos et al. 2007). However, to prevent premature Nek2 activation and inappropriate centrosome

separation in interphase, Nek2 is inactivated through dephosphorylation by protein phosphatase 1 (PP1), which binds to a KVHF motif in the non-catalytic C-terminal region of Nek2 (Helps et al. 2000; Mi et al. 2007). PP1 is also able to dephosphorylate the Nek2 substrate C-Nap1 (Helps et al. 2000). At the onset of mitosis, PP1 is inactivated leading to Nek2 activation (Li et al. 2007). However, following mitotic entry, Nek2A is rapidly degraded in an APC/C-dependent manner (Hames et al. 2001; Hayes et al. 2006).

Nek2 is not the only mammalian Nek regulating spindle assembly. Nek6, Nek7 and Nek9 also play a role. Nek6 and Nek7 are highly similar in sequence. They encode little more than a catalytic domain with no C-terminal extensions (Kandli et al. 2000). Evidence suggests that these two kinases are part of a Nek cascade regulating progression through mitosis (Belham et al. 2003). In the cascade, Nek6 and Nek7 act downstream of another Nek kinase, Nek9, which phosphorylates a serine residue within the activation loop of Nek6 and Nek7, to stimulate their kinase activity (Roig et al. 2002; Belham et al. 2003). Nek9 may also bind and induce activation of the kinases via an allosteric mechanism (Richards et al. 2009).

Recent data indicates that Nek6 and Nek7 are both activated in mitosis and both have been shown to localise to spindle poles (O'Regan & Fry 2009). Interestingly, Nek6 also localises to spindle microtubules in metaphase and anaphase and to the midbody during cytokinesis (O'Regan & Fry 2009). There is now good evidence that Nek6 and Nek7 both play important roles in mitotic spindle organisation. Overexpression of catalytically-inactive Nek6 or Nek7, or depletion of these proteins causes cells to exhibit spindle defects, nuclear abnormalities, mitotic arrest and apoptosis (Yissachar et al. 2006; Yin et al. 2003; Kim et al. 2007; O'Regan & Fry 2009).

Although, the expression of Nek9 protein remains constant through the cell cycle, its kinase activity also increases in mitosis (Roig et al. 2002; Holland et

al. 2002). In addition to a coiled coil dimerization motif, the Nek9 C-terminal non-catalytic domain contains an RCC1 homology region (O'Connell et al. 2003), which is thought to be required for autoinhibition of Nek9 (Roig et al. 2002). Total Nek9 is diffusely distributed within the cytoplasm in interphase and mitosis (Roig et al. 2002; Holland et al. 2002; Pelka et al. 2007), although active Nek9 has been observed to concentrate on spindle poles during mitosis (Roig et al. 2005). Functional studies support a role for Nek9 in mitotic spindle organisation. Expression of inactive and truncated Nek9 mutants resulted in missegregation of chromosomes, while injection of anti-Nek9 antibodies into cells caused defects in mitotic spindle formation (Roig et al. 2002). In addition, a number of Nek9 binding partners have been identified including components of the  $\gamma$ TuRC, the Ran GTPase, and BicD2, suggesting that Nek9 may play some role in microtubule nucleation and anchoring (Roig et al. 2005; Roig et al. 2002; Holland et al. 2002).

The similarity in defects that arise from interference with either Nek9 or Nek6/7 has led to the working model that suggests that activation of Nek9 leads to activation of its downstream substrates, Nek6 and Nek7, which independently co-ordinate the formation and/or maintenance of the mitotic spindle (O'Regan et al. 2007; O'Regan & Fry 2009).

#### **1.4.3.2 DNA damage response Neks: Nek10 and Nek11**

Recently, Nek10 has been reported to play a function in mediating G<sub>2</sub>/M arrest in response to DNA damage (Moniz & Stambolic 2011). Expression of Nek10 in cells resulted in an increase in ERK1/2 and MEK1 activation in response to UV irradiation but not in response to mitogens (Moniz & Stambolic 2011). Consistent with this, depletion of Nek10 led to impaired MEK/ERK activation in response to UV irradiation but not in response to mitogens (Moniz & Stambolic 2011). ERK1/2 is a mitogen activated protein kinase (MAPK) that responds to extracellular stimuli via a MAPK cascade and regulates various cellular activities such as gene expression, cell proliferation and cell differentiation. The kinase

cascade is composed of the MAPK (ERK1/2), activated by the MAPKK (MEK1/2), which is activated by more than one MAPKKK in response to different stimuli, for example c-Raf, in response to growth factors (Chang & Karin 2001). It is proposed that in response to UV irradiation, Nek10 associates with MEK1 in a Raf-dependent manner promoting its autophosphorylation leading to activation of ERK1/2 which is required for G<sub>2</sub>/M arrest (Moniz & Stambolic 2011).

Initial studies on Nek11 indicated that it is expressed as at least two alternative splice variants: a long isoform (Nek11L ~74 kDa) and a short isoform (Nek11S ~54 kDa), although the short isoform is rarely detected in somatic cells (Noguchi et al. 2002). Nek11L shows a cell cycle-dependent expression pattern with low levels in G<sub>1</sub> and increased abundance in S/G<sub>2</sub>/M phase, suggesting that Nek11L may play a role in cell cycle regulation (Noguchi et al. 2002). Using indirect immunofluorescence microscopy, Noguchi and colleagues (2002) found that the subcellular localisation of Nek11 also changes through the cell cycle. At interphase, nuclei were stained by an anti-Nek11 antibody, whereas in early mitosis staining was observed on polar microtubules. During anaphase, Nek11 staining became more diffuse, and cells in late mitosis displayed little specific staining. In a later study, the subcellular localisation was described as being more specifically nucleolar at interphase, whereas mitotic Nek11 was detected at perichromosomal regions (Noguchi et al. 2004). Although still far from being clearly defined, localisation does seem to be cell cycle-dependent, supporting the notion that Nek11 may have different roles in different phases of the cell cycle.

Importantly, while studying Nek11 kinase activity during cell cycle progression, it was unexpectedly found that replication inhibitors and genotoxic agents caused an increase in Nek11 kinase activity (Noguchi et al. 2002). These stresses cause the activation of DNA damage response (DDR) pathways including cell cycle checkpoint mechanisms. In support of this, Nek11 has now been shown to contribute to the DNA damage induced G<sub>2</sub>/M checkpoint by regulating the

phosphorylation of Cdc25A (Melixetian et al. 2009). In response to DNA damage, Nek11 is phosphorylated by Chk1 (checkpoint kinase 1) resulting in its activation; active Nek11 then phosphorylates Cdc25A targeting it for degradation via the SCF ubiquitin ligase, thus inducing G<sub>2</sub>/M arrest (Melixetian et al. 2009). In the absence of Nek11, proteasome-dependent degradation of Cdc25A is inhibited and cells fail to arrest in the presence of DNA damage, suggesting that Nek11 is an important component of the G<sub>2</sub>/M checkpoint (Melixetian et al. 2009; Sørensen et al. 2010).

Intriguingly, Nek2A has been reported to co-localise with nucleolar Nek11 and phosphorylate the non-catalytic region of Nek11 (Noguchi et al. 2004). As the non-catalytic region of Nek11 has an autoinhibitory function by interacting with the catalytic N-terminal domain, this led to the suggestion that phosphorylation of Nek11 by Nek2 might relieve the autoinhibitory activity and produce activated Nek11 (Noguchi et al. 2004). However, DNA damage leads to loss of Nek2A activity (Fletcher et al. 2004), so it is not clear how this interaction contributes to the activation of Nek11 in the DDR.

#### **1.4.3.3 Ciliary Neks: Nek1 and Nek8**

The first mammalian NIMA-related gene to be cloned was Nek1 (Letwin et al. 1992). However, apart from showing high expression in the testis, its function remained obscure. Then, almost a decade later, two different mutations (*kat* and *kat*<sup>2J</sup>) known to cause polycystic kidney disease (PKD) in mice were mapped to the murine Nek1 gene. This was the first clue that the mammalian Neks might have roles related to cilia. These mice exhibited a slowly progressing form of PKD as well as facial dysmorphism, male sterility, and other developmental abnormalities (Upadhyaya et al. 2000). PKD is said to be cilia-related as evidence indicates that dysfunctional ciliary signalling is the proximal cause of kidney cyst development (Quarmby & Parker 2005). In further support of the connection between Nek1 and PKD, a yeast two-hybrid assay using human Nek1 as bait reported an interaction with proteins known to be involved

in the development of PKD, such as the kinesin motor protein, KIF3A, and the tumour suppressor protein, tuberin (Surpili et al. 2003). More recently, Nek1 has been shown to localise to primary cilia, basal bodies and centrosomes while its overexpression was found to inhibit ciliogenesis. Indeed, its mutation in *kat<sup>2J</sup>* MEFs also led to abnormal cilia (Mahjoub et al. 2005; Shalom et al. 2008; White & Quarmby 2008). The additional localisation of Nek1 to the nucleus has led to the hypothesis that Nek1 may transduce signals between the primary cilium and the nucleus to regulate gene expression (Hilton et al. 2009).

Interestingly, interactions between Nek1 and several proteins that participate in DNA repair pathways have also been identified (Surpili et al. 2003). Moreover, there is evidence that the expression and activity of Nek1 are stimulated following DNA damage and that active Nek1 redistributes to sites of DNA double-strand breaks (Polci et al. 2004). Additionally, Nek1 has been shown to be important not only for efficient DNA damage checkpoint control, as in the absence of functional Nek1 cells fail to arrest in response to DNA damage, whilst overexpression of wild-type Nek1 rescues the checkpoint response, but also for proper DNA damage repair, as without functional Nek1 excessive numbers of chromosome breaks are observed that persist long after low dose ionising radiation (Chen et al. 2008; Pelegriani et al. 2010). Hence, Nek1 may have a dual role in both ciliogenesis and the DNA damage response.

Soon after identifying mutations in the Nek1 gene that cause PKD, a mutation that caused cystic kidney disease in another mouse model (*jck*) was mapped to the gene encoding Nek8. Confirmation of a cilia-related role for Nek8 came from showing that injection of zebrafish embryos with a morpholino anti-sense oligonucleotide corresponding to the orthologue of Nek8 resulted in the PKD phenotype (Liu et al. 2002). Overexpression of inactive Nek8 mutants in renal epithelial cells resulted in the formation of enlarged, multinucleated cells with an abnormal actin cytoskeleton and a reduced number of actin stress fibres. Thus, Nek8 is thought to be involved in regulating the cytoskeletal structure and possibly cell division in such cells (Liu et al. 2002). Moreover, overexpression

of kinase-deficient Nek8 in U2OS cells led to decreased actin expression (Bowers & Boylan 2004). Nek8 has been shown to localise to the proximal region of the primary cilium (Mahjoub et al. 2005) and, more specifically, to the inversin compartment at the base of primary cilia, where the Inv (inversin) protein accumulates (Shiba et al. 2010). Mutations of Nek8 result in mislocalisation of the protein from these regions (Mahjoub et al. 2005; Trapp et al. 2008; Otto et al. 2008; Sohara et al. 2008).

There is now evidence to suggest that Nek8 might be implicated in two human cystic diseases, ADPKD (autosomal dominant polycystic kidney disease) and NPHP (nephronophthisis) (Cai & Somlo 2008). Specifically, amino acid substitution mutations in *NEK8* have been identified in families with NPHP and it has been proposed that Nek8 is the *NPHP9* causative gene (Otto et al. 2008). Inversin is another NPHP causative protein and has been reported to interact with Nek8 in the inversin compartment. Moreover, Nek8 protein has been reported to associate with the ADPKD protein, polycystin-2, and in *jck* mutants an increase in abnormal phosphorylation of polycystin-2 has been reported to be associated with lengthened cilia and increased expression of polycystins (Sohara et al. 2008).

#### **1.4.3.4 Signal transducing Neks: Nek3**

Nek3 has a typical N-terminal serine/threonine kinase domain; however, the C-terminal regulatory domain lacks the predicted coiled-coil regions present in NIMA and most other human Neks. In contrast to the well-studied kinase, Nek2, no correlation between Nek3 expression levels and the proliferative index of particular organs has been found (Tanaka & Nigg 1999; Kimura & Okano 2001). In fact, evidence suggests there is very little variation in Nek3 protein and kinase activity levels through the cell cycle. Moreover, the kinase was expressed more highly in G<sub>0</sub>-arrested than proliferating Swiss 3T3 fibroblast cells (Tanaka & Nigg 1999). In contrast to this, though, there is one report of increased Nek3 expression in mitotically active cells (Chen et al. 1999).

Indirect immunofluorescence microscopy and chemical fractionation of cultured cells expressing Nek3 indicated that the protein kinase was predominantly cytoplasmic and there was no evidence that Nek3 associated with centrosomes (Tanaka & Nigg 1999). In an attempt to identify a function for Nek3, Nek3 antibodies were microinjected into Swiss 3T3 cells while epitope-tagged wild type and kinase-inactive Nek3 constructs were expressed in U2OS cells. However, these studies provided no evidence for a cell cycle-related role for Nek3 (Tanaka & Nigg 1999). Unexpectedly, yeast-two hybrid analyses and co-immunoprecipitation studies found a direct interaction between Nek3 and members of the Vav family of guanine nucleotide exchange factors in response to signalling from the prolactin receptor (Miller et al. 2005). These studies suggested that prolactin receptor stimulation induced Nek3 kinase activity causing Vav2 to interact with the kinase domain of Nek3 and become phosphorylated. Phosphorylated Vav proteins then activate downstream signalling targets involved in tumour progression. Overexpression of Nek3 was shown to potentiate prolactin-mediated cytoskeletal re-organisation of cells; however, if Nek3 was depleted then cytoskeletal re-organisation was attenuated as was cell migration and invasion. Therefore, current evidence suggests that activation of the prolactin receptor increases the proliferation and motility of human breast cancer cells with Nek3 implicated in the pathway (Miller et al. 2005; Miller et al. 2007). Nek3 has also been reported recently to regulate cytoskeletal dynamics in neurons by altering levels of acetylated tubulin, thus raising the possibility of a role for Nek3 in neuronal disorders (Chang et al. 2009).

## **1.5 Cell cycle-dependent kinases as targets in cancer**

Cancer refers to a wide range of pathologies related by unrestrained cellular proliferation. The development and progression of a tumour is a multistep process in which cells sustain genetic damage over a prolonged period of time that drives the transformation of normal cells into highly malignant derivatives (Hanahan & Weinberg 2000). Misregulation of cell cycle kinases might result in

cancer-associated defects including unscheduled proliferation and aberrant cell division leading to genomic instability (Malumbres & Barbacid 2007).

Indeed, many of the protein kinase families discussed above and that are known to be important in regulating cell cycle progression, have been linked to cancer progression. For example, the genes encoding the three members of the human Aurora protein kinase family map to chromosomal loci that are frequently altered in different cancer types, and overexpression of these proteins has been detected in human cancer cell lines (Carmena & Earnshaw 2003). Plk1 is overexpressed in a broad spectrum of cancer types, and its expression often correlates with poor prognosis and a lower overall survival rate (Schöffski 2009; Malumbres & Barbacid 2007). Among the NIMA-related kinases, Nek2 mRNA and protein expression levels are upregulated in a range of human cancer cell lines suggesting that this protein kinase may be implicated in cancer progression (Wai et al. 2002; de Vos et al. 2003; Hayward et al. 2004; Barbagallo et al. 2009). There is evidence that Nek3 is enriched in malignant human breast carcinomas (Miller et al. 2005; Miller et al. 2007). Furthermore, the Nek3 gene is located in the chromosomal region 13q14, which is frequently deleted in several types of human cancer (Kimura & Okano 2001; Hernández & Almeida 2006). A Nek3 alternative splice variant has been identified and a single adenine insertion/deletion polymorphism has been observed in the coding region of Nek3 (Hernández & Almeida 2006). Interestingly, data indicates that the adenine insertion (which involves a stretch of 8 adenines) was statistically higher in cancer samples with frequent 13q14 alterations in prostate cancer, whereas normal controls had a higher frequency of 7 adenine nucleotides (Hernández & Almeida 2006). This evidence suggests that there is an association between Nek3 and cancers with frequent 13q14 deletion. Similarly, Nek6 has been mapped to a locus at which loss of heterozygosity has been associated with several cancers (Hashimoto et al. 2002), and recently the transcript, protein and kinase levels of Nek6 were found to be highly elevated in malignant tumours and human cancer cell lines (Nassirpour et al. 2010). Nek8 might also be implicated in cancer progression as, like Nek2 and Nek3, it is upregulated in human breast tumours (Bowers & Boylan 2004).

Mitotic kinases have only relatively recently been implicated in cancer development (Malumbres & Barbacid 2007). However, advances in our understanding of how cell cycle events are regulated and the roles that these processes play in cancer development are expected to lead to the development of highly specific inhibitors designed to treat tumour-specific lesions. Indeed, RNAi-mediated depletion of Nek2, for example, blocks proliferation of breast, colorectal and cholangiocarcinoma cancer cells (Kokuryo et al. 2007; Tsunoda et al. 2009; Suzuki et al. 2010). Hence, evidence to date indicates that Neks have a potential of serving as novel targets for the management of cancers, and therefore detailed research into the mechanisms of their functions is required.

## **1.6 Project aims and objectives**

Although the mammalian Neks are structurally similar to each other, it is clear they do not all have the same function. At the onset of this project, the regulation and function of Nek3 and Nek11 remained relatively obscure. Moreover, there was no published data on Nek5 whatsoever. The aims of this project were therefore to use a variety of biochemical and cell biology based assays to carry out a broad characterisation of Nek3, Nek5 and Nek11. Furthermore, a particular emphasis would be placed on characterising a potential role for Nek5.

The specific experimental objectives which form the basis for the four Results chapters were as follows:

1. To generate, affinity-purify and characterise anti-Nek5 and anti-Nek11 antibodies that could be used for functional analyses of Nek5 and Nek11. Antibodies would be raised in rabbits against bacterially-expressed C-terminal fragments of Nek5 and Nek11 in order to maximise the chances of generating specific antibodies. Following purification, these would initially be used to assess cell cycle-dependent localisation. Similarly, a commercially available Nek3 antibody would be characterised for use in studies on Nek3.

2. To optimise assays for the purpose of examining Nek3, Nek5 and Nek11 localisation, expression and activity. This admittedly broad study was considered fundamental to determine where efforts should be focused for more detailed functional studies.
3. To investigate the effect of RNAi depletion of Nek5 on cell cycle progression using flow cytometry and immunofluorescence microscopy.
4. To characterise the centrosome and cell cycle phenotypes observed upon interference with Nek5 function as a result of RNAi depletion or expression of a kinase-inactive version of the protein.

Nek3, Nek5 and Nek11 clones (GenBank accession ID: BC019916, BC063885 and BC028587, respectively) used in this research project were purchased from GeneCopoeia (Rockville, USA). Using these clone sequences, the key structural features of the Nek family were examined using tools to predict PEST motifs (<http://mobyle.pasteur.fr/cgi-bin/portal.py?form=epestfind>) and coiled-coil domains (<http://www.isrec.isb-sib.ch/software/software.html>). Human full-length Nek3 is a 506 amino acid protein with an N-terminal kinase domain (aa 4-258) and two C-terminal PEST domains (aa 443-460, 469-495); no coiled-coil domains were identified in this protein (Figure 1.10). Human Nek5 is a 708 amino acid protein with an N-terminal kinase domain (aa 4-259), and a C-terminal coiled-coil domain (aa 456-498); no PEST motifs were identified in this protein (Figure 1.11). Alignment of the protein sequence for the Nek11 clone used in this project (Nek11c), with the published Nek11-long (Nek11L) and Nek11-short (Nek11S) sequences, revealed high similarity between Nek11S and Nek11c. Only the last four amino acid residues of Nek11S differed compared to Nek11c, after which, the Nek11c protein sequence extends for another 12 amino acid residues (Figure 1.12). Human Nek11c is a 482 amino acid protein with an N-terminal kinase domain (aa 29-286) and, within the C-terminus, this protein has two coiled-coil domains (aa 287-317, 341-388) and two PEST motifs (aa 410-422, 426-450). Like Nek11S, Nek11c lacks the third PEST motif present in Nek11L (aa 466-501) (Figure 1.13).

**A**

```

1  MDDYMLRMI GECSFORALLVQHESSNQMFAMKEIRLPKSFSTQNSRKEAVLLAKMKHP 60
61  NIVAFKESFEAEGLHYIVMEYCDGGDLMQIKQKQKGLFPEDMILNWFQMLGVNHIHK 120
121  KRVLHRDIKSKNIFLTQNGKVKLGDGFSARLLSNPMAFACTYVGTPTYVPEIWNLPYN 180
181  NKSDIWSLGCILYELCTLKHPFQANSWKNLILKVCQGCISPLPSHYSYELQFLVKQMFKR 240
241  NPSHRPSATLLSRGIVARLVQKCLPPEI IMEYGEVLEEIKNSKHNTPRKKINPSRIRI 300
301  ALGNEASTVQEEEQDRKGSHTDLESINENLVESALRRVNRREEKGNKSVHLRKASSPNLHR 360
361  RQWEKNVPNTALTALENASILTSSLTAEDDRGGSVIKYSKNTTRKQWLKETPDTLLNLIK 420
421  NADLSLAFQTYTYIRPGSEGF LKGPLSEETEASDSVDGGHDSVILDPERLEPLGDEEDTD 480
481  FEEEDDNPDWVSELKKRAGWQGLCDR 506

```

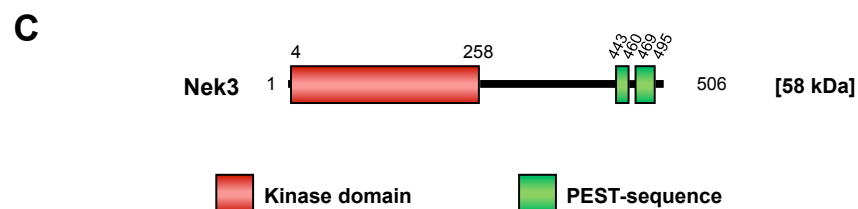
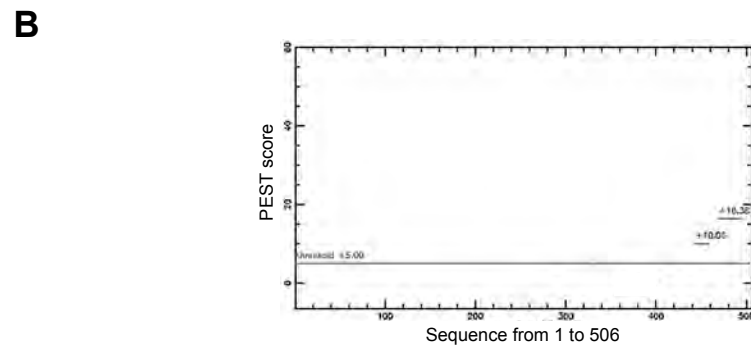


**Figure 1.10 Structural features of human Nek3**

**(A)** Amino acid sequence of human Nek3, a 506-amino acid protein. Amino acid residue numbers are shown. The protein kinase domain is boxed. Amino acid residues that have been underlined are sites that have been mutated to create a kinase-inactive mutant. **(B)** Identification of PEST sequences (<http://mobyli.pasteur.fr/cgi-bin/portal.py?form=epestfind>); only sequences that scored above +5 were included as putative PEST sequences. **(C)** A schematic view of the Nek3 structure, showing the kinase domain and PEST sequences, and predicted molecular weight.

**A**

```

1 MDKVDVIRKAIQGQAFGKAYLAKGKSDSKHCVIKEINFEKMPIQEKEASKKEVILLEMKH 60
61 PNIVAFFNSFQENGRLFIVMEYCDGGDLMKRINRQGVLFSEDDQILGWVQISLQLKHTH 120
121 DRKILHRDIKAQNIFLSKNGMVAKLGDFGIARVLNNSMELARTCIGTPYYLSPEICQNKP 180
181 YNNKTDIWSLGCVLVELCTLKHPFEGNNLQQVLVKICQAHFAPISPGFSRELHSLISQLF 240
241 QVSPDRRPSINSILKRPFLENLIPKYLTPEVIQEESHMLICRAGAPASRHAGKVVQKCK 300
301 IQKVRVFGKCPFRSRISVPIKRNAILHRNEWRPAGAQAQKARSIKMIERPKIAAVCGHYDY 360
361 YYAQLDMLRRRAHKPSYHIPQENTGVEDYGGQETRHGSPSPQWPAEYLQRKFEAQYKLLK 420
421 VEKQLGLRPSSAEPNYNQRQELRSNGEPRFQELPFRKNEMKEQYWKQLEEIRQQYHND 480
481 MKEIRKKMGREPEENSKISHKTYLVKKSNLPHQDASEGEAPVQMEFRSCCPGWSAMARS 540
541 WLTATSASQDIEKDLKQMLQNTKESYNPEQKYAKKGVKFEINLDKCISDENILQEEEA 600
601 MDIPNETLTFEDGMKFKKEYECVKEHGDYTDKAFKELHCEAGFSTQIVAAVGNRRQWDGG 660
661 APQILLQMAVADITSICPTGPDSSEVLSVSRQEGKTKDPYSPVLILM 708

```

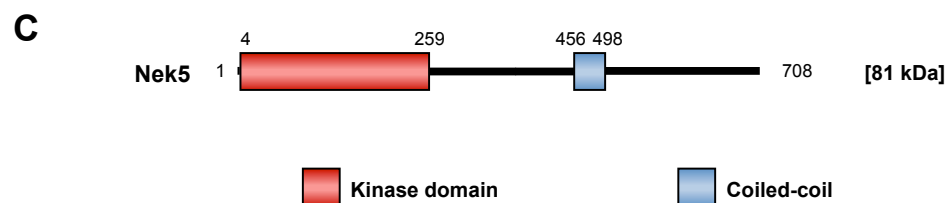
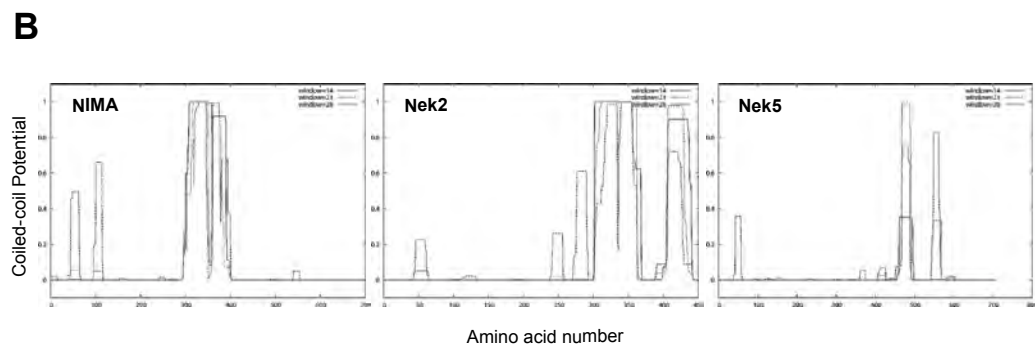


**Figure 1.11 Structural features of human Nek5**

(A) Amino acid sequence of human Nek5, a 708-amino acid protein. Amino acid residue numbers are shown. The protein kinase domain is boxed and its subdomains are shown in Roman numerals. Amino acid residues that have been underlined are sites that have been mutated to create a kinase-inactive mutant. (B) Diagram of the coiled-coil conformation probability calculated for Nek5 protein, and for comparison, NIMA and Nek2 proteins, using the COILS program (<http://www.isrec.isb-sib.ch/software/software.html>). (C) A schematic view of the Nek5 structure, showing the kinase domain and single strongest predicted coiled-coil region, and predicted molecular weight.

```

Nek11L 1 MLKFQEAARKCVSGSTAISTYFKTLIARRYVLQQKLGSGSFGIVVYLVSDKKAKRGEELKVL
Nek11S 1 .....
Nek11c 1 .....

Nek11L 61 KEISVGEINFNETVQANLEAQLLSKLDHPAIVKFHASFVEQDNFCIIITEYCEGRDLDDKI
Nek11S 61 .....
Nek11c 61 .....

Nek11L 121 QEYKQAGKIFPENQIIENFIQLLGVDYMHERRILHRDLKSKNVFLKNNLLKIGDFGVSR
Nek11S 121 .....
Nek11c 121 .....

Nek11L 181 LLMGSCDLATTLTGTPHYMSFEALKHQGYDTKSDIWSLACILYEMCCMNHAFAGSNFLSI
Nek11S 181 .....
Nek11c 181 .....

Nek11L 241 VLKIVEGDTPSLPERYPKELNAIMESMLNKNPSLRPSAIEILKIPYLDEQLQNLMCRYSE
Nek11S 241 .....
Nek11c 241 .....

Nek11L 301 MILEDKNLDCQKEAAHIINAMQKRIHLQTLRALSEVQKMTPPRERMLRKLQAADEKARKL
Nek11S 301 .....
Nek11c 301 .....

Nek11L 361 KKIVEEKYEENSKRMQELRSRNFQQLSVDVLHEKTHLKGMEEKEEQPEGRLSCSPQDEDE
Nek11S 361 .....
Nek11c 361 .....

Nek11L 421 ERWQGREEESEDEPTLENLPESQPIPSMDLHELESIVEDATSDLGYHEIPEDPLVAEYYA
Nek11S 421 .....ATHS
Nek11c 421 .....GDCNLISLD.YWKN

Nek11L 481 DAFDSYCVESDEEEEEIALERPEKEIRNEGSQPAYRTNQQDSDIEALARCLENVLGCTSL
Nek11S
Nek11c 481 EK

Nek11L 541 DTKTITTMAEDMSFGPPIFNSVMARTKMKRMRESAMQKLGTEVFEEVYNYLKRARHQNAS
Nek11S
Nek11c

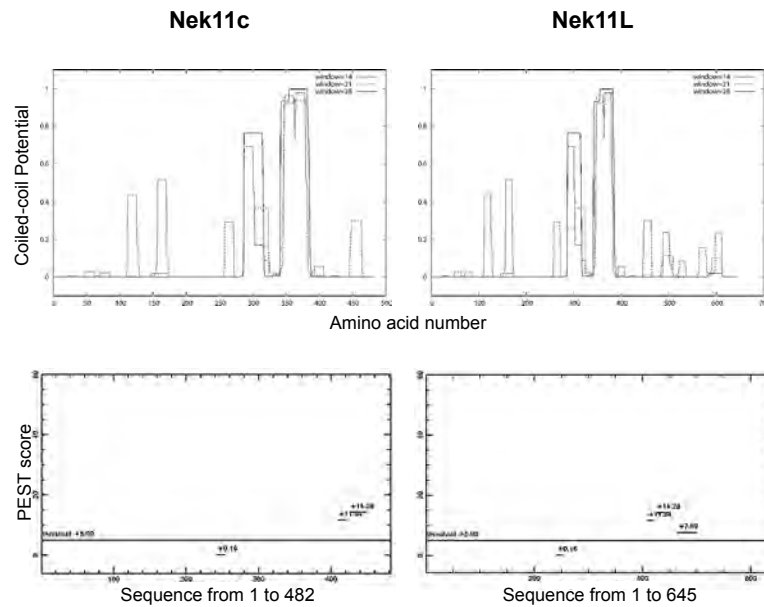
Nek11L 601 EAEIRECLEKVVFPQASDCFEVDQLLYFEEQLLITMGKEPTLQNHL
Nek11S
Nek11c

```

**Figure 1.12 Alignment of Human Nek11 isoforms**

Amino acid sequence alignment of Nek11 short (S) and long (L) isoforms with the sequence for the Nek11 clone (c) used in the project. Nek11c is a 482-amino acid protein. Amino acid residue numbers are shown and, where sequences are identical, the lower two sequences are simply indicated with dots. The protein kinase domain is boxed. Amino acid residues that have been underlined are sites that have been mutated to create a kinase-inactive mutant.

**A**



**B**

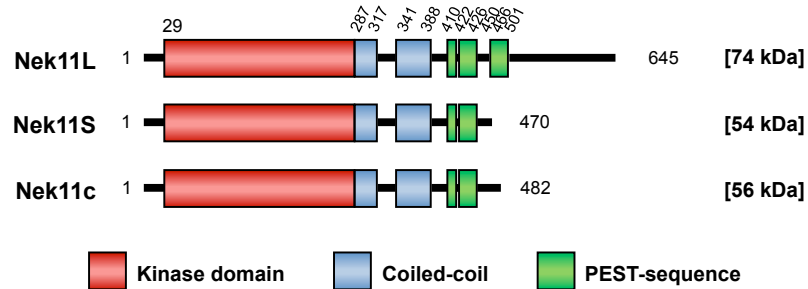


**Figure 1.13 Structural features of human Nek11**

**(A)** Diagram of the coiled-coil conformation probability calculated for the Nek11c and Nek11L proteins, using the COILS program (<http://www.isrec.isb-sib.ch/software/software.html>). Putative PEST sequences have also been identified (<http://mobyli.pasteur.fr/cgi-bin/portal.py?form=epestfind>) for these proteins. **(B)** A schematic view of the protein structures of the three Nek11 isoforms. The kinase domains, predicted coiled-coil regions and putative PEST sequences are shown, together with their predicted molecular weights.

## **Chapter 2**

### **Materials and Methods**

## 2.1 Materials

### 2.1.1 Suppliers and manufacturers

All chemicals were of analytical grade purity or higher and supplied by Sigma-Aldrich, Roche (Lewes, UK), or as stated below. All cell culture solutions were supplied by Gibco Invitrogen (Paisley, UK).

Reagent	Supplier
CNBr activated sepharose	Amersham (Buckinghamshire, UK)
Poly-prep columns Precision Plus all blue protein standards	Bio-rad (Hemel Hempstead, UK)
Hoechst 33258 Leptomycin B	Calbiochem (Nottingham, UK)
siRNA oligonucleotides	Dharmacon (Lafayette, USA)
GeneRuler 1 kb DNA ladder PageRuler Plus prestained protein ladder	Fermentas (York, UK)
Glacial acetic acid EDTA; EGTA; NaCl; KCl; Na <sub>2</sub> HPO <sub>4</sub> ; KH <sub>2</sub> PO <sub>4</sub> Ethanol Methanol	Fisher Scientific (Loughborough, UK)
ProtoFLOWgel (30% w/v acrylamide)	Flowgen Bioscience (Nottingham, UK)
Bovine serum albumin (fraction V)	Fluka (Gillingham, UK)
Super RX X-Ray film	Fuji Photo Film (Tokyo, Japan)
Ethidium Bromide GeneTailor site directed mutagenesis kit dNTP Mix (dATP, dCTP, dGTP, dTTP) Taq DNA polymerase SuperScript III reverse transcriptase NI-NTA agarose Dynabeads Protein G Oligonucleotide primers Lipofectamine 2000 Oligofectamine	Invitrogen/Gibco (Paisley, UK)
Rosetta 2 (DE3) <i>E. coli</i> competent cells	Novagen (Nottingham, UK)
Bacto-agar Bacto-tryptone Yeast extract	Oxoid (Basingstoke, UK)
ECL Western blotting reagent Coomassie (Bradford) protein assay reagent	Pierce (Rockford, USA)
TNT T7 quick coupled transcription/translation kit	Promega (Southampton, UK)
Skimmed milk powder (Marvel)	Premiere Beverages (Stafford, UK)
QIAfilter plasmid miniprep spin kit QIAfilter plasmid maxiprep kit	Qiagen (Hilden, Germany)

QIAquick PCR purification kit	
Nitrocellulose transfer membrane	Schleicher & Schuell (Dassel, Germany)
Histone H1 His <sub>6</sub> Nek3 His <sub>6</sub> Nek11	Upstate (Millipore) (Dundee, UK)
3MM chromatography paper	Whatman International (Maidstone, UK)

## 2.1.2 Radioisotopes

Isotope	Specific Activity	Supplier
[ <sup>35</sup> S]-methionine	43.5 Tbq/mmol	NEN Life Sciences Products
[γ- <sup>32</sup> P]-ATP	167 Tbq/mmol	Perkin Elmer

## 2.1.3 Vectors

Vector	Application	Supplier
pETM-11	Bacterial protein expression	EMBL
pFLAG-CMV-2	Eukaryotic expression vector	Sigma
pEGFP-T7	Eukaryotic expression vector	Fry lab

## 2.1.4 Antibodies

### 2.1.4.1 Primary antibodies

Antibody	Dilution ([Ab])*	Supplier
Anti-FLAG (mouse) <i>Clone M2; F3165</i>	1:1000 (5 µg/ml)	Sigma
Anti-FLAG (rabbit) <i>F7425</i>	1:500 (2 µg/ml)	
Anti-γ-tubulin (mouse) <i>Clone GTU-88; T6557</i>	1:1000	
Anti-γ-tubulin (rabbit) <i>T3559</i>	1:1000	
Anti-acetylated tubulin (mouse) <i>Clone 6-11B-1; T6793</i>	1:1000 (1 µg/ml)	
Anti-α-tubulin (mouse) <i>Clone B-5-1-2; T5168</i>	1:2000 (0.3 µg/ml)	
Anti-HIS (mouse) <i>Clone HIS-1; H1029</i>	1:1000	

Anti-GFP (mouse) <i>Clone GFP-20; G6539</i>	1:500 (0.25 µg/ml)	
Anti-α-tubulin (rabbit) <i>ab15246</i>	1:200	Abcam
Anti-GFP (rabbit) <i>ab6556</i>	1:1000 (0.5 µg/ml)	
Anti-Nek2 (mouse) <i>Clone 20; 610594</i>	1:100 (2.5 µg/ml)	BD Biosciences
Anti-C-Nap1 (mouse) <i>Clone 42; 611374</i>	1:1000 (0.25 µg/ml)	
Anti-Nek3 (mouse) <i>H00004752-P01</i>	1:500 (1 µg/ml)	Abnova
Anti-Nek5 (rabbit)	1:500 (2 µg/ml)	This study
Anti-Nek11 (rabbit)	1:250 (2 µg/ml)	

\*Where known, final antibody concentrations are stated in brackets after the working dilution

#### 2.1.4.2 Secondary antibodies

Antibody	Dilution ([Ab])*	Supplier
Anti-mouse horseradish peroxidase conjugate <i>A4416</i>	1:1000	Sigma (Poole, UK)
Anti-rabbit horseradish peroxidase conjugate <i>A6154</i>	1:1000	
Anti-mouse Alexa 488 nm <i>A-11001</i>	1:200 (10 µg/ml)	Invitrogen (Paisley, UK)
Anti-rabbit Alexa 488 nm <i>A-11008</i>	1:200 (10 µg/ml)	
Anti-mouse Alexa 594 nm <i>A-11005</i>	1:200 (10 µg/ml)	
Anti-rabbit Alexa 594 nm <i>A-11012</i>	1:200 (10 µg/ml)	

\*Where known, final antibody concentrations are stated in brackets after the working dilution

## **2.2 Molecular biology techniques**

### **2.2.1 Cloning**

A basic cloning procedure was followed involving amplification of insert DNA by polymerase chain reaction (PCR), restriction digestion of purified PCR products and destination vector, and then ligation of the two under appropriate conditions as outlined below. A PCR screening approach was then employed to identify colonies likely to contain plasmid with insert DNA, after which DNA was prepared from bacterial cultures in the appropriate manner. The specific details of each stage are described below.

#### **2.2.1.1 Oligonucleotide design**

Oligonucleotides for PCR-based cloning were designed to be 18-24 nucleotides in length with a GC:AT ratio of ~50%, thus ensuring a practical annealing temperature of around 55-60°C. To incorporate appropriate restriction enzyme sites for cloning, additional bases were added to the 5' end of the primer sequences with extra bases added in to ensure the maintenance of the correct reading frame upon insertion into the destination vector, as necessary. A GC clamp (4 bases), was added 5' to the restriction site sequence to allow for efficient digestion.

#### **2.2.1.2 Polymerase chain reaction**

To obtain insert DNA for cloning, PCR amplification was carried out using Expand high fidelity proof-reading DNA polymerase (Roche). A standard reaction mixture was 50 µl in volume and typically contained ~12.5 ng template DNA, 400 nM forward primer, 400 nM reverse primer, 1x PCR amplification buffer, 1.5 mM MgCl<sub>2</sub>, 0.2 mM dNTPs, 2.6 U DNA polymerase and the appropriate volume of water to complete reaction volume. Annealing temperatures and elongation times suitable for each set of primers and template, respectively, were employed as appropriate, however the basic PCR

reaction consisted of one cycle of denaturation at 94°C for 2 mins, followed by 25 cycles of denaturation at 94°C for 30 secs, annealing at the appropriate temperature for 30 secs and elongation at 72°C for the appropriate extension time (1 min per kb), followed by one cycle of extension at 72°C for 7 mins. PCR products were then analysed by agarose gel electrophoresis to assess yield.

#### **2.2.1.3 Agarose gel electrophoresis**

DNA was combined with loading buffer (50% v/v glycerol, 0.1 M EDTA, 0.3% v/v bromophenol blue) in a 5:1 ratio and resolved by electrophoresis on a 1% (w/v) agarose gel made by dissolving agarose in 1x TBE (89 mM Tris, 89 mM Boric acid, 2 mM EDTA pH 8.0) supplemented with ethidium bromide (0.5 µg/ml). Electrophoresis was carried out at 80 V for 45 mins after which resolved DNA was analysed by UV transillumination (302 nm) and images captured using a GeneGenius gel imaging system (Syngene).

#### **2.2.1.4 Purification of PCR products for cloning**

Upon verification that the PCR reaction had been successful and sufficient product of the appropriate size obtained, PCR products were purified for cloning using a QIAquick PCR purification kit (QIAGEN) according to the manufacturer's instructions. Purified DNA was eluted in 20-30 µl of sterile water and product yield assessed by agarose gel electrophoresis.

#### **2.2.1.5 Restriction enzyme digest and purification**

Purified insert DNA and destination vectors were digested with the appropriate restriction enzymes using suitable buffer conditions and temperature, as specified by the manufacturer. Typically, 2 µg of DNA was incubated with 1 U of restriction endonuclease and appropriate buffer at 37°C for 2 hrs. Following digestion, the destination vector was dephosphorylated to prevent self-ligation. The 5' phosphates of the linearised vector were removed by incubating the

entire vector reaction volume (40  $\mu$ l) with 4 U Shrimp Alkaline Phosphatase (Roche) in 1x dephosphorylation buffer and sterile water to complete the reaction volume to 50  $\mu$ l, for 15 mins at 37°C. The total reaction volumes of digested insert DNA and digested, dephosphorylated destination vector were then purified using the QIAquick PCR purification kit as described in section 2.2.1.4 above. DNA yield was assessed by agarose gel electrophoresis in order to assess DNA concentrations for ligation.

#### **2.2.1.6 DNA ligation**

Ligation reactions were carried out using a rapid DNA ligation kit (Roche). Typically a vector:insert molar ratio of 1:3 was employed in a standard reaction mix of 75 ng vector DNA, 150 ng insert DNA and 5 U DNA ligase diluted in the appropriate volume of ligation buffer. Reactions were incubated 15 mins at room temperature.

#### **2.2.1.7 Bacterial transformation**

For cloning, 100 ng of ligated DNA was added to 100  $\mu$ l of DH5 $\alpha$  competent cells, which had been thawed on ice, and the two were mixed by gently tapping the side of the tube. The mix was incubated on ice for 10 mins, heat shocked at 42°C for 45 secs to induce plasmid DNA uptake, and then returned to the ice for a further 2 mins. 900  $\mu$ l of Luria Broth (LB) media (1% w/v NaCl, 1% w/v tryptone, 0.5% w/v yeast extract) was added to the cells and the transformation mix was incubated for 1 hr at 37°C, 225 rpm. Following incubation, 100  $\mu$ l of the cell suspension was spread onto LB agar plates (LB plus 2% w/v agar) containing the appropriate antibiotic for selection (ampicillin at 100  $\mu$ g/ml, chloramphenicol at 34  $\mu$ g/ml or kanamycin at 50  $\mu$ g/ml, as appropriate). Plates were incubated for 16 hrs at 37°C, and then colonies picked for insert screening by PCR and plasmid preparation.

#### **2.2.1.8 DNA insert verification**

PCR screening of colony DNA was used to verify the presence of appropriate DNA insert using Taq DNA polymerase (Invitrogen). A standard reaction mixture was 20 µl in volume and typically contained 0.5 µM forward primer, 0.5 µM reverse primer, 1x PCR amplification buffer plus MgCl<sub>2</sub>, 0.2 mM dNTPs, 2.5 U DNA polymerase and the appropriate volume of water to complete reaction volume. Colonies to be screened were picked and cells added to the PCR reaction mix. PCR reaction cycles were as described above in section 2.2.1.2. Colonies which proved positive by PCR screen were then grown up for DNA isolation and further insert verification by DNA sequencing.

#### **2.2.1.9 Isolation of plasmid DNA by DNA miniprep**

Individual bacterial colonies were picked off LB agar plates, inoculated into 5 ml LB containing the appropriate antibiotic and incubated for 16 hrs at 37°C, 250 rpm. Following incubation, cells were recovered by centrifugation (2000 rpm, 10 mins) and DNA was isolated using the QIAprep Spin Miniprep kit (QIAGEN) according to the manufacturer's instructions. DNA was eluted into 50 µl of sterile water.

#### **2.2.1.10 DNA sequencing**

Automated DNA sequencing was employed to verify the presence of the appropriate insert and the correct reading frame. This was carried out by the Protein Nucleic Acid Chemistry Laboratory (PNAACL, Leicester).

#### **2.2.2 Isolation of plasmid DNA by DNA maxiprep**

For isolation of large quantities of ultrapure transfection grade plasmid DNA, DNA plasmid maxipreps were used. Starter cultures were made by inoculating 5 ml LB containing the appropriate antibiotic and incubating for 8 hrs at 37°C, 250 rpm. These were used to inoculate 100 ml LB + antibiotic at a dilution of

1:500 which were likewise grown at 37°C, 250 rpm for 16 hrs. Cells were then harvested by centrifugation at 6000 xg for 15 mins at 4°C before plasmid DNA was isolated using a QIAfilter™ Plasmid Maxi kit (QIAGEN) according to the manufacturer's instructions. Isolated plasmid DNA was resuspended in 500 µl water and DNA concentration was determined by measuring OD<sub>260</sub>.

## **2.2.3 Site-directed mutagenesis**

### **2.2.3.1 Oligonucleotide design**

Primers for site-directed mutagenesis were approximately 30 nucleotides in length. The forward primer consisted of an overlapping region of ~20 bases 5' of the mutation site, the mutation site, and an extended region of at least 10 bp 3' of the mutation site. The reverse primer consisted of a region overlapping the forward primer from the mutation site to the 5' end of the forward primer and extended beyond this for a further ~10 bp.

### **2.2.3.2 Site-directed mutagenesis reaction**

To induce nucleotide changes in plasmid DNA, the Genetailor™ Site-Directed Mutagenesis System (Invitrogen) was used according to the manufacturer's instructions. In brief, 100 ng of target plasmid was methylated by incubation with 8 U of DNA methylase in appropriate buffer conditions for 1 hr at 37°C. Methylated DNA was then amplified by PCR with appropriate mutagenesis primers at a final concentration of ~12.5 ng in a reaction mix containing 300 nM each forward and reverse primer, 0.3 mM dNTPs and 2.6 U Expand DNA polymerase in appropriate buffer conditions. The PCR amplification cycle consisted of denaturation at 94°C for 2 mins, followed by 25 cycles of denaturation at 94°C for 30 secs, annealing at 55°C for 30 secs and elongation at 68°C for 1 min/kb template DNA, and a final elongation step of 68°C for 10 mins. Amplification was confirmed by agarose gel electrophoresis, following which plasmid DNA was transformed into DH5α-T1<sup>R</sup> *E. coli* and transformants containing plasmid DNA selected on appropriate selective media. Individual

transformants were selected, plasmid DNA was isolated and the mutation was verified by DNA sequencing.

#### **2.2.4 RT-PCR**

Total RNA was prepared as described in section 2.6.7 and used for first strand cDNA synthesis with Superscript III reverse transcriptase (Invitrogen) according to the manufacturer's instructions. Briefly, 5 µg RNA was used in a reaction containing 25 ng oligo(dT)<sub>12-18</sub>, 0.5 mM dNTPs, 5 mM DTT, 2 U Recombinant RNase inhibitor and 10 U Superscript III reverse transcriptase. RNA was denatured by incubation at 65°C for 5 mins after which first strand synthesis was carried out at 50°C for 1 hour. The reaction was inactivated by heating at 70°C for 15 mins. 25% of the first strand reaction was then used in the PCR reaction mixture, 25 µl total volume, containing 1.5 mM MgCl<sub>2</sub>, 0.2 mM dNTPs, 0.8 µM each forward and reverse primer and 1 U *Taq* DNA polymerase (Invitrogen). Annealing temperatures suitable for the primers used were employed as appropriate, however the basic PCR reaction consisted of one cycle of denaturation at 94°C for 2 mins, followed by 35 cycles of denaturation at 95°C for 1.5 mins, annealing at the appropriate temperature for 2 mins and elongation at 72°C for 1 min, followed by one cycle of extension at 72°C for 10 mins. PCR products were then analysed by agarose gel electrophoresis to assess yield as described in section 2.2.1.3.

### **2.3 Protein analysis techniques**

#### **2.3.1 SDS-PAGE**

Protein samples were resolved on 12% discontinuous polyacrylamide gels that had been cast using the Mini-PROTEAN 3 polyacrylamide gel electrophoresis (PAGE) system (Bio-Rad). Resolving gel (40% ProtoFLOWgel (30% w/v acrylamide), 375 mM Tris-HCl pH 8.8, 0.10% w/v SDS, 0.13% w/v APS, 0.08% v/v TEMED) was overlaid with stacking gel (13% ProtoFLOWgel (30% w/v acrylamide), 126 mM Tris-HCl pH 6.8, 0.10% w/v SDS, 0.15% w/v APS, 0.10%

v/v TEMED). Samples to be resolved were mixed with an appropriate volume of 3x Laemmli buffer (62.5 mM Tris-HCl pH 6.8, 10% v/v glycerol, 2% w/v SDS, 5% v/v  $\beta$ -mercaptoethanol, 0.01% w/v bromophenol blue) and denatured at 95°C for 5 mins. Electrophoresis was carried out at a standard of 180 V for ~1 hr using an SDS-running buffer (1% w/v SDS, 3% w/v Tris, 14.4% w/v glycine). Polyacrylamide gels were then further analysed by Coomassie Blue staining or Western blotting.

### **2.3.2 Coomassie Blue staining**

To directly visualise proteins after electrophoretic separation, resolving gels were submerged in Coomassie Blue solution (0.25% w/v Coomassie Brilliant Blue, 40% v/v IMS, 10% v/v Acetic acid) and then gently agitated for at least 20 mins at room temperature. The Coomassie Blue solution was then decanted and protein bands were distinguished by repeated washes in destain solution (25% v/v IMS, 7.5% v/v Acetic acid) until the background was clear. Gels were then dried onto 3 MM paper (Whatmann) under a vacuum at 80°C as appropriate. Radiolabelled proteins were visualised by autoradiography where necessary.

### **2.3.3 Western blotting**

Using semi-dry electrophoretic blotting, resolved proteins were transferred to nitrocellulose membrane for immunodetection. Briefly, the resolving gel, nitrocellulose membrane (Schleicher and Schuell), and 3MM chromatography paper were soaked in Western blotting transfer buffer (25 mM Tris, 192 mM glycine, 10% v/v methanol) before being sandwiched together in a TE 77 semi-dry transfer unit (Amersham), as directed by the manufacturer. Transfer was carried out for 1 hour at 1 mA/cm<sup>2</sup> membrane. Following transfer, equality of loading was visualised by ponceau red stain solution (0.1% w/v Ponceau S, 5% v/v acetic acid) and the position of size markers and lanes marked. Prior to immunoblotting, membranes were incubated in 5% w/v non-fat milk powder in PBST [0.1% v/v Tween-20 in PBS (137 mM NaCl, 2.7 mM KCl, 8.1 mM

$\text{Na}_2\text{HPO}_4$ , 1.4 mM  $\text{KH}_2\text{PO}_4$ )] for 30 mins to block non-specific antibody binding. The blocked membrane was then incubated with primary antibody at the appropriate dilution in 5% non-fat milk powder/PBST for 1 hour at room temperature or overnight at 4°C. Membranes were then washed three times in PBST to remove unbound antibody before being incubated with the horseradish peroxidase-conjugated secondary antibody for a further 1 hour at room temperature. Membranes were then washed a further three times to remove unbound secondary antibody, after which they were developed in enhanced chemiluminescence (ECL) Western blotting detection solution (Pierce), and the proteins visualised by autoradiography on X-ray film.

#### **2.3.3.1 Quantification of Western blot band intensities**

For comparative quantification of protein band intensities on Western blots, Adobe Photoshop software was used. Briefly, autoradiographs in which protein exposures were judged to be in the linear phase were scanned and Adobe Photoshop used to select a region of interest (to encompass the largest band to be analysed) and mean pixel intensity within this region of interest calculated for each band to be analysed, with background intensity subtracted.

#### **2.3.4 *In vitro* translation**

The TNT T7 quick coupled transcription/translation system was used to verify the expected molecular weight of proteins synthesised from plasmid constructs. Briefly, 1 µg plasmid DNA was incubated with 2 µl [ $^{35}\text{S}$ ]-labelled methionine (10 mCi/ml stock) and 8 µl T7 Quick Master Mix (Promega) for 90 mins at 30°C. The *in vitro* translated radiolabelled protein was visualised by autoradiography following SDS-PAGE and Coomassie Blue staining.

### **2.3.5 Immunoprecipitation**

Immunoprecipitation experiments were carried out on whole cell lysates (see section 2.6.6 for cell lysis) using the mouse GFP monoclonal antibody bound to Dynabeads Protein G (Invitrogen). Briefly, 50  $\mu$ l of washed Protein G beads was incubated in 100  $\mu$ l of GFP (mouse) antibody solution (20  $\mu$ g antibody in PBS) for 40 mins with gentle mixing after which the antibody solution was removed. After washing the beads again to remove unbound antibody, 1 mg cell lysate in NEB buffer (50 mM HEPES-KOH pH 7.4, 5 mM  $MnCl_2$ , 10 mM  $MgCl_2$ , 5 mM EGTA, 2 mM EDTA, 100 mM NaCl, 5 mM KCl, 0.1% v/v NP-40, 30  $\mu$ g/ml RNase A, 30  $\mu$ g/ml DNase I, 1 mM PMSF, 5 mM  $\beta$ -glycerophosphate, 5 mM NaF, 1x Protease inhibitor cocktail (PIC) (Sigma)) was added and rotated for 1 hr at 4°C. Beads were then prepared for further analysis by washing 3x in PBS.

### **2.3.6 *In vitro* kinase assays**

Kinase assays were carried out using either 10  $\mu$ l washed immune complex beads, prepared as described above, or 0.1  $\mu$ g of purified kinase. Briefly, proteins were incubated with 5  $\mu$ g of the appropriate substrate and 1  $\mu$ Ci of [ $\gamma$ - $^{32}P$ ]-ATP in 40  $\mu$ l kinase buffer (50 mM Hepes-KOH pH 7.4, 5 mM  $MnCl_2$ , 5 mM  $\beta$ -glycerophosphate, 5 mM NaF, 4  $\mu$ M ATP, 1 mM DTT) for 30 mins at 30°C. Reactions were stopped by addition of 50  $\mu$ l 3x Laemmli buffer and analysed by SDS-PAGE and autoradiography. In order to pre-activate purified kinase for *in vitro* kinase assays, the reaction was incubated for 30 mins at 30°C, prior to and after the addition of 1  $\mu$ Ci of [ $\gamma$ - $^{32}P$ ]-ATP.

## **2.4 Bacterial protein expression and purification**

### **2.4.1 Protein expression in *E. coli***

To generate His-tagged antigens for antibody production, Nek5 and Nek11 DNA fragments (corresponding to amino acid residues 505-708 for Nek5, and

residues 288-446 for Nek11) were amplified by PCR and inserted into the pETM-11 bacterial expression vector as described in section 2.2.1. Plasmids were transformed into *E. coli* Rosetta 2(DE3) cells (Novagen). Briefly, 1  $\mu$ g DNA was added to 50  $\mu$ l of chemically competent Rosetta cells, which had been thawed on ice, and the two were mixed by gently tapping the side of the tube. The mix was incubated on ice for 5 mins, heat shocked at 42°C for 30 secs to induce plasmid DNA uptake, and then returned to the ice for a further 2 mins. 250  $\mu$ l of LB media was added to the cells and the transformation mix was incubated for 1 hr at 37°C, 225 rpm. Following incubation, 100  $\mu$ l of the cell suspension was spread onto LB agar plates containing the appropriate antibiotics for selection (chloramphenicol at 34  $\mu$ g/ml and kanamycin at 50  $\mu$ g/ml). Plates were incubated for 16 hrs at 37°C. Individual colonies were used to inoculate cultures of LB supplemented with the appropriate antibiotics (chloramphenicol at 34  $\mu$ g/ml and kanamycin at 50  $\mu$ g/ml). Cultures were grown at 37°C, 225 rpm until an OD<sub>600</sub> of ~0.5 was reached. The temperature was then adjusted to 22°C and expression was induced using 0.1 mM IPTG for 18 hrs, 180 rpm. Cells were then collected by centrifugation at 4000 xg for 20 mins and the recombinant protein purified.

#### **2.4.2 Recombinant protein purification**

Following harvesting by centrifugation, bacterial cells were resuspended in lysis buffer (50 mM NaH<sub>2</sub>PO<sub>4</sub>, 300 mM NaCl, pH 8.0) supplemented with 10 mM imidazole, 2 mM DTT, and 1x PIC. The cells were lysed by incubation on ice for 30 mins with lysozyme (1 mg/ml), followed by sonication on ice (MSE Soniprep 150, 10 mm probe, amplitude 12  $\mu$ m) using 9 cycles of 60 secs sonication followed by 10 secs cooling. The lysates were then clarified by centrifugation at 16000 rpm for 1 hr at 4°C. The cleared lysates were stored at -80°C or immediately mixed with 1 ml Ni-NTA agarose slurry (Invitrogen) and rotated at 4°C for 1 hr. The lysate-bead slurry was then loaded onto a column and subjected to two rounds of washing with lysis buffer supplemented with 20 mM imidazole. Bound protein was then eluted in lysis buffer supplemented with

250 mM imidazole in several 500  $\mu$ l fractions. Protein recovery was determined by SDS-PAGE and Coomassie Blue analysis of aliquots of each fraction and those containing highest protein levels were pooled.

### **2.4.3 Quantification of protein concentration**

Total protein content of purified elutions, and also mammalian cell lysates (section 2.6.6), was determined using the Coomassie (Bradford) protein assay reagent (Pierce), which exploits the quantitative colorimetric interaction of the acidic environment of the reagent and protein peptide bonds. Typically, 5  $\mu$ l of the protein solution (or appropriate dilutions of the protein solution) were incubated with 1 ml of Coomassie reagent for 10 mins at room temperature. Then  $A_{595}$  was measured alongside BSA standards of known concentrations so that a standard curve could be generated from which the protein concentration of each unknown sample could be determined.

SDS-PAGE and Coomassie Blue analysis of the pooled purified recombinant protein antigen fractions (section 2.4.2) was also used to determine the total protein concentration by comparison against BSA standards on a gel.

## **2.5 Antibody generation and purification**

### **2.5.1 Antibody generation**

For production of anti-Nek5 and anti-Nek11 antibodies, pre-selected rabbits were immunised by Cambridge Research Biochemicals with 2 mg of purified recombinant protein antigens (section 2.4). Rabbit bleeds were screened for reactivity against recombinant and endogenous Nek5 and Nek11 by Western blotting of HEK293 whole cell lysates and immunofluorescence microscopy of methanol-fixed U2OS cells as described in sections 2.3.3 and 2.7, respectively.

## **2.5.2 Affinity purification of antibodies**

Antibodies were affinity purified using the Nek5 or Nek11 peptides against which the antibodies were raised, covalently bound to a CNBr activated sepharose column, made according to the manufacturer's instructions (Amersham). Briefly, ~5 mg of peptide was coupled to 1 ml of swollen CNBr activated sepharose beads by incubation in coupling buffer (0.2 M NaHCO<sub>3</sub>, 0.5 M NaCl pH 8.5) and after several washes, 2 ml of the final bleed antisera (diluted 1:5 in 10 mM Tris pH 7.5) was passed over the peptide column. Specific antibodies were eluted under low pH conditions with 100 mM glycine pH 2.5 and then high pH conditions with 100 mM Triethylamine (TEA) pH 11.5 into tubes containing neutralising quantities of 1 M Tris-HCl pH 8.0. Abundance of antibodies was assessed by SDS-PAGE and Coomassie Blue staining, after which the specificity of the affinity purified antibodies was assessed by Western blot and immunofluorescence microscopy, as described (sections 2.3.3 and 2.7, respectively).

## **2.6 Mammalian cell culture techniques**

### **2.6.1 Maintenance of human cell lines**

All cell lines were maintained in a humidified 5% CO<sub>2</sub> atmosphere at 37°C and passaged upon reaching ~80% confluency. To passage, growth media was aspirated off adherent cell populations, cells were washed in 1x PBS and harvested by either incubation in 1x PBS supplemented with 0.5 mM EDTA, or by incubation in Trypsin/EDTA (Invitrogen), according to the cell line. Cells were then seeded into fresh, pre-warmed growth media at the appropriate density. HEK293, U2OS, HeLa and HeLa-GFP-centrin, as well as colorectal (SW620, SW480, HT29, HCT116), breast (HBL100) and pancreatic (MIA-Pa-Ca-2, Panc-1) cancer cell lines were cultured in Dulbecco's Modified Eagle's medium (DMEM) (Invitrogen). Other breast (MDA-MB-468) and pancreatic (AsPc, BxPc-3) cancer cell lines were cultured in RPMI 1640 media (Invitrogen). hTERT-RPE1 cells were cultured in DMEM/Ham's F12 (1:1) supplemented with 0.348% sodium bicarbonate solution. All cell lines were supplemented with

10% v/v heat inactivated foetal bovine serum (FBS) and penicillin-streptomycin (Pen/Strep) (100 U/ml and 100 µg/ml, respectively).

### **2.6.2 Storage of human cell lines**

For long-term storage, cell lines were cryopreserved in liquid nitrogen. Briefly, cells were washed and harvested before being collected by centrifugation (1100 rpm, 5 mins). After a second wash, cells were resuspended in FBS supplemented with 10% v/v DMSO and transferred to cryotubes for freezing in steps (-20°C overnight; -80°C overnight; liquid nitrogen).

### **2.6.3 Transient transfection of mammalian cells**

Transient transfection of cultured mammalian cells to induce expression of appropriate recombinant proteins was achieved using Lipofectamine 2000 (Invitrogen) with U2OS and hTERT-RPE1 cells or Fugene HD (Roche) with HEK293 cells, according to the manufacturer's instructions.

#### **2.6.3.1 Lipofectamine 2000**

Briefly, cells were seeded in appropriate culture vessels 24 hrs prior to transfection to reach 80% confluency on the day of transfection. Plasmid DNA and lipofectamine were mixed at optimal ratio for each construct (typically 1:4) in Opti-MEM, according to the manufacturer's instructions, and added dropwise to cells on which the growth media had been replaced with Opti-MEM media. Following a 4 hr incubation period (5% CO<sub>2</sub>, 37°C), transfection media was replaced with the appropriate complete media and cells were allowed to express recombinant protein for the appropriate length of time (24-48 hrs) before transfected cells were processed as required.

### **2.6.3.2 Fugene HD**

Unlike with Lipofectamine 2000, cells were freshly seeded using complete growth media just before addition of the transfection reaction. Plasmid DNA and Fugene HD were mixed at optimal ratio for each construct (typically 1:6) in Opti-MEM, according to the manufacturer's instructions. The mixture was then added dropwise to cells which were then returned to the incubator (5% CO<sub>2</sub>, 37°C) for 24-48 hrs until they were ready to be processed as required.

### **2.6.4 Nuclear export block**

Leptomycin B (20 nM; Calbiochem) was added to cells for 3 hrs to block nuclear export.

### **2.6.5 Induction of primary cilia formation**

Primary cilia formation was induced by culturing hTERT-RPE1 cells in serum free media for at least 48 hrs.

### **2.6.6 Preparation of cell lysates**

Whole cell lysates were prepared for SDS-PAGE and Western blotting or immunoprecipitation in either RIPA lysis buffer (50 mM Tris-HCl pH 8, 150 mM NaCl, 0.5% w/v sodium deoxycholate, 1% v/v NP-40, 0.1% w/v SDS, 1 mM PMSF, 1 mM DTT, 1x PIC) or NEB lysis buffer. Briefly, cells were washed in 1x PBS, harvested and collected by centrifugation and then lysed in an appropriate volume of lysis buffer. Lysis was carried out on ice for 30 mins after which RIPA lysates were centrifuged at 4°C, 13000 rpm for 10 mins to remove insoluble material whereas NEB lysates were passed 10 times through a 27G needle and then centrifuged. Supernatants were either used directly as required or stored at -80°C.

### **2.6.7 Preparation of RNA extracts**

To prepare RNA for RT-PCR, cells were homogenised with Tri reagent (Sigma). Tri reagent was added directly to washed cells adhering to the culture vessel and the subsequent homogenate collected. RNA isolation was performed according to the manufacturer's instructions. Briefly, the homogenate was separated into aqueous and organic phases by addition of chloroform and centrifugation. RNA, partitioned to the aqueous phase, was then precipitated with isopropanol before washing with ethanol and solubilisation in RNase-free water. Total RNA concentration was calculated by measuring  $A_{260}$  and samples were stored at  $-80^{\circ}\text{C}$ .

### **2.6.8 Cell synchronisation**

Cells were first cultured in the appropriate complete growth medium to a suitable (usually ~60-70%) confluency. Cells were then synchronised in  $G_1/S$  by 16 hr treatment with 2 mM thymidine, and where required released for 4 hrs by replacing drug media with fresh complete growth media. To then examine expression during progression into mitosis, cells were treated with 0.5  $\mu\text{g/ml}$  nocodazole and samples taken every 2 hrs for 12 hrs as cells progressed into and arrested in mitosis. Whole cell populations were collected (including rounded mitotic cells that were collected by gently pipetting off the floating population) and processed as described in section 2.6.7 for RT-PCR analysis (see 2.2.4). Synchronization was confirmed by flow cytometry.

### **2.6.9 Flow cytometric analysis**

To determine cell cycle distributions, cell populations for analysis were harvested and collected by centrifugation, then washed in 1x PBS before being resuspended in 1 ml 70% ice-cold ethanol to fix cells. Cells were maintained in ethanol at  $-20^{\circ}\text{C}$  for a minimum of 30 mins before being stained with propidium iodide. Briefly, cells were washed twice in 1x PBS to completely remove all traces of ethanol, and resuspended in 1x PBS supplemented with 200  $\mu\text{g/ml}$

RNase A and 20 µg/ml propidium iodide. Cells were stained in the dark at 4°C for a minimum of 4 hrs. Cells were then analysed via flow cytometry, using a BD FACSCanto II analyzer and BD FACSDiva software.

### 2.6.10 RNA interference

Cells were seeded into a 6-well dish the day before transfection so as to reach a confluency of ~30% for transfection. 100 nM siRNA oligonucleotides and Oligofectamine (Invitrogen) transfection reagent were mixed according to the manufacturer's instructions and added dropwise to cells whose normal growth media had been replaced with medium without FBS or Pen/Strep. Following a 4 hour incubation period (5% CO<sub>2</sub>, 37°C), antibiotic free media containing 30% v/v FBS was added and cells incubated again (5% CO<sub>2</sub>, 37°C) for 72 hours before being processed as required.

<b>Human Nek3 siRNA</b>	
Duplex #1	GAUAAUGCCUGAGGAAAUGUU
Duplex #2	GGAAUAUGGUGAGGAAGUAUU
Duplex #3	CGAUAGAGGUGGUUCUGUAUU
Duplex #4	CAAUGUGCCUUGGAGUAAUU
<b>Human Nek5 siRNA</b>	
Duplex #4	GAGAAUGGCAGGCUGUUUAAUU
Duplex #5	GAAUAAACCCUACAACAAUUU
Duplex #6	GACCGACCAUCCAUAAAUUUU
Duplex #19	GGGGUAAGGUCACCGAUUAAUU
<b>Human Nek11 siRNA</b>	
Duplex #1	GAACAAGAAUCCUUCAUUAAUU
Duplex #2	GAAGGAGGCUGCUCAUUAUUU
Duplex #3	GAACCUBAAUGUGUAGAUUUUU
Duplex #5	GCCGAGAUCUGGACGAUAAUU

### 2.6.11 siRNA-plasmid co-transfection

To perform siRNA-plasmid co-transfection using Lipofectamine 2000, cells were seeded in appropriate culture vessels 24 hrs prior to transfection to reach ~80%

confluency on the day of transfection using media without Pen/Strep. Briefly, transfection mixes containing 1 µg plasmid DNA, 100 nM final concentration of siRNA duplex(es) and 4 µl lipofectamine in Opti-MEM were prepared, according to the manufacturer's instructions. The DNA-siRNA-lipofectamine complexes were added dropwise to cells and following a 4 hr incubation period (5% CO<sub>2</sub>, 37°C), transfection media was replaced with fresh media without Pen/Strep and cells were returned to the incubator (5% CO<sub>2</sub>, 37°C) until they needed to be processed as required.

## **2.7 Indirect immunofluorescence microscopy**

Cells grown on acid-etched coverslips were either (i) fixed and permeabilised using ice-cold methanol for a minimum of 10 mins before processing for immunofluorescence microscopy; (ii) pre-extracted for 30 secs in pre-extraction buffer (80 mM PIPES pH 6.8, 1 mM MgCl<sub>2</sub>, 1 mM EGTA, 0.5% v/v Triton X-100) and then methanol fixed as in (i); or (iii) fixed and permeabilised using ice-cold methanol as in (i), then washed twice in 1x PBS prior to being post-extracted for 30 secs using post-extraction buffer (80 mM PIPES pH 6.8, 1 mM MgCl<sub>2</sub>, 1 mM EGTA, 0.2% v/v NP-40). Briefly, after appropriate fixation with or without extraction, cells were rehydrated by three 5 min washes in 1x PBS. Non-specific antibody binding was blocked by incubation for 10 mins in 1x PBS supplemented with 1% w/v BSA. Coverslips were incubated with an appropriate volume (~100 µl) of primary antibody solution diluted to a suitable concentration in 1x PBS supplemented with 3% w/v BSA. Incubation with primary antibodies was for a minimum of 1 hr at room temperature. Coverslips were then subjected to three 5 min washes in 1x PBS to remove unbound antibody before incubation with appropriate secondary antibodies diluted in 1x PBS supplemented with 3 % w/v BSA and 0.3 µg/ml Hoechst 33258 in the dark for 1 hr at room temperature. Coverslips were then subjected to a final round of washes before being mounted on glass microscope slides in mountant (80% v/v glycerol, 35% w/v n-propyl gallate in PBS). Images were obtained with a TE300 inverted microscope (Nikon) using an ORCA-R<sup>2</sup> camera (Hamamatsu) using

Openlab software (Improvision), and images were processed using Adobe Photoshop 7.

### **2.7.1 Data analysis and quantification techniques**

The relative abundance of protein at centrosomes was quantified using the relevant immunofluorescence images, captured and processed using Openlab software. All images to be measured for a given experiment were captured under identical conditions and processed identically. Briefly, a region of interest of the appropriate size (the average size of one centrosome) was selected and saved. Total pixel intensity within this region was calculated and background intensity subtracted for each image to be analysed.

## **Chapter 3**

# **Generation and Characterisation of Antibodies against Nek3, Nek5 and Nek11**

### 3.1 Introduction

Initial studies on Nek11 raised the prospect of it being a cell cycle regulated kinase with increased mRNA expression through S to G<sub>2</sub>/M phase and changes in subcellular localisation in a cell cycle dependent manner (Noguchi et al. 2002). Meanwhile, activation of Nek11 kinase activity in response to various DNA-damaging agents and DNA replication inhibitors suggested that this kinase plays a role in the G<sub>1</sub>/S DNA damage checkpoint (Noguchi et al. 2002). Upon further investigation of the molecular mechanism of Nek11L activation, Nek11 was reported to be a target of Nek2A in G<sub>1</sub>/S-arrested cells with Nek2 phosphorylation activating Nek11 (Noguchi et al. 2004). However, it has recently been demonstrated that the checkpoint protein CHK1 directly activates Nek11 to regulate CDC25A phosphatase degradation and enforce DNA damage-induced G<sub>2</sub>/M arrest (Melixetian et al. 2009).

As for Nek3, early studies revealed mRNA expression in multiple tissues and cell lines, but indicated no change during cell cycle progression (Tanaka & Nigg 1999; Kimura & Okano 2001). A few years later, it was reported that Nek3 kinase activity is induced in response to signalling from the prolactin receptor causing members of the Vav family of guanine nucleotide exchange factors to interact with the kinase domain of Nek3 and become activated by transient phosphorylation, leading to activation of downstream signalling targets involved in tumour progression (Miller et al. 2005). Subsequently, it was shown that Nek3 depletion in breast cancer cells attenuated cytoskeletal re-organisation as well as cell migration and invasion (Miller et al. 2007). Hence, roles in both cell signalling and cytoskeleton organisation have been proposed.

However, it is clear that much still remains to be learnt about the function, as well as regulation, of both Nek3 and Nek11. Meanwhile, there is no published data yet on Nek5. In order to begin to characterise these protein kinases, specific antibodies would be required for applications such as Western blotting to analyse protein expression and test knockdown by siRNA-mediated

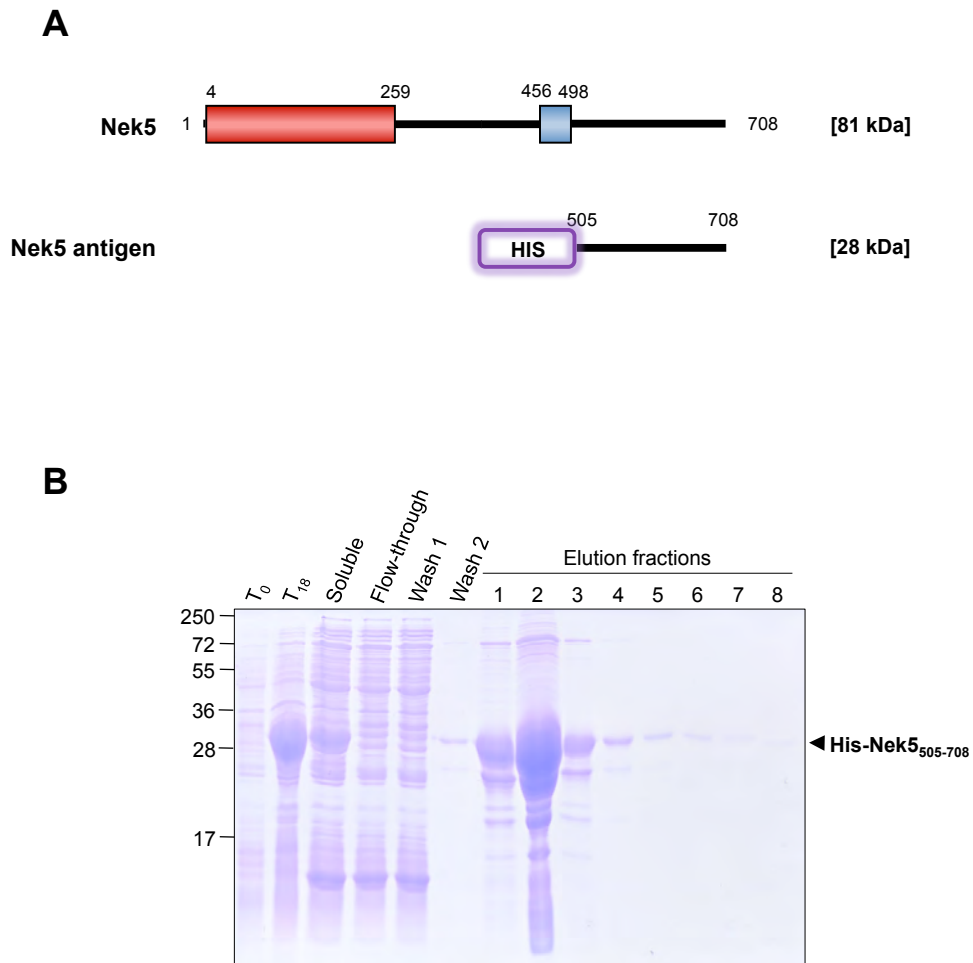
depletion, immunofluorescence microscopy to study subcellular localisation, and immunoprecipitation to assay activity and isolate interacting regulators and substrates. At the time of this study, no Nek5 or Nek11-specific antibodies were commercially available. Therefore, polyclonal antibodies specific for human Nek5 and Nek11 were raised in rabbits, affinity purified and characterised for use in studies of Nek5 and Nek11 function. To study human Nek3, a commercial antibody was available which we could characterise for specificity.

## 3.2 Results

### 3.2.1 Expression of Nek5 and Nek11 antigens in bacteria

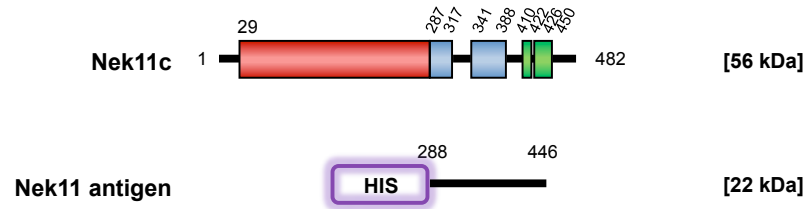
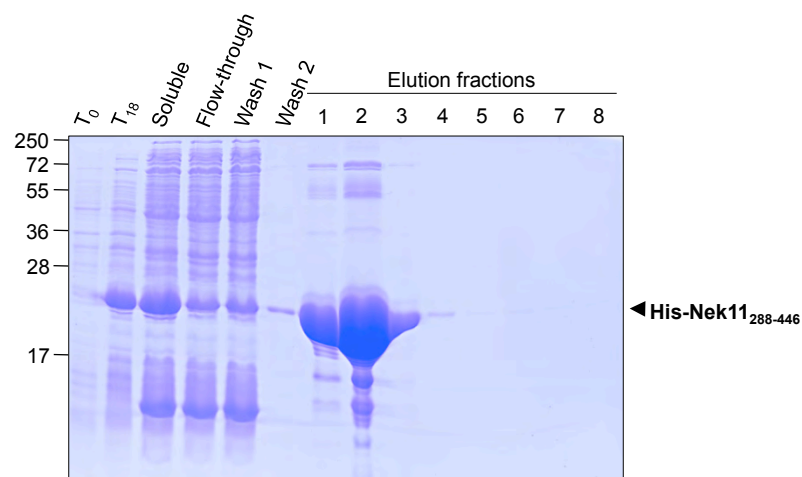
Neks have conserved N-terminal catalytic kinase domains, approximately 40-85% identical to each other, whereas their C-terminal non-catalytic regions are highly divergent. For this reason, bacterially expressed His-tagged peptides designed to correspond to the C-terminal amino acid sequences of Nek5, residues 505-708, and Nek11, residues 288-446, were used as antigens for immunisation of rabbits for antibody generation (Figure 3.1A and 3.2A, respectively).

Expression of these proteins was extremely poor in the most widely used host *E. coli* background for protein expression, BL21. However, this problem was overcome by using a host strain derived from BL21, Rosetta 2, that has been designed to enhance the expression of eukaryotic proteins that contain codons rarely used in *E. coli*. The expression of His-Nek5 and His-Nek11 peptides was successfully induced in these competent cells at a temperature of 22°C using IPTG at a final concentration of 0.1 mM. After 18 hours, the soluble protein lysate was obtained by sonication and then incubated with Ni-NTA slurry to purify the His-Nek5 peptide in native soluble form. By SDS-PAGE analysis, an intense band at ~28 kDa, as expected for His-Nek5<sub>505-708</sub> protein, was present after protein induction, and this affinity purified predominantly into the first three fractions following elution with imidazole (Figure 3.1B). A similar result was obtained for His-Nek11<sub>288-446</sub>, for which the band migrated at the expected size of ~22 kDa (Figure 3.2B). Contaminating proteins larger than the desired antigens co-purified at low concentrations in the elution fractions (Figures 3.1B and 3.2B). These contaminants could have been removed using more stringent wash conditions; however for the purpose of generating antibodies to be used with mammalian cells, time was not spent optimising the removal of these low abundance bacterial contaminants. The bands with a smaller molecular weight than the desired antigens may well represent truncated fragments of the antigen produced by premature translation termination or protein degradation during expression and purification.



**Figure 3.1 Expression of Nek5 protein fragment for antibody production**

**(A)** Schematic representation of the full-length Nek5 protein and the His-tagged Nek5 (amino acids 505-708) protein generated using a pETM-11 expression vector for antibody generation. Amino acid numbers and predicted molecular weights are indicated. **(B)** Purification of the His-Nek5 (aa 505-708) protein.  $T_0$ , uninduced Rosetta 2 (DE3) competent cells;  $T_{18}$ , cell sample taken 18 hours after protein expression was induced using IPTG (0.1 mM). Molecular weights (kDa) are indicated on the left.

**A****B**

**Figure 3.2 Expression of Nek11 protein fragment for antibody production**

**(A)** Schematic representation of the full-length Nek11c isoform and the His-tagged Nek11 (amino acids 288-446) protein generated using a pETM-11 expression vector for antibody generation. Amino acid numbers and predicted molecular weights are indicated. **(B)** Purification of the His-Nek11 (aa 288-446) protein.  $T_0$ , uninduced Rosetta 2 (DE3) competent cells;  $T_{18}$ , cell sample taken 18 hours after protein expression was induced using IPTG (0.1 mM). Molecular weights (kDa) are indicated on the left.

### **3.2.2 Immunisation of rabbits for Nek5 and Nek11 antibody generation**

The purified His-tagged peptides were used as antigens without removal of the His-tag as the small tag is poorly immunogenic. Hence, after purification, the peak fractions of purified antigen were pooled and protein concentrations quantified against BSA standards (Figure 3.3). After quantification, 2 mg of both recombinant peptides were sent to Cambridge Research Biochemicals (CRB) for immunisation of rabbits. Two rabbits were immunised for each antigen and each rabbit was subjected to four cycles of immunisation and bleeding.

However, prior to immunisation, screening of the sera from 8 rabbits was performed to test their “pre-immune” reactivity using Western blot analysis on HEK293 whole cell lysates (Figure 3.4) and by immunofluorescence microscopy of methanol fixed U2OS cells (Figure 3.5). Rabbits that had the lowest background reactivity (3214, 3216, 3217 and 3219) were selected for immunisation with the peptide antigens.

Western blot analysis of the Nek5 antisera from rabbit 3217, used at a 1:250 dilution, revealed several strong bands with the post-immunisation antisera, which were absent with the pre-immune sera (Figure 3.6A). However, Western blot analysis of the Nek5 antisera from rabbit 3219 used at a 1:250 dilution, revealed a more specific reactivity with bands at ~72 kDa with the post-immunisation antisera, which were absent with the pre-immune sera (Figure 3.6B). These blots also showed that the Nek5 antisera from both rabbits (3217 and 3219) detected recombinant Nek5 protein in transfected HEK293 cell lysates (TAP-tagged and FLAG-tagged Nek5, respectively). There is no published data on Nek5 protein; however, the ‘full length’ Nek5 protein sequence currently available on the NCBI Resource Database is 708 amino acid residues (~81 kDa). Hence, it is possible that the band detected at ~72 kDa by rabbit sera 3219 could be endogenous Nek5 protein.

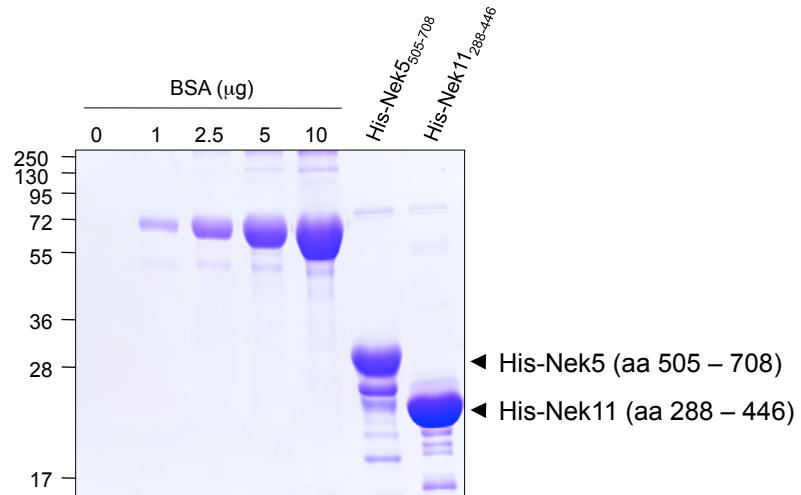


**Figure 3.3 Quantification of Nek5 and Nek11 recombinant protein fragments**

Coomassie Blue stained SDS-polyacrylamide gel with BSA standards and His-Nek5 and His-Nek11 peptides. The amount of BSA loaded (in  $\mu\text{g}$ ) is indicated. Molecular weights (kDa) are indicated on the left.

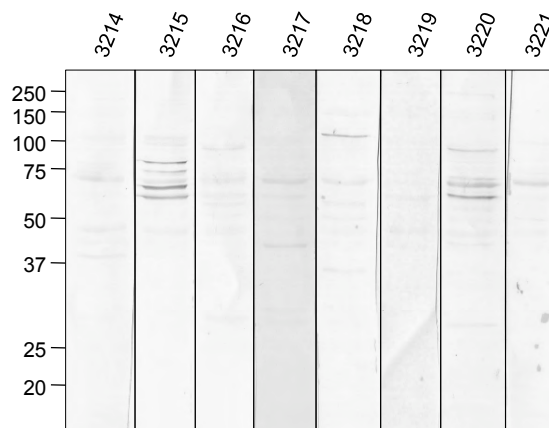


**Figure 3.4 Characterisation of rabbit sera prior to immunisation by Western blot**

Immunoblot analysis of the reactivity of pre-immune serum from eight different rabbits (3214-3221) with human proteins from untransfected HEK293 total cell lysate (20  $\mu$ g per lane). Molecular weights (kDa) are indicated on the left.

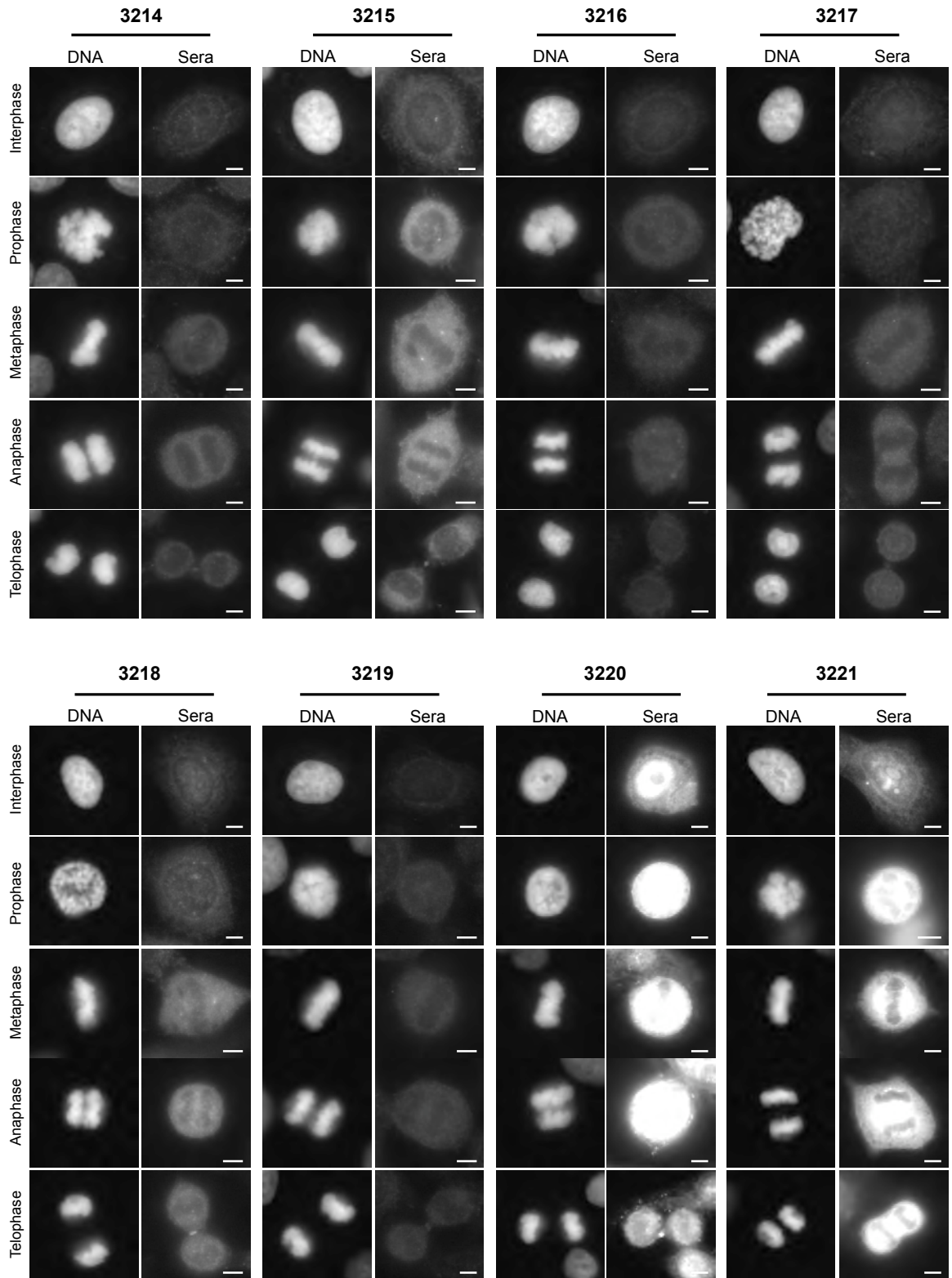


**Figure 3.5 Characterisation of rabbit sera prior to immunisation by immunofluorescence microscopy**

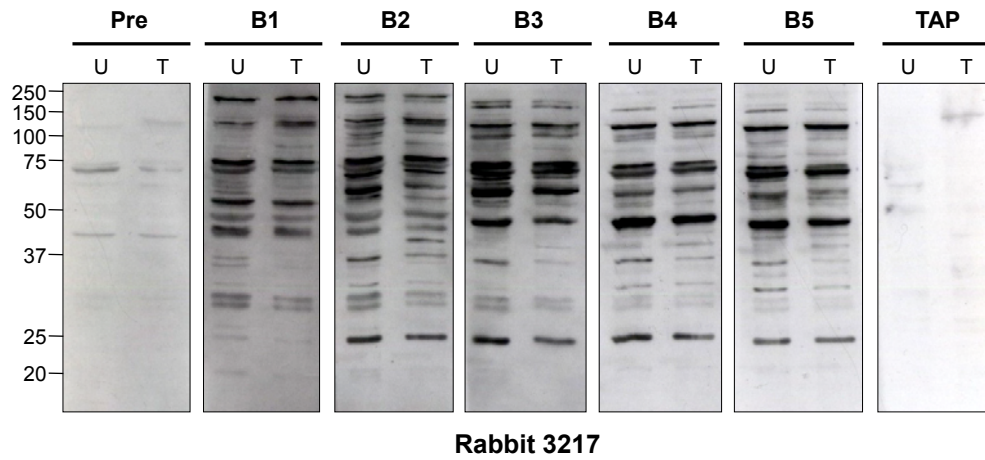
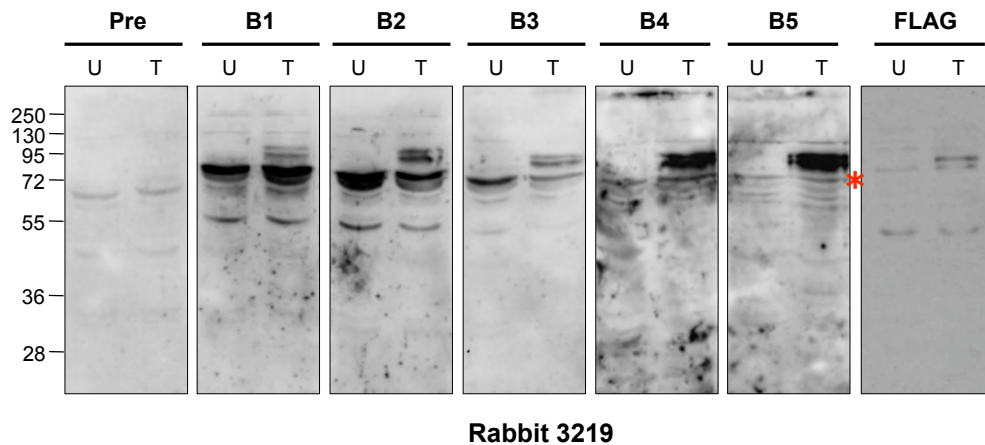
Analysis of the reactivity of pre-immune sera from eight different rabbits (3214-3221) with human proteins at different stages of cell cycle progression using immunofluorescence microscopy. Asynchronously growing U2OS cells were fixed in methanol and stained using pre-immune rabbit serum (1:250); DNA was stained using Hoechst 33258. Scale bars 5  $\mu\text{m}$ .

Western blot analysis of the Nek11 antisera from rabbit 3214, used at a 1:250 dilution, revealed a band above 100 kDa in the post-immunisation sera, which was absent from the pre-immune sera and increased in intensity from bleed one to five (Figure 3.7A). However, Western blot analysis of the Nek11 antisera from rabbit 3216, used at a 1:250 dilution, revealed a strong band at ~75 kDa and two bands at ~50 kDa in the final bleed, which are absent from the pre-immune sera (Figure 3.7B). These blots also show that Nek11 antisera from both rabbits (3214 and 3216) detected recombinant FLAG-Nek11c protein in transfected HEK293 cell lysates. Nek11 is expressed as alternative splice variants (Noguchi et al. 2002): a long isoform, Nek11L (~74 kDa), and a short isoform, Nek11S (~54 kDa). Moreover, a third isoform is present in the NCBI database representing the Nek11c clone that we obtained (56 kDa). Hence, it is possible that for rabbit 3216 the band detected at ~75 kDa could be endogenous Nek11L, and those bands at ~50 kDa could be endogenous Nek11S and Nek11c.

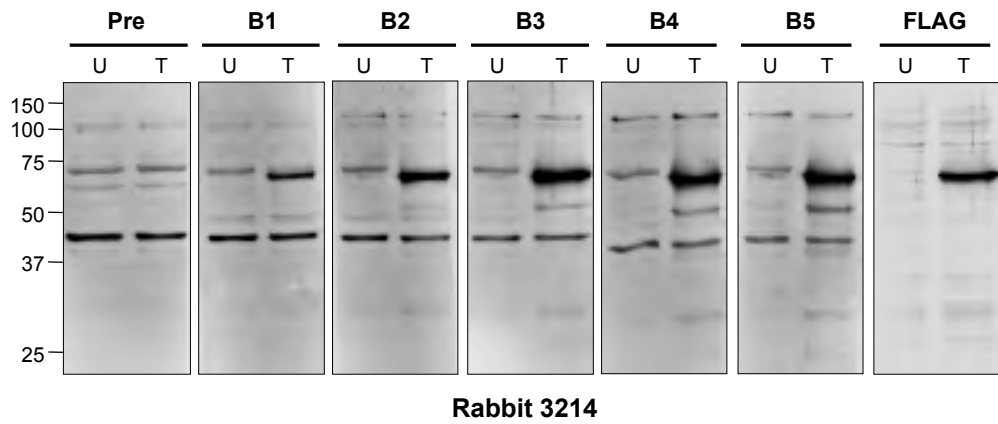
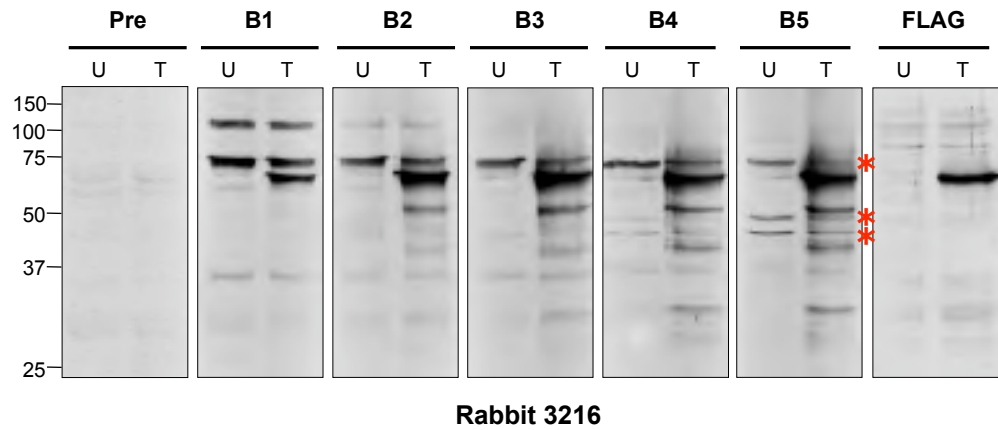
### **3.2.3 Affinity purification of human anti-Nek5 and anti-Nek11 antibodies**

Of the rabbits immunised, rabbit 3219 showed the most specific response to the His-Nek5<sub>505-708</sub> peptide, whilst rabbit 3216 showed the most avid and specific response to the His-Nek11<sub>288-446</sub> peptide, suggesting that antisera from these two rabbits would be most suitable for use in antibody purification.

Nek5 and Nek11 antisera from bleed 5 of rabbit 3219 and 3216, respectively, were first incubated with CNBr-activated sepharose covalently bound to control His-tagged peptides in order to remove any antibodies against the His-tag of the Nek5 and Nek11 peptide antigens, and then using the corresponding peptide antigen covalently bound to a column of CNBr-activated sepharose. The antibodies were then eluted, first in a low pH glycine buffer (pH 2.5) and then in a high pH TEA buffer (pH 11.5) in case the interaction of the antibody with the antigen was specifically sensitive to either low or high pH. The purity of these antibodies was tested by SDS-PAGE and Coomassie Blue staining (Figure 3.8),

**A****B****Figure 3.6 Characterisation of Nek5 antisera by Western blot analysis**

Reactivity of anti-Nek5 antisera taken from two different rabbits, 3217 (**A**) and 3219 (**B**), was characterised by Western blot analysis at a dilution of 1/250 against HEK293 whole cell lysates that were either untransfected (U) or transfected with either TAP-Nek5 or FLAG-Nek5 (T), respectively. Pre, pre-immune sera, B1-5, antisera from bleeds 1-5, respectively. The asterisk (\*) indicates a band detected by 3219 that could potentially represent endogenous Nek5. Molecular weights (kDa) are indicated on the left.

**A****B****Figure 3.7 Characterisation of Nek11 antisera by Western blot analysis**

Reactivity of anti-Nek11 antisera taken from two different rabbits, 3214 (**A**) and 3216 (**B**), was characterised by Western blot analysis at a dilution of 1/250 against HEK293 whole cell lysates that were either untransfected (U) or transfected with FLAG-Nek11 (T). Pre, pre-immune sera, B1-5, antisera from bleeds 1-5, respectively. The asterisks (\*) indicate three bands detected by 3216 that could potentially represent endogenous Nek11L, Nek11c and Nek11S isoforms. Molecular weights (kDa) are indicated on the left.

which revealed the presence of little rabbit serum albumin (RSA), and strong bands at the molecular weights expected for heavy and light chains of the purified antibodies. Using low pH elution buffer, the elution of antibody chains peaked in fractions 2 and 3 after which only RSA was present in the collected fractions; however, using high pH elution buffer, the elution of antibody chains remained relatively constant. Presumably, had more elution fractions been collected, their presence would have declined as elution became complete. Glycine fractions 2 and 3 were pooled for each antibody and concentrated; anti-Nek5 (3219) TEA fractions 2 to 6 were pooled and concentrated; and anti-Nek11 (3216) TEA fractions 1-10 were pooled and concentrated.

Aliquots of the Nek5 and Nek11 antisera (bleed 5) from rabbit 3219 and 3216, respectively, were independently purified by CRB. Antibodies were purified by eluting in a low pH buffer and then a high pH buffer as described above. A comparison of the different Nek5 affinity purified antibodies revealed that the Nek5 antibodies purified by CRB contain predominantly RSA, and only after concentration of these antibodies can the IgG heavy chain be observed using Coomassie Blue staining (Figure 3.9). In comparison, my own preparations contained predominantly IgGs with antibody heavy and light chains clearly visible. Hence, future studies were undertaken with the antibodies purified in Leicester.

#### **3.2.4 Characterisation of purified anti-Nek5 and anti-Nek11 antibodies**

Methanol-fixed U2OS cells which had been transfected with either FLAG-Nek5 or FLAG-Nek11 were co-stained with anti-FLAG antibodies and affinity-purified antibodies to test reactivity of the antibodies by immunofluorescence microscopy. Co-localisation of the FLAG antibody signal with the purified Nek5 antibody showed that the purified Nek5 antibody specifically detected the recombinant Nek5 protein that was predominantly nuclear in interphase cells (Figure 3.10A). Similarly, co-localisation of FLAG antibody with purified Nek11

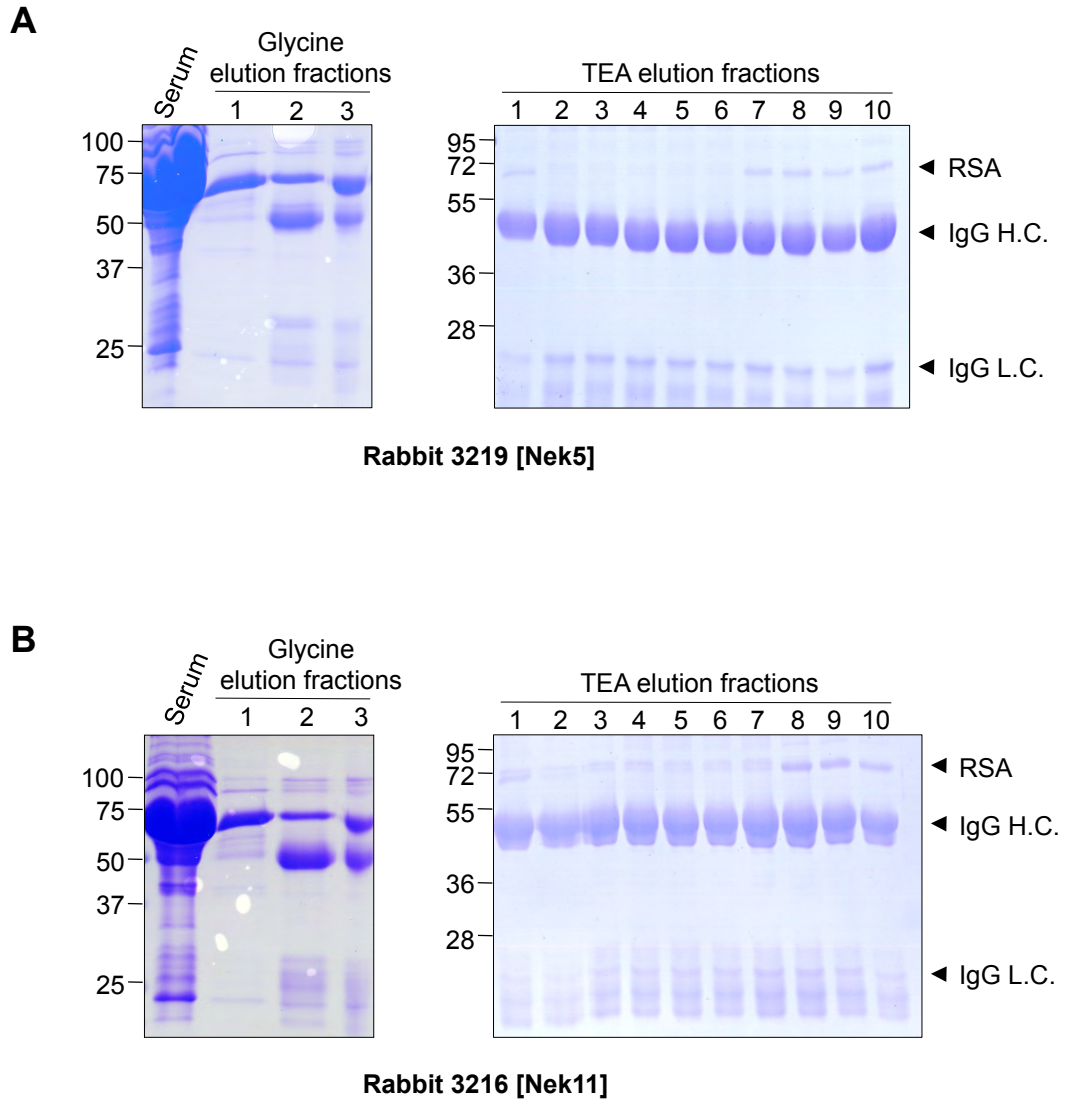


**Figure 3.8 Affinity purification of anti-Nek5 and anti-Nek11 antibodies**

Anti-Nek5 (3219) and anti-Nek11 (3216) antisera, **(A)** and **(B)** respectively, were purified on a column of His-Nek5 or His-Nek11 peptide, respectively, covalently bound to CNBr-activated sepharose beads and eluted using glycine pH 2.5 or triethylammonium chloride (TEA) pH 11.5. Purification efficiency was tested by SDS-PAGE and Coomassie Blue staining of unpurified antiserum and protein in elution fractions. The positions of rabbit serum albumin (RSA), the IgG heavy chain (H.C.), and IgG light chain (L.C.) are indicated. Molecular weights (kDa) are indicated on the left.

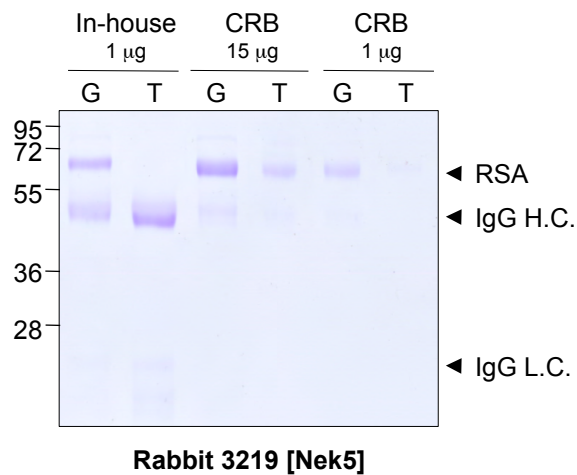


**Figure 3.9 Comparison of different affinity purified anti-Nek5 antibodies**

Anti-Nek5 (3219) serum was also purified by Cambridge Research Biochemicals (CRB) using affinity chromatography and eluted using glycine (G) pH 2.5 and then triethylammonium chloride (T) pH 11.5. Purification efficiency was tested by SDS-PAGE and Coomassie Blue staining by loading glycine and TEA antibodies that had been eluted in-house (Figure 3.8) for comparison with eluate provided by the CRB. The positions of rabbit serum albumin (RSA), the IgG heavy chain (H.C.), and IgG light chain (L.C.) are indicated. Molecular weights (kDa) are indicated on the left.

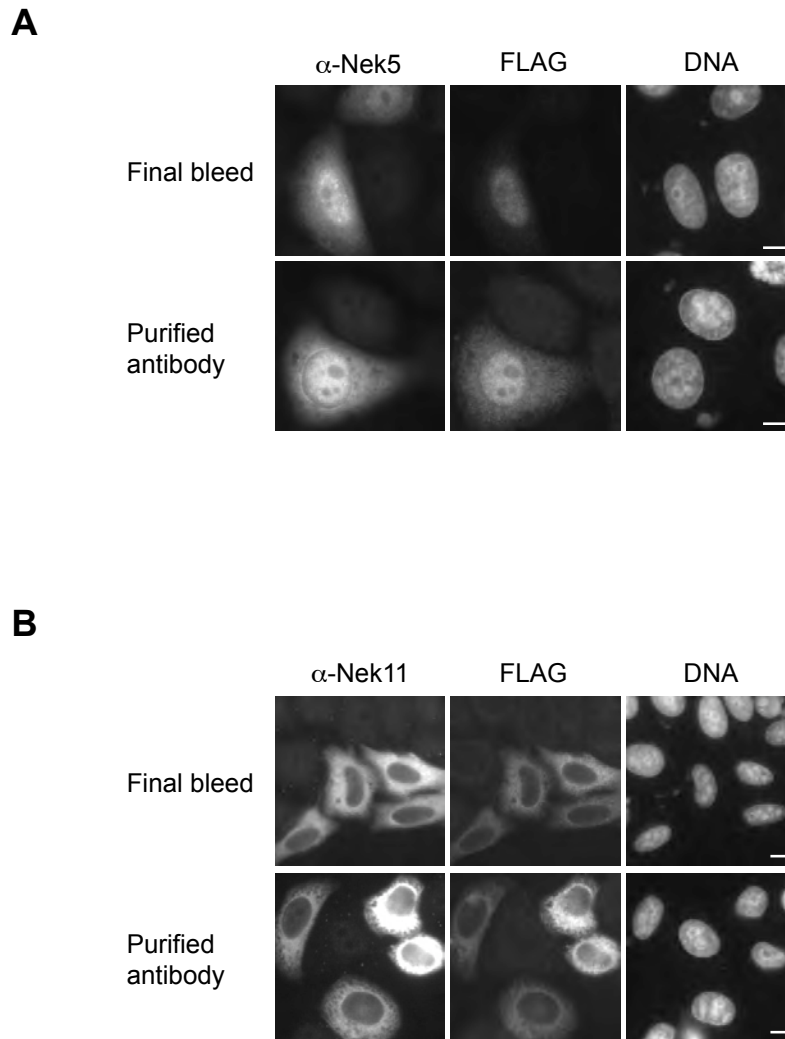
antibody indicated that this antibody specifically detected the recombinant protein, which was predominantly cytoplasmic (Figure 3.10B).

The reactivity and specificity of the purified anti-Nek5 and anti-Nek11 antibodies was further tested by Western blotting against HEK293 whole cell lysates that were either untransfected or transfected with FLAG-Nek5 or FLAG-Nek11 constructs. The purified antibodies only detected the Nek protein against which they were generated (Figure 3.11).

### **3.2.5 Characterisation of a commercially available Nek3 antibody**

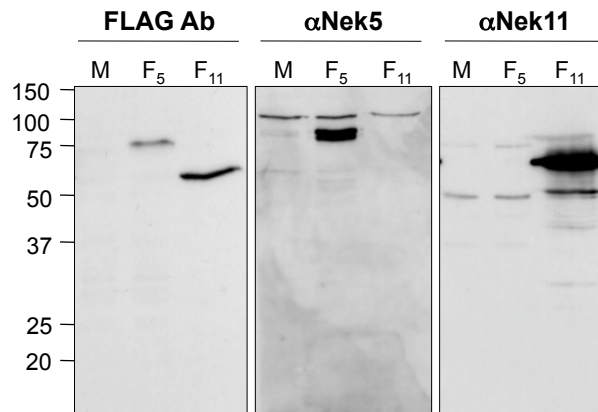
TAP-tagged Nek3, Nek5 and Nek11c proteins (Figure 3.12A) were generated by *in vitro* translation in the presence of [<sup>35</sup>S]methionine. Analysis by SDS-PAGE and autoradiography confirmed that the proteins made from these constructs were of the correct size (Figure 3.12B). The reactivity of a commercially available monoclonal Nek3 antibody (clone 2F8, Abnova) was then tested by Western blot analysis using whole cell lysates from untransfected cells and cells transfected with empty TAP-vector or TAP-Nek3 constructs (Figure 3.12C). Using the Nek3 antibody, recombinant Nek3 protein was detected at ~80 kDa in the lysate from cells transfected with TAP-Nek3 plasmid and not in the control lysates. This commercial antibody also detected apparent protein doublets at ~60 kDa and ~40 kDa in both control and transfected lysates. These correspond to the molecular weights expected to be produced by endogenous Nek3 splice variants, as described by Hernández & Almeida (2006).

To determine whether the proteins detected by the anti-Nek3 antibody were indeed endogenous Nek3 isoforms, four individual siRNA duplexes targeting the Nek3 mRNA were transfected into HEK293 cells to deplete the protein. On this occasion, SDS-PAGE and Western blot analysis clearly identified three distinct proteins at ~60 kDa, 45 kDa and 40 kDa. The abundance of all three proteins



**Figure 3.10 Characterisation of affinity-purified anti-Nek5 and anti-Nek11 antibodies**

Indirect immunofluorescence microscopy to test reactivity of purified antibodies (glycine eluates) on either Flag-Nek5-transfected U2OS cells **(A)** or Flag-Nek11-transfected U2OS cells **(B)**. Cells were transfected as appropriate, methanol fixed and processed for immunofluorescence microscopy. Recombinant proteins are detected with antibodies against the Flag epitope tag and either Nek5 or Nek11 final bleed serum (1:250) and equivalent purified antibodies (1  $\mu$ g/ml); DNA is stained with Hoechst 33258. Scale bars, 5  $\mu$ m.

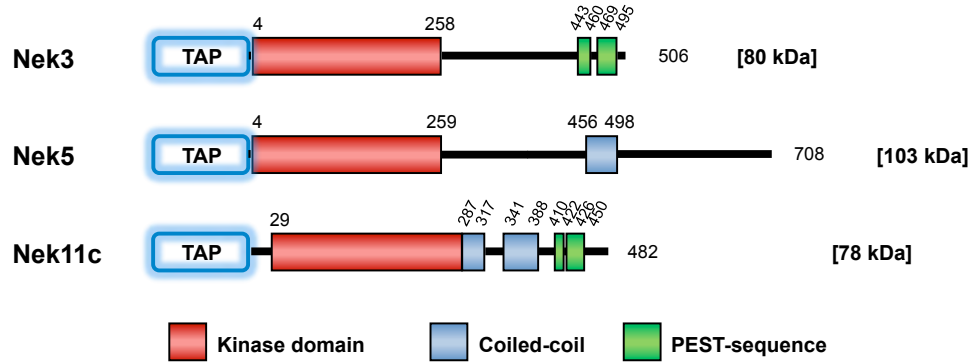
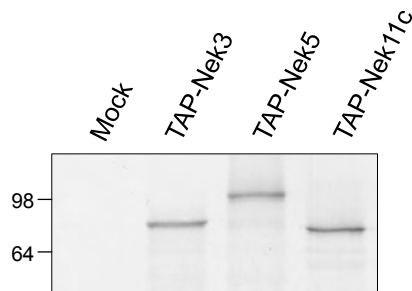
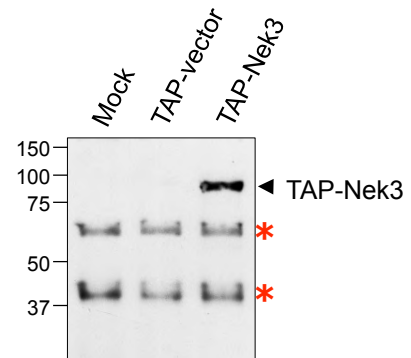


**Figure 3.11 Nek5 and Nek11 affinity purified antibodies do not detect the complementary protein**

Western blot analysis of Flag-Nek5 (F<sub>5</sub>) and Flag-Nek11 (F<sub>11</sub>) transfected as well as mock transfected (M) HEK293 whole cell lysates with affinity-purified anti-Nek5 (glycine eluate), anti-Nek11 (glycine eluate), and anti-Flag antibody to determine whether the Nek5 antibody recognises recombinant Nek11 and vice versa. Molecular weights (kDa) are indicated on the left.

was reduced in lysates from cells treated with the Nek3 specific siRNA duplexes for 72 hours (Figure 3.13A). Quantification of the blots indicated that, in comparison to mock treated cells, cells treated with Nek3 specific siRNA duplexes for 24 hours had no significant change in the abundance of protein; however, treatment with Nek3 siRNA duplexes for 72 hours resulted in ~40-50% reduction in the combined protein level compared to mock treated cells (Figure 3.13B).

However, reproducibility of this data proved difficult due to the weak detection of the endogenous proteins. Hence, to ensure that the Nek3 specific siRNA duplexes were efficient at depleting Nek3 protein, cells transiently transfected with recombinant Nek3 were treated with the individual siRNA duplexes. TAP-Nek3 was successfully depleted in cells co-transfected with a pool of the four Nek3 siRNA oligonucleotides or with the Nek3 specific siRNA oligonucleotides individually, whereas in mock or control siRNA transfected cells expression of TAP-Nek3 protein remained stable (Figure 3.13C). Furthermore, RT-PCR analysis of total mRNA extracted from cells treated with the pool of the four Nek3 siRNA oligos indicated that Nek3 was successfully depleted at the mRNA level (Figure 3.13D). Hence, these siRNA duplexes are specific for Nek3 and can effectively deplete Nek3 protein.

**A****B****C****Figure 3.12 Expression of TAP-tagged Nek3, Nek5 and Nek11c**

**(A)** Schematic representation of TAP-Nek3, -Nek5, and -Nek11c proteins generated using a pCMV-TAP mammalian expression vector. The TAP tag consists of protein A, a TEV (tobacco etch virus) protease cleavage site and a calmodulin binding peptide (CBP). Amino acid numbers are indicated. **(B)** The TAP-tagged proteins translated *in vitro* in the presence of [<sup>35</sup>S]methionine were analysed by SDS-PAGE and autoradiography. Mock represents a no DNA control. **(C)** Reactivity of commercially available Nek3 antibody against HEK293 whole cell lysates that were either mock, empty TAP-vector, or TAP-Nek3 transfected. The asterisk (\*) indicates bands detected that could potentially represent endogenous Nek3 variants. Molecular weights (kDa) are indicated on the left.

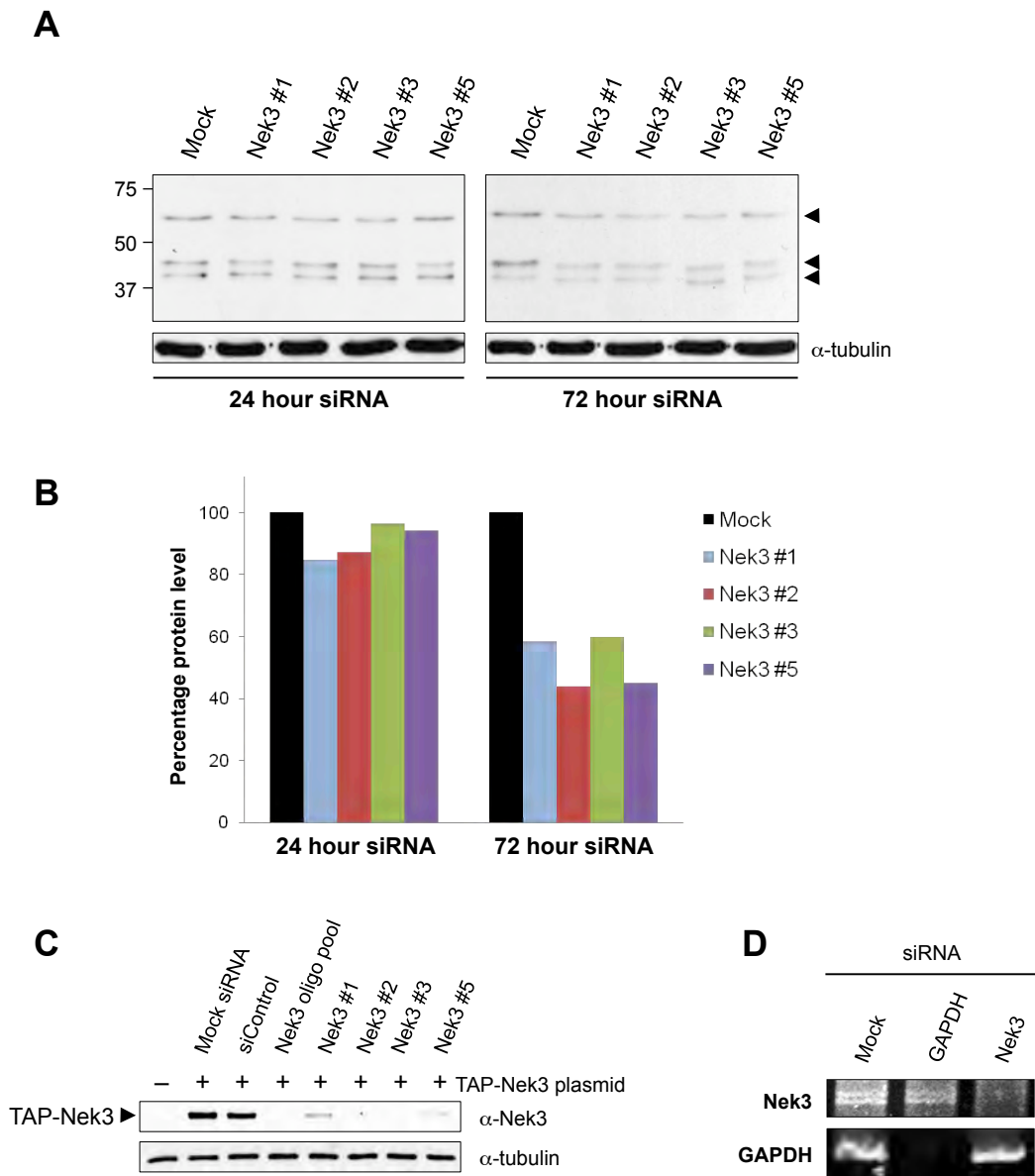


**Figure 3.13 Identification of endogenous Nek3 on Western blot using siRNA**

**(A)** U2OS cells were transfected with four individual Nek3 specific siRNA oligonucleotides for either 24 or 72 hrs before cells were lysed and analysed by SDS-PAGE and Western blot with anti-Nek3 and anti- $\alpha$ -tubulin antibodies. Potential endogenous Nek3 proteins are indicated (arrowheads). Molecular weights (kDa) are indicated on the left. **(B)** Knockdown efficiency of all three bands combined as a total was quantified using Adobe Photoshop software. Protein remaining after knockdown is shown as a percentage of protein in mock extracts minus background for both 24 hr and 72 hr siRNA treatments. **(C)** U2OS cells were co-transfected with either a pool of four Nek3 siRNA oligonucleotides, or Nek3 specific oligonucleotides individually, and with TAP-Nek3 plasmid. After 48 hrs plasmid-siRNA co-transfection, cells were harvested, lysed, and then analysed by SDS-PAGE and Western blot with anti-Nek3 and anti- $\alpha$ -tubulin antibodies. **(D)** Total RNA was collected after 48 hr siRNA treatment of U2OS cells transfected with a pool of four Nek3 siRNA oligonucleotides, and used to perform semi-quantitative RT-PCR analysis using Nek3 or GAPDH specific primers.

### 3.3 Discussion

Of the eleven human Neks, Nek2, Nek6, Nek7 and Nek9 play a role in cell cycle progression, whereas Nek1 and Nek8 are implicated in microtubule organisation in cilia. The remaining human Neks are much less well studied. The current hypothesis is that all Neks may contribute to the regulation of microtubule organisation and thereby co-ordinate cell proliferation and/or ciliogenesis. Hence, to investigate the roles of Nek3, Nek5 and Nek11 and determine whether they have a function in cell cycle progression and/or ciliogenesis, it was essential to have specific antibodies available.

As the human Nek family have highly conserved N-terminal catalytic domains, peptides corresponding to regions of the highly divergent C-terminal non-catalytic regions of Nek5 and Nek11 were expressed and purified for generation of Nek-specific antibodies. The two rabbits immunised with the Nek5 peptide produced sera that had very different patterns of bands when analysed by Western blot. Of these, the rabbit serum that was selected for antibody purification strongly detected recombinant FLAG-Nek5 protein and bands at ~72 kDa that could be endogenous Nek5 protein. For Nek11, the two immunised rabbits produced sera that strongly detected recombinant FLAG-Nek11c protein. The rabbit antisera that was chosen for antibody purification also potentially detected endogenous Nek11 proteins, as bands at ~75 kDa and ~50 kDa, corresponding to the predicted sizes of Nek11L and Nek11S isoforms were detected. The Nek11L and Nek11S cDNA sequences encode full length products encoding proteins predicted to be 74 and 54 kDa proteins, respectively (Noguchi et al. 2002). The Nek11c isoform used in this study is very similar to the Nek11S sequence, being just 12 amino acid residues longer in sequence and making a protein of approximately 56 kDa.

Consistent with the Western blot data, the purified Nek5 and Nek11 antibodies when used for immunofluorescence microscopy specifically detected recombinant Nek5 and Nek11 proteins, respectively. FLAG-Nek5 was

observed to be predominantly nuclear in interphase cells, whereas FLAG-Nek11 was predominantly cytoplasmic. Analysis of both endogenous and recombinant Nek5 and Nek11 subcellular localisation using the affinity purified Nek antibodies and antibodies against the recombinant proteins have led to more distinct patterns of localisation being observed (see subsequent chapters).

A commercially available Nek3 antibody detected recombinant Nek3 protein by Western blot analysis, as well as bands at approximately 60, 45 and 40 kDa in untransfected samples. These correspond to the expected sizes of endogenous full length Nek3 and the variants described by Hernández & Almeida (2006). The variants have been reported to result from alternative splicing of exon 10 and a single adenine insertion/deletion polymorphism at the end of exon 9, leading to the production of four hypothetical Nek3 proteins (Hernández & Almeida 2006): (i) full length Nek3 with a stretch of 8 adenine residues: 58 kDa (506 aa); (ii) Nek3-short produced if there is a stretch of 7 adenine residues, as this results in a premature stop codon: 34 kDa (299 aa); (iii) Nek3 $\alpha$ : lacking exon 10 with a stretch of 7 adenine residues: 56 kDa (489 aa); (iv) Nek3 $\alpha$ -short produced if there is a stretch of 8 adenine residues, as this results in a premature stop codon: 34 kDa (298 aa).

Hence, these variants at 34 kDa, 56 kDa and 58 kDa may correspond to the proteins being detected by the commercial Nek3 antibody. The specificity of the antibody was confirmed using cell lysates that had been depleted for Nek3 with siRNA duplexes. However, significant depletion of the 'endogenous' proteins was difficult to reproducibly observe using Western blot analysis. For this reason, the ability of these oligonucleotides to deplete Nek3 was confirmed using Western blot analysis of cells transfected with recombinant proteins, as well as by RT-PCR analysis.

In summary, generation and characterisation of antibodies for some of these least studied Nek protein kinases, Nek3, Nek5 and Nek11, has now enabled their roles in cell cycle progression and ciliogenesis to be investigated.

## **Chapter 4**

### **Nek3, Nek5 and Nek11: Subcellular localisation, expression and activity studies**

## 4.1 Introduction

At the start of this project, only limited information was available on the expression, localisation and activity of Nek3 and Nek11, and nothing was known about Nek5. To provide a first set of clues as to their function, we therefore decided to undertake a broad analysis of these aspects of their biology that could then act as guides to future, more hypothesis-driven experiments. Here, I summarise what was known prior to these studies.

Recombinant tagged versions of active and inactive Nek3 were diffusely distributed throughout the cytoplasm in U2OS and CHO cells (Tanaka & Nigg 1999; Miller et al. 2007). Consistent with this, subcellular fractionation to separate nuclear and cytoplasmic proteins indicated that endogenous Nek3 was predominantly cytoplasmic (Tanaka & Nigg 1999). Likewise, the subcellular distribution of endogenous Nek3 was also reported to be primarily cytoplasmic in neuronal cells (Chang et al. 2009). Interestingly, there is no evidence to suggest that Nek3 localises to centrosomes. Hence, for Nek3 there is reasonably consistent data that it is a cytoplasmic kinase. Little variation in Nek3 protein levels through the cell cycle has been observed, although in quiescent cells expression is enhanced (Tanaka & Nigg 1999). Consistent with this, Nek3 kinase activity is constant through the cell cycle, but increased in quiescent cells (Tanaka & Nigg 1999). These studies were undertaken with mouse Nek3. Initial studies with human Nek3, however, reported that Nek3 mRNA is prominently expressed in mitotically active tissues, leading to the suggestion that Nek3 may play a role in mitotic control (Chen et al. 1999). However, a separate study reported that human Nek3 mRNA levels are cell cycle-independent, consistent with the expression profile of mouse Nek3 (Kimura & Okano 2001). Hence, data on Nek3 expression are not completely consistent but do not yet strongly support a cell cycle role.

Initial studies on Nek11 also showed no localisation of this protein kinase to centrosomes (Noguchi et al. 2002; Noguchi et al. 2004). Using Western blot

analysis of whole cell lysates it was demonstrated that the short isoform of Nek11 was rarely detected indicating that the long isoform is the major Nek11 protein in most somatic cells (Noguchi et al. 2002). In HeLa cells, the subcellular localisation of Nek11 changed through the cell cycle being found in nuclei at interphase and on polar microtubules in early mitosis. However, staining became relatively diffuse and weak in late mitotic cells (Noguchi et al. 2002). In a later study, the same researchers reported an enrichment of Nek11 in nucleoli at interphase and in the perichromosomal localisation in mitosis (Noguchi et al. 2004). In contrast, overexpressed exogenous Nek11 was reported to be predominantly cytoplasmic, however, the splice variant used was not specified (Noguchi et al. 2004). Like NIMA and Nek2, expression of the long isoform of Nek11 was reported to be cell cycle regulated at mRNA and protein level, with peak levels at S/G<sub>2</sub>/M phase of the cell cycle (Noguchi et al. 2002). The kinase activity of Nek11 too was reported to be cell cycle regulated, with a 2-fold increase in activity in cells that had been G<sub>1</sub>/S arrested in comparison to asynchronously growing cells (Noguchi et al. 2002). Hence, Nek11 localisation, expression and kinase activity do appear to be cell-cycle regulated, although systematic analysis of the different Nek11 isoforms remains to be done.

Here, the localisation, expression and kinase activity of these Neks, together with that of human Nek5 for which there is currently no published data, was examined in an attempt to shed light on their potential functions.

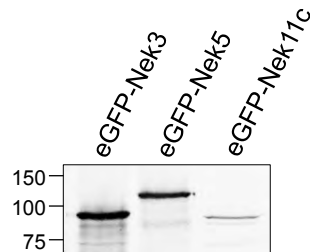
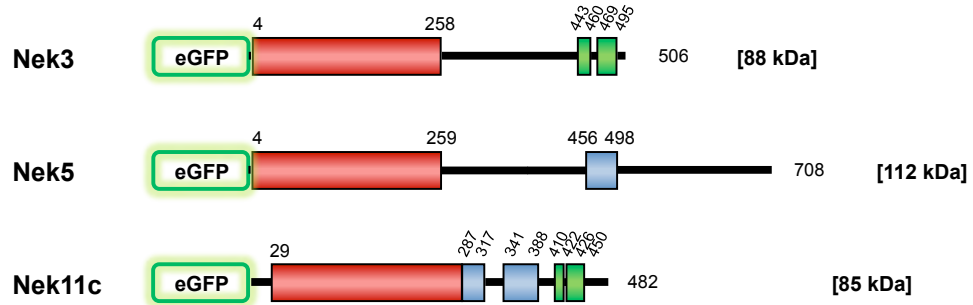
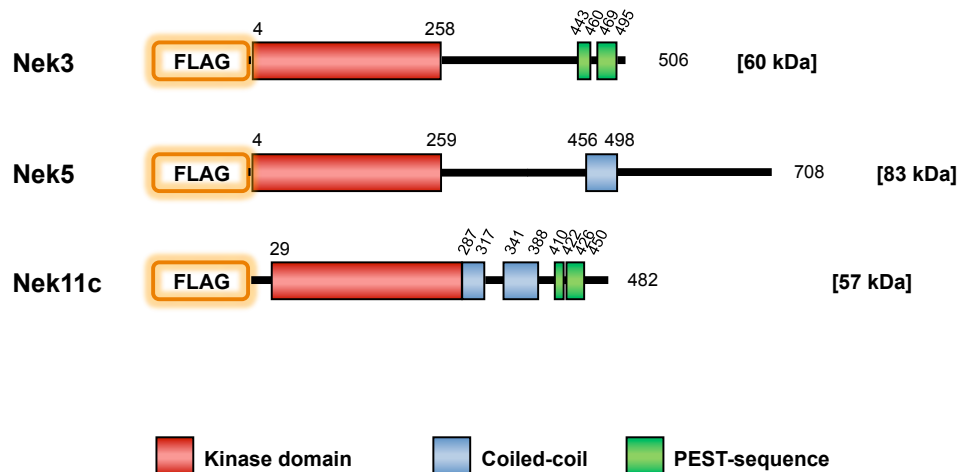
## 4.2 Results

In order to analyse the subcellular localisation of Nek3, Nek5 and Nek11c, human cDNAs for each of these proteins were cloned into pEGFP-T7 and pFLAG-CMV-2 mammalian expression vectors to generate recombinant proteins with N-terminal eGFP and FLAG tags, respectively (Figure 4.1). As there was a T7 bacteriophage promoter present in the eGFP vector, these constructs were also used for *in vitro* translation and the products analysed by SDS-PAGE and autoradiography confirming that the resulting proteins were of the correct size (Figure 4.1).

### 4.2.1 Subcellular localisation of recombinant Nek3

The localisation of recombinantly tagged Nek3 was examined using indirect immunofluorescence microscopy following transient transfection into U2OS cells. Cells were fixed in ice-cold methanol after 24 hours and processed for immunofluorescence microscopy with either anti-GFP or anti-FLAG antibodies. Both eGFP and FLAG-tagged Nek3 proteins localised predominantly to the cytoplasm during interphase (Figure 4.2), consistent with previous studies (Tanaka & Nigg 1999; Miller et al. 2007; Chang et al. 2009).

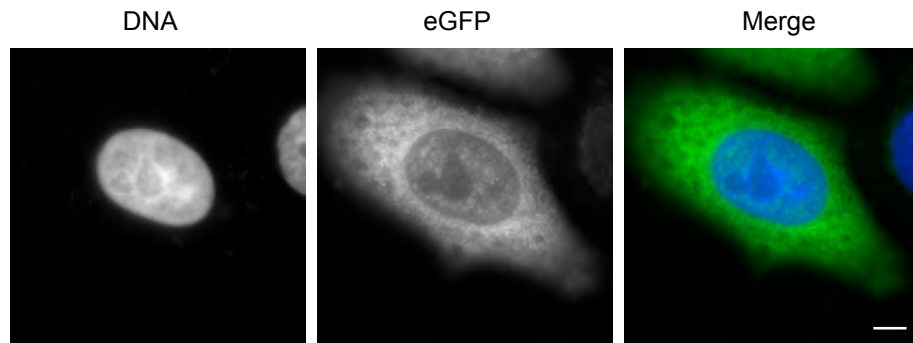
To specifically test whether there was localisation at the centrosome in this cell line, transfected U2OS cells were stained using an anti- $\gamma$ -tubulin antibody to detect centrosomes. Recombinant Nek3 proteins were found not to co-localise with  $\gamma$ -tubulin at centrosomes during interphase (Figure 4.3A-B). Equally, during mitosis, there was no co-localisation of eGFP-Nek3 with  $\gamma$ -tubulin at spindle poles. Interestingly though, recombinant Nek3 was weakly observed on fibrous structures reminiscent of spindle microtubules in metaphase (Figure 4.4). Co-staining with an anti- $\alpha$ -tubulin antibody to detect microtubules would be required to support this potential localisation to these mitotic structures. The subcellular localisation of recombinant Nek3 was also examined in an untransformed cell type, hTERT-RPE1 cells. These cells were transiently

**A****B**

**Figure 4.1 Recombinant Nek3, Nek5, Nek11c constructs generated for expression in mammalian cells**

**(A)** Schematic representation of the eGFP-Nek3, -Nek5, and -Nek11c constructs generated using a pEGFP-T7 mammalian expression vector. Lower panel shows these eGFP-tagged proteins translated *in vitro* in the presence of [<sup>35</sup>S]methionine and analysed by SDS-PAGE and autoradiography. **(B)** Schematic representation of the FLAG-Nek3, -Nek5, and -Nek11c constructs generated using a pFLAG-CMV-2 mammalian expression vector.

**A**



**B**

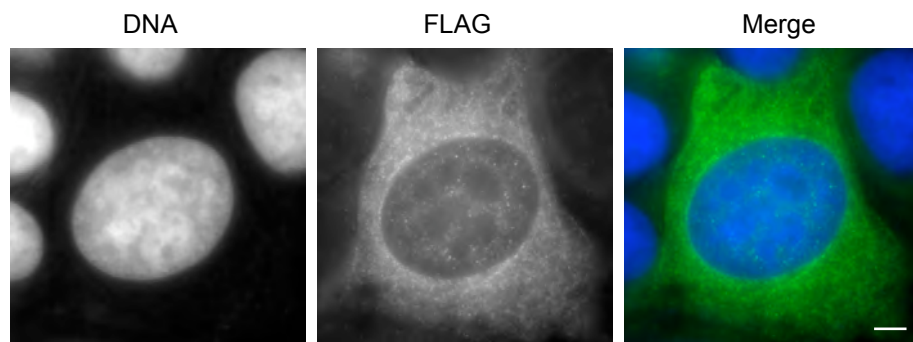


**Figure 4.2 Recombinant Nek3 proteins localise to the cytoplasm during interphase**

U2OS cells were transiently transfected with either eGFP-Nek3 (**A**) or FLAG-Nek3 (**B**) for 24 hrs before being fixed and permeabilised in ice-cold methanol and processed for immunofluorescence microscopy. eGFP-Nek3 and FLAG-Nek3 proteins were stained with anti-GFP and anti-FLAG antibodies, respectively, (green on merge). DNA is stained with Hoechst 33258 (blue on merge). Scale bars, 5  $\mu$ m.

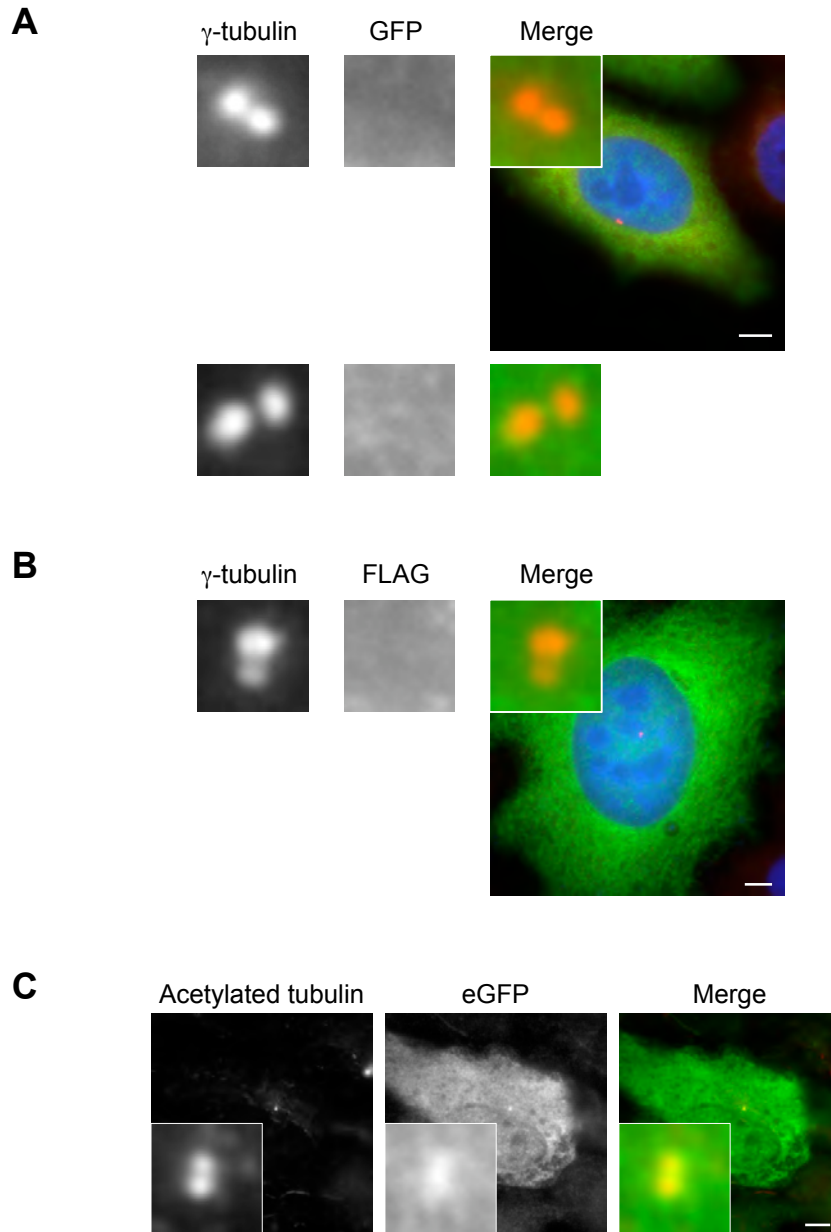


**Figure 4.3 Localisation of recombinant Nek3 proteins to centrosomes during interphase is cell-type dependent**

U2OS cells were transiently transfected with either eGFP-Nek3 (**A**) or FLAG-Nek3 (**B**) for 24 hrs before being fixed and permeabilised in ice-cold methanol and processed for immunofluorescence microscopy. Cells were immunostained with anti- $\gamma$ -tubulin antibodies to detect centrosomes (red on merge). eGFP-Nek3 and FLAG-Nek3 proteins were stained with anti-GFP and anti-FLAG antibodies, respectively (green on merge). DNA was stained with Hoechst 33258 (blue on merge). An additional magnified example is shown in (A). (**C**) RPE1 cells were transiently transfected with eGFP-Nek3 for 24 hrs, then fixed in methanol. Cells were immunostained with anti-acetylated tubulin antibodies to detect stable microtubules (red on merge). eGFP-Nek3 protein was stained with anti-GFP antibodies (green on merge). Scale bars, 5  $\mu$ m.

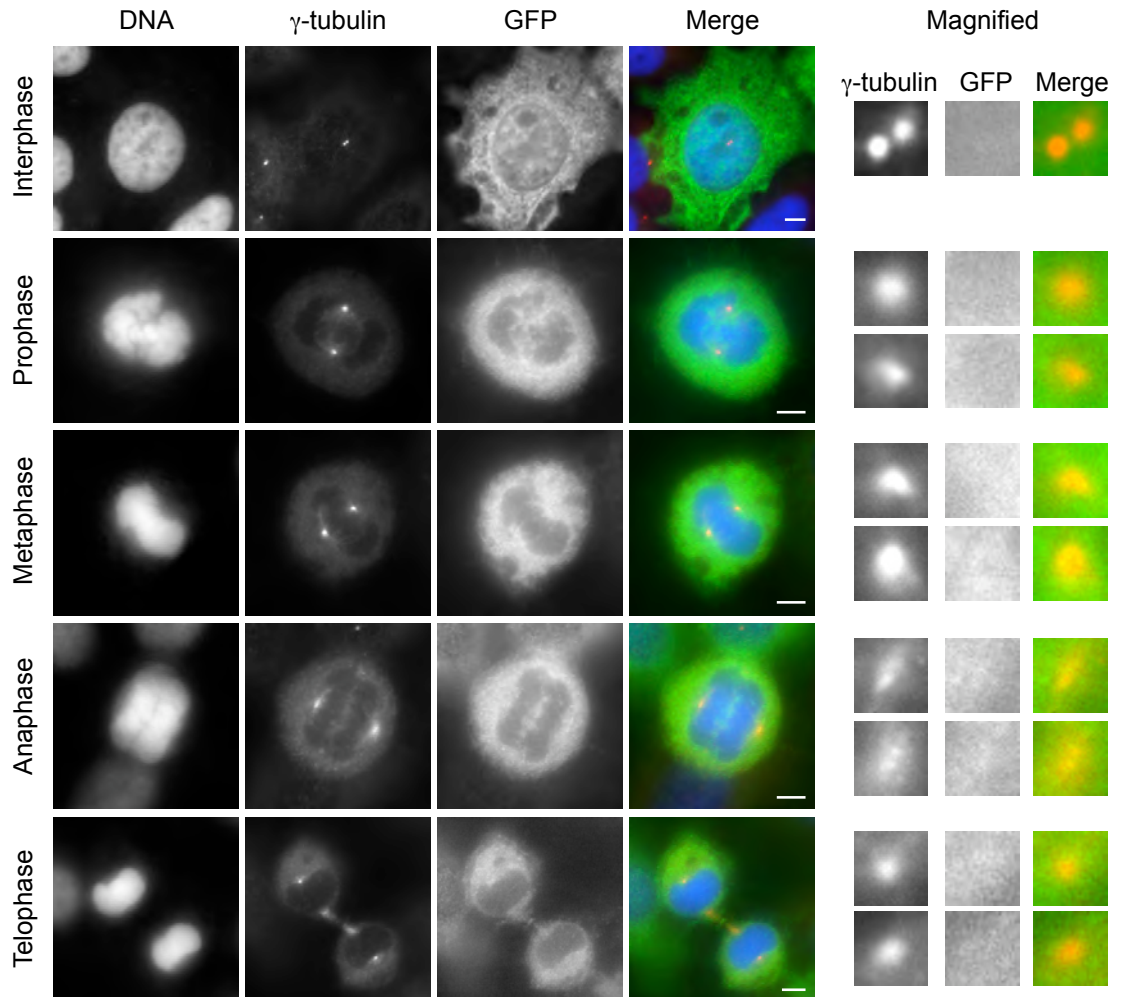


**Figure 4.4 Recombinant Nek3 protein does not localise to mitotic spindle poles**

U2OS cells were transiently transfected with eGFP-Nek3 for 24 hrs before being fixed and permeabilised in ice-cold methanol and processed for immunofluorescence microscopy. Cells were immunostained with anti- $\gamma$ -tubulin antibodies to detect centrosomes (red on merge). eGFP-Nek3 was stained with anti-GFP antibodies (green on merge). DNA was stained with Hoechst 33258 (blue on merge). Scale bars, 5  $\mu$ m.

transfected with eGFP-Nek3, fixed in methanol after 24 hours, and then processed for immunofluorescence microscopy with anti-GFP antibodies. Anti-acetylated tubulin antibody was also used to detect stable microtubule structures. As in U2OS cells, eGFP-Nek3 was found to be predominantly cytoplasmic during interphase. However, in RPE1 cells recombinant Nek3 also co-localised with acetylated tubulin at centrosomes (Figure 4.3C). Hence, under the conditions used here, localisation of recombinant Nek3 to centrosomes during interphase appears to be cell-type dependent.

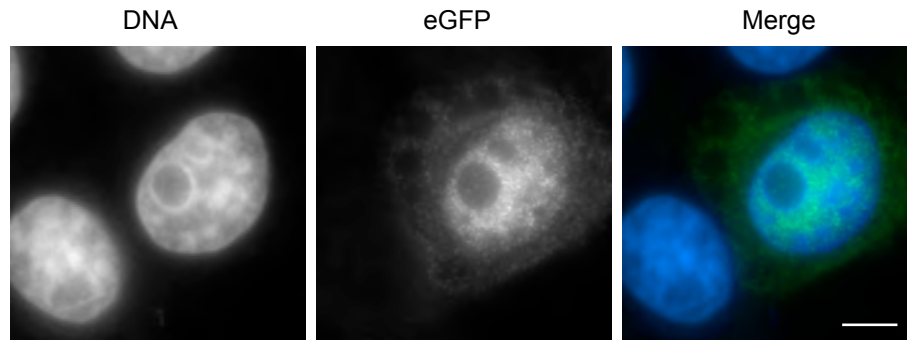
The localisation data for recombinant Nek3 could not be further supported by studying endogenous Nek3 subcellular localisation as the commercial Nek3 antibody characterised in Chapter 3 did not perform reliably by immunofluorescence microscopy. U2OS cells fixed in ice-cold methanol were processed for staining with this antibody at a concentration of up to 10 µg/ml; however, the weak staining of this antibody made it difficult to visually observe any specific localisation pattern.

#### **4.2.2 Subcellular localisation of recombinant Nek5**

Next, the localisation of recombinantly tagged Nek5 was examined. U2OS cells were transiently transfected for 24 hours with either eGFP- or FLAG-tagged Nek5 constructs, then fixed in ice-cold methanol and processed for immunofluorescence microscopy with either anti-GFP or anti-FLAG antibodies. In contrast to Nek3, recombinant Nek5 proteins predominantly localised to the nucleus during interphase and appeared to be excluded from nucleoli in these cells (Figure 4.5).

Using an anti- $\gamma$ -tubulin antibody to detect centrosomes, recombinant Nek5 was initially found not to localise at centrosomes during interphase under standard methanol fixation conditions (Figure 4.6A-B). However, using a different cell-type, RPE1 cells, FLAG-Nek5 strongly localised to the nucleus and co-localised

**A**



**B**

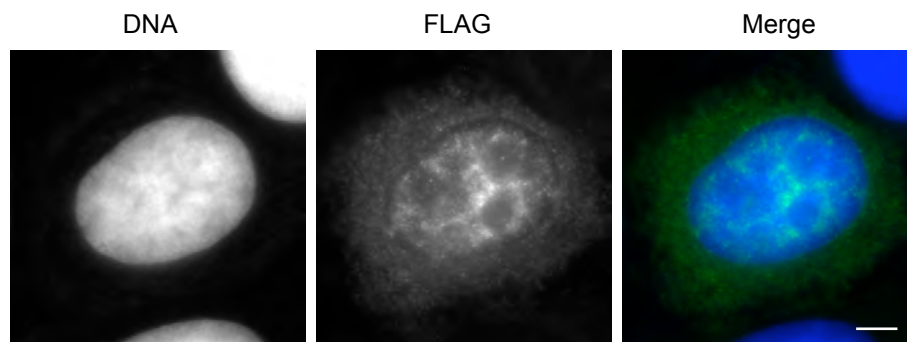


**Figure 4.5 Recombinant Nek5 proteins localise to the nucleus during interphase**

U2OS cells were transiently transfected with either eGFP-Nek5 (**A**) or FLAG-Nek5 (**B**) for 24 hrs before being fixed and permeabilised in ice-cold methanol and processed for immunofluorescence microscopy. eGFP-Nek5 and FLAG-Nek5 proteins were stained with anti-GFP and anti-FLAG antibodies, respectively, (green on merge). DNA is stained with Hoechst 33258 (blue on merge). Scale bars, 5  $\mu$ m.

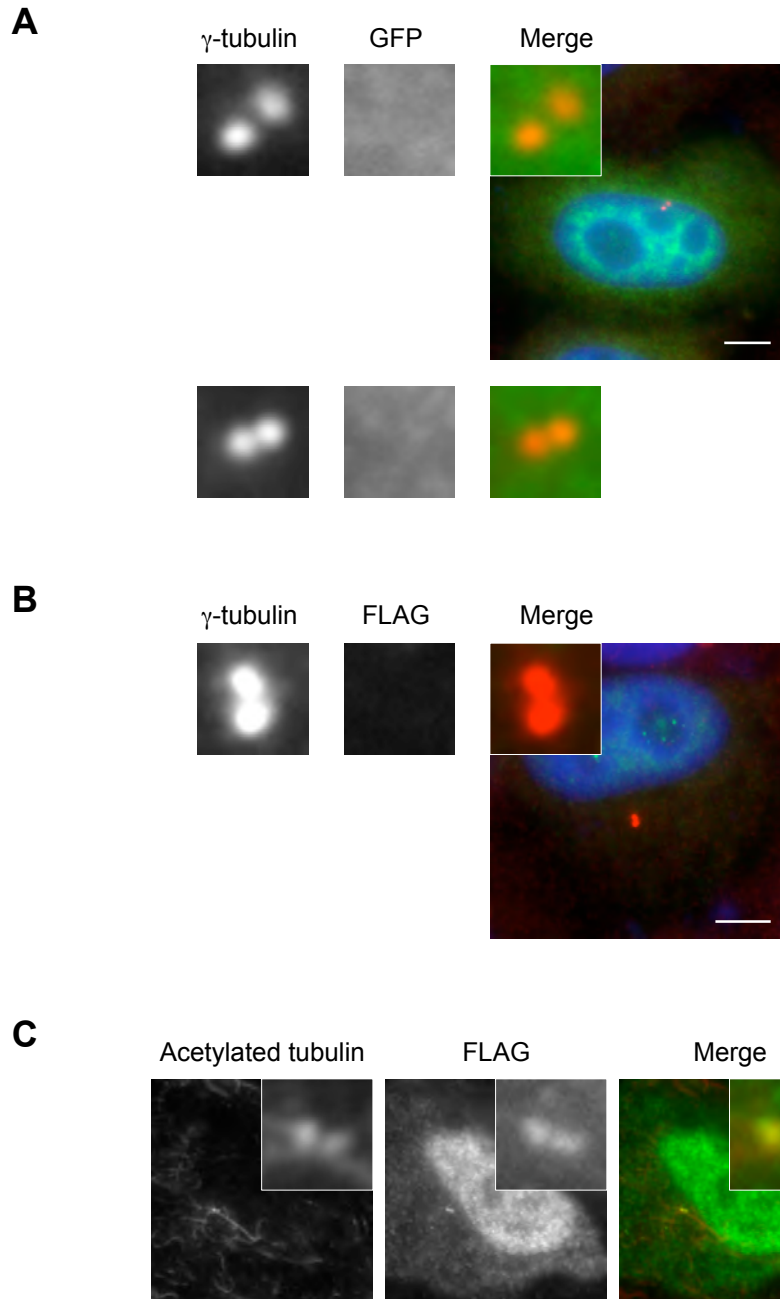


**Figure 4.6 Localisation of recombinant Nek5 proteins to interphase centrosomes following methanol fixation is cell-type dependent**

U2OS cells were transiently transfected with either eGFP-Nek5 (**A**) or FLAG-Nek5 (**B**) for 24 hrs before being fixed and permeabilised in ice-cold methanol and processed for immunofluorescence microscopy. Cells were immunostained with anti- $\gamma$ -tubulin antibodies to detect centrosomes (red on merge). eGFP-Nek5 and FLAG-Nek5 proteins were stained with anti-GFP and anti-FLAG antibodies, respectively, (green on merge). DNA was stained with Hoechst 33258 (blue on merge). An additional magnified example is shown in (A). (**C**) RPE1 cells were transiently transfected with FLAG-Nek5 for 24 hrs, then fixed in methanol. Cells were immunostained with anti-acetylated tubulin antibodies to detect stable microtubules (red on merge). FLAG-Nek5 protein was stained with anti-FLAG antibodies (green on merge). Scale bars, 5  $\mu$ m.

with acetylated tubulin at centrosomes under standard methanol fixation conditions (Figure 4.6C). After further characterisation of endogenous Nek5 protein localisation, described in the following Chapter, localisation in U2OS cells was revisited using pre-extraction with a buffer containing Triton X-100 prior to fixation in ice-cold methanol and staining with either anti-GFP or anti-FLAG antibodies. The purpose of pre-extraction was to remove soluble proteins from the cells, leaving structures that can then be visualised against a reduced background signal. Under these fixation conditions, recombinant Nek5 appeared not only within the nucleus but also at centrosomes during interphase (Figure 4.7), thus strengthening the data obtained in the second cell type tested, RPE1 cells.

#### **4.2.3 Subcellular localisation of recombinant Nek11c**

Most data previously published on Nek11 has been obtained using the long isoform of the protein. Here, in order to examine the subcellular localisation of Nek11c, recombinantly tagged versions were transiently transfected into U2OS cells. Cells were fixed in ice-cold methanol after 24 hours, and then processed for immunofluorescence microscopy with either anti-GFP or anti-FLAG antibodies. Recombinant Nek11c protein localised predominantly to the cytoplasm during interphase (Figure 4.8). Using two different cell types, U2OS and RPE1 cells, and either an anti- $\gamma$ -tubulin antibody to detect centrosomes or anti-acetylated tubulin antibody to detect stable microtubule structures, respectively, recombinant Nek11c was found not to localise at centrosomes during interphase (Figure 4.9).

#### **4.2.4 Localisation of endogenous Nek11**

To investigate the subcellular localisation of endogenous Nek11 protein, the affinity-purified anti-Nek11 antibodies generated as described in Chapter 3 were employed. U2OS cells were grown on acid-etched coverslips then incubated briefly in a pre-extraction buffer containing Triton X-100 detergent prior to fixation in ice-cold methanol. These samples were then processed for

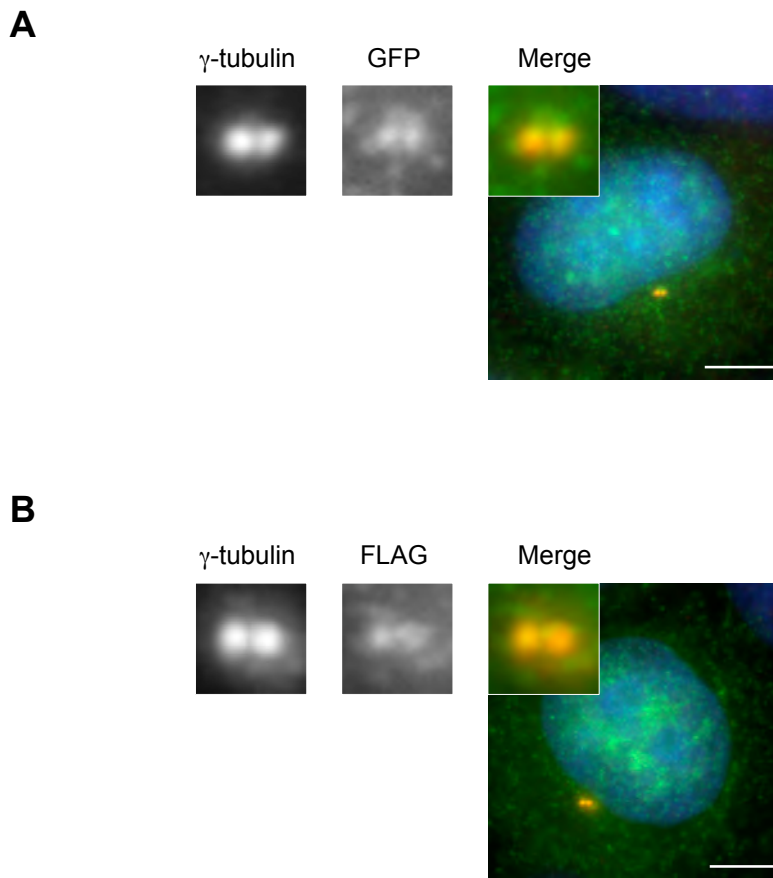
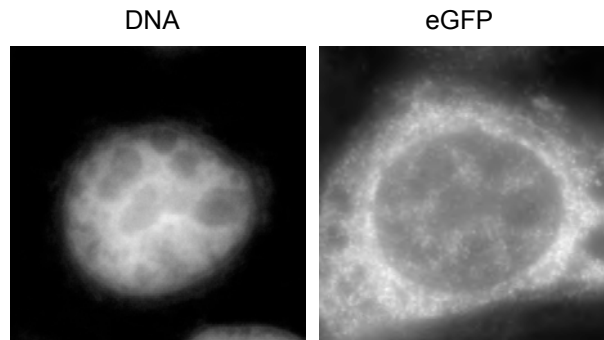


**Figure 4.7 Pre-extraction of cells reveals centrosomal localisation of recombinant Nek5 proteins in U2OS cells**

U2OS cells were transiently transfected with either eGFP-Nek5 (**A**) or FLAG-Nek5 (**B**) for 24 hrs before being incubated in Triton X-100 pre-extraction buffer for 30 seconds, then fixed and permeabilised in ice-cold methanol and processed for immunofluorescence microscopy. Cells were immunostained with anti- $\gamma$ -tubulin antibodies to detect centrosomes (red on merge). eGFP-Nek5 and FLAG-Nek5 proteins were stained with anti-GFP and anti-FLAG antibodies, respectively, (green on merge). DNA was stained with Hoechst 33258 (blue on merge). Scale bars, 5  $\mu$ m.

**A**



**B**

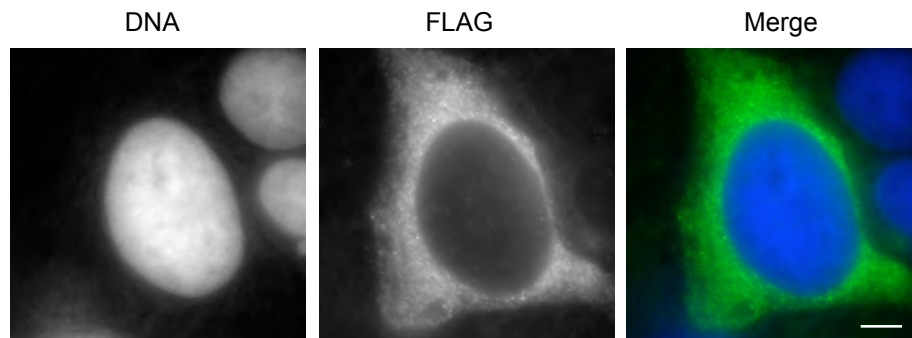


**Figure 4.8 Recombinant Nek11c localises to the cytoplasm during interphase**

U2OS cells were transiently transfected with either eGFP-Nek11c (**A**) or FLAG-Nek11c (**B**) for 24 hrs before being fixed and permeabilised in ice-cold methanol and processed for immunofluorescence microscopy. eGFP-Nek11c and FLAG-Nek11c proteins were stained with anti-GFP and anti-FLAG antibodies, respectively, (green on merge). DNA is stained with Hoechst 33258 (blue on merge). Scale bars, 5  $\mu$ m.

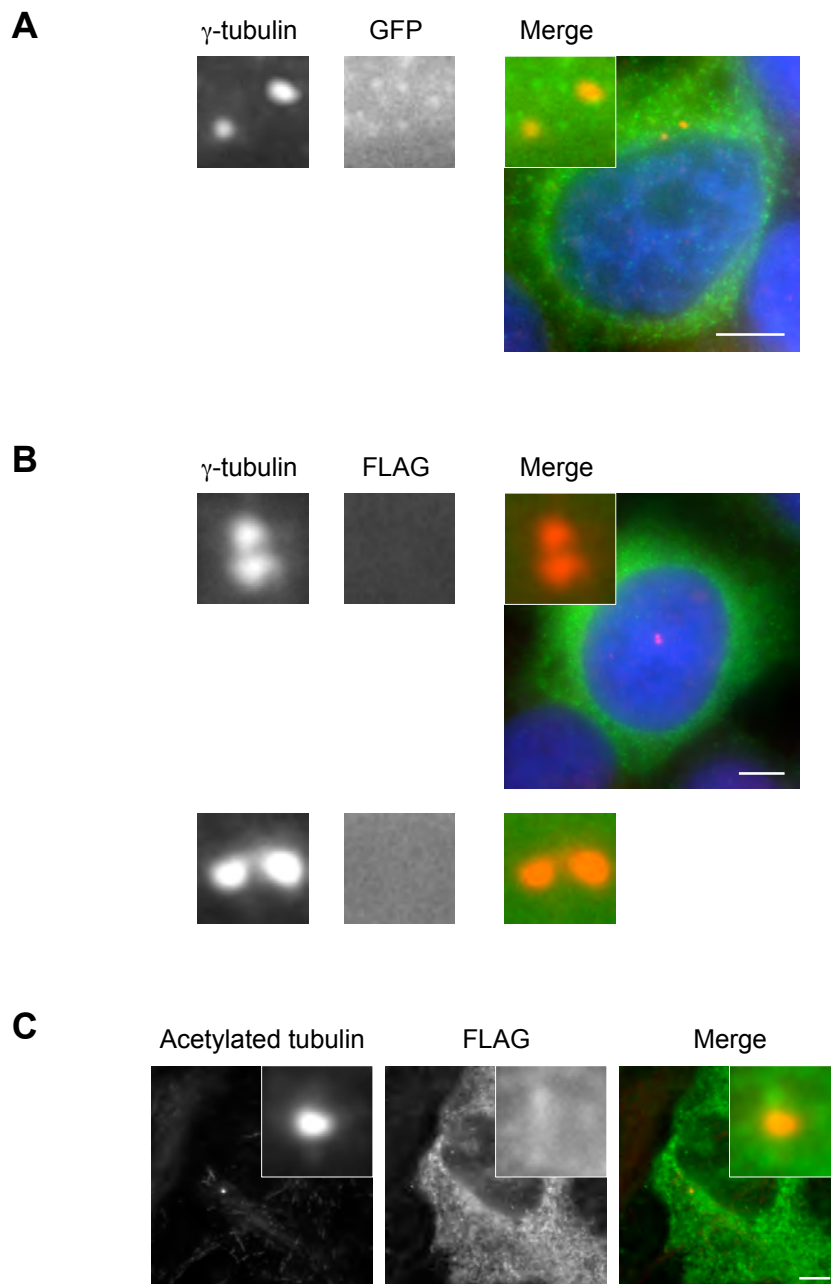


**Figure 4.9 Recombinant Nek11c proteins do not localise to centrosomes during interphase**

U2OS cells were transiently transfected with either eGFP-Nek11c (**A**) or FLAG-Nek11c (**B**) for 24 hrs before being fixed and permeabilised in ice-cold methanol and processed for immunofluorescence microscopy. Cells were immunostained with anti- $\gamma$ -tubulin antibodies to detect centrosomes (red on merge). eGFP-Nek11c and FLAG-Nek11c proteins were stained with anti-GFP and anti-FLAG antibodies, respectively, (green on merge). DNA was stained with Hoechst 33258 (blue on merge). An additional magnified example is shown in (B). (**C**) RPE1 cells were transiently transfected with FLAG-Nek11c for 24 hrs, then fixed in methanol. Cells were immunostained with anti-acetylated tubulin antibodies to detect stable microtubules (red on merge). FLAG-Nek11c protein was stained with anti-FLAG antibodies (green on merge). Scale bars, 5  $\mu$ m.

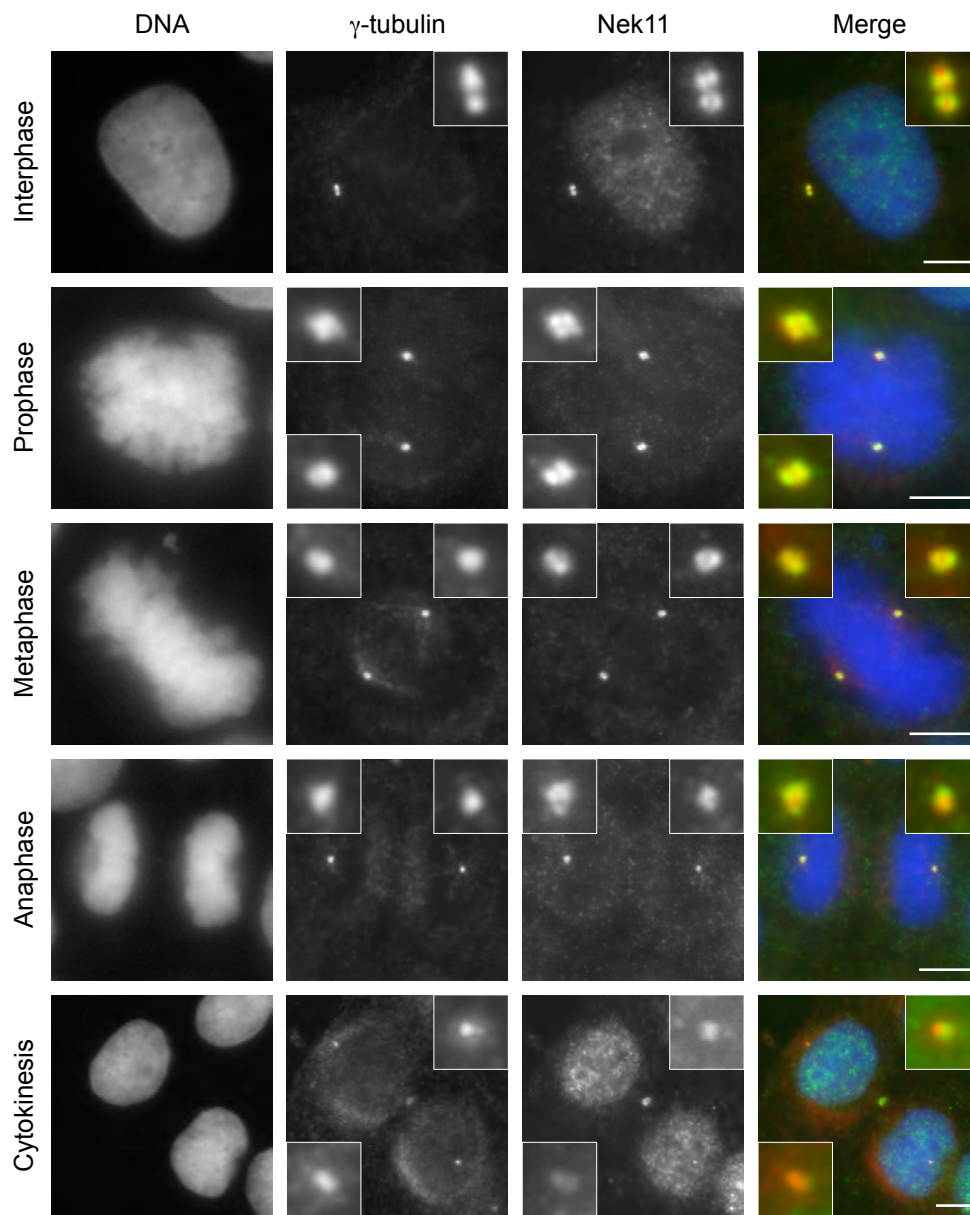


**Figure 4.10 Endogenous Nek11 localises to the nucleus and to centrosomes during interphase and on spindle poles through mitosis**

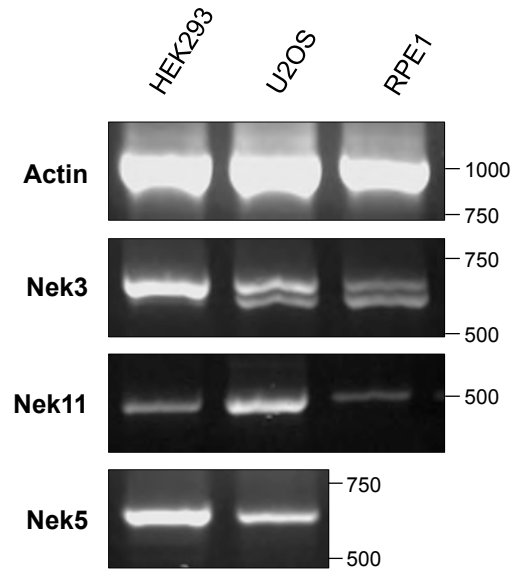
U2OS cells were grown asynchronously on acid-etched coverslips before being pre-extracted, fixed and permeabilised in ice-cold methanol and processed for immunofluorescence microscopy. Cells were immunostained with affinity-purified anti-Nek11 antibodies to detect endogenous Nek11 protein (green on merge). Centrosomes were stained with anti- $\gamma$ -tubulin antibodies (red on merge). DNA was stained with Hoechst 33258 (blue on merge). Scale bars, 5  $\mu$ m.

immunofluorescence microscopy with anti-Nek11 and anti- $\gamma$ -tubulin antibodies. During interphase, Nek11 appeared to be predominantly nuclear and there was clearly co-localisation with  $\gamma$ -tubulin at the centrosome. More specifically, a 1:2 ratio of  $\gamma$ -tubulin:Nek11 dots was observable suggesting that Nek11 was concentrating on the individual centrioles (Figure 4.10). In mitotic cells, Nek11 strongly accumulated at the mitotic spindle poles and as cells progressed through the cell cycle into cytokinesis, the association of Nek11 with spindle poles seemed weaker and the ratio of  $\gamma$ -tubulin:Nek11 returned to a 1:2 ratio in each daughter cell. Furthermore, although Nek11 began to accumulate in the nuclei of the daughter cells a strong signal was detected at the midbody (Figure 4.10). These data support previously published work suggesting that endogenous Nek11 protein is nuclear in interphase cells; however, localisation at centrosomes during interphase and at spindle poles through mitosis has not previously been reported. Additional work will be required to verify these localisation patterns.

#### **4.2.5 Optimisation of RT-PCR conditions for Nek3, Nek5 and Nek11**

In order to begin to assess whether there is any change in Nek3, Nek5 or Nek11 expression through the cell cycle, we undertook semi-quantitative RT-PCR on mRNA extracted from synchronised cell populations. Firstly, primers specific for Nek3, Nek5 and Nek11 were designed that spanned intron sequences so as to avoid amplifying genomic DNA. The Nek3 primers were designed to amplify the region of Nek3 reported to be alternatively spliced (Hernández & Almeida 2006). These primers were tested on mRNA extracted from asynchronous HEK293, U2OS and RPE1 cells (Figure 4.11A). Based on size, results indicated that both Nek3 variants were expressed at similar levels in RPE1 cells. U2OS cells expressed the longer Nek3 variant at higher abundance than the splice variant lacking exon 10; HEK293 cells appeared to express the mRNA for the longer Nek3 variant only (Figure 4.11A). Nek11 mRNA abundance was highest in U2OS cells, whilst mRNA expression levels were comparable in HEK293 and RPE1 cells. Primers specific for Nek11 short and long isoforms were then designed and expression of these was tested

**A**



**B**

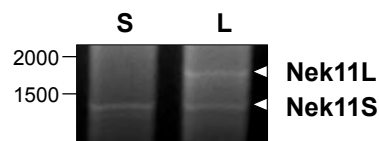


**Figure 4.11 Expression of Nek3, Nek5 and Nek11 mRNA in human cell lines**

**(A)** Cells were lysed using Tri reagent and mRNA isolated. This was used to carry out RT-PCR reactions with primers specific for Nek3, Nek5, Nek11 and actin (positive control) at exon/exon boundaries on the mRNA. Size markers (bp) are indicated on the right. **(B)** Using mRNA extracted from HEK293 cells, expression of Nek11 short (1410 bp) and long (1935 bp) isoforms was analysed using primers specific for either the short isoform (S) or the full length long isoform (L). Size markers (bp) are indicated on the left.

using RNA isolated from HEK293. These primers revealed roughly equal abundance of the two isoforms in HEK293 cells (Figure 4.11B). Nek5 mRNA levels were higher in HEK293 cells than U2OS cells. Expression of this protein kinase at the level of mRNA in asynchronous RPE1 cells is demonstrated in a later experiment (Figure 4.13). This data provides evidence that the cell lines used in this project do express the Nek kinases being studied at least at the level of transcription.

To draw conclusions about comparative mRNA expression levels, conditions for semi-quantitative RT-PCR analysis were then established to optimise PCR cycle number and amount of mRNA added. To optimise cycle number, RT-PCR reactions were carried out with Nek3, Nek5 and Nek11 specific primers on 5 µg total RNA extracted from asynchronous HEK293 cells with cycle numbers increasing from 10-35 cycles in steps of 5 cycles; as control, primers specific for GAPDH were used. Analysis of DNA yield by agarose gel electrophoresis revealed that the optimal cycle number, i.e. clear detection without plateau, was 25 cycles for Nek3, 30 cycles for Nek5 and Nek11, and 15 cycles for GAPDH (Figure 4.12A). To optimise total mRNA content, RT-PCR reactions were carried out on mRNA derived from asynchronous HEK293 cell populations using a range from 0 to 5 µg total mRNA and the optimal number of PCR reaction cycles established for each mRNA. Analysis of DNA yield by agarose gel electrophoresis revealed that the optimal amount of mRNA was 5 µg for Nek3, Nek5 and Nek11, and 1 µg for GAPDH (Figure 4.12B).

Semi-quantitative RT-PCR was then carried out on RNA extracted from synchronized RPE1 cell populations. RPE1 cells were synchronised by thymidine treatment, released for 4 hrs and then treated with nocodazole to arrest cells in M phase with samples collected every 2 hrs after nocodazole addition. The synchrony of these samples was confirmed by flow cytometry (Figure 4.13B). Analysis of RT-PCR products by agarose gel electrophoresis showed that Nek5 mRNA was expressed in asynchronous RPE1 cells. However, its expression was strongly cell cycle regulated being undetectable

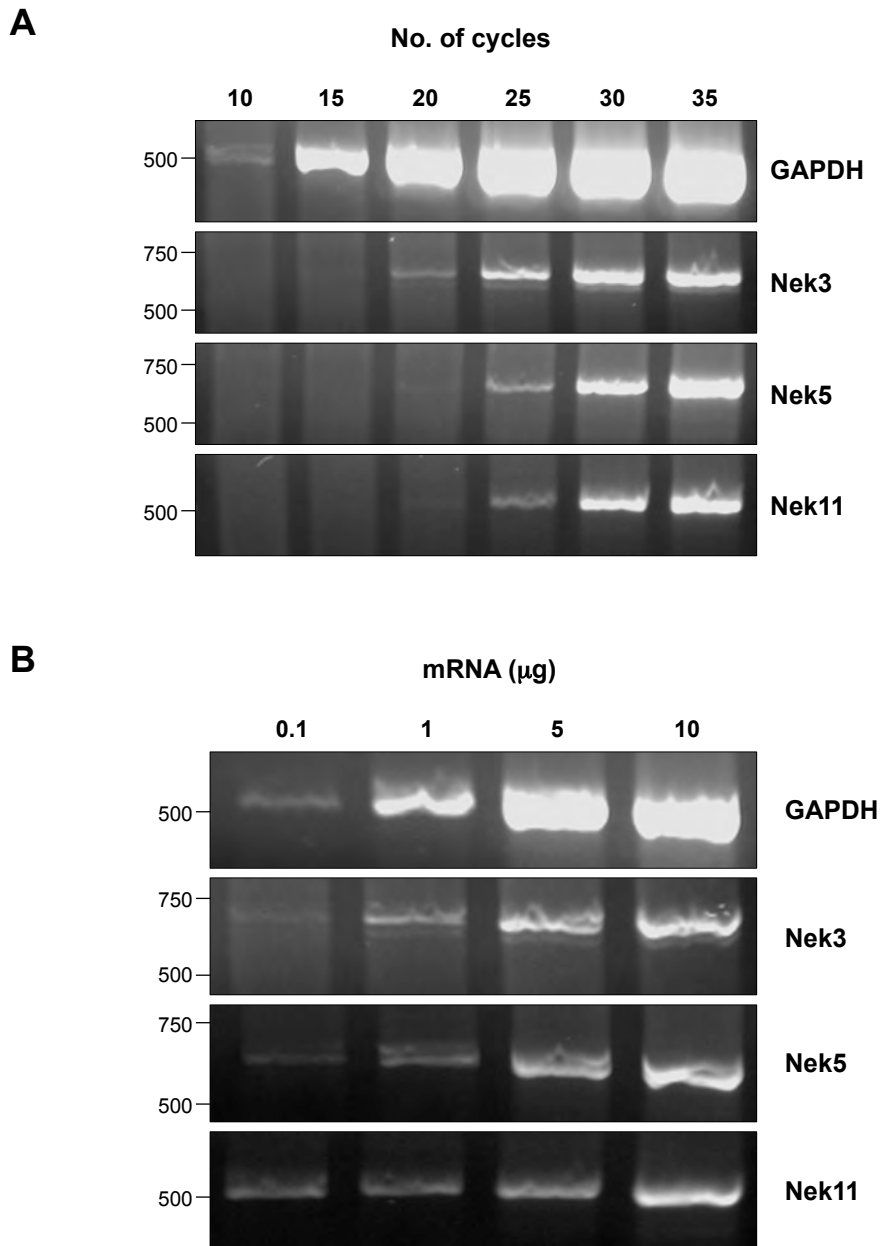


**Figure 4.12 Optimisation of Nek3, Nek5 and Nek11 semi-quantitative RT-PCR**

**(A)** RT-PCR reactions were carried out using Nek3, Nek5, Nek11 or GAPDH primers and increasing number of amplification cycles. 5  $\mu\text{g}$  total RNA from HEK293 cells was used. **(B)** RT-PCR was carried out using Nek3, Nek5, Nek11 or GAPDH primers and increasing amounts of total mRNA as indicated. For Nek3, 25 amplification cycles were used; for Nek5 and Nek11, 30 cycles; and for GAPDH, 15 cycles were used. Size markers (bp) are indicated on the left.

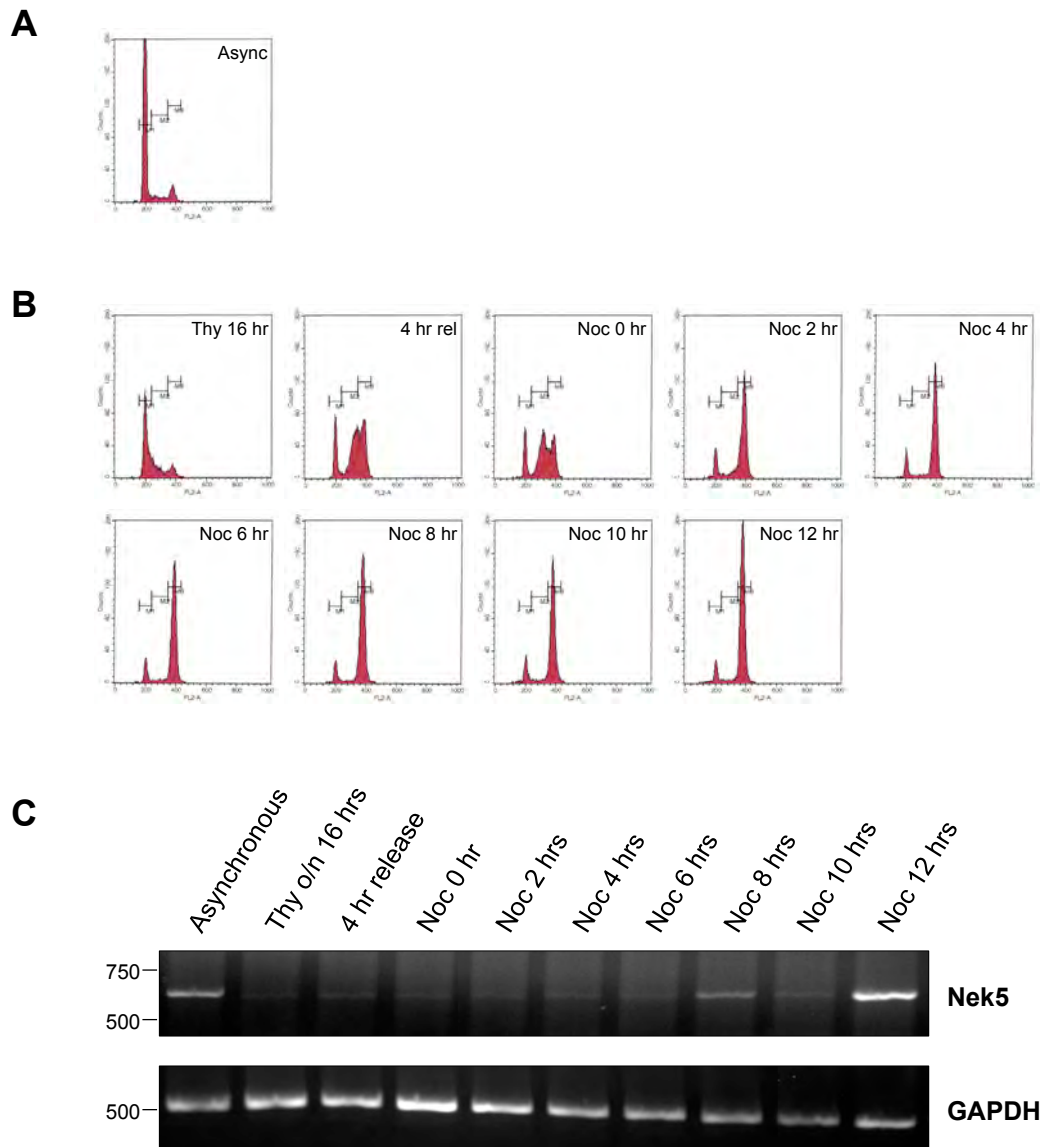


**Figure 4.13 Nek5 mRNA levels are cell cycle regulated**

RPE1 cell synchronisation was confirmed using flow cytometry analysis of cells fixed in 70% ice-cold ethanol and stained with propidium iodide. **(A)** Asynchronous RPE1 cells. **(B)** RPE1 cells were pre-synchronised by incubation with thymidine (Thy) for 16 hours, released from the drug arrest for 4 hours, and then treated with nocodazole (Noc) to arrest cells in M-phase during which time samples were taken every 2 hours for analysis. **(C)** Total RNA was collected from synchronised RPE1 cell samples, and semi-quantitative RT-PCR was performed using specific primers against Nek5 or GAPDH. Size markers (bp) are indicated on the left.

during S and G<sub>2</sub> and only becoming apparent as cells approached M phase (Figure 4.13C).

#### **4.2.6 mRNA expression in human cancer cell lines**

To determine whether Nek3, Nek5 or Nek11 kinases might show altered expression in cancer cell lines, semi-quantitative RT-PCR was carried out on RNA extracted from a control immortalised breast epithelial cell line, HBL100, and a panel of nine colorectal, breast, and pancreatic cancer cell lines. Analysis of the RT-PCR products by agarose gel electrophoresis showed that Nek3 mRNA was expressed as three variants and, in comparison to HBL100, total Nek3 mRNA expression levels were elevated in all cancer cell lines tested (Figure 4.14). A single Nek3 product was generated using HBL100 cells; however, in addition to this band, a larger Nek3 variant was expressed by 3 out of 4 colorectal cancer cell lines (SW480, HT29 and HCT116) and a smaller Nek3 variant was expressed by 3 out of the other 5 cancer cell lines, including those of breast (MDA-MB-468) and pancreatic (AsPc and MIA-Pa-Ca-2) origin. Nek5 mRNA expression was substantially upregulated in 7 out of 9 cancer cell lines including those of colorectal (SW620, SW480, HT29 and HCT116), breast (MDA-MB-468) and pancreatic (BxPc-3 and MIA-Pa-Ca-2) origin, whilst 1 out of 4 pancreatic cell lines (Panc-1) apparently downregulated Nek5 mRNA expression as no product was detected on the agarose gel (Figure 4.14). In comparison to Nek3 and Nek5, the level of Nek11 mRNA expressed in the non-transformed cell line, HBL100, was significantly higher but this then remained relatively constant across the majority of cancer cell lines. Only 2 out of those tested (AsPc and BxPc-3, both of pancreatic origin) showed downregulation of this kinase at the mRNA level (Figure 4.14). In summary, Nek3 shows potentially interesting changes in splicing, Nek5 shows consistently elevated expression, whilst Nek11 exhibits no substantial difference.

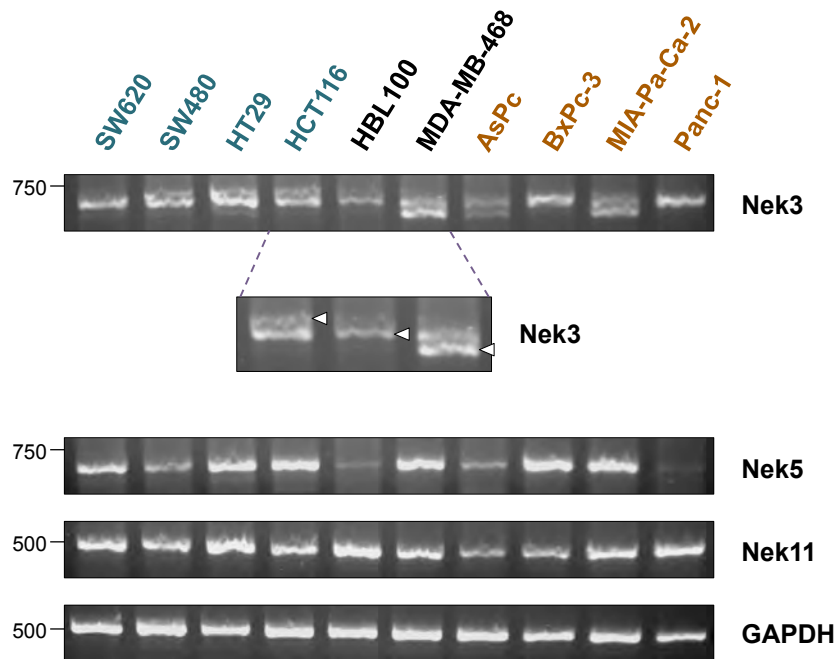


**Figure 4.14 Expression of Nek3, Nek5 and Nek11 mRNA in cancer cell lines**

Semi-quantitative RT-PCR was performed using specific primers against Nek3, Nek5, Nek11 or GAPDH on equalized amounts of total RNA collected from various cancer cell lines (in blue font: colorectal; in black font: breast; in orange font: pancreatic). As control, immortalised breast epithelial cells (HBL100) have been used (bold). Arrows indicate variants of Nek3 expressed. Size markers (bp) are indicated on the left.

#### 4.2.7 Analysis of Nek3 and Nek11c kinase activity *in vitro*

Recombinant purified, active His<sub>6</sub>Nek3 and His<sub>6</sub>Nek11c proteins were commercially available from Millipore Corporation and were therefore used to establish assays and identify a suitable substrate with which to test kinase activity. These recombinant proteins were first characterised by SDS-PAGE and Coomassie Blue staining to check their purity and ensure the recombinant proteins were of the expected molecular weight. Results from this analysis together with data from Western blots using anti-HIS, anti-Nek3 and anti-Nek11 antibodies confirmed the purity and size of the proteins (Figure 4.15).

In terms of substrates, *A. nidulans* NIMA, as well as most known mammalian Neks, phosphorylates  $\beta$ -casein *in vitro* (Osmani et al. 1991; Lu et al. 1993; Letwin et al. 1992; Fry et al. 1995; Minoguchi et al. 2003; Holland et al. 2002). Furthermore, although NIMA kinase activity requires Mg<sup>2+</sup> (Lu et al. 1993), mammalian Neks tend to have a preference for Mn<sup>2+</sup> to co-ordinate the ATP (Letwin et al. 1992; Fry et al. 1995; Holland et al. 2002; Minoguchi et al. 2003). Indeed, Nek3 kinase activity has been successfully measured using  $\beta$ -casein as an exogenous substrate in the presence of Mn<sup>2+</sup> (Tanaka & Nigg 1999) and Mg<sup>2+</sup> (Miller et al. 2005). Similarly, both Mn<sup>2+</sup> and Mg<sup>2+</sup> have been reported as suitable divalent cations for Nek11L kinase assays, although this kinase poorly phosphorylated  $\beta$ -casein, whilst strongly phosphorylating histones (H1, H2A, and H3) and myelin basic protein (Noguchi et al. 2002). Here, in order to establish our own assays,  $\beta$ -casein, Histone H1 or MBP, were tested as substrates for Nek3 and Nek11c in the presence of either Mg<sup>2+</sup> or Mn<sup>2+</sup> divalent cations.

The commercial His<sub>6</sub>Nek3 kinase was first incubated in kinase buffer containing either Mg<sup>2+</sup> or Mn<sup>2+</sup>, [ $\gamma$ -<sup>32</sup>P]-ATP, and either  $\beta$ -casein, MBP or Histone H1 as a substrate for 30 min at 30°C. Analysis of substrate phosphorylation by SDS-PAGE, Coomassie Blue staining and autoradiography demonstrated that  $\beta$ -casein was the best substrate for Nek3 kinase in the presence of Mn<sup>2+</sup> ions,

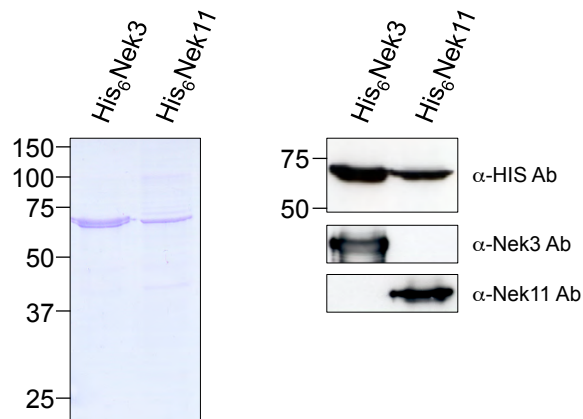


**Figure 4.15 Characterisation of commercial recombinant Nek3 and Nek11c proteins**

His<sub>6</sub>Nek3 and His<sub>6</sub>Nek11c recombinant kinases purchased from Millipore Corporation were subjected to SDS-PAGE, Coomassie Blue staining (left panel) and Western blotting with anti-HIS, anti-Nek3 and anti-Nek11 antibodies (right panel). Molecular weights (kDa) are indicated.

whilst the presence of  $Mg^{2+}$  ions strongly inhibited phosphorylation of  $\beta$ -casein by Nek3 (Figure 4.16). Under these conditions, Nek3 underwent autophosphorylation, although this was most obvious in the presence of weaker exogenous substrates (Figure 4.16). This is most likely due to  $\beta$ -casein competing with autophosphorylation in the presence of this substrate.

His<sub>6</sub>Nek11c kinase was also tested using the experimental assay described above. However, an additional pre-activation step was found to be required for kinase activity. His<sub>6</sub>Nek11c was incubated in kinase buffer containing either  $Mg^{2+}$  or  $Mn^{2+}$ , and either  $\beta$ -casein, MBP or Histone H1 for 30 min at 30°C to first activate the kinase.  $[\gamma\text{-}^{32}\text{P}]\text{-ATP}$  was then added and the samples were incubated for a further 30 min at 30°C. Analysis of substrate phosphorylation by SDS-PAGE, Coomassie Blue staining and autoradiography demonstrated that although  $\beta$ -casein was a good exogenous substrate, MBP was the best substrate for Nek11c kinase in the presence of  $Mg^{2+}$  ions, whilst the presence of  $Mn^{2+}$  ions inhibited phosphorylation of these substrates by this kinase (Figure 4.17). Under these conditions, autophosphorylation of Nek11c could not be seen presumably because autophosphorylation had occurred during the activation step in the absence of  $[\gamma\text{-}^{32}\text{P}]\text{-ATP}$  (Figure 4.17).

In further experiments using  $\beta$ -casein, it was found that the kinase activities of both Nek3 and Nek11c was sensitive to salt concentration with phosphorylation greatest in the absence of NaCl, and reduction with increasing concentrations of NaCl (Figure 4.18). Hence, salt inhibits both Nek3 and Nek11c kinase activity, as observed for Nek2 (Fry et al. 1995). Autophosphorylation of Nek3 and Nek11c could be detected most prominently in the absence of substrate (Figure 4.18).

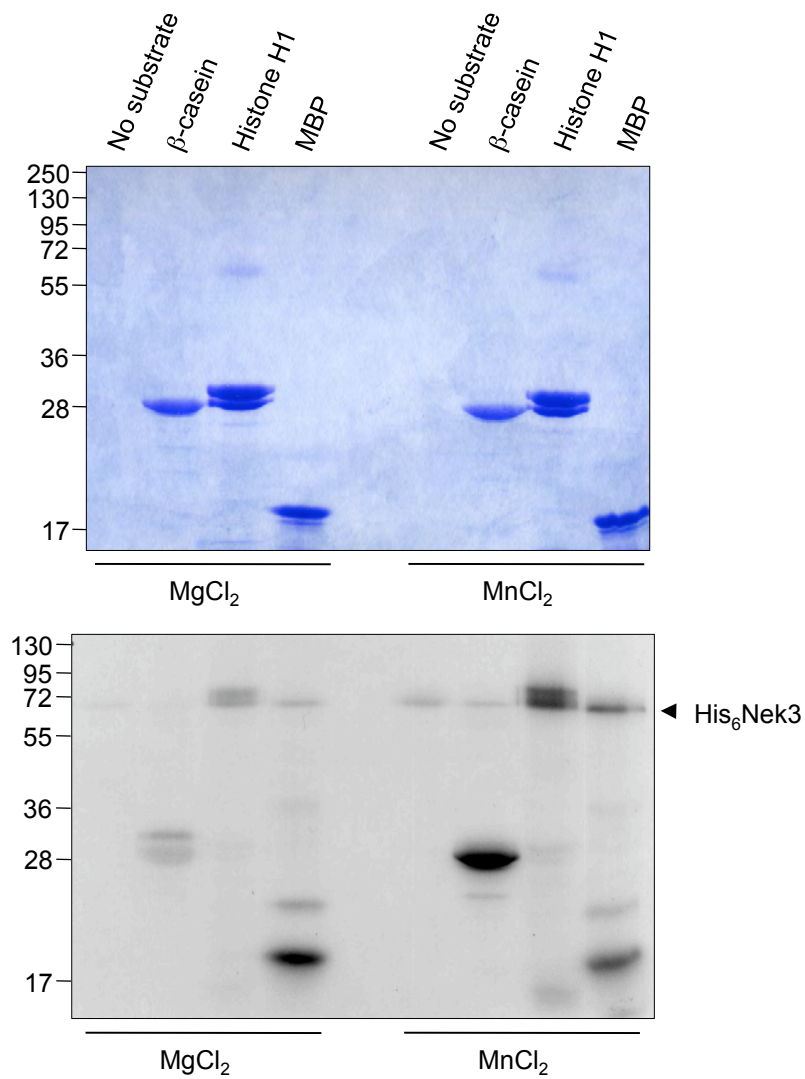


**Figure 4.16 β-casein is a good *in vitro* substrate for the Nek3 kinase**

His<sub>6</sub>Nek3 recombinant kinase was incubated in kinase buffer containing [ $\gamma$ -<sup>32</sup>P]-ATP and either β-casein, Histone H1, or MBP as a substrate for 30 min at 30°C. Samples were subjected to SDS-PAGE, Coomassie Blue staining (upper panel) and autoradiography (lower panel). Arrowhead indicates autophosphorylated His<sub>6</sub>Nek3. Molecular weights (kDa) are indicated on the left.

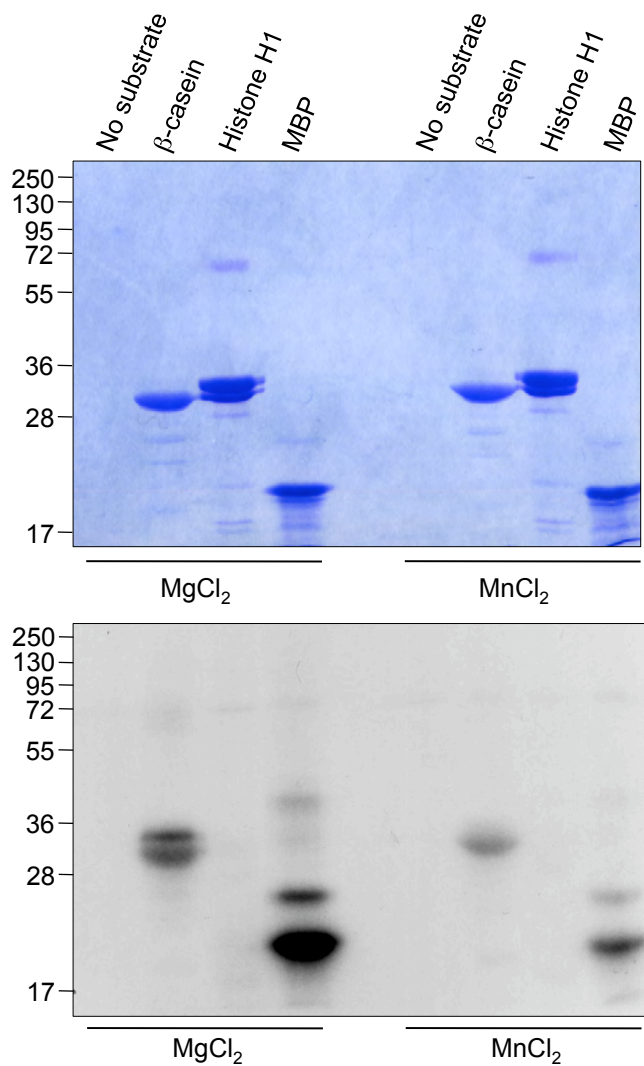


**Figure 4.17 MBP is a good *in vitro* substrate for the Nek11c kinase**

His<sub>6</sub>Nek11c recombinant kinase was incubated in kinase buffer containing either β-casein, Histone H1, or MBP as a substrate for 30 min at 30°C to pre-activate the kinase. Then [ $\gamma$ -<sup>32</sup>P]-ATP was added and incubated for a further 30 min at 30°C. Samples were subjected to SDS-PAGE, Coomassie Blue staining (upper panel) and autoradiography (lower panel). Molecular weights (kDa) are indicated on the left.

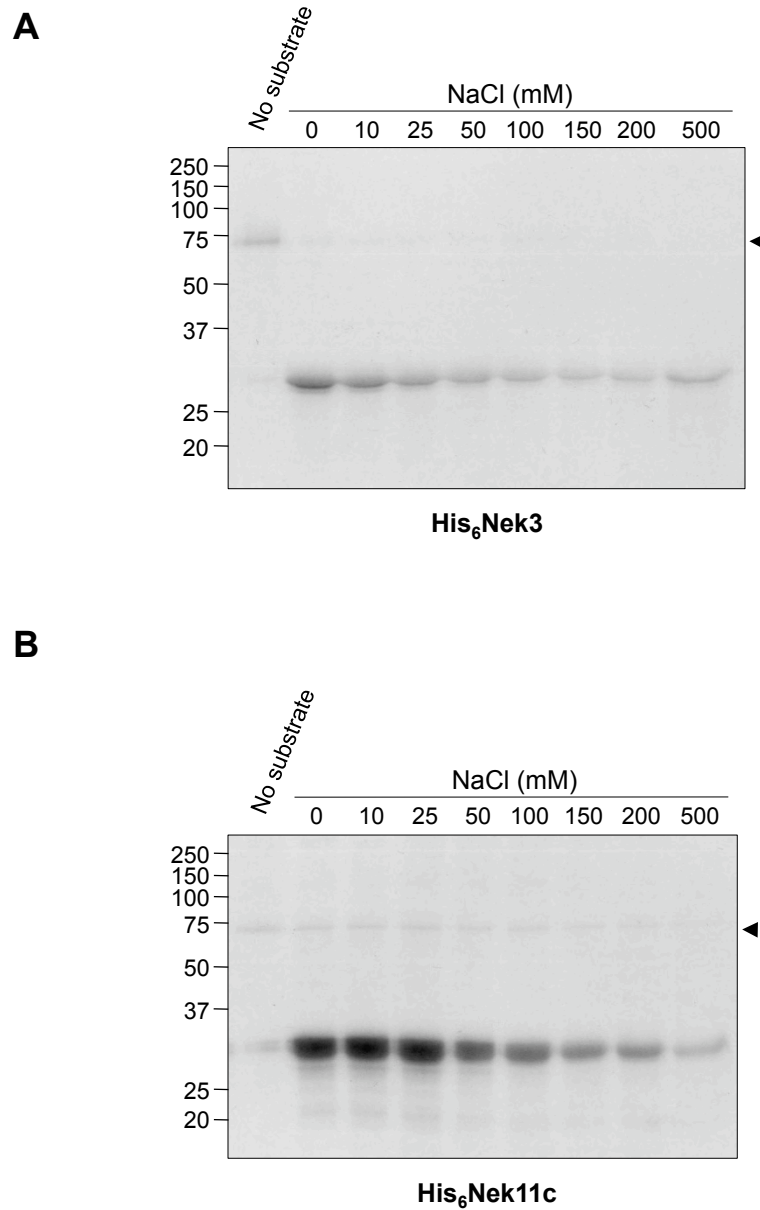


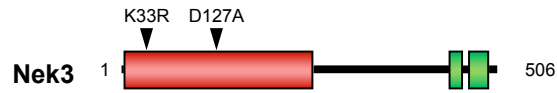
**Figure 4.18 NaCl inhibits Nek3 and Nek11c kinase activity *in vitro***

(A) His<sub>6</sub>Nek3 and (B) His<sub>6</sub>Nek11c recombinant kinases were incubated in kinase buffer containing  $\beta$ -casein, increasing concentrations of NaCl (as indicated), and [ $\gamma$ -<sup>32</sup>P]-ATP for 30 min at 30°C. Samples were subjected to SDS-PAGE, Coomassie Blue staining and autoradiography. Arrowheads indicate kinase autophosphorylation. Molecular weights (kDa) are indicated on the left.

#### **4.2.8 Assay for Nek3 activity from transfected cells**

To establish Nek3 kinase assays from transfected cells, a catalytically inactive mutant was generated by mutating the critical catalytic residues, Lys33 and Asp127 (Figure 4.19A). eGFP-tagged wild-type Nek3 and the K33R/D127A mutant were expressed in HEK293 cells for 24 hrs after which cell lysates were prepared. Transfection efficiency was determined by analysing samples of the lysates by SDS-PAGE and Western blotting with anti-GFP antibodies (Figure 4.19B). An equal amount of protein from each lysate was then subjected to immunoprecipitation with anti-GFP antibodies. Successful immunoprecipitation was confirmed by analysing samples of immune complexes by SDS-PAGE and Western blotting with anti-GFP antibodies (Figure 4.19B). The remaining immune complexes were used in a kinase assay with  $\beta$ -casein as substrate. Analysis of substrate phosphorylation by SDS-PAGE, Coomassie Blue staining and autoradiography demonstrated that wild-type Nek3 strongly phosphorylated  $\beta$ -casein substrate and was capable of autophosphorylation, whilst the double mutation (K33R/D127A) resulted in complete loss of kinase activity and loss of autophosphorylation (Figure 4.19B).

**A**



**B**

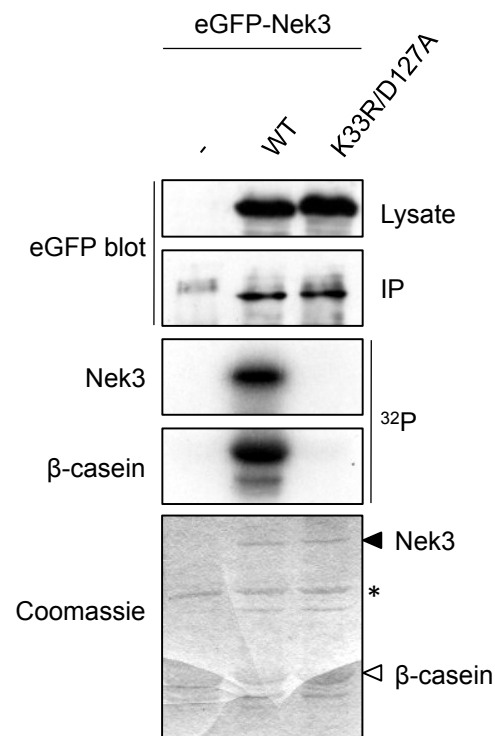


**Figure 4.19 Kinase assay of immunoprecipitated Nek3**

**(A)** Schematic representation of the Nek3 kinase-inactive mutant. Amino acid residues that have been mutated are indicated. **(B)** HEK293 cells were transiently transfected with eGFP-tagged Nek3 constructs, as indicated, for 24 h before cells were lysed and subjected to immunoprecipitation with anti-GFP antibodies. The amount of kinase precipitated was determined by Western blotting with anti-GFP antibodies and the immunoprecipitates used for kinase assays, with  $\beta$ -casein as a substrate. Autoradiographs ( $^{32}\text{P}$ ) are shown of the Nek3 and  $\beta$ -casein proteins. The asterisk (\*) indicates IgG heavy chain.

### 4.3 Discussion

Those Neks from mammals and lower eukaryotic species for which a function is known are involved in microtubule organisation, cell cycle regulation and ciliogenesis. However, for Nek3, Nek5 and Nek11, there was no clear idea of their cellular function at the onset to this project. It was therefore of considerable interest to optimise conditions that would enable the subcellular localisation, expression and activity of these less well researched Neks to be determined, and to test to what extent these properties resembled those of the other Neks.

Typically, mitotic protein kinases are localized to subcellular structures where they exert their effects at the appropriate time. Here, examination by immunofluorescence microscopy of the subcellular distribution of recombinant proteins indicated that in U2OS cells Nek3 is a cytoplasmic protein at interphase, but appears to become associated with fibrous spindle-like structures during prophase/prometaphase and metaphase, and the spindle midzone during anaphase. There was though no apparent localisation to centrosomes or spindle poles. This pattern of localisation suggests that Nek3 may have a role in regulation of mitotic spindle organisation. However, further studies using antibodies to co-stain spindle microtubules (e.g.  $\alpha$ -tubulin) would be required to confirm localisation of recombinant Nek3 to mitotic spindle structures. Interestingly, in a different mammalian cell type, RPE1 cells, the subcellular distribution of recombinant Nek3 was also cytoplasmic but, in addition, recombinant Nek3 localised to the centrosome.

The cytoplasmic localisation of Nek3 is consistent with published research (Tanaka & Nigg 1999; Miller et al. 2007). However, no previous studies identified association with either centrosomes or mitotic spindle fibres. However, this data was obtained upon overexpression of a recombinant tagged protein. Hence, it is possible that this may be an artefact of overexpression. Hence, it will be essential to use a Nek3 specific antibody to study localisation

of the endogenous kinase and confirm data observed with overexpressed protein. Several Nek3 antibodies are commercially available; however, they need to be characterised for use in different applications. The anti-Nek3 antibody described in Chapter 3 was considered not suitable for immunofluorescence microscopy analysis with fixation conditions used here as the antibody signal was too weak to observe. However, it is also possible that endogenous Nek3 expression was too low for the antibody to detect. Overall, this data does fit the postulated cytoplasmic role for Nek3 in prolactin signalling (Miller et al. 2005). Nek3 has been shown to interact with and contribute to the prolactin-mediated phosphorylation of the guanine nucleotide exchange factor Vav2 (Miller et al. 2005), which when activated, targets downstream effectors including the Rho family of GTP binding proteins (Abe et al. 2000; Miller et al. 2005). Activation of the Rho family has been linked to cytoskeletal reorganisation (Miller et al. 2005; Miller et al. 2007), supporting a role for Nek3 in regulation of the actin cytoskeleton.

As with Nek3, the subcellular localisation of recombinant Nek11c was predominantly cytoplasmic in the cell types tested. In previous studies, data on the localisation of recombinant Nek11 isoforms has not been presented using immunofluorescence microscopy analysis, although it has been stated that exogenous Nek11 (isoform not mentioned) is abundant in the cytoplasm (Noguchi et al. 2004). However, using the Nek11 antibody described in Chapter 3, endogenous Nek11 localised to nuclei, as well as centrosomes during interphase and to spindle poles through mitosis. Previous studies also point to a nuclear localisation for Nek11 (Noguchi et al. 2002; Noguchi et al. 2004), and report the major expressed isoform of Nek11 to be Nek11L in somatic cells (Noguchi et al. 2002). Hence, the data suggests that Nek11c localises preferentially to the cytoplasm, but the pattern of localisation observed with Nek11 antibodies support the idea that the major expressed isoform, Nek11L, is probably nuclear. The nuclear localisation of Nek11 observed here would fit the role reported for Nek11 in the DNA damage response pathway (Melixetian et al. 2009). However, further studies are required with recombinant versions of

Nek11L to confirm this hypothesis. Moreover, RNAi is needed to confirm that the localisation detected by the antibodies is indeed Nek11.

In terms of expression, Nek3 mRNA was transcribed in all cancer cell lines examined, but showed interesting differences in the pattern of splice variants depending on the tissue of origin. Previously it has been reported that a total of 4 possible Nek3 mRNA transcripts can be generated due to alternative splicing of exon 10 and a single adenine insertion/deletion polymorphism at the end of exon 9 (Hernández & Almeida 2006) (Table 4.1). Nek3 transcripts can be (i) full length Nek3 (506 aa) with a stretch of 8 adenines; (ii) Nek3-short (299 aa) with a stretch of 7 adenines causing a premature stop codon in Nek3 sequence; (iii) Nek3 $\alpha$  (489 aa) lacking exon 10 with a stretch of 7 adenines; or (iv) Nek3 $\alpha$ -short (298 aa) lacking exon 10 with a stretch of 8 adenines causing a premature stop codon in Nek3 sequence (Hernández & Almeida 2006). A stretch of 8 adenines has been reported to be statistically higher in prostate cancer samples with frequent alterations in the chromosomal region 13q14 where the Nek3 gene is located, whereas normal controls had a higher frequency of 7 adenine nucleotides (Hernández & Almeida 2006). This could apply to the data found here: control HBL100 cells may be expressing mRNA encoding Nek3 $\alpha$  which has a stretch of 7 adenines, whilst, in addition to this transcript, cancer cell lines of colorectal origin may be expressing Nek3 full length (stretch of 8 adenines). This would explain the presence of a larger band on an agarose gel. Meanwhile, the cancer cell lines of breast and pancreatic origin may be expressing Nek3 $\alpha$ -short (stretch of 8 adenines) hence producing a smaller sized band on the agarose gel. This of course needs to be further investigated by sequencing the different Nek3 RT-PCR products from the various cancer cell lines to confirm the association between the type of cancer and Nek3 variant expressed.

Recent research has demonstrated that Nek11 is highly expressed in 35% of colon adenomas and carcinomas in comparison to normal tissue (Sørensen et al. 2010). Data presented here did not detect any significant alteration in Nek11

Genome	Alternatively spliced (skips exon 10)?	mRNA length exon 8-11 (bp)	Premature stop codon?	Protein length (aa)
<b>Nek3-FL</b> A8 : A8	<i>x</i>	431	<i>x</i>	506
<b>Nek3-short</b> A7 : A7	<i>x</i>	431-1	<b>yes</b>	299
<b>Nek3<math>\alpha</math></b> A7 : A7	<b>yes</b>	381	<i>x</i>	489
<b>Nek3<math>\alpha</math>-short</b> A8 : A8	<b>yes</b>	381+1	<b>yes</b>	298

**Table 4.1 Potential Nek3 variants**

A table summarising the four possible Nek3 variants reported by Hernández & Almeida (2006) that can be generated as a result of alternative splicing of exon 10 and a single adenine insertion/deletion polymorphism at the end of exon 9.

mRNA expression levels in the cancer cells lines examined, although a small decrease in expression was observable in 2 out of 4 pancreatic cancer cell lines. Using the affinity-purified antibody, Nek11 protein expression in various cancer cell lines can now be examined to determine whether there are significant alterations in cancer cells.

In terms of the biochemical properties and *in vitro* substrate specificity of Nek3 and Nek11c, the kinase assays performed here revealed similarities but also differences with the well studied Nek2 kinase. Like *A. nidulans* NIMA, most mammalian Neks phosphorylate  $\beta$ -casein *in vitro* (Osmani et al. 1991; Lu et al. 1993; Letwin et al. 1992; Fry et al. 1995; Minoguchi et al. 2003; Holland et al. 2002) and although NIMA kinase requires  $Mg^{2+}$  (Lu et al. 1993), mammalian Neks tend to have a preference for  $Mn^{2+}$  (Letwin et al. 1992; Fry et al. 1995; Holland et al. 2002; Minoguchi et al. 2003). Supporting these data, Nek3 was found to preferentially phosphorylate  $\beta$ -casein *in vitro* with a preference for  $Mn^{2+}$  as a cofactor. Nek11c, however, displays different properties; although it is capable of phosphorylating  $\beta$ -casein, it has a higher preference for MBP as substrate and prefers the presence of  $Mg^{2+}$  as a cofactor. With *in vitro* kinase assays established for these two Neks, their activity during cell cycle progression could be assessed to better understand whether they might have roles in cell cycle control.

Interestingly, data in this chapter provide the first evidence not only that Nek5 is a nuclear protein but also that it localises to centrosomes in dividing cells. This is studied in more detail in the subsequent chapters. Nek5 mRNA expression may be cell cycle regulated as an increase at the  $G_2/M$  transition was observed. However, this needs to be repeated. Also of interest, was the observation that Nek5 expression was elevated in 7 out of the 9 cancer cell lines analysed including those of colorectal, breast and pancreatic origin.

Overall, further characterisation of Nek3 and Nek11 function can now be studied using the reagents developed and experimental conditions optimised here. However, due to the intriguing localisation and expression data on Nek5, together with the lack of published data on Nek5, we decided to focus on Nek5 for the remainder of this project. We hypothesised that Nek5 may contribute to regulation of centrosomes through the cell cycle and so further experiments presented in this thesis were designed to test this specific hypothesis.

## **Chapter 5**

### **Subcellular localisation of Nek5**

## 5.1 Introduction

The eukaryotic cell is a highly ordered system where the subcellular localisation of proteins at particular sites is critical for its structural and functional integrity. Hence, determining the subcellular localisation of a protein kinase gives an important clue to understanding its functions and potential substrates and interacting partners. Here, the subcellular localisation of Nek5 was investigated to provide insights into its function.

The localisation of NIMA and a few of the mammalian Neks has been studied indicating potential roles in cell cycle progression and ciliogenesis. An enrichment of recombinant NIMA in subnuclear regions undergoing chromosome condensation was demonstrated, and as cells progressed further into mitosis, NIMA displayed staining on spindle microtubules and at spindle pole bodies (De Souza et al. 2000). The revelation of a chromatin-like pattern of localisation for NIMA led to its correlation with histone H3 phosphorylation in early mitosis suggesting a role for NIMA in chromatin condensation. Localisation to spindle microtubules and spindle pole bodies strengthened the hypothesis that this kinase has a role in regulating microtubule dynamics during spindle formation (De Souza et al. 2000; Osmani et al. 1988). Mammalian Nek2 has been shown to localise to centrosomes, where it plays a role in centrosome disjunction at the G<sub>2</sub>/M transition (Fry et al. 1998b). Activated Nek9 has been shown to concentrate on spindle poles during mitosis leading to suggestions that this protein kinase may play a role in regulating spindle organisation (Roig et al. 2005). Nek7, a downstream target of Nek9, has been reported to localise to centrosomes in interphase and mitosis leading to proposals that this protein kinase also contributes to organisation of spindle microtubules (Kim et al. 2007). Similarly, Nek6, another substrate of Nek9, plays a role in mitotic spindle organisation localising to spindle poles in early mitosis, and to microtubules of the mitotic spindle and central spindle (O'Regan & Fry 2009). In contrast, Nek1 and Nek8 have been implicated in cilia function, with Nek8 localising to the inversin compartment in the proximal region of primary cilia (Mahjoub et al. 2005), and Nek1 localising to primary cilia, basal

bodies, centrosomes and nuclei (Mahjoub et al. 2005; Shalom et al. 2008; Hilton et al. 2009).

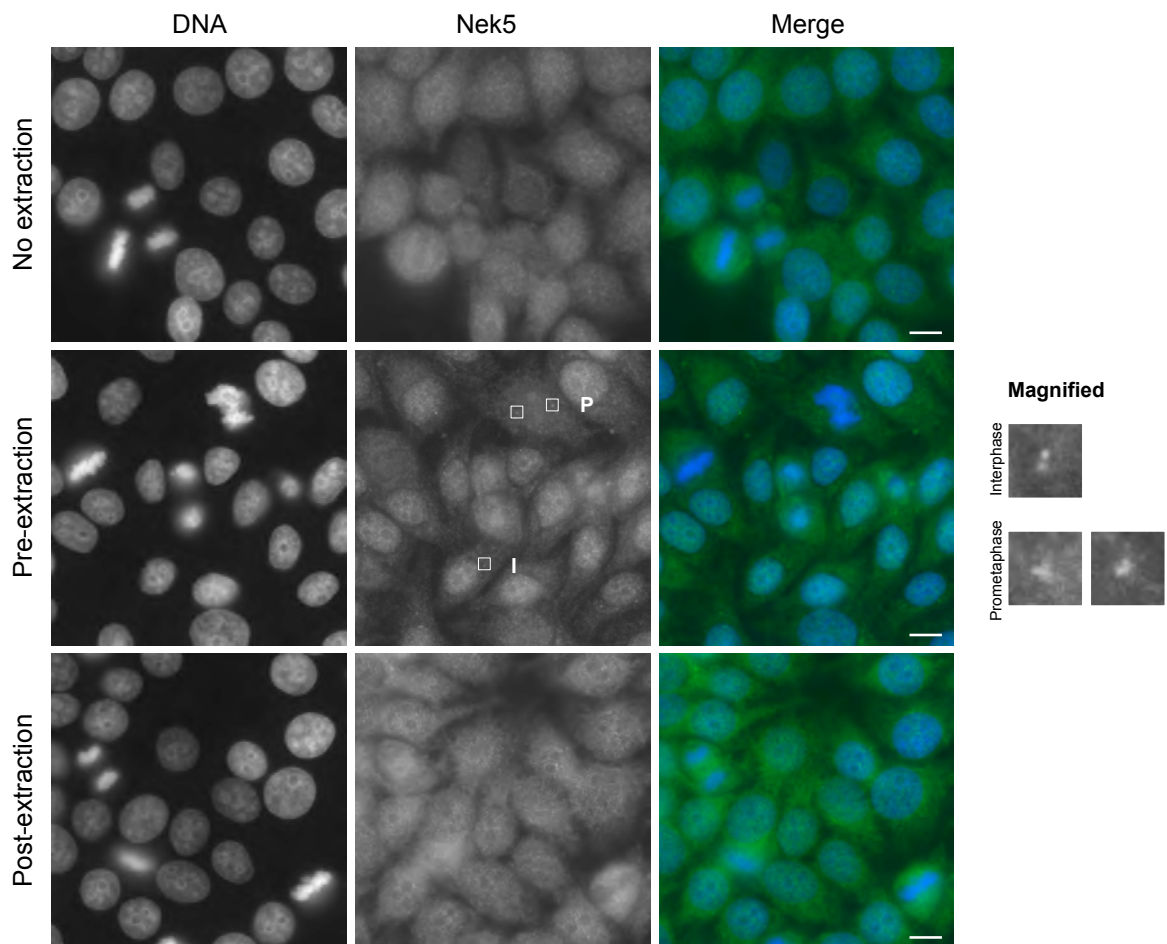
Hence, the conserved theme is that these Neks localise to structures where they perform functions in regulating microtubules in dividing and non-dividing cells. In the previous chapter, recombinant Nek5 protein was found to localise to cell nuclei and centrosomes in interphase. Here, the localisation of human Nek5 was characterised in more detail to determine whether or not this kinase also plays a role in microtubule organisation.

## 5.2 Results

### 5.2.1 Cell-cycle dependent localisation of endogenous Nek5

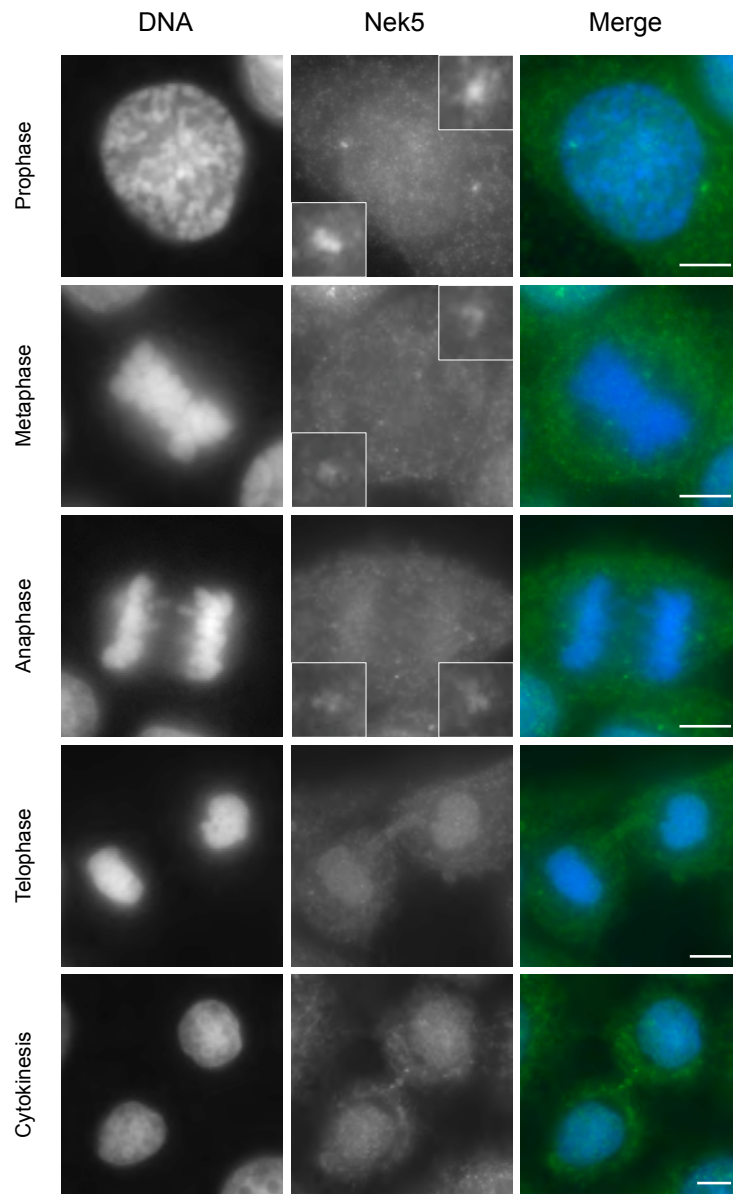
To study the subcellular localisation of endogenous Nek5, the affinity-purified anti-Nek5 antibodies were used in combination with different extraction techniques. This was done based on previous studies shown in Chapter 4 which indicate that this could improve imaging of proteins localised to insoluble structures by removing soluble proteins. Prior to processing U2OS cells for immunofluorescence microscopy, asynchronously growing cells were either fixed and permeabilised with ice-cold methanol (Figure 5.1 upper panel), pre-extracted in Triton X-100 buffer and then fixed with methanol (Figure 5.1 middle panel), or fixed and permeabilised with ice-cold methanol and then post-extracted in NP-40 buffer (Figure 5.1 lower panel). Cells that were fixed and analysed without extraction or post-extracted showed a diffuse whole cell stain. However, following pre-extraction, the affinity-purified anti-Nek5 antibody more clearly detected a nuclear localisation in interphase cells. Furthermore, centrosome-like dots could also be detected using this technique. Examination of pre-extracted mitotic U2OS cells revealed that during prophase, staining could be observed at the separated centrosomes; however, this localisation to spindle poles weakened as cells progressed through metaphase and anaphase. By telophase and cytokinesis, staining was no longer visible at the spindle poles but became focused once more in nuclei of daughter cells (Figure 5.2). The similarity of the nuclear and centrosome stain with this antibody and the recombinant protein (Figure 4.6) strongly suggest that this pattern is genuinely reflective of Nek5.

In order to confirm that the staining pattern observed did reflect centrosomes, pre-extracted U2OS cells were fixed and processed for immunofluorescence microscopy using anti-Nek5 antibodies and anti- $\gamma$ -tubulin antibodies as a marker for centrosomes. Nek5 co-localised with  $\gamma$ -tubulin at centrosomes in interphase, and to spindle poles during prophase, metaphase and anaphase of mitosis (Figure 5.3A). To strengthen the observation that Nek5 localisation at



**Figure 5.1 Comparison of staining patterns with Nek5 antibodies in U2OS cells upon different fixation-extraction techniques**

**Upper panel:** U2OS cells were grown on acid-etched coverslips before being fixed and permeabilised with ice-cold methanol and processed for immunofluorescence microscopy. **Middle panel:** U2OS cells were grown on acid-etched coverslips before being pre-extracted in Triton X-100 buffer for 30 secs and then fixed and permeabilised with ice-cold methanol and processed for immunofluorescence microscopy. Detection of Nek5 at centrosomes in interphase (I) and prometaphase (P) cells has been magnified. **Lower panel:** U2OS cells were grown on acid-etched coverslips before being fixed and permeabilised with ice-cold methanol and then post-extracted in NP-40 buffer for 30 secs and processed for immunofluorescence microscopy. Cells were stained with affinity purified anti-Nek5 antibodies (green on merge); DNA was stained with Hoechst 33258 (blue on merge). Scale bars, 10  $\mu$ m.

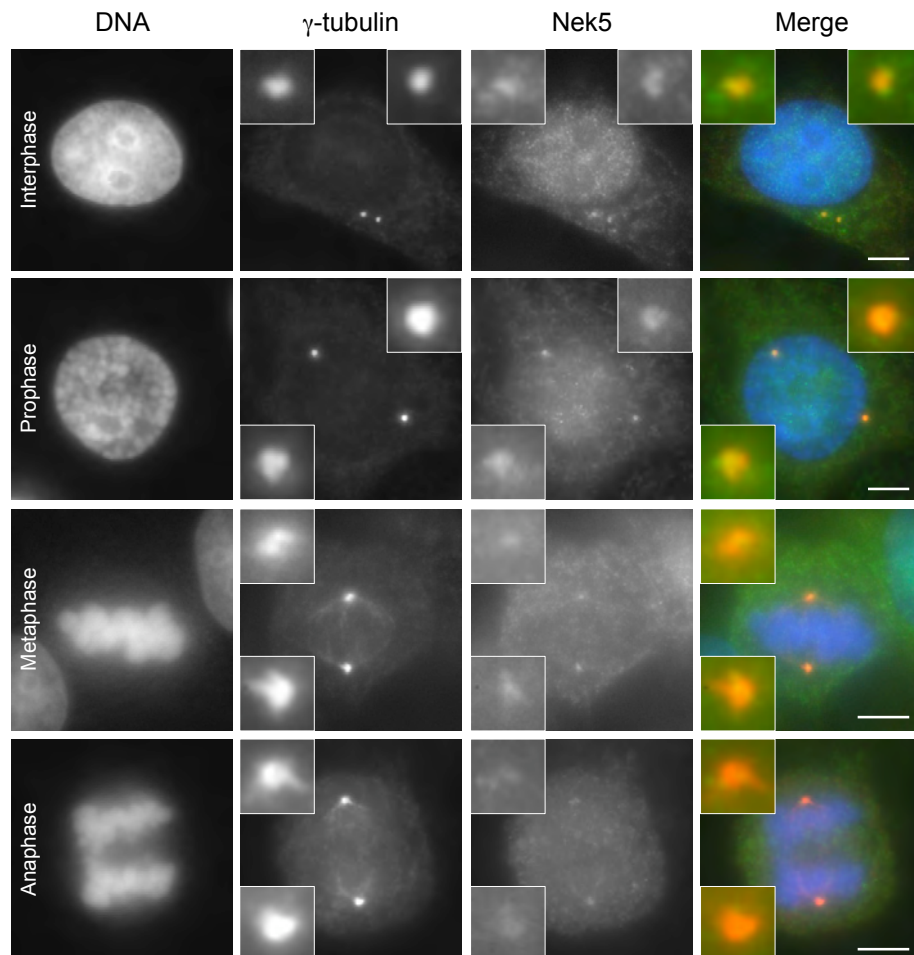
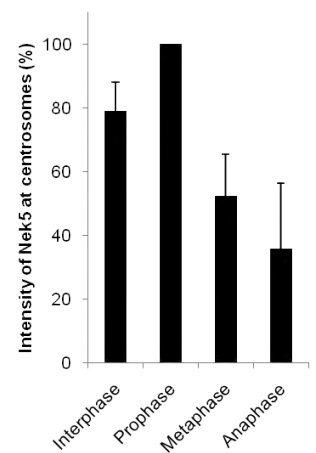


**Figure 5.2 Localisation of endogenous Nek5 protein through mitosis in U2OS cells**

U2OS cells were grown on acid-etched coverslips before being pre-extracted in Triton X-100 buffer, then fixed and permeabilised with ice-cold methanol and processed for immunofluorescence microscopy. Cells at different stages of mitosis were imaged as indicated. Cells were stained with affinity purified anti-Nek5 antibodies (green on merge); DNA was stained with Hoechst 33258 (blue on merge). Scale bars, 5  $\mu$ m.

centrosomes was cell cycle-dependent, the intensity of Nek5 at centrosomes was measured. As staining of centrosomes using the anti-Nek5 antibodies was strongest during prophase, the intensity of centrosomal Nek5 during the other cell cycle stages examined was calculated as percentage intensity of centrosomes in cells at prophase. Data revealed that the intensity of Nek5 at centrosomes in interphase cells was ~80% of cells in prophase. This intensity decreased significantly as cells progressed through mitosis with a level of ~35% at anaphase (Figure 5.3B).

Thus, these data on the subcellular localisation of endogenous Nek5 supports the localisation pattern of recombinant Nek5 described in the previous chapter. Importantly, the specificity of the affinity purified anti-Nek5 antibodies was confirmed using siRNA according to conditions described in Chapter 6. U2OS cells were treated with the Nek5-specific siRNA oligos for 72 hours before being pre-extracted in Triton X-100 buffer and then fixed in methanol. The cells were processed for immunofluorescence microscopy using anti-Nek5 antibodies and anti- $\gamma$ -tubulin antibodies to detect centrosomes. There was no co-localisation of endogenous Nek5 with  $\gamma$ -tubulin at centrosomes upon depletion of Nek5 protein using the siRNA duplexes either individually or combined. In contrast, in mock and GL2 siRNA treated cells, there was co-localisation of the signal detected by anti-Nek5 antibodies at the centrosomes with  $\gamma$ -tubulin (Figure 5.4). The strong nuclear localisation of endogenous Nek5 protein that was observed in mock and GL2 control cells was also lost upon Nek5 siRNA treatment of cells leaving a weaker background staining pattern uniform throughout the cell (Figure 5.4). Hence, the affinity-purified anti-Nek5 antibodies are suitable for immunofluorescence microscopy applications as they specifically detect endogenous Nek5 in nuclei and at centrosomes. Together, these findings provide the first evidence for a cell cycle-dependent localisation of endogenous Nek5 at centrosomes/spindle poles and cell nuclei.

**A****B**

**Figure 5.3 Nek5 localises at centrosomes and spindle poles in a cell cycle-dependent manner**

**(A)** U2OS cells were grown on acid-etched coverslips before being pre-extracted in Triton X-100, then fixed and permeabilised with ice-cold methanol and processed for immunofluorescence microscopy. Cells in interphase and at different stages of mitosis were imaged as indicated. Cells were immunostained with anti- $\gamma$ -tubulin antibodies to detect centrosomes (red on merge) and with affinity purified anti-Nek5 antibodies (green on merge); DNA was stained with Hoechst 33258 (blue on merge). Scale bars, 5  $\mu$ m. **(B)** Histogram displaying the intensity of Nek5 at the centrosome at different cell cycle stages is indicated as a percentage of intensity in cells during prophase minus background intensities; data shown represent means ( $\pm$  S.E.) of at least 20 centrosomes.

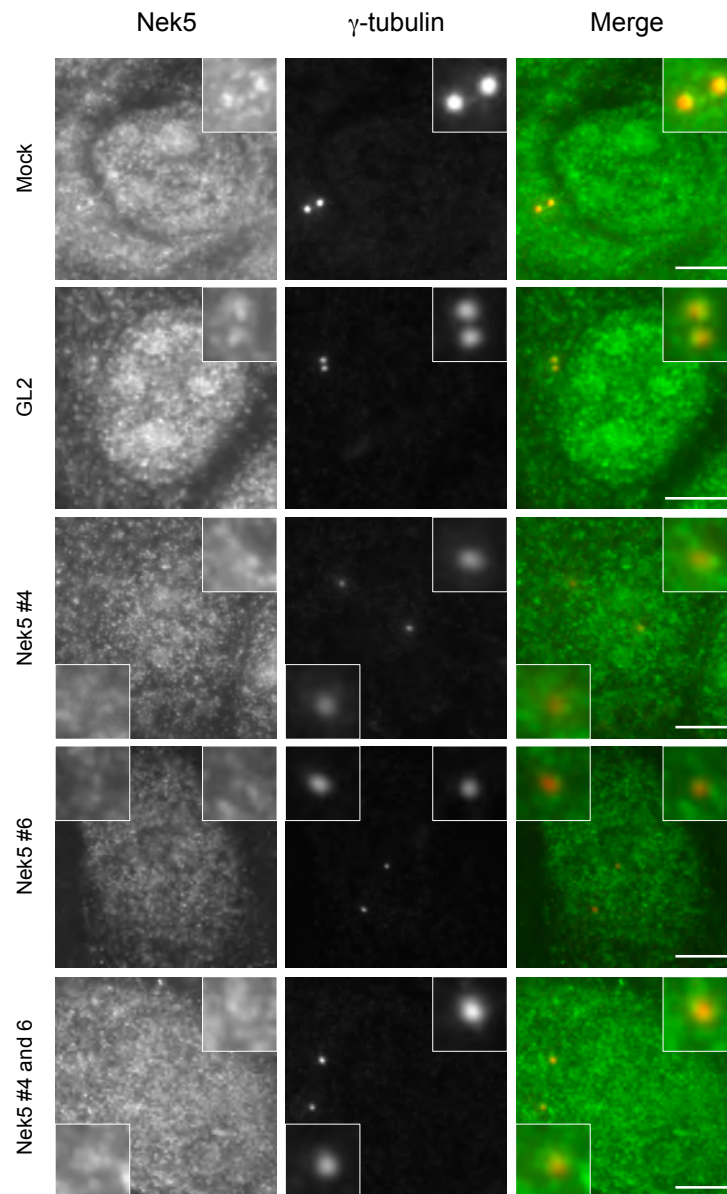


**Figure 5.4 RNAi knockdown of Nek5 leads to loss of centrosome staining**

U2OS cells were either mock transfected or transfected with two individual Nek5 siRNA oligonucleotides (#4, 6), a pool of two siRNA oligonucleotides (#4 and 6), or GL2 specific RNAi oligos for 72 hrs before being pre-extracted then methanol-fixed and immunostained with anti- $\gamma$ -tubulin antibodies to detect centrosomes (red on merge) and with affinity purified anti-Nek5 antibodies (green on merge). Scale bars, 5  $\mu$ m.

### **5.2.2 Nek5 localises to centrosomes and basal bodies in RPE1 cells**

To assess the localisation pattern in a different cell type, asynchronous RPE1 cells were pre-extracted in Triton X-100 buffer and fixed in ice-cold methanol, then processed for immunofluorescence microscopy with affinity purified anti-Nek5 antibodies. Additional co-stains used were either anti- $\gamma$ -tubulin antibodies to detect centrosomes or anti- $\alpha$ -tubulin antibodies to detect the microtubule network. Without an additional co-stain, anti-Nek5 antibodies stained nuclei and appeared to stain centrosomes during interphase (Figure 5.5A). This centrosomal localisation was confirmed by co-localisation with  $\gamma$ -tubulin, whilst co-staining with anti- $\alpha$ -tubulin antibodies demonstrated that the microtubules emanated from the site of Nek5 localisation (Figure 5.5A). Next, RPE1 cells were serum-starved to promote ciliogenesis and after pre-extraction and fixation they were processed for immunofluorescence microscopy with affinity purified anti-Nek5 antibodies and co-stained with anti-acetylated tubulin antibodies to detect microtubule structures, centrosomes and primary cilia. These data showed that endogenous Nek5 co-localised with acetylated tubulin specifically at the two basal bodies of primary cilia (Figure 5.5B).

### **5.2.3 Nek5 localises towards the proximal ends of centrioles**

The centrosome and basal body staining pattern in U2OS and RPE1 cells indicated more specifically a centriolar pattern of localisation for Nek5. Distal-end, centrin, and proximal-end, C-Nap1, centriole markers were therefore used to co-stain cells to confirm this observation. GFP-centrin expressing HeLa cells were grown on acid-etched coverslips then incubated in Triton X-100 pre-extraction buffer prior to fixation in ice-cold methanol. These samples were then processed for immunofluorescence microscopy with anti-Nek5 and anti-GFP antibodies. Endogenous Nek5 was observed localising adjacent to GFP-centrin; more specifically, the pattern of Nek5 localisation was often between the two centrin dots, suggesting a more proximal centriolar localisation of Nek5 (Figure 5.6A). HeLa and U2OS cells were then grown on acid-etched coverslips, incubated in Triton X-100 pre-extraction buffer prior to fixation in ice-cold methanol and processed for immunofluorescence microscopy with anti-

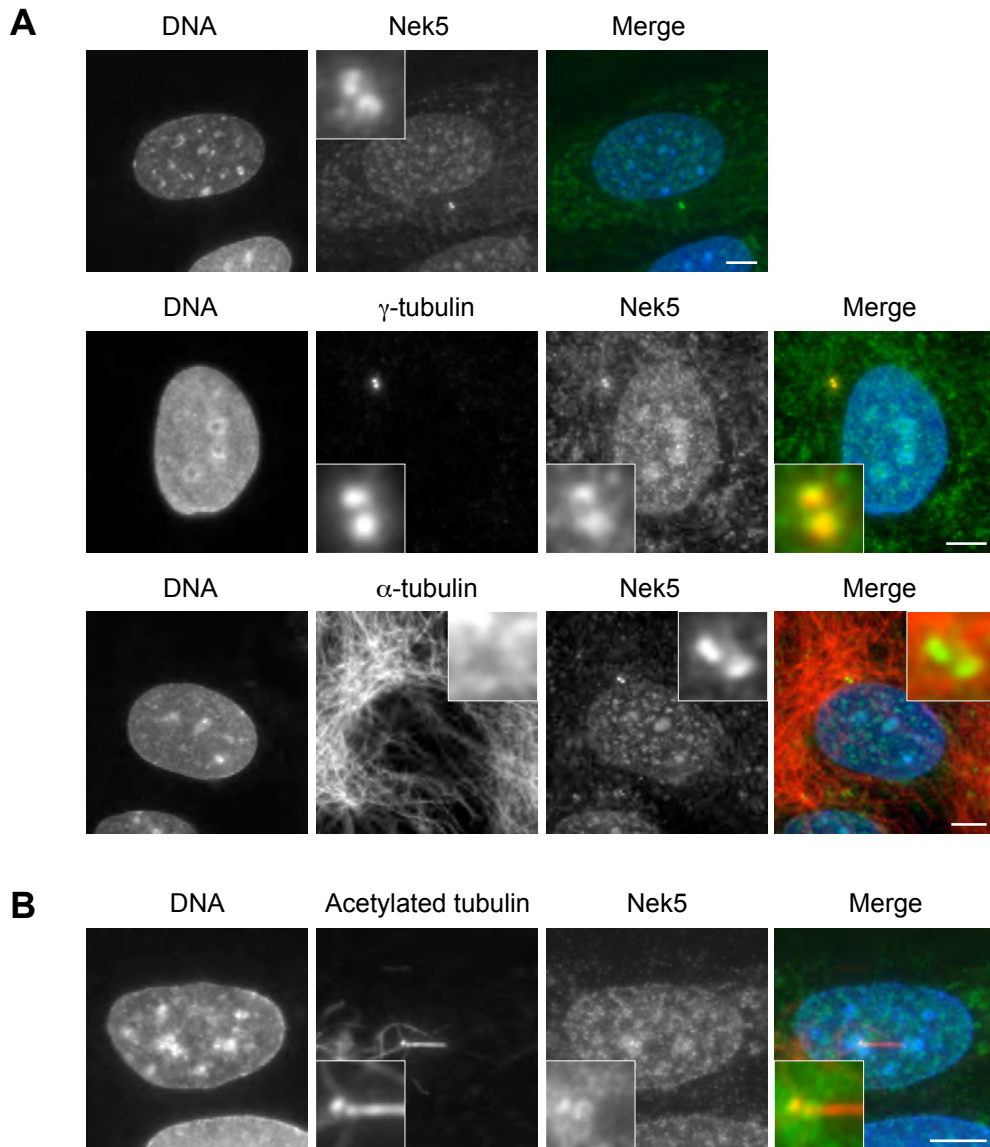


**Figure 5.5 Nek5 localises to centrosomes in cycling RPE1 cells and to basal bodies in ciliated RPE1 cells**

(A) Asynchronous RPE1 cells were grown on acid-etched coverslips before being pre-extracted in Triton X-100 buffer, then fixed and permeabilised with ice-cold methanol and processed for immunofluorescence microscopy. Cells were stained with affinity purified anti-Nek5 antibodies (green on merge) alone, or immunostained with either  $\gamma$ -tubulin antibodies to detect centrosomes or  $\alpha$ -tubulin antibodies to detect microtubules, as indicated (red on merge); DNA was stained with Hoechst 33258 (blue on merge). (B) RPE1 cells were serum starved for 72 hours prior to pre-extraction and fixation as in (A). Cells were stained with affinity purified anti-Nek5 antibodies (green on merge) and acetylated-tubulin antibodies to detect cilia (red on merge); DNA was stained with Hoechst 33258 (blue on merge). Scale bars, 5  $\mu$ m.

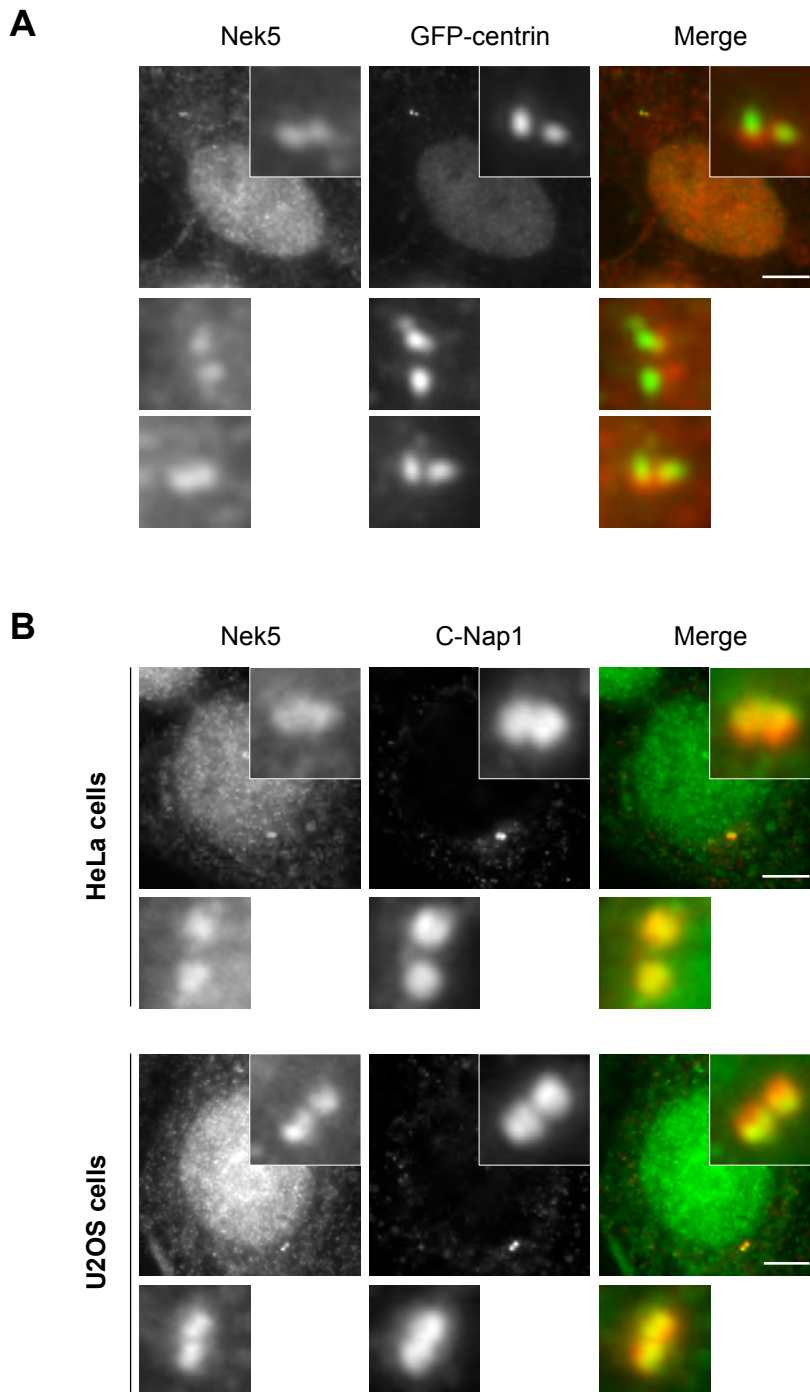


**Figure 5.6 Nek5 localises towards the proximal ends of centrioles**

**(A)** HeLa-GFP-centrin cells were grown on acid-etched coverslips before being pre-extracted in Triton X-100, then fixed and permeabilised with ice-cold methanol and processed for immunofluorescence microscopy. Cells were stained with affinity purified anti-Nek5 antibodies (red on merge) and anti-GFP antibodies (green on merge). Two additional magnified examples are shown. **(B)** HeLa and U2OS cells were grown on acid-etched coverslips before being pre-extracted in Triton X-100 buffer, then fixed and permeabilised with ice-cold methanol and processed for immunofluorescence microscopy, as indicated. Cells were stained with affinity purified anti-Nek5 antibodies (green on merge) and anti-C-Nap1 antibodies (red on merge). An additional magnified example is shown in each case. Scale bars, 5  $\mu$ m.

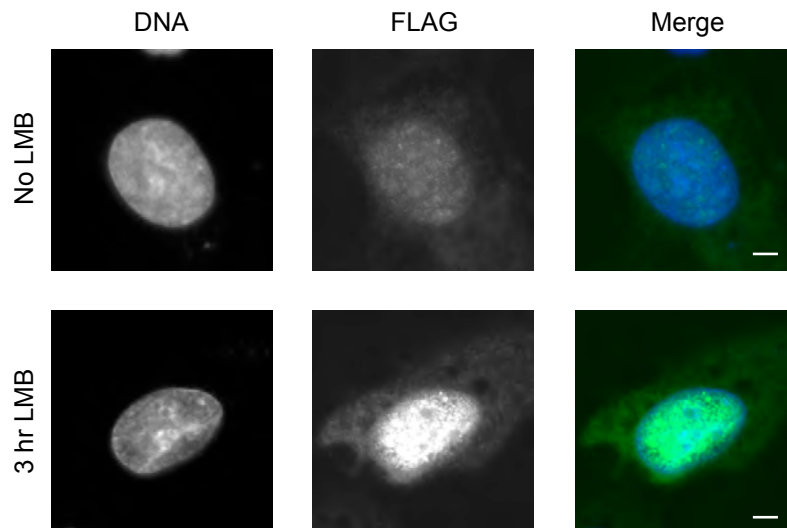
Nek5 and anti-C-Nap1 antibodies. There was a much closer overlap, albeit still not precise, between these two antibodies than between centrin and Nek5 antibodies (Figure 5.6B). Based on this evidence we propose that Nek5 is localised close to the proximal ends of centrioles.

#### **5.2.4 Nek5 accumulates in the nucleus upon inhibition of nuclear export**

As recombinant Nek5 displayed a nuclear localisation in interphase cells, we next investigated the nuclear translocation of this protein. The drug Leptomycin B (LMB) binds to and inhibits CRM1, an essential protein required for nuclear export of proteins containing nuclear export signals (NES). To test the effects of LMB on the subcellular localisation of Nek5, U2OS cells were transiently transfected with FLAG-Nek5 and then treated for 3 hrs with LMB 24 hrs post-transfection. Following fixation in ice-cold methanol, cells were processed for immunofluorescence microscopy with anti-FLAG antibodies. In cells treated with LMB, the relative intensity of FLAG-Nek5 within nuclei, as compared to the cytoplasm, was significantly increased in comparison to untreated cells, indicating that this protein accumulated in the nucleus in response to LMB treatment (Figure 5.7). This suggests that Nek5 either has a functional NES that is blocked by LMB or that Nek5 exits the nucleus via interaction with another NES-bearing protein.

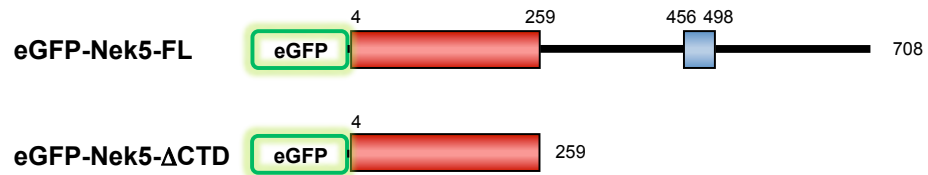
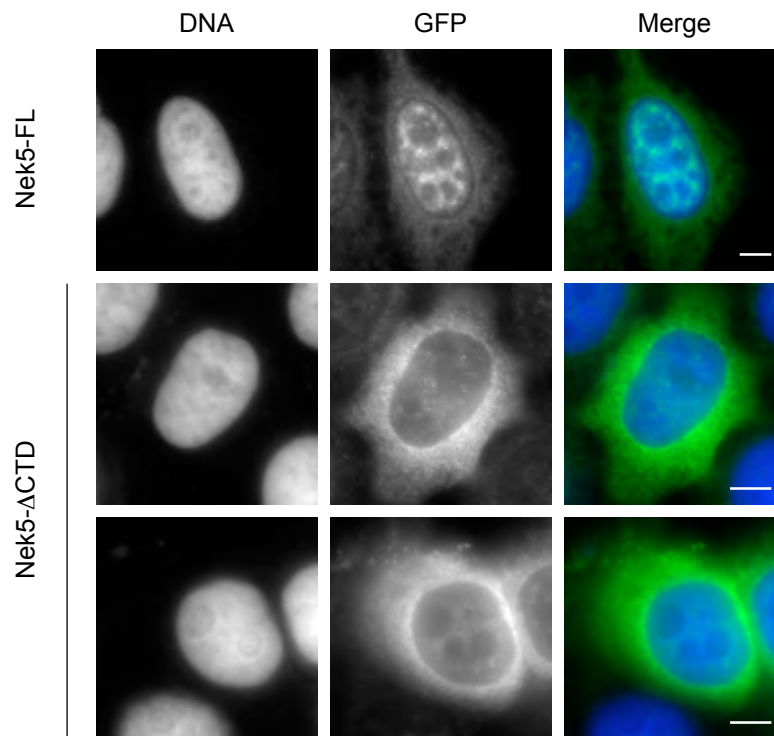
#### **5.2.5 Nek5 nuclear localisation is dependent on residues 380-460**

In order to determine the region of Nek5 responsible for its nuclear localisation, a truncated Nek5 construct lacking the non-catalytic C-terminal domain (Nek5- $\Delta$ CTD) was generated (Figure 5.8A). U2OS cells were transiently transfected with eGFP-tagged full-length Nek5 and Nek5- $\Delta$ CTD for 24 hours, then fixed in methanol and processed for immunofluorescence microscopy with antibodies against the GFP tag. The Nek5- $\Delta$ CTD protein exhibited a cytoplasmic pattern of localisation in contrast to the full-length protein that was nuclear. Hence, the C-terminal non-catalytic domain of Nek5 is required for nuclear localisation (Figure 5.8B).



**Figure 5.7 Recombinant Nek5 accumulates in the nucleus in response to treatment with the nuclear export inhibitor Leptomycin B**

U2OS cells were transiently transfected with FLAG-Nek5 for 24 hrs and then treated with leptomycin B for 3 hrs before being fixed and permeabilised in ice-cold methanol and processed for immunofluorescence microscopy. FLAG-Nek5 proteins were stained with anti-FLAG antibodies (green on merge). DNA was stained with Hoechst 33258 (blue on merge). Scale bars, 5  $\mu$ m.

**A****B**

**Figure 5.8 The non-catalytic region of Nek5 is required for nuclear localisation**

**(A)** Schematic representation of the full-length (FL) and C-terminal truncated eGFP-tagged Nek5 constructs. The kinase domain is indicated in red and coiled-coil domain in blue. **(B)** U2OS cells were transiently transfected with either eGFP-Nek5-FL or eGFP-Nek5-ΔCTD for 24 hrs before being fixed and permeabilised in ice-cold methanol and processed for immunofluorescence microscopy. eGFP-Nek5 proteins were stained with anti-GFP antibodies (green on merge). DNA was stained with Hoechst 33258 (blue on merge). Scale bars, 5  $\mu$ m.

We therefore analysed the non-catalytic region of Nek5 for a putative nuclear localisation signal (NLS) sequence. A sequence rich in lysines and arginines was identified between residues 480-508 (Figure 5.9A). Typically, positively charged amino acids target proteins to nuclei by binding to a nuclear import receptor. Hence, a Nek5 construct was generated where a consecutive sequence of three basic residues (RKK<sup>487</sup>) was mutated to alanine residues (Figure 5.9A). U2OS cells were then transfected with FLAG-tagged full-length Nek5 and Nek5-RKK<sup>487</sup>/AAA for 24 hours, then fixed in methanol and processed for immunofluorescence microscopy with antibodies against the epitope tag. Both full-length Nek5 and the RKK<sup>487</sup> mutant localised to the nucleus, suggesting that this stretch of amino acids does not direct nuclear import (Figure 5.9B).

A series of FLAG-tagged Nek5 truncations were then generated to define the region within the C-terminus of Nek5 required for nuclear localisation (Figure 5.10). These were transiently transfected into U2OS cells for 24 hours, following which the cells were fixed in ice-cold methanol and processed for immunofluorescence microscopy with anti-FLAG antibodies. Full-length Nek5, and the 1-620, 1-540 and 1-460 constructs localised to the nucleus. However, the 1-380 and 1-300 proteins distributed in both the nucleus and cytoplasm (Figure 5.11). These data suggest that residues 380-460 are required for efficient nuclear localisation of the protein. This region is rich in basic amino acid residues (lysines, arginines and histidines), which constitute approximately 17% of the amino acids in this region.

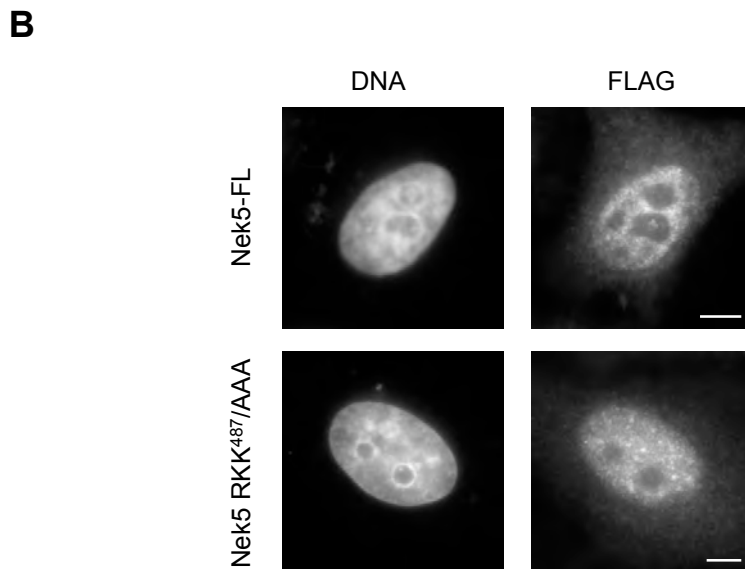
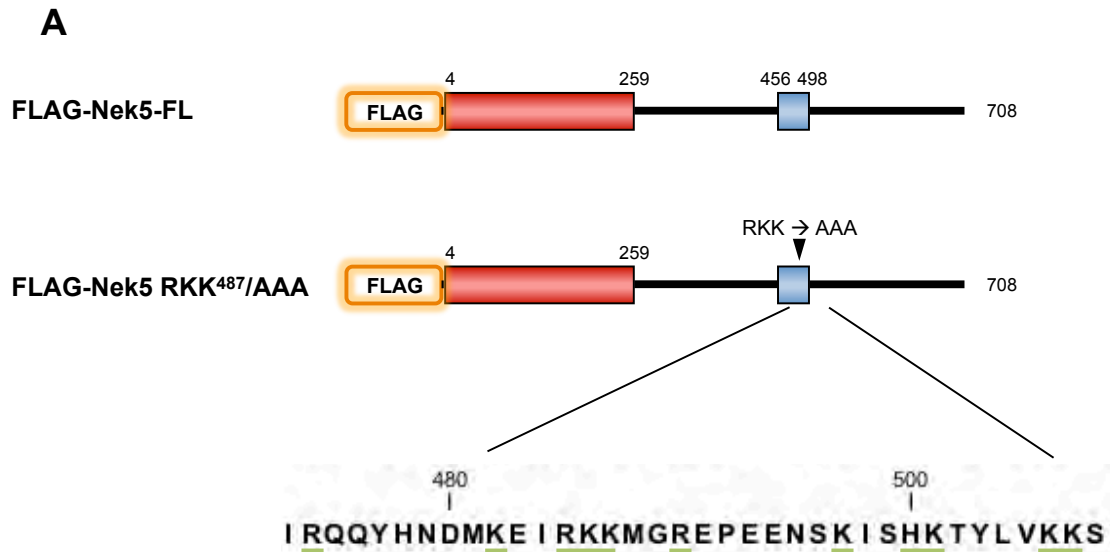


**Figure 5.9 Nuclear localisation of Nek5 is not affected by mutation of a putative nuclear localisation sequence**

**(A)** Schematic representation of a putative nuclear localisation signal and the mutant constructs generated. The region of positively charged lysine and arginine residues (RKK<sup>487</sup>) mutated to alanine (AAA) residues is indicated. The kinase domain is indicated in red and the coiled-coil domain in blue. **(B)** U2OS cells were transiently transfected with either FLAG-Nek5 FL or FLAG-Nek5 RKK<sup>487</sup>/AAA for 24 hrs before being fixed and permeabilised in ice-cold methanol and processed for immunofluorescence microscopy. FLAG-Nek5 proteins were stained with anti-FLAG antibodies and DNA was stained with Hoechst 33258. Scale bars, 5  $\mu$ m.

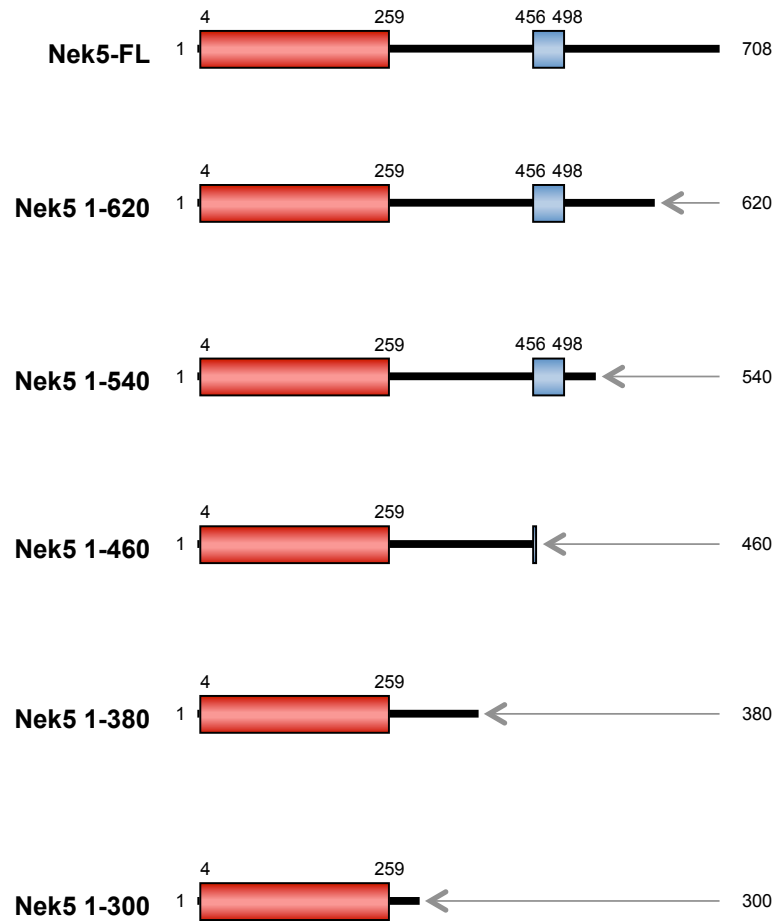


**Figure 5.10 Nek5 C-terminal truncations generated to identify nuclear targeting region**

Schematic representation of the C-terminal truncation constructs of Nek5 generated in order to identify the region required for the nuclear localisation of Nek5. The kinase domain is indicated in red and the coiled-coil domain in blue. Amino acid residue numbers are indicated.

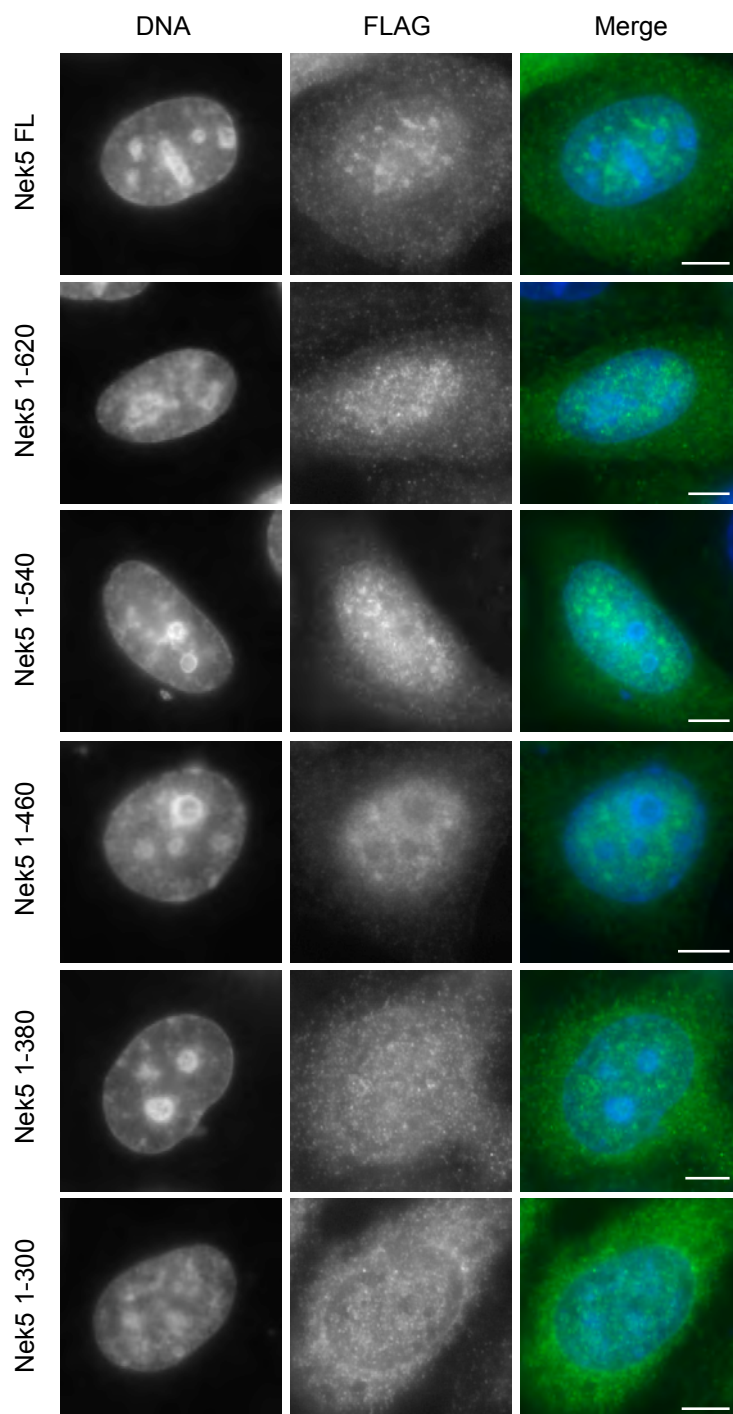


**Figure 5.11 Residues 380-460 are required for nuclear localisation of the Nek5 protein**

U2OS cells were transiently transfected with the FLAG-Nek5 C-terminal truncation constructs indicated for 24 hrs before being fixed and permeabilised in ice-cold methanol and processed for immunofluorescence microscopy. FLAG-Nek5 proteins were stained with anti-FLAG antibodies (green on merge). DNA was stained with Hoechst 33258. Scale bars, 5  $\mu$ m.

### 5.3 Discussion

Examination of the subcellular localisation of Nek5 by immunofluorescence microscopy has shown that Nek5 is a nuclear protein that can also associate with centrosomes, spindle poles and basal bodies. More specifically, localisation to centrosomes occurs towards the proximal ends of centrioles and occurs in a cell cycle-dependent manner.

The nuclear and centrosomal localisation data obtained here using affinity-purified Nek5 antibodies was similar in the different cell types tested. Importantly, the specificity of this antibody for Nek5 was confirmed using RNAi, which resulted in the loss of signal at these sites upon Nek5 depletion. In addition, these data are in agreement with that obtained using recombinant Nek5 proteins, strongly suggesting that the nuclear and centrosomal localisation patterns are reflective of Nek5.

During interphase the bulk of Nek5 is located within nuclei. Inhibition of nuclear export increased the amount of recombinant Nek5 in the nucleus indicating that the protein probably shuttles in and out of the nucleus. In terms of nuclear import, truncation studies revealed that amino acid residues 380-460 within the non-catalytic C-terminal region are important for localising Nek5 to the nucleus. This region has a high abundance of basic amino acid residues; however, using the PredictNLS tool (<http://cubic.bioc.columbia.edu/predictNLS>), a nuclear localisation signal could not be identified within this region. This suggests that Nek5 may have a cryptic NLS or that Nek5 traffics to nuclei via interaction with other proteins that would associate with Nek5 via residues 380-460. There is evidence that Nek5 may play a role in DNA damage/repair pathways (Fletcher et al. 2004; Noguchi et al. 2004; Melixetian et al. 2009; Moniz & Stambolic 2011). Hence, it is possible that nuclear localisation of Nek5 enables this protein to contribute to these pathways, or indirectly regulate expression of genes encoding proteins required for the regulation of cell division. It might also be possible that Nek5 localises to nuclei during interphase and in late stages of

mitosis as it may play a role in regulating chromatin condensation, like NIMA, or nuclear architecture.

In addition to the nucleus, Nek5 protein kinase also localised to centrosomes, spindle poles during early mitosis and basal bodies. Previously, mammalian Neks 2, 6, 7 and 9 were found to localise to centrosomes at specific stages of the cell cycle (De Souza et al. 2000; Fry et al. 1998b; O'Regan & Fry 2009; Kim et al. 2007; Roig et al. 2005). For these mammalian Neks, there is now substantial evidence that they have functions in regulating mitotic events, specifically centrosome organisation and spindle assembly. In comparison, Nek1 and Nek8 have been reported to play microtubule-dependent roles in non-dividing ciliated cells (O'Regan et al. 2007). Hence, it is possible that, like these Neks, Nek5 may contribute to similar processes, including centrosome separation, mitotic progression, spindle organisation or ciliogenesis. It is also possible that Nek5 may work in conjunction with at least one of these other mammalian Neks, in a similar manner to the cooperation of Nek9, Nek6 and Nek7.

Furthermore, the Nek5 protein kinase specifically localised towards the proximal ends of both mother and daughter centrioles. The centrosome contains a pair of centrioles that are tethered together at their proximal ends by a fibrous, intercentriolar link (Doxsey 2001; Bettencourt-Dias & Glover 2007). Previously, it has been shown that components of the intercentriolar linker, a proximal end centriolar protein, C-Nap1 (Fry et al. 1998a) and the fibrous protein emanating from proximal ends of centrioles, rootletin (Bahe et al. 2005), tether centrioles together, and at the onset of mitosis, phosphorylation of these proteins by Nek2 results in centrosome disjunction and formation of a bipolar spindle (Fry et al. 1998b). It is therefore possible that Nek5 might regulate the maintenance or contribute to the formation of this intercentriolar linker at proximal ends of centrioles.

However, whilst localisation studies can point towards roles for Nek5, functional studies need to be performed in order to properly understand whether Nek5 regulates microtubule organisation in dividing and/or non-dividing cells. For this purpose, Nek5 depletion studies were performed and are described in the next chapter.

## **Chapter 6**

### **An insight into Nek5 function through RNAi-mediated depletion**

## 6.1 Introduction

Of the eleven mammalian Neks, there is now substantial evidence that Nek2, Nek6, Nek7 and Nek9 have functions in regulating mitotic events involving microtubule organisation and mitotic spindle assembly, whilst Nek1 and Nek8 play roles in regulating microtubules of cilia in non-dividing cells (O'Regan et al. 2007). There are no functional studies published yet on Nek5. Hence, the consequences of RNAi-mediated Nek5 depletion and overexpression of kinase-inactive Nek5 were examined to provide insights into the roles of this protein kinase.

RNA interference (RNAi) is a well conserved mechanism in eukaryotic cells and a powerful research tool to mediate the sequence-specific degradation of target mRNA. This in turn results in suppression of target protein expression (Bonetta 2004; Dharmacon 2004). Briefly, RNAi can be induced by introducing sequence-specific double-stranded small interfering RNAs (siRNAs) into the cell cytoplasm directly by transfection. In the cytoplasm, these siRNAs associate with a protein complex called RNA-inducing silencing complex (RISC) resulting in activation of its helicase activity which unwinds the siRNA duplex. This then enables the siRNA strand to probe the target mRNA for complementary sequences. Upon identifying a region of complementarity, nuclease activity within the RISC complex mediates mRNA cleavage. Hence, target mRNA is rapidly degraded resulting in suppressed protein expression (Bonetta 2004; Dharmacon 2004). On the other hand, overexpression of an inactive kinase is another method used to provide insights into protein kinase functions. The catalytic kinase domain is typically essential for function; hence, mutation to abolish its activity and then overexpression of the kinase-inactive mutant can have a dominant-negative effect by binding substrates in a non-productive manner. Hence, both of these techniques are useful tools to investigate Nek5 function.

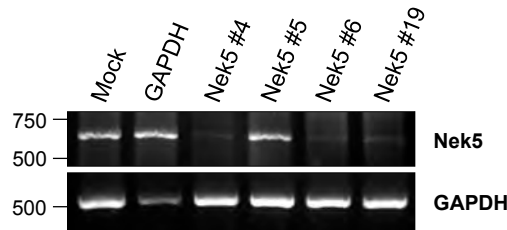
Data presented so far in this thesis provide evidence that Nek5 is a nuclear protein capable of also localising to the proximal ends of centrioles in a cell cycle dependent manner, with strongest localisation to centrioles during prophase. Functional experiments therefore concentrated on the importance of Nek5 at these structures by making phenotypic observations of cell cycle progression and centrosome organisation.

## 6.2 Results

### 6.2.1 Optimisation of RNAi-mediated depletion of Nek5

In order to analyse the effect of Nek5 depletion on cell cycle progression, four individual oligonucleotides were designed to specifically silence Nek5. The ability of these small interfering RNA oligonucleotides (siRNA oligos) to effectively deplete Nek5 was first assessed by Western blot and RT-PCR. U2OS cells treated with a pool of the four siRNA duplexes for 24 hours were transiently transfected with recombinant FLAG-Nek5 and then harvested at four different time points. As an additional control, this experiment was also performed with recombinant Nek2 and Nek2-specific siRNAs previously shown to efficiently deplete Nek2 protein. FLAG-Nek5 was successfully expressed in mock siRNA treated cells by 24 hours post plasmid transfection after which recombinant protein levels decreased. In comparison, FLAG-Nek5 was not expressed in cells co-transfected with the pool of Nek5 siRNA oligonucleotides (Figure 6.1A). Similar results were obtained with the Nek2 control experiment: Myc-Nek2 was expressed in mock siRNA treated cells at 24 hour and 48 hour time points, but not in Nek2 siRNA treated cells (Figure 6.1A).

In order to test the efficiency of depletion of each individual Nek5 siRNA oligo, U2OS cells were treated with the four Nek5 duplexes individually for 72 hours. Semi-quantitative RT-PCR analysis of the mRNA extracted from these cells showed that Nek5 was successfully depleted at the mRNA level with 3 out of the 4 duplexes (#4, 6, and 19) (Figure 6.1B). Immunofluorescence microscopy analysis using the affinity purified anti-Nek5 antibodies revealed that the Nek5 siRNA duplexes 4 and 6 produced the most efficient depletion of Nek5 (Figure 6.2). Hence, all subsequent RNAi experiments were carried out with these two oligonucleotides individually or combined.

**A****B****Figure 6.1 Characterising Nek5 siRNA oligos**

**(A)** U2OS cells were transfected with a pool of either four Nek5 or two Nek2 siRNA oligonucleotides for 24 hrs and then recombinant Nek5 and Nek2 were transfected into the appropriate siRNA treated cells. Cells were harvested at different time points following plasmid transfection, lysed and analysed by SDS-PAGE and Western blot with anti-Nek5 and anti-Nek2 antibodies. **(B)** Total RNA was collected after 72 hr siRNA treatment of U2OS cells transfected with no oligonucleotides (mock) or siRNA oligonucleotides against GAPDH or Nek5. Four individual Nek5 siRNA oligonucleotides were used. Semi-quantitative RT-PCR analysis was performed using Nek5 or GAPDH specific primers. Size markers (bp) are indicated on the left.

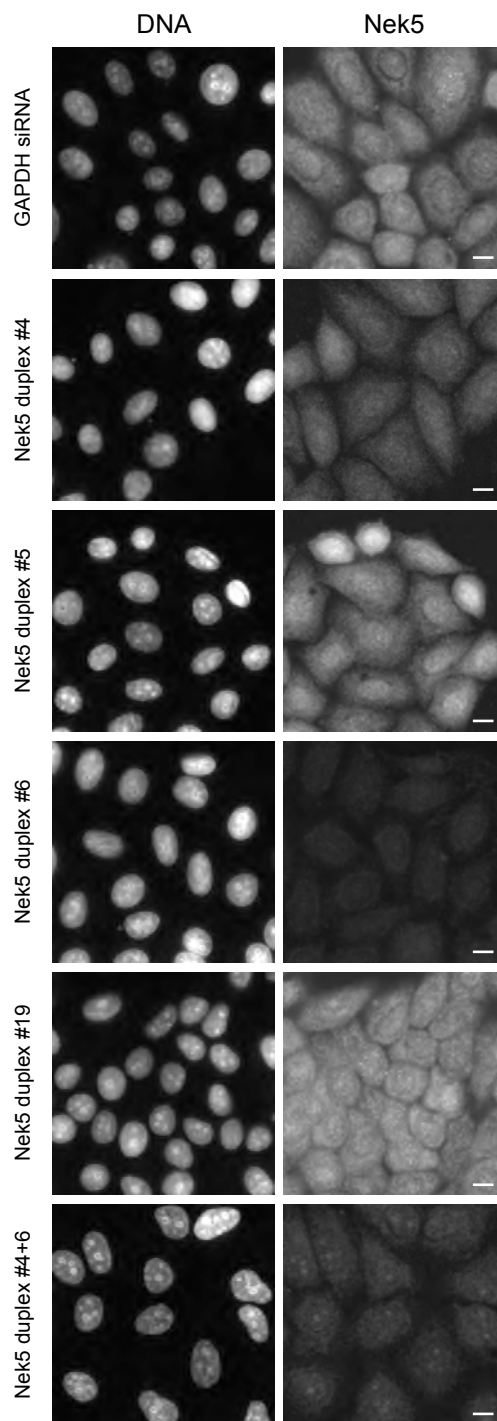


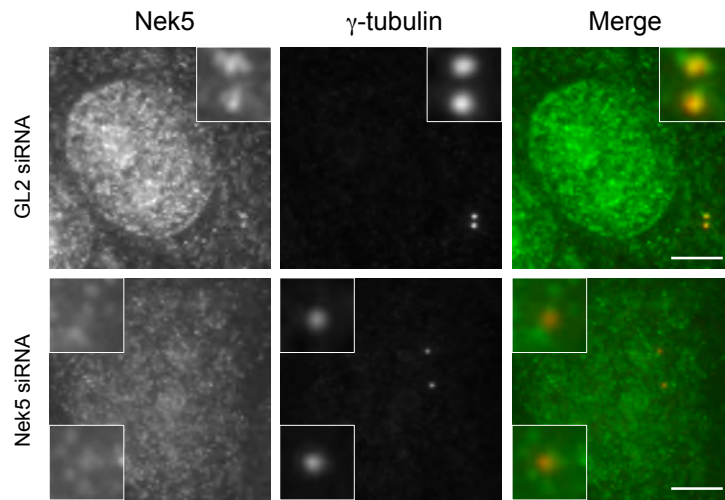
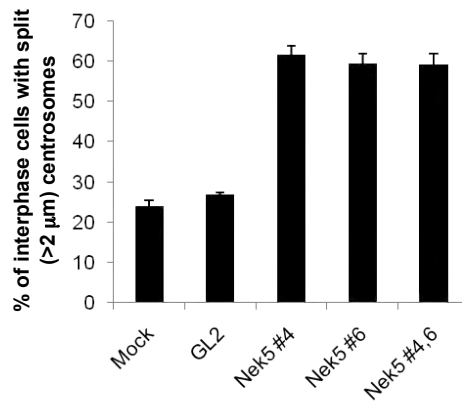
**Figure 6.2 Optimising RNAi knockdown of Nek5 in U2OS cells**

U2OS cells were transfected with four individual Nek5 siRNA oligonucleotides (#4, 5, 6, 19) or a pool of two siRNA oligonucleotides (#4 and 6) for 72 hrs before being pre-extracted then methanol-fixed and stained with anti-Nek5 antibodies; DNA was stained with Hoechst 33258. Scale bars, 10  $\mu$ m.

### **6.2.2 Nek5 depletion or expression of kinase-inactive Nek5 induces centrosome splitting**

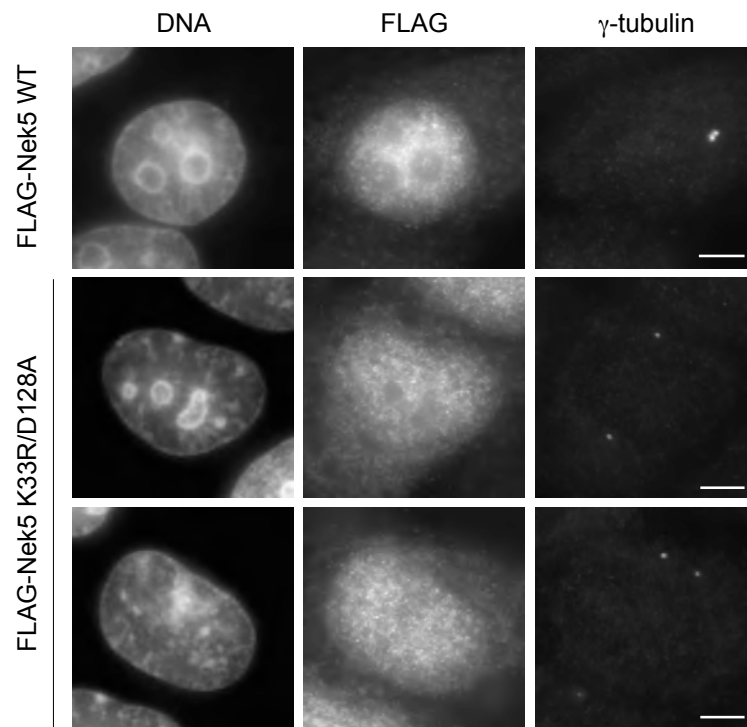
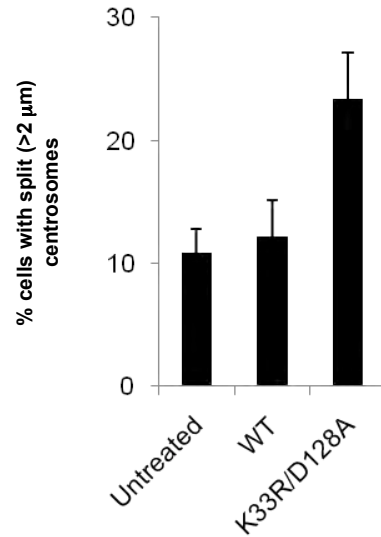
To determine whether Nek5 might play a role in centrosome organisation, U2OS cells were treated with the Nek5-specific siRNA oligos for 72 hours before being pre-extracted in Triton X-100 buffer, methanol fixed and then processed for immunofluorescence microscopy using anti-Nek5 antibodies and anti- $\gamma$ -tubulin antibodies to detect centrosomes. Strikingly, Nek5 depletion led to premature splitting of centrosomes. Upon depletion using either individual or combined duplexes, the percentage of interphase cells with centrosomes that were separated by more than 2  $\mu$ m increased by almost 3-fold in comparison to control depleted cells. Specifically, whilst, 25% of mock treated cells displayed split centrosomes, this percentage increased to 60% upon Nek5 depletion (Figure 6.3).

In order to determine whether centrosome cohesion is dependent on the kinase activity of Nek5, a recombinant Nek5 construct was generated with two conserved catalytic residues (K33 and D128) mutated. U2OS cells were transiently transfected with recombinant wild-type Nek5 and the kinase-inactive mutant (K33R/D128A) for 24 hours. Cells were then fixed in ice-cold methanol and processed for immunofluorescence microscopy with anti-FLAG and anti- $\gamma$ -tubulin antibody. Overexpression of the kinase-inactive Nek5 mutant also induced centrosome splitting, with approximately 2-fold more interphase cells displaying split centrosomes upon overexpression of K33R/D128A mutant in comparison to untransfected and Nek5 wild-type expressing cells (Figure 6.4). This suggests that centrosome cohesion in normal cells is dependent on the kinase activity of Nek5; however, the loss of kinase activity in the K33R/D128A mutant remains to be confirmed. It is also noteworthy that recent preliminary findings (data not shown) suggest that centrosome splitting may be repressed upon overexpression of wild-type Nek5; however, this needs further study.

**A****B**

**Figure 6.3 Nek5 depletion induces centrosome splitting**

(A) U2OS cells were transfected with Nek5 or GL2 specific siRNA oligonucleotides for 72 hrs before being pre-extracted then methanol-fixed and immunostained with anti- $\gamma$ -tubulin antibodies to detect centrosomes (red on merge) and with affinity purified anti-Nek5 antibodies (green on merge). Scale bars, 5  $\mu$ m. (B) The percentage of interphase cells with split centrosomes (>2  $\mu$ m) was calculated; data represent means ( $\pm$ S.E.) of three independent experiments with counts of 200 cells for each condition.

**A****B**

**Figure 6.4 Overexpression of kinase-inactive Nek5 induces split centrosomes**

(A) U2OS cells were transiently transfected with FLAG-tagged wild-type (WT) Nek5 and kinase-inactive Nek5 (K33R/D128A) for 24 hours. Cells were then methanol-fixed and immunostained with anti-FLAG antibodies and anti- $\gamma$ -tubulin antibodies to detect centrosomes. Scale bars, 5  $\mu$ m. (B) The percentage of transfected cells with split centrosomes (>2  $\mu$ m) was calculated; data represent means ( $\pm$ S.E.) of three independent experiments where n=30 in each case.

### **6.2.3 Nek5 depletion leads to loss of $\gamma$ -tubulin from centrosomes**

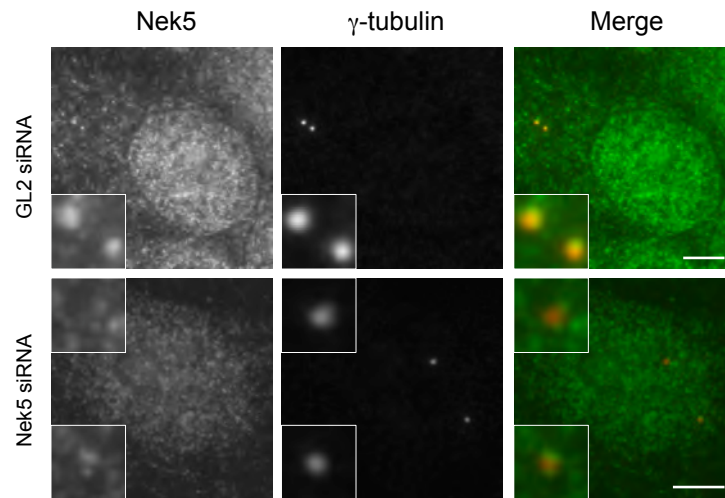
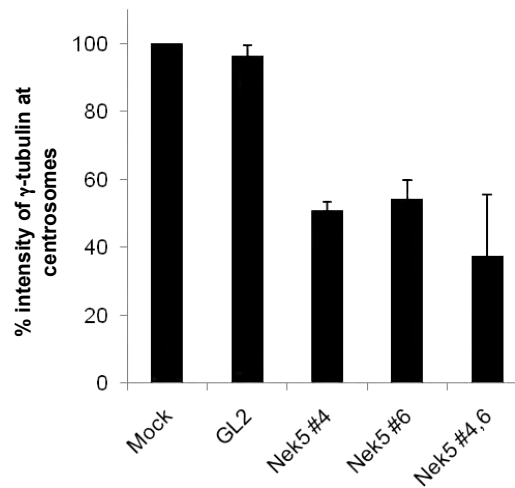
Further analysis of the Nek5 depleted cells revealed a striking loss of  $\gamma$ -tubulin from centrosomes. This was quantified by measuring the fluorescence intensity of  $\gamma$ -tubulin at centrosomes of Nek5 depleted interphase cells imaged under identical conditions and calculating this relative to the intensity of  $\gamma$ -tubulin at centrosomes of mock treated cells. In comparison to mock and GL2 siRNA treated cells, the intensity of  $\gamma$ -tubulin at centrosomes decreased by approximately 50-60% in cells depleted of Nek5 using siRNA oligos either individually or combined (Figure 6.5).

### **6.2.4 Nek5 depletion leads to split centrosomes during cytokinesis**

We then examined whether Nek5 depletion altered centrosome appearance in mitotic cells and observed a difference in cells undergoing cytokinesis. During cytokinesis, cells were scored in three categories: (i) both daughter cells had centrosomes that were close together ( $<2 \mu\text{m}$  apart); (ii) one daughter cell displayed split centrosomes ( $>2 \mu\text{m}$  apart); (iii) both daughter cells had split centrosomes ( $>2 \mu\text{m}$  apart). In mock and GL2 control siRNA treated cells, the vast majority (80-90%) of cells fell into the first category with the remainder of cells falling into category two. In comparison, upon Nek5 depletion, the percentage of cells undergoing cytokinesis in category one, where both daughter cells displayed unsplit centrosomes, decreased to only 40-50%. Of the remaining cells,  $\sim$ 30-35% fell in to category two and  $\sim$ 20-30% into category three (Figure 6.6). Hence, it would appear that in the absence of Nek5, the two centrioles in emerging daughter cells undergo disengagement but then fail to establish cohesion.

### **6.2.5 Depletion of Nek5 results in a delay in prometaphase**

We next investigated whether there was an effect on cell cycle progression upon depletion of Nek5. First of all, the cell cycle distribution of populations of U2OS cells treated with specific siRNA oligos for 72 hours was analysed by flow

**A****B****Figure 6.5 Nek5 depletion causes loss of  $\gamma$ -tubulin from centrosomes**

**(A)** U2OS cells were transfected with Nek5 or GL2 specific siRNA oligonucleotides for 72 hrs before being pre-extracted then methanol-fixed and immunostained with anti- $\gamma$ -tubulin antibodies to detect centrosomes (red on merge) and with affinity purified anti-Nek5 antibodies (green on merge). Scale bars, 5  $\mu$ m. **(B)** The fluorescence intensity of  $\gamma$ -tubulin at centrosomes of interphase cells in siRNA treated cells is expressed relative to the intensity of  $\gamma$ -tubulin at centrosomes of mock treated cells. Intensities were determined as indicated in Materials and Methods. Data represent means ( $\pm$ S.E.) of three independent experiments where n=at least 25 cells for each condition.

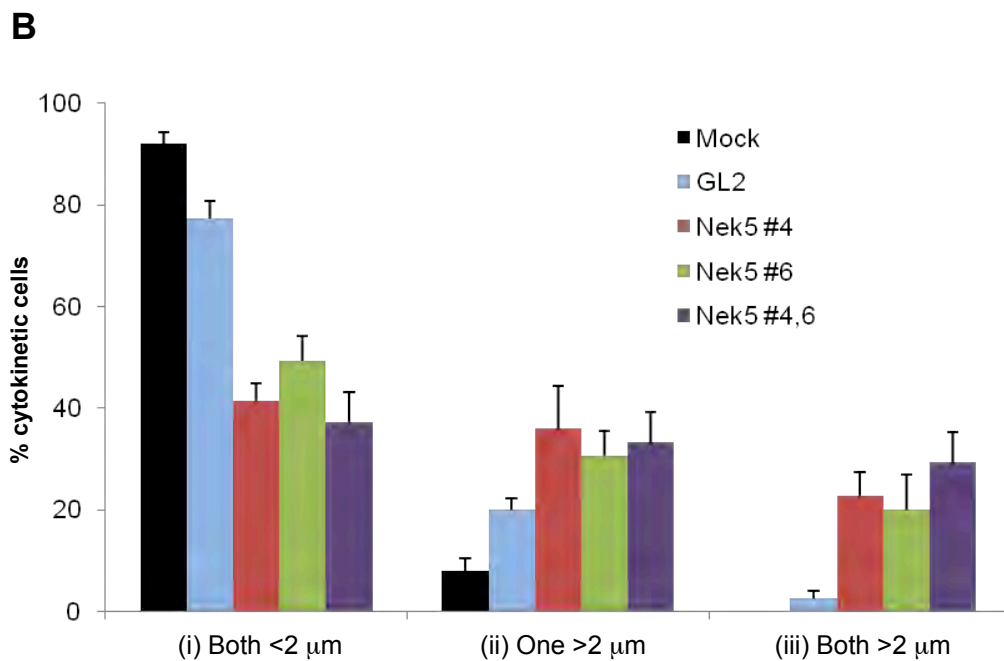
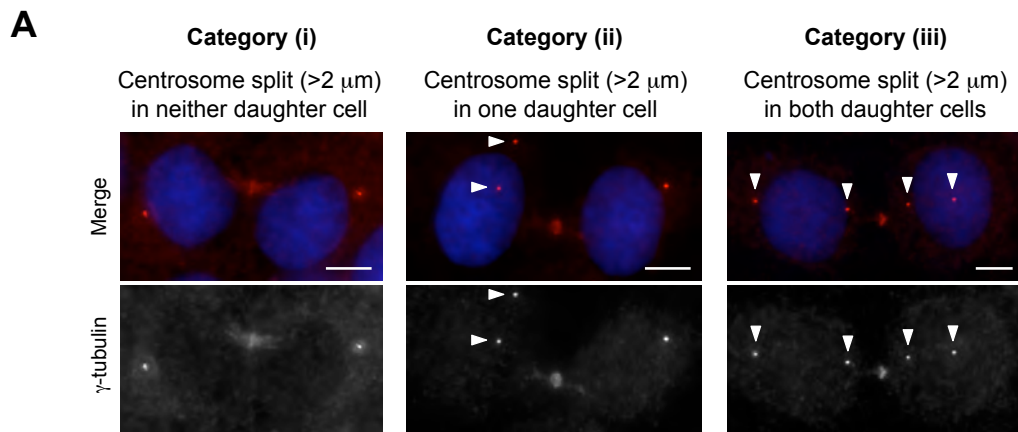


**Figure 6.6 Nek5 depletion increases the frequency of split centrosomes during cytokinesis**

**(A)** U2OS cells were transfected with Nek5 or GL2 specific siRNA oligonucleotides for 72 hrs before being pre-extracted, methanol-fixed and immunostained with anti- $\gamma$ -tubulin antibodies to detect centrosomes (red on merge) and Hoechst 33258 to stain DNA (blue on merge). Scale bars, 5  $\mu\text{m}$ . Cells in cytokinesis were scored as (i) unsplit centrosomes (<2  $\mu\text{m}$ ) in both daughter cells, (ii) split centrosomes (>2  $\mu\text{m}$ ) in one daughter cell, or (iii) split centrosomes in both daughter cells. **(B)** The percentage of cytokinetic cells in the three different categories for depleted cells is shown. Data represent means ( $\pm$ S.E.) of three independent experiments where n=25 for each condition.

cytometry. Mock, GL2 and Nek5 siRNA treated cells were fixed in ethanol and stained with propidium iodide (PI) to quantitatively bind DNA so that the fluorescence intensity of the stained cells would correlate with the amount of DNA they contained. The acquired cell cycle distribution data revealed a broader G<sub>2</sub>/M peak in samples depleted of Nek5 in comparison to control siRNA treated cells (Figure 6.7A). This may be indicative of a delay in mitotic progression. Mitotic index counts were made on depleted U2OS cells. For this purpose, cells were siRNA transfected with the Nek5-specific siRNA oligos for 72 hours before being pre-extracted in Triton X-100 buffer, methanol fixed and then processed for immunofluorescence microscopy. The percentage of mitotic cells in the population treated with Nek5-specific siRNA oligos did not show any significant difference in comparison to mock and GL2 siRNA treated cells (Figure 6.7B). Although the overall mitotic index was unaffected by depletion of Nek5, counts were then performed to determine if there was an effect of Nek5 depletion on the fraction of cells within different phases of mitosis (prophase and prometaphase, metaphase, anaphase, telophase and cytokinesis). In mock and GL2 siRNA treated cells, the mean percentage of cells in prophase/prometaphase was ~15-18%; upon Nek5 depletion, this percentage increased ~2-fold to ~30%. Conversely, the percentage of cells in metaphase decreased to 25-30% in cells treated with Nek5 siRNA duplexes, compared to 38% in mock and GL2 treated cells. The percentage of cells in anaphase and telophase/cytokinesis remained unaffected, at ~15% and 30% respectively (Figure 6.7C). This data therefore suggests that Nek5 depletion causes a delay in the prophase and prometaphase stages of mitosis.

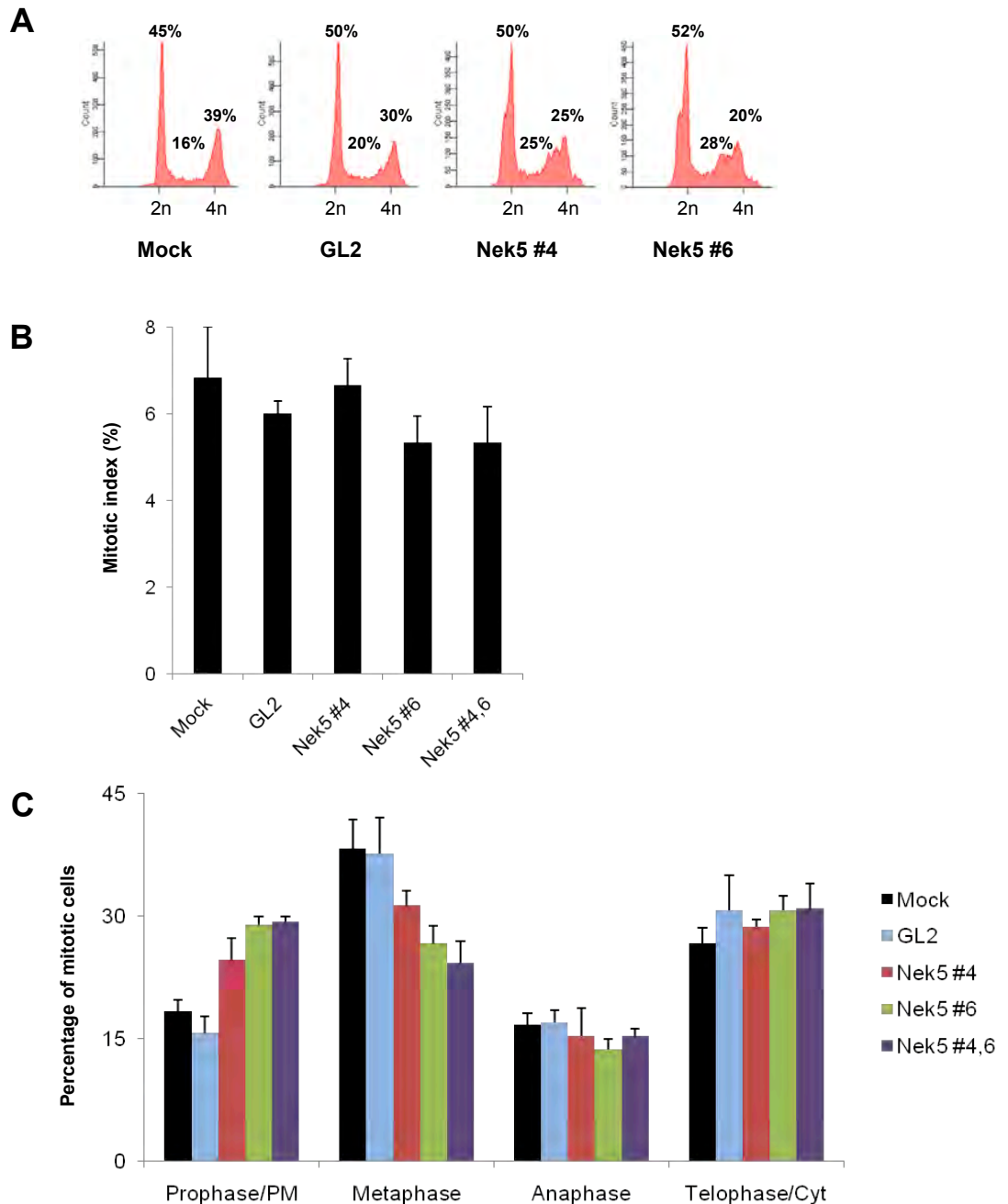


**Figure 6.7 Depletion of Nek5 results in an early mitotic delay**

(A) U2OS cells were mock transfected or transfected with either Nek5 or GL2 specific siRNA oligonucleotides for 72 hrs before being harvested and fixed, and then stained with propidium iodide and cell cycle distribution analysed by flow cytometry. (B) U2OS cells were transfected with Nek5 or GL2 specific siRNA oligonucleotides for 72 hrs before being pre-extracted, methanol-fixed and immunostained with anti- $\gamma$ -tubulin antibodies to detect centrosomes and with affinity purified anti-Nek5 antibodies; DNA was stained with Hoechst 33258. The percentage of mitotic cells in each condition was counted; data represent means ( $\pm$ S.E.) of three independent experiments where  $n=200$  for each condition. (C) The percentage of cells in different stages of mitosis, as indicated, was calculated; data represent means ( $\pm$ S.E.) of three independent experiments where  $n=100$  for each condition.

### 6.3 Discussion

There is currently no data published on the mammalian Nek5 protein kinase. Results obtained here provide the first direct evidence in support of a cell cycle role for human Nek5. Having shown that endogenous Nek5 localises to centrosomes, specifically the proximal ends of centrioles, in a cell-cycle dependent manner, potential insights into Nek5 function were sought using RNAi-mediated depletion. Importantly, depletion of Nek5 produced two striking consequences, namely, centrosome splitting and loss of  $\gamma$ -tubulin from centrosomes. Centrosome splitting also occurred upon overexpression of a Nek5 kinase-inactive mutant, suggesting that Nek5 kinase activity is important in preventing premature centrosome separation. This result is extremely interesting as a centrosome splitting phenotype has previously been reported upon deregulation of another NIMA-related kinase, Nek2 (Fry et al. 1998b). However, the results are quite distinct in that whilst depletion of Nek5 induced splitting, Nek2 induced splitting only upon overexpression of active kinase (Fry et al. 1998b).

Nek2 is the most well studied mammalian Nek kinase and plays a role in bipolar spindle formation through initiating centrosome disjunction at the G<sub>2</sub>/M transition. It does this via interaction with, phosphorylation and displacement of components forming the intercentriolar linkage, C-Nap1 and rootletin, which normally hold centrosomes together in close proximity during interphase (Fry et al. 1998a; Bahe et al. 2005; O'Regan et al. 2007). The findings here suggest that Nek5 may also play a role in regulating centrosome cohesion, although in this case it may act to hold centrosomes in close proximity. It could be that as Nek5 is localised at proximal ends of centrioles, it may contribute directly to Nek2 kinase regulation. By directly interacting with or phosphorylating Nek2 during interphase it may prevent premature centrosome separation. Alternatively, Nek5 may be capable of interacting with and phosphorylating the intercentriolar linkage components, C-Nap1 and rootletin, at the proximal ends of centrioles. Conversely, active Nek2 may phosphorylate Nek5 to inactivate it and induce centrosome separation. These suggestions though remain to be

tested. Initially, one could examine Nek2 activity as well as Nek2, C-Nap1 and rootletin localisation in cells depleted of Nek5. Next one could test interactions by co-immunoprecipitation. Isolating additional interacting partners of Nek5 through co-immunoprecipitation and mass spectrometry would help shed further light on how Nek5 may be contributing to the regulation of centrosome separation, and whether this involves the same pathway through which Nek2 functions.

Loss of  $\gamma$ -tubulin from centrosomes also suggests that Nek5 is involved in regulating the integrity of the PCM. Interestingly, loss of  $\gamma$ -tubulin from centrosomes has also been observed upon overexpression of Nek2 concomitant with centrosome splitting (Fry et al. 1998b). It will be interesting to examine whether centrosome splitting is always accompanied by  $\gamma$ -tubulin loss suggesting that attachment of PCM to centrosomes is weakened upon loss of centrosome cohesion.  $\gamma$ -tubulin loss was also observed in Nek7-suppressed cells, which led to the suggestion that Nek7 is required for the microtubule nucleation activity of the centrosome (Kim et al. 2007). Hence, it could be that Nek5 may also contribute to the regulation of microtubule nucleation.

In terms of mitotic progression, the evidence presented here suggests that depletion of Nek5 leads to a delay in prophase or prometaphase. This delay may be a result of the loss of  $\gamma$ -tubulin from centrosomes causing a delay in centrosome maturation or spindle formation. Microtubules are required for both nuclear envelope breakdown and chromosome congression. Hence, either of these processes may be delayed. However, the increased amount of Nek5 seen on spindle poles in early mitosis might suggest an unidentified distinct role. Furthermore, observation of cytokinesis in Nek5 depleted cells, revealed that the emerging daughter cells tended to have prematurely separated centrosomes. This is likely to reflect a similar mechanism of Nek5 in regulating centrosome cohesion as observed in interphase cells. In other words, after the two centrioles at each pole undergo disengagement, they fail to then acquire

the protein required for centrosome cohesion in the ensuing interphase. Thus, after these daughter cells have completed abscission, the new cells progress into the next round of division with already split centrosomes.

Overall, this first set of functional experiments lead us to conclude that, like Nek2, Nek6, Nek7 and Nek9, Nek5 also plays a role in mitotic events. Also like Nek2, Nek6 and Nek7, Nek5 is likely to play important roles in centrosome regulation and microtubule organisation.

Interestingly, my preliminary findings (data not shown) also suggest that Nek5 may be implicated in ciliogenesis as upon Nek5 depletion there was an apparent reduction in primary cilia formation. However, this needs careful repetition to generate clear data. In support of this, Nek5 has recently been identified as a target gene regulated by the FOXJ1 transcription factor (Thomas et al. 2010). FOXJ1 governs motile cilia assembly by regulating genes involved in cilia biogenesis and physiology (Thomas et al. 2010), hence Nek5 may well also be implicated in ciliogenesis. Although this requires further investigation, it would not be surprising if Nek5 plays a role in microtubule organisation within cilia as there is a close link between the biology of centrosomes, cilia and cell cycle control and there is precedent for other Neks to be intimately involved in ciliogenesis.

**Chapter 7**  
**Discussion**

The NIMA-related kinase family represents one of the least studied groups of protein kinases. Yet it is becoming clear that they play important roles in cell cycle control, centrosome biology and ciliogenesis. Moreover, their deregulation may contribute to the progression of various diseases, including cancer. This, together with the fact that kinases are eminently druggable enzymes, means that Neks may be appropriate therapeutic targets in different contexts. Hence, a comprehensive understanding of their regulation and function is urgently required. Yet, at the onset of this project, research on Nek3 and Nek11 function was limited, and still to date, there have been no publications on Nek5. The work presented in this thesis therefore provides the first insight into Nek5 function as well as a more broad analysis of Nek3 and Nek11 properties.

## **7.1 Nek5 is a nuclear protein**

The development of an antibody specific for Nek5, together with generation of epitope-tagged Nek5 constructs, has enabled the subcellular localisation of Nek5 to be examined. Data presented here indicates that both recombinant and endogenous Nek5 protein localise to nuclei in all cell types examined. Nek5 appears to be excluded from nucleoli and is diffusely distributed through the nucleoplasm, albeit with a speckled pattern suggestive of localisation to specific subnuclear compartments. Upon inhibition of nuclear export, Nek5 concentration in the nucleus increased, suggesting that this protein kinase is likely to shuttle between the cytoplasm and nucleus. Furthermore, using a series of truncation mutants of Nek5, the protein sequence region required for localisation to the nucleus was found to be between amino acid residues 380-460 within the C-terminal non-catalytic domain.

*Aspergillus* NIMA accumulates in the nucleus through interaction with nuclear pore complex components SONA and SONB (Wu et al. 1998; De Souza et al. 2003). Here, NIMA is thought to carry out at least some of its mitotic functions, including the phosphorylation of histone H3 to promote chromatin condensation

(De Souza et al. 2000). Of the mammalian Neks, Nek2, Nek1 and Nek9 have all been reported to localise to the nucleus. Previously, a strong bipartite NLS, RKX<sub>10</sub>KKK, was identified in Nek2C that was also present but weaker in Nek2A (Wu et al. 2007). However, an NLS within the region required for Nek5 nuclear localisation could not be identified suggesting that Nek5 may have a cryptic NLS or that Nek5 trafficks to nuclei via interaction with other proteins that associate with Nek5 via residues 380-460. Nek1 has also been reported to contain functional NLSs, and a truncated fragment of Nek9 has been reported to localise to the nucleus (Hilton et al. 2009; Hames & Fry 2002; Wu et al. 2007; Pelka et al. 2007). However, the functions of these Neks in nuclei remain to be determined. Similarly, the function of Nek5 in the nucleus is yet to be determined. It might be that like NIMA, Nek5 may play a role in regulating chromatin condensation. To investigate this, the effect of Nek5 expression on histone H3 phosphorylation could be examined using phospho-H3 antibodies. Alternatively, Nek5 might interact with and regulate other nuclear proteins, including those involved in the expression of genes required for the regulation of cell division. Hence, to understand the function of Nek5 in the nucleus, future efforts will be required to identify substrates and interacting partners of Nek5, as well as study potential defects in nuclear-mediated events upon alteration of Nek5 expression. Finally, it cannot be ruled out that Nek5 is sequestered in the nucleus in interphase to limit its activity in the cytoplasm.

## **7.2 Nek5 localises to the proximal ends of centrioles**

In addition to localising to nuclei, recombinant and endogenous Nek5 proteins were observed at the centrosome during interphase in all cell types examined. Having observed an increase in Nek5 mRNA expression levels at M phase, the localisation of Nek5 to centrosomes was also found to be cell cycle-dependent. The intensity of Nek5 at centrosomes reached a peak in early mitosis. Interestingly, after maximal intensity during prophase, there was a progressive decrease in intensity to levels lower than in interphase as cells progressed into late mitosis. These data indicate that Nek5 may have a mitotic role, as other mitotic Neks, Nek2, Nek6, Nek7 and Nek9, have been localised to the

centrosome (Fry et al. 1998a; Hames et al. 2005; O'Regan & Fry 2009; Roig et al. 2005). More specifically, Nek5 localisation appeared to be centriolar, as co-staining with centrin as a distal-end marker and C-Nap1 as a proximal end marker indicated that Nek5 antibodies preferentially stained the proximal ends of centrioles. Further studies will be required to determine the region of Nek5 that targets it to the proximal ends of centrioles, to examine whether this association is independent of microtubules, and to identify components of the centrosome with which Nek5 may be interacting. Furthermore, proximal end localisation of Nek5 might implicate Nek5 in a role in centriole biogenesis or centrosome cohesion. Indeed, data presented in this thesis supports the hypothesis that Nek5 does indeed regulate centrosome cohesion.

### **7.3 Nek5 regulates centrosome cohesion**

From a functional perspective, we have demonstrated that interfering with Nek5 function, either by siRNA-mediated depletion or expression of a catalytically-inactive mutant, results in premature centrosome splitting during interphase. Of the other mammalian Neks, Nek2A has been shown to play a role in centrosome disjunction. The current working model for Nek2A is that at the onset of mitosis, activated Nek2A phosphorylates at least two components of the intercentriolar linker, C-Nap1 and rootletin, which hold centrosomes together in close proximity. Phosphorylation of these components leads to their dissociation from the centrosome resulting in a loss of centrosome cohesion (Fry et al. 1998a, 1998b; Fletcher et al. 2005; Bahe et al. 2005; Mardin et al. 2010). However, in contrast to the data obtained for Nek5, RNAi-mediated depletion of Nek2A inhibits centrosome separation, whilst overexpression of active, but not catalytically-inactive, Nek2 stimulates premature centrosome splitting in interphase cells (Fletcher et al. 2005; Mardin et al. 2010; Fry et al. 1998b; Faragher & Fry 2003). Hence, together these data suggest that active Nek5 might contribute to the inhibition of Nek2A in order to prevent premature centrosome disjunction (Figure 7.1). In order to address this hypothesis, Nek2 activity should be measured as well as the localisation of C-Nap1 and rootletin examined in Nek5 depleted cells. Similarly, the activity of Mst2, which has been

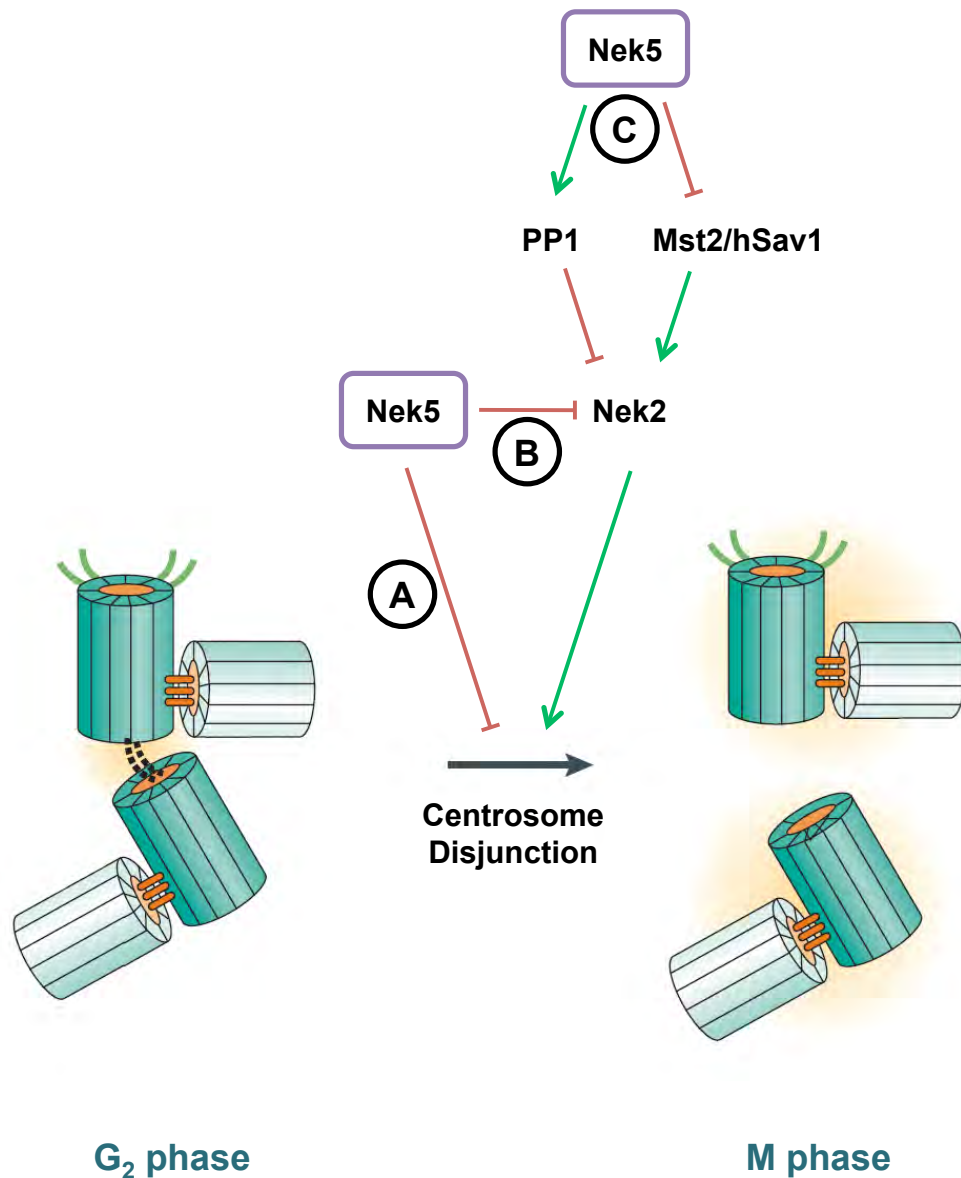


**Figure 7.1 Putative roles of Nek5 in centrosome disjunction**

Schematic model showing alternative mechanisms through which Nek5 might regulate centrosome disjunction. Nek5 might inhibit centrosome disjunction directly in a mechanism independent of Nek2 (**A**); Nek5 might directly inhibit Nek2 in order to prevent premature centrosome disjunction (**B**); or it may be that Nek5 regulates centrosome disjunction by acting on upstream regulators of Nek2 kinase (**C**).

reported to stimulate Nek2A function (Mardin et al. 2010), could be assessed in Nek5 depleted cells.

Interestingly, data presented in this thesis revealed that Nek5 depletion also led to prematurely separated centrosomes in daughter cells emerging during cytokinesis. Upon exit from mitosis, centriole disengagement normally occurs where the orthogonal association between mother and daughter centrioles is lost. However, the two centrioles are thought to quickly become tethered by an intercentriolar link that assembles between their proximal ends (Lim et al. 2009; Azimzadeh & Bornens 2007). Hence, one interpretation of our data is that, in the absence of Nek5, the centrioles fail to recruit the proteins required for centrosome cohesion in the ensuing interphase. This could be investigated by examining the localisation of known intercentriolar components, C-Nap1 and rootletin, in Nek5 depleted cells undergoing cytokinesis. Furthermore, time-lapse imaging of cells progressing through mitosis upon Nek5 depletion could be performed, using, for example, GFP-tagged rootletin cells to determine whether formation of the intercentriolar linker is disrupted in the absence of Nek5 protein.

#### **7.4 Nek5 regulates $\gamma$ -tubulin recruitment**

In addition to premature centrosome splitting, another striking phenotype observed upon depletion of Nek5 was a loss of  $\gamma$ -tubulin from these centrosomes. Although the overall mitotic index of Nek5 depleted cells was unaffected, the percentage of Nek5 depleted mitotic cells in prophase and prometaphase increased, potentially indicating a delay in this phase of cell cycle progression. This delay may indeed be due to the reduced  $\gamma$ -tubulin observed on prematurely separated centrosomes; this could reduce the microtubule nucleating activity causing a delay in mitotic progression due to activation of the SAC in the presence of a weak spindle.

Many key mitotic regulators, including Plk1, Aurora A, Nek2 and Nek7, are centrosomal proteins which have been reported to control microtubule nucleation and anchoring activity. Like Nek5, interference with the functions of these mitotic regulators has been shown to cause reduction in the  $\gamma$ -tubulin levels at centrosomes (Sumara et al. 2004; van Vugt et al. 2004; Giet et al. 2002; Liu & Ruderman 2006; Sonn et al. 2004; Kim et al. 2007). Hence, it seems likely that Nek5 may play similar roles in centrosome maturation and/or microtubule nucleation by regulating  $\gamma$ -tubulin recruitment. Clearly, future efforts will be required to determine whether Nek5 directly interacts with  $\gamma$ -tubulin. To study potential alterations in microtubule nucleating activity in interphase or mitotic cells, microtubule re-growth assays would need to be performed. It would also be useful to perform time-lapse imaging of Nek5 depleted cells stably expressing GFP-tagged  $\alpha$ -tubulin to observe the microtubule network and follow progression into mitosis to investigate the delay in prophase.

## **7.5 Future directions with Nek3 and Nek11**

Consistent with previous data on Nek3 (Tanaka & Nigg 1999), the studies presented here indicate that Nek3 is predominantly cytoplasmic during interphase in the cell types examined. Localisation of recombinant Nek3 during cell cycle progression indicated no strikingly obvious association to any cellular structures, although weak staining of fibrous spindle-like structures was observed during early mitosis. This observation has not been identified in previous studies, and could be explored in the future using antibodies to co-stain spindle microtubules. If this observation is confirmed, it might suggest that Nek3 may also play a role in regulating mitotic spindle organisation. In addition, data presented in this thesis demonstrated a cell type dependent localisation of recombinant Nek3 protein to centrosomes. This may, however, reflect the low levels of Nek3 which actually associate with the centrosome. Again, this is the first report of an association of Nek3 with centrosomes. Using optimised co-immunoprecipitation conditions, future experiments could be directed towards isolating substrates and interacting partners to gain a better insight into whether or not Nek3 plays a role in cell cycle progression and/or ciliogenesis.

In terms of mRNA expression, interesting differences were observed in the pattern of Nek3 splice variants according to the type of cancer origin. The RT-PCR product sizes appeared consistent with the four possible Nek3 mRNA transcripts that have been previously described to result from alternative splicing and a single adenine insertion/deletion polymorphism (Hernández & Almeida 2006). However, it will be necessary to sequence the different products generated from the different cancer types to determine whether or not an association does exist between the type of cancer and Nek3 variant expressed. Recently published work strongly argues that Nek3 plays a role in the prolactin mediated cytoskeletal re-organisation of breast cancer cells (Miller et al. 2005; Miller et al. 2007). Future investigations could therefore focus on characterising the localisation, interacting partners and functional mechanisms of the different Nek3 variants in relation to prolactin signalling.

Previously published data on the subcellular localisation of Nek11 were inconsistent (Noguchi et al. 2002; Noguchi et al. 2004). Data presented in this thesis, showed Nek11c is predominantly cytoplasmic, whilst affinity-purified Nek11 antibodies, suggested that the major endogenous Nek11 isoform – likely to be Nek11L – is predominantly nuclear in interphase. However, findings presented here showed that Nek11 also localised to centrosomes in interphase and on spindle poles through mitosis. There are no previous studies reporting an association between Nek11 with centrosomes, hence further research will require confirmation of the Nek11 antibody specificity using siRNA-mediated depletion to show loss of centrosomal staining.

With conditions for *in vitro* kinase assays optimised, data reporting a functional interaction between Nek11 and Nek2A in which Nek2 phosphorylates and activates Nek11 could be confirmed in cells depleted of Nek2. However, during the course of this project, persuasive evidence has been presented that Nek11 plays a key role in the G<sub>2</sub>/M DNA damage response (Melixetian et al. 2009). As targets of the DNA damage checkpoint, e.g. Plk1 and Cdc25, have been localised to the centrosome, it will be intriguing to study the localisation of

Nek11 in response to DNA damage and ask whether Nek11 contributes to transfer of the signal from the nucleus to the centrosome.

## **7.6 Concluding remarks**

Clearly, much work remains to be done in order to fully elucidate the pathways by which Nek3, Nek5 and Nek11 contribute to cell cycle control. However, evidence is mounting that multiple human Neks function in a range of cell cycle events including G<sub>2</sub>/M progression, mitotic spindle formation and DNA damage checkpoint signalling. Interestingly, increased expression of several Neks in cancer cells has been reported. For example, data is presented here showing upregulation of Nek5 in cancer cell lines, and altered pattern of Nek3 splice variant expression. It is becoming clear then that deregulation of NIMA-related kinases may contribute to the progression of various diseases, including cancer, making Neks potentially important therapeutic drug targets. However, one must be careful in this regard as there is now evidence indicating a role for Nek5, as well as Nek1 and Nek8, in ciliogenesis (Thomas et al. 2010). Hence, Neks are likely to be involved in microtubule organisation within cilia in addition to cell cycle control. Thus, a comprehensive understanding of their regulation, function and structure is required to be able to utilise them as therapeutic targets and design selective inhibitors.

**Chapter 8**  
**Bibliography**

- Abe K, Rossman KL, Liu B, Ritola KD, Chiang D, Campbell SL, Burridge K, Der CJ. 2000.** Vav2 is an activator of Cdc42, Rac1, and RhoA. *The Journal of biological chemistry* **275**: 10141-9.
- Abou Alaiwi WA, Lo ST, Nauli SM. 2009.** Primary cilia: highly sophisticated biological sensors. *Sensors* **9**: 7003-20.
- Adams RR, Maiato H, Earnshaw WC, Carmena M. 2001.** Essential roles of Drosophila inner centromere protein (INCENP) and aurora B in histone H3 phosphorylation, metaphase chromosome alignment, kinetochore disjunction, and chromosome segregation. *The Journal of cell biology* **153**: 865-80.
- Ahmad FJ, Yu W, McNally FJ, Baas PW. 1999.** An essential role for katanin in severing microtubules in the neuron. *The Journal of cell biology* **145**: 305-15.
- Alberts B, Johnson A, Lewis J, Raff M, Roberts K, Walter P. 2002.** *Molecular biology of the cell*. New York: Garland Science.
- Anderson CT, Castillo AB, Brugmann SA, Helms JA, Jacobs CR, Stearns T. 2008.** Primary cilia: cellular sensors for the skeleton. *The anatomical record*. **291**: 1074-8.
- Andrews PD, Ovechkina Y, Morrice N, Wagenbach M, Duncan K, Wordeman L, Swedlow JR. 2004.** Aurora B regulates MCAK at the mitotic centromere. *Developmental cell* **6**: 253-68.
- Archambault V, Glover DM. 2009.** Polo-like kinases: conservation and divergence in their functions and regulation. *Nature reviews molecular cell biology* **10**: 265-75.
- Azimzadeh J, Bornens M. 2007.** Structure and duplication of the centrosome. *Journal of cell science* **120**: 2139-42.
- Bahe S, Stierhof Y, Wilkinson CJ, Leiss F, Nigg EA. 2005.** Rootletin forms centriole-associated filaments and functions in centrosome cohesion. *The Journal of cell biology* **171**: 27-33.
- Barbagallo F, Paronetto MP, Franco R, Chieffi P, Dolci S, Fry AM, Geremia R, Sette C. 2009.** Increased expression and nuclear localization of the centrosomal kinase Nek2 in human testicular seminomas. *The Journal of pathology* **217**: 431-41.
- Bartek J, Lukas J. 2001.** Pathways governing G<sub>1</sub>/S transition and their response to DNA damage. *FEBS letters* **490**: 117-22.
- Barton AB, Davies CJ, Hutchison CA 3rd, Kaback DB. 1992.** Cloning of chromosome I DNA from *Saccharomyces cerevisiae*: analysis of the FUN52 gene, whose product has homology to protein kinases. *Gene* **117**: 137-40.

- Bastos RN, Barr FA. 2010.** Plk1 negatively regulates Cep55 recruitment to the midbody to ensure orderly abscission. *The Journal of cell biology* **191**: 751-60.
- Bates S, Parry D, Bonetta L, Vousden K, Dickson C, Peters G. 1994.** Absence of cyclin D/cdk complexes in cells lacking functional retinoblastoma protein. *Oncogene* **9**: 1633-40.
- Bayliss R, Sardon T, Vernos I, Conti E. 2003.** Structural basis of Aurora-A activation by TPX2 at the mitotic spindle. *Molecular cell* **12**: 851-62.
- Becker WM, Kleinsmith LJ, Hardin J, Bertoni GP. 2008.** *The world of the cell*. San Francisco, CA: Pearson/Benjamin Cummings.
- Belham C, Roig J, Caldwell JA, Aoyama Y, Kemp BE, Comb M, Avruch J. 2003.** A mitotic cascade of NIMA family kinases. Nerc1/Nek9 activates the Nek6 and Nek7 kinases. *The Journal of biological chemistry* **278**: 34897-909.
- Bettencourt-Dias M, Glover DM. 2007.** Centrosome biogenesis and function: centrosomes bring new understanding. *Nature reviews molecular cell biology* **8**: 451-63.
- Bettencourt-Dias M, Rodrigues-Martins A, Carpenter L, Riparbelli M, Lehmann L, Gatt MK, Carmo N, Balloux F, Callaini G, Glover DM. 2005.** SAK/PLK4 is required for centriole duplication and flagella development. *Current biology* **15**: 2199-207.
- Blagden SP, Glover DM. 2003.** Polar expeditions--provisioning the centrosome for mitosis. *Nature cell biology* **5**: 505-11.
- Blangy A, Lane HA, d'Hérin P, Harper M, Kress M, Nigg EA. 1995.** Phosphorylation by p34<sup>cdc2</sup> regulates spindle association of human Eg5, a kinesin-related motor essential for bipolar spindle formation in vivo. *Cell* **83**: 1159-69.
- Bonetta L. 2004.** RNAi: silencing never sounded better. *Nature methods* **1**: 79-86.
- Bowers AJ, Boylan JF. 2004.** Nek8, a NIMA family kinase member, is overexpressed in primary human breast tumors. *Gene* **328**: 135-42.
- Bradley BA, Quarmby LM. 2005.** A NIMA-related kinase, Cnk2p, regulates both flagellar length and cell size in *Chlamydomonas*. *Journal of cell science* **118**: 3317-26.
- Burns TF, Fei P, Scata KA, Dicker DT, El-Deiry WS. 2003.** Silencing of the novel p53 target gene Snk/Plk2 leads to mitotic catastrophe in paclitaxel (taxol)-exposed cells. *Molecular and cellular biology* **23**: 5556-71.

- Cai Y, Somlo S. 2008.** Too much of a good thing: does Nek8 link polycystic kidney disease and nephronophthisis? *Journal of the American society of nephrology* **19**: 418-20.
- Carmena M, Earnshaw WC. 2003.** The cellular geography of aurora kinases. *Nature reviews molecular cell biology* **4**: 842-54.
- Carvajal RD, Tse A, Schwartz GK. 2006.** Aurora kinases: new targets for cancer therapy. *Clinical cancer research* **12**: 6869-75.
- Casenghi M, Barr FA, Nigg EA. 2005.** Phosphorylation of Nlp by Plk1 negatively regulates its dynein-dynactin-dependent targeting to the centrosome. *Journal of cell science* **118**: 5101-8.
- Casenghi M, Meraldi P, Weinhart U, Duncan PI, Körner R, Nigg EA. 2003.** Polo-like kinase 1 regulates Nlp, a centrosome protein involved in microtubule nucleation. *Developmental cell* **5**: 113-25.
- Chan CSM, Botstein D. 1993.** Isolation and characterization of chromosome-gain and increase-in-ploidy mutants in yeast. *Genetics* **135**: 677-91.
- Chan EH, Santamaria A, Silljé HH, Nigg EA. 2008.** Plk1 regulates mitotic Aurora A function through betaTrCP-dependent degradation of hBora. *Chromosoma* **117**: 457-69.
- Chang L, Karin M. 2001.** Mammalian MAP kinase signalling cascades. *Nature* **410**: 37-40.
- Chang J, Baloh RH, Milbrandt J. 2009.** The NIMA-family kinase Nek3 regulates microtubule acetylation in neurons. *Journal of cell science* **122**: 2274-82.
- Chellappan SP, Hiebert S, Mudryj M, Horowitz JM, Nevins JR. 1991.** The E2F transcription factor is a cellular target for the RB protein. *Cell* **65**: 1053-61.
- Chen A, Yanai A, Arama E, Kilfin G, Motro B. 1999.** NIMA-related kinases: isolation and characterization of murine nek3 and nek4 cDNAs, and chromosomal localization of nek1, nek2 and nek3. *Gene* **234**: 127-37.
- Chen Y, Chen P, Chen C, Jiang X, Riley DJ. 2008.** Never-in-mitosis related kinase 1 functions in DNA damage response and checkpoint control. *Cell cycle* **7**: 3194-201.
- Chen HL, Tang CJ, Chen CY, Tang TK. 2005.** Overexpression of an Aurora-C kinase-deficient mutant disrupts the Aurora-B/INCENP complex and induces polyploidy. *Journal of biomedical science* **12**: 297-310.
- Chin CF, Yeong FM. 2010.** Safeguarding entry into mitosis: the antepause checkpoint. *Molecular and cellular biology* **30**: 22-32.

- Ciliberto A, Shah JV. 2009.** A quantitative systems view of the spindle assembly checkpoint. *The EMBO journal* **28**: 2162-173.
- Cizmecioglu O, Warnke S, Arnold M, Duensing S, Hoffmann I. 2008.** Plk2 regulated centriole duplication is dependent on its localization to the centrioles and a functional polo-box domain. *Cell cycle* **7**: 3548-55.
- Crasta K, Lim HH, Zhang T, Nirantar S, Surana U. 2008.** Consorting kinases, end of destruction and birth of a spindle. *Cell Cycle* **7**: 2960-6.
- Dawe HR, Farr H, Gull K. 2007.** Centriole/basal body morphogenesis and migration during ciliogenesis in animal cells. *Journal of cell science* **120**: 7-15.
- De Souza CP, Horn KP, Masker K, Osmani SA. 2003.** The SONB(NUP98) nucleoporin interacts with the NIMA kinase in *Aspergillus nidulans*. *Genetics* **165**: 1071-81.
- De Souza CP, Osmani AH, Wu LP, Spotts JL, Osmani SA. 2000.** Mitotic histone H3 phosphorylation by the NIMA kinase in *Aspergillus nidulans*. *Cell* **102**: 293-302.
- DeLuca JG, Gall WE, Ciferri C, Cimini D, Musacchio A, Salmon ED. 2006.** Kinetochore microtubule dynamics and attachment stability are regulated by Hec1. *Cell* **127**: 969-82.
- Debec A, Sullivan W, Bettencourt-Dias M. 2010.** Centrioles: active players or passengers during mitosis? *Cellular and molecular life sciences* **67**: 2173-94.
- Delgehyr N, Sillibourne J, Bornens M. 2005.** Microtubule nucleation and anchoring at the centrosome are independent processes linked by ninein function. *Journal of cell science* **118**: 1565-75.
- Dharmacon. 2004.** *RNA interference technical reference & application guide*. Lafayette, CO: Dharmacon RNA Technologies.
- Ditchfield C, Johnson VL, Tighe A, Ellston R, Haworth C, Johnson T, Mortlock A, Keen N, Taylor SS. 2003.** Aurora B couples chromosome alignment with anaphase by targeting BubR1, Mad2, and Cenp-E to kinetochores. *The Journal of cell biology* **161**: 267-80.
- Doonan JH, Kitsios G. 2009.** Functional evolution of cyclin-dependent kinases. *Molecular biotechnology* **42**: 14-29.
- Dorée M, Galas S. 1994.** The cyclin-dependent protein kinases and the control of cell division. *FASEB Journal* **8**: 1114-21.
- Doxsey S. 2001.** Re-evaluating centrosome function. *Nature reviews molecular cell biology* **2**: 688-98.

- Dulić V, Kaufmann WK, Wilson SJ, Tlsty TD, Lees E, Harper JW, Elledge SJ, Reed SI. 1994.** p53-dependent inhibition of cyclin-dependent kinase activities in human fibroblasts during radiation-induced G<sub>1</sub> arrest. *Cell* **76**: 1013-23.
- Elia AE, Cantley LC, Yaffe MB. 2003a.** Proteomic screen finds pSer/pThr-binding domain localizing Plk1 to mitotic substrates. *Science* **299**: 1228-31.
- Elia AEH, Rellos P, Haire LF, Chao JW, Ivins FJ, Hoepker K, Mohammad D, Cantley LC, Smerdon SJ, Yaffe MB. 2003b.** The molecular basis for phosphodependent substrate targeting and regulation of Plks by the Polo-box domain. *Cell* **115**: 83-95.
- Elowe S, Hümmer S, Uldschmid A, Li X, Nigg EA. 2007.** Tension-sensitive Plk1 phosphorylation on BubR1 regulates the stability of kinetochore microtubule interactions. *Genes & development* **21**: 2205-19.
- Fang G. 2002.** Checkpoint protein BubR1 acts synergistically with Mad2 to inhibit anaphase-promoting complex. *Molecular biology of the cell* **13**: 755-66.
- Faragher AJ, Fry AM. 2003.** Nek2A kinase stimulates centrosome disjunction and is required for formation of bipolar mitotic spindles. *Molecular biology of the cell* **14**: 2876-89.
- Fardilha M, Wu W, Sá R, Fidalgo S, Sousa C, Mota C, da Cruz e Silva OA, da Cruz e Silva EF. 2004.** Alternatively spliced protein variants as potential therapeutic targets for male infertility and contraception. *Annals of the New York academy of sciences* **1030**: 468-78.
- Fletcher L, Cerniglia GJ, Nigg EA, Yend TJ, Muschel RJ. 2004.** Inhibition of centrosome separation after DNA damage: a role for Nek2. *Radiation research* **162**: 128-35.
- Fletcher L, Cerniglia GJ, Yen TJ, Muschel RJ. 2005.** Live cell imaging reveals distinct roles in cell cycle regulation for Nek2A and Nek2B. *Biochimica et biophysica acta* **1744**: 89-92.
- Fode C, Motro B, Yousefi S, Heffernan M, Dennis JW. 1994.** Sak, a murine protein-serine/threonine kinase that is related to the *Drosophila* polo kinase and involved in cell proliferation. *Proceedings of the national academy of sciences of the United States of America* **91**: 6388-92.
- Fry AM. 2002.** The Nek2 protein kinase: a novel regulator of centrosome structure. *Oncogene* **21**: 6184-94.
- Fry AM, Baxter JE. 2006.** Sealed with a Kiz: how Plk1 ensures spindle pole integrity. *Developmental cell* **11**: 431-2.
- Fry AM, Nigg EA. 1995.** The NIMA kinase joins forces with Cdc2. *Current biology* **5**: 1122-5.

- Fry AM, Arnaud L, Nigg EA. 1999.** Activity of the human centrosomal kinase, Nek2, depends on an unusual leucine zipper dimerization motif. *The Journal of biological chemistry* **274**: 16304-10.
- Fry AM, Mayor T, Meraldi P, Stierhof YD, Tanaka K, Nigg EA. 1998a.** C-Nap1, a novel centrosomal coiled-coil protein and candidate substrate of the cell cycle-regulated protein kinase Nek2. *The Journal of cell biology* **141**: 1563-74.
- Fry AM, Meraldi P, Nigg EA. 1998b.** A centrosomal function for the human Nek2 protein kinase, a member of the NIMA family of cell cycle regulators. *The EMBO journal* **17**: 470-81.
- Fry AM, Schultz SJ, Bartek J, Nigg EA. 1995.** Substrate specificity and cell cycle regulation of the Nek2 protein kinase, a potential human homolog of the mitotic regulator NIMA of *Aspergillus nidulans*. *The Journal of biological chemistry* **270**: 12899-905.
- Giet R, Glover DM. 2001.** Drosophila aurora B kinase is required for histone H3 phosphorylation and condensin recruitment during chromosome condensation and to organize the central spindle during cytokinesis. *The Journal of cell biology* **152**: 669-82.
- Glotzer M, Murray AW, Kirschner MW. 1991.** Cyclin is degraded by the ubiquitin pathway. *Nature* **349**: 132-38.
- Glover DM, Leibowitz MH, McLean DA, Parry H. 1995.** Mutations in aurora prevent centrosome separation leading to the formation of monopolar spindles. *Cell* **81**: 95-105.
- Goto H, Kiyono T, Tomono Y, Kawajiri A, Urano T, Furukawa K, Nigg EA, Inagaki M. 2006.** Complex formation of Plk1 and INCENP required for metaphase-anaphase transition. *Nature cell biology* **8**: 180-7.
- Goto H, Yasui Y, Nigg EA, Inagaki M. 2002.** Aurora-B phosphorylates Histone H3 at serine28 with regard to the mitotic chromosome condensation. *Genes to cells* **7**: 11-7.
- Grallert A, Hagan IM. 2002.** *Schizosaccharomyces pombe* NIMA-related kinase, Fin1, regulates spindle formation and an affinity of Polo for the SPB. *The EMBO journal* **21**: 3096-107.
- Grallert A, Krapp A, Bagley S, Simanis V, Hagan IM. 2004.** Recruitment of NIMA kinase shows that maturation of the *S. pombe* spindle-pole body occurs over consecutive cell cycles and reveals a role for NIMA in modulating SIN activity. *Genes & development* **18**: 1007-21.
- Habedanck R, Stierhof YD, Wilkinson CJ, Nigg EA. 2005.** The Polo kinase Plk4 functions in centriole duplication. *Nature cell biology* **7**: 1140-6.

- Hamanaka R, Maloid S, Smith MR, O'Connell CD, Longo DL, Ferris DK. 1994.** Cloning and characterization of human and murine homologues of the *Drosophila polo* serine-threonine kinase. *Cell growth & differentiation* **5**: 249-57.
- Hames RS, Fry AM. 2002.** Alternative splice variants of the human centrosome kinase Nek2 exhibit distinct patterns of expression in mitosis. *The Biochemical journal* **361**: 77-85.
- Hames RS, Crookes RE, Straatman KR, Merdes A, Hayes MJ, Faragher AJ, Fry AM. 2005.** Dynamic recruitment of Nek2 kinase to the centrosome involves microtubules, PCM-1, and localized proteasomal degradation. *Molecular biology of the cell* **16**: 1711-24.
- Hames RS, Wattam SL, Yamano H, Bacchieri R, Fry AM. 2001.** APC/C-mediated destruction of the centrosomal kinase Nek2A occurs in early mitosis and depends upon a cyclin A-type D-box. *The EMBO journal* **20**: 7117-27.
- Hanahan D, Weinberg RA. 2000.** The hallmarks of cancer. *Cell* **100**: 57-70.
- Hanisch A, Wehner A, Nigg EA, Silljé HHW. 2006.** Different Plk1 functions show distinct dependencies on Polo-Box domain-mediated targeting. *Molecular biology of the cell* **17**: 448-59.
- Hanks SK. 2003.** Genomic analysis of the eukaryotic protein kinase superfamily: a perspective. *Genome biology* **4**: 111.
- Hansen DV, Loktev AV, Ban KH, Jackson PK. 2004.** Plk1 regulates activation of the anaphase promoting complex by phosphorylating and triggering SCFbetaTrCP-dependent destruction of the APC inhibitor Emi1. *Molecular biology of the cell* **15**: 5623-34.
- Harbour JW, Luo RX, Santi AD, Postigo AA, Dean DC. 1999.** Cdk phosphorylation triggers sequential intramolecular interactions that progressively block Rb functions as cells move through G1. *Cell* **98**: 859-69.
- Hartman JJ, Mahr J, McNally K, Okawa K, Iwamatsu A, Thomas S, Cheesman S, Heuser J, Vale RD, McNally FJ. 1998.** Katanin, a microtubule-severing protein, is a novel AAA ATPase that targets to the centrosome using a WD40-containing subunit. *Cell* **93**: 277-87.
- Hartwell LH, Weinert TA. 1989.** Checkpoints: controls that ensure the order of cell cycle events. *Science* **246**: 629-34.
- Hashimoto Y, Akita H, Hibino M, Kohri K, Nakanishi M. 2002.** Identification and characterization of Nek6 protein kinase, a potential human homolog of NIMA histone H3 kinase. *Biochemical and biophysical research communications* **293**: 753-8.

- Hauf S, Cole RW, LaTerra S, Zimmer C, Schnapp G, Walter R, Heckel A, van Meel J, Rieder CL, Peters JM. 2003.** The small molecule Hesperadin reveals a role for Aurora B in correcting kinetochore-microtubule attachment and in maintaining the spindle assembly checkpoint. *The Journal of cell biology* **161**: 281-94.
- Hauf S, Roitinger E, Koch B, Dittrich CM, Mechtler K, Peters J. 2005.** Dissociation of cohesin from chromosome arms and loss of arm cohesion during early mitosis depends on phosphorylation of SA2. *PLoS biology* **3**: e69.
- Hayes MJ, Kimata Y, Wattam SL, Lindon C, Mao G, Yamano H, Fry AM. 2006.** Early mitotic degradation of Nek2A depends on Cdc20-independent interaction with the APC/C. *Nature cell biology* **8**: 607-14.
- Hayward DG, Clarke RB, Faragher AJ, Pillai MR, Hagan IM, Fry AM. 2004.** The centrosomal kinase Nek2 displays elevated levels of protein expression in human breast cancer. *Cancer research* **64**: 7370-6.
- Helps NR, Luo X, Barker HM, Cohen PT. 2000.** NIMA-related kinase 2 (Nek2), a cell-cycle-regulated protein kinase localized to centrosomes, is complexed to protein phosphatase 1. *The biochemical journal* **349**: 509-18.
- Hernández M, Almeida TA. 2006.** Is there any association between nek3 and cancers with frequent 13q14 deletion? *Cancer investigation* **24**: 682-8.
- Hilton LK, White MC, Quarmby LM. 2009.** The NIMA-related kinase NEK1 cycles through the nucleus. *Biochemical and biophysical research communications* **389**: 52-6.
- Hinchcliffe EH, Miller FJ, Cham M, Khodjakov A, Sluder G. 2001.** Requirement of a centrosomal activity for cell cycle progression through G1 into S phase. *Science* **291**: 1547-50.
- Hirano T. 2000.** Chromosome cohesion, condensation, and separation. *Annual review of biochemistry* **69**: 115-44.
- Hochegger H, Takeda S, Hunt T. 2008.** Cyclin-dependent kinases and cell-cycle transitions: does one fit all? *Nature reviews molecular cell biology* **9**: 910-6.
- Holland PM, Milne A, Garka K, Johnson RS, Willis C, Sims JE, Rauch CT, Bird TA, Virca GD. 2002.** Purification, cloning, and characterization of Nek8, a novel NIMA-related kinase, and its candidate substrate Bicd2. *The Journal of biological chemistry* **277**: 16229-40.
- Honda R, Körner R, Nigg EA. 2003.** Exploring the functional interactions between Aurora B, INCENP, and survivin in mitosis. *Molecular biology of the cell* **14**: 3325-41.

- Hoyer-Fender S. 2010.** Centriole maturation and transformation to basal body. *Seminars in cell & developmental biology* **21**: 142-7.
- Hudson JW, Kozarova A, Cheung P, Macmillan JC, Swallow CJ, Cross JC, Dennis JW. 2001.** Late mitotic failure in mice lacking Sak, a polo-like kinase. *Current biology* **11**: 441-6.
- Hutterer A, Berdnik D, Wirtz-Peitz F, Zigman M, Schleiffer A, Knoblich JA. 2006.** Mitotic activation of the kinase Aurora-A requires its binding partner Bora. *Developmental cell* **11**: 147-57.
- Jeong Y, Lee J, Kim K, Yoo JC, Rhee K. 2007.** Characterization of NIP2/centrobin, a novel substrate of Nek2, and its potential role in microtubule stabilization. *Journal of cell science* **120**: 2106-16.
- Johnson DG, Walker CL. 1999.** Cyclins and cell cycle checkpoints. *Annual review of pharmacology and toxicology* **39**: 295-312.
- Jones DG, Rosamond J. 1990.** Isolation of a novel protein kinase-encoding gene from yeast by oligodeoxyribonucleotide probing. *Gene* **90**: 87-92.
- Kaelin WG Jr. 1999.** Functions of the retinoblastoma protein. *BioEssays* **21**: 950-8.
- Kambouris NG, Burke DJ, Creutz CE. 1993.** Cloning and genetic analysis of the gene encoding a new protein kinase in *Saccharomyces cerevisiae*. *Yeast* **9**: 141-50.
- Kandli M, Feige E, Chen A, Kilfin G, Motro B. 2000.** Isolation and characterization of two evolutionarily conserved murine kinases (Nek6 and nek7) related to the fungal mitotic regulator, NIMA. *Genomics* **68**: 187-96.
- Khodjakov A, Rieder CL. 2001.** Centrosomes enhance the fidelity of cytokinesis in vertebrates and are required for cell cycle progression. *The Journal of cell biology* **153**: 237-42.
- Khodjakov A, Cole RW, Oakley BR, Rieder CL. 2000.** Centrosome-independent mitotic spindle formation in vertebrates. *Current biology* **10**: 59-67.
- Kim S, Lee K, Rhee K. 2007.** NEK7 is a centrosomal kinase critical for microtubule nucleation. *Biochemical and biophysical research communications* **360**: 56-62.
- Kimura M, Okano Y. 2001.** Molecular cloning and characterization of the human NIMA-related protein kinase 3 gene (NEK3). *Cytogenetics and cell genetics* **95**: 177-82.
- Kimura M, Matsuda Y, Yoshioka T, Okano Y. 1999.** Cell cycle-dependent expression and centrosome localization of a third human aurora/lpl1-related protein kinase, AIK3. *The Journal of biological chemistry* **274**: 7334-40.

- Kitada K, Johnson AL, Johnston LH, Sugino A. 1993.** A multicopy suppressor gene of the *Saccharomyces cerevisiae* G<sub>1</sub> cell cycle mutant gene *dbf4* encodes a protein kinase and is identified as CDC5. *Molecular and cellular biology* **13**: 4445-57.
- Kleylein-Sohn J, Westendorf J, Le Clech M, Habedanck R, Stierhof YD, Nigg EA. 2007.** Plk4-induced centriole biogenesis in human cells. *Developmental cell* **13**: 190-202.
- Knowlton AL, Lan W, Stukenberg PT. 2006.** Aurora B is enriched at merotelic attachment sites, where it regulates MCAK. *Current biology* **16**: 1705-10.
- Ko MA, Rosario CO, Hudson JW, Kulkarni S, Pollett A, Dennis JW, Swallow CJ. 2005.** Plk4 haploinsufficiency causes mitotic infidelity and carcinogenesis. *Nature genetics* **37**: 883-8.
- Koff A, Giordano A, Desai D, Yamashita K, Harper JW, Elledge S, Nishimoto T, Morgan DO, Franza BR, Roberts JM. 1992.** Formation and activation of a cyclin E-cdk2 complex during the G<sub>1</sub> phase of the human cell cycle. *Science* **257**: 1689-94.
- Kokuryo T, Senga T, Yokoyama Y, Nagino M, Nimura Y, Hamaguchi M. 2007.** Nek2 as an effective target for inhibition of tumorigenic growth and peritoneal dissemination of cholangiocarcinoma. *Cancer research* **67**: 9637-42.
- Kops GJPL, Saurin AT, Meraldi P. 2010.** Finding the middle ground: how kinetochores power chromosome congression. *Cellular and molecular life sciences* **67**: 2145-61.
- Krause A, Hoffmann I. 2010.** Polo-like kinase 2-dependent phosphorylation of NPM/B23 on serine 4 triggers centriole duplication. *PLoS one* **5**: e9849.
- Krien MJE, Bugg SJ, Palatsides M, Asouline G, Morimyo M, O'Connell MJ. 1998.** A NIMA homologue promotes chromatin condensation in fission yeast. *Journal of cell science* **111**: 967-76.
- Krien MJE, West RR, John UP, Koniaras K, McIntosh JR, O'Connell MJ. 2002.** The fission yeast NIMA kinase Fin1p is required for spindle function and nuclear envelope integrity. *The EMBO journal* **21**: 1713-22.
- Kuriyama R, Bettencourt-Dias M, Hoffmann I, Arnold M, Sandvig L. 2009.** Gamma-tubulin-containing abnormal centrioles are induced by insufficient Plk4 in human HCT116 colorectal cancer cells. *Journal of cell science* **122**: 2014-23.
- Lampson MA, Renduchitala K, Khodjakov A, Kapoor TM. 2004.** Correcting improper chromosome-spindle attachments during cell division. *Nature cell biology* **6**: 232-7.

- Lan W, Zhang X, Kline-Smith SL, Rosasco SE, Barrett-Wilt GA, Shabanowitz J, Hunt DF, Walczak CE, Stukenberg PT. 2004.** Aurora B phosphorylates centromeric MCAK and regulates its localization and microtubule depolymerization activity. *Current biology* **14**: 273-86.
- Lane HA, Nigg EA. 1996.** Antibody microinjection reveals an essential role for human polo-like kinase 1 (Plk1) in the functional maturation of mitotic centrosomes. *The Journal of cell biology* **135**: 1701-13.
- Lee KS, Yuan YL, Kuriyama R, Erikson RL. 1995.** Plk is an M-phase-specific protein kinase and interacts with a kinesin-like protein, CHO1/MKLP-1. *Molecular and cellular biology* **15**: 7143-51.
- Lees JA, Buchkovich KJ, Marshak DR, Anderson CW, Harlow E. 1991.** The retinoblastoma protein is phosphorylated on multiple sites by human cdc2. *The EMBO journal* **10**: 4279-90.
- Letwin K, Mizzen L, Motro B, Ben-David Y, Bernstein A, Pawson T. 1992.** A mammalian dual specificity protein kinase, Nek1, is related to the NIMA cell cycle regulator and highly expressed in meiotic germ cells. *The EMBO Journal* **11**: 3521 -31.
- Li B, Ouyang B, Pan H, Reissmann PT, Slamon DJ, Arceci R, Lu L, Dai W. 1996.** *Prk*, a cytokine-inducible human protein serine/threonine kinase whose expression appears to be down-regulated in lung carcinomas. *The Journal of biological chemistry* **271**: 19402-8.
- Li M, Satinover DL, Brautigan DL. 2007.** Phosphorylation and functions of inhibitor-2 family of proteins. *Biochemistry* **46**: 2380-9.
- Liby K, Wu H, Ouyang B, Wu S, Chen J, Dai W. 2001.** Identification of the human homologue of the early-growth response gene *Snk*, encoding a serum-inducible kinase. *DNA sequence* **11**: 527-33.
- Lim HH, Zhang T, Surana U. 2009.** Regulation of centrosome separation in yeast and vertebrates: common threads. *Trends in cell biology* **19**: 325-33.
- Lindqvist A, Rodríguez-Bravo V, Medema RH. 2009.** The decision to enter mitosis: feedback and redundancy in the mitotic entry network. *The Journal of cell biology* **185**: 193-202.
- Lipp JJ, Hirota T, Poser I, Peters JM. 2007.** Aurora B controls the association of condensin I but not condensin II with mitotic chromosomes. *Journal of cell science* **120**: 1245-55.
- Liu S, Lu W, Obara T, Kuida S, Lehoczky J, Dewar K, Drummond IA, Beier DR. 2002.** A defect in a novel Nek-family kinase causes cystic kidney disease in the mouse and in zebrafish. *Development* **129**: 5839-46.

- Liu D, Vader G, Vromans MJ, Lampson MA, Lens SM. 2009.** Sensing chromosome bi-orientation by spatial separation of aurora B kinase from kinetochore substrates. *Science* **323**: 1350-3.
- Liu X, Zhou T, Kuriyama R, Erikson RL. 2004.** Molecular interactions of Polo-like-kinase 1 with the mitotic kinesin-like protein CHO1/MKLP-1. *Journal of cell science* **117**: 3233-46.
- Llamazares S, Moreira A, Tavares A, Girdham C, Spruce BA, Gonzalez C, Karess RE, Glover DM, Sunkel CE. 1991.** *polo* encodes a protein kinase homolog required for mitosis in *Drosophila*. *Genes & development* **5**: 2153-65.
- Lu KP, Hunter T. 1995.** Evidence for a NIMA-like mitotic pathway in vertebrate cells. *Cell* **81**: 413-24.
- Lu KP, Kemp BE, Means AR. 1994.** Identification of substrate specificity determinants for the cell cycle-regulated NIMA protein kinase. *The Journal of biological chemistry* **269**: 6603-7.
- Lu KP, Osmani SA, Means AR. 1993.** Properties and regulation of the cell cycle-specific NIMA protein kinase of *Aspergillus nidulans*. *The Journal of biological chemistry* **268**: 8769-76.
- Lundberg AS, Weinberg RA. 1998.** Functional inactivation of the retinoblastoma protein requires sequential modification by at least two distinct cyclin-cdk complexes. *Molecular and cellular biology* **18**: 753-61.
- Lénárt P, Petronczki M, Steegmaier M, Di Fiore B, Lipp JJ, Hoffmann M, Rettig WJ, Kraut N, Peters J. 2007.** The small-molecule inhibitor BI 2536 reveals novel insights into mitotic roles of polo-like kinase 1. *Current biology* **17**: 304-15.
- Ma S, Charron J, Erikson RL. 2003a.** Role of Plk2 (Snk) in mouse development and cell proliferation. *Molecular and cellular biology* **23**: 6936-43.
- Ma S, Liu MA, Yuan YL, Erikson RL. 2003b.** The serum-inducible protein kinase Snk is a G1 phase polo-like kinase that is inhibited by the calcium- and integrin-binding protein CIB. *Molecular cancer research* **1**: 376-84.
- Macurek L, Lindqvist A, Medema RH. 2009.** Aurora-A and hBora join the game of Polo. *Cancer research* **69**: 4555-8.
- Macůrek L, Lindqvist A, Lim D, Lampson MA, Klompaker R, Freire R, Clouin C, Taylor SS, Yaffe MB, Medema RH. 2008.** Polo-like kinase-1 is activated by aurora A to promote checkpoint recovery. *Nature* **455**: 119-23.

- Mahjoub MR, Montpetit B, Zhao L, Finst RJ, Goh B, Kim AC, Quarmby LM. 2002.** The FA2 gene of *Chlamydomonas* encodes a NIMA family kinase with roles in cell cycle progression and microtubule severing during deflagellation. *Journal of cell science* **115**: 1759-68.
- Mahjoub MR, Trapp ML, Quarmby LM. 2005.** NIMA-related kinases defective in murine models of polycystic kidney diseases localize to primary cilia and centrosomes. *Journal of the American society of nephrology* **16**: 3485-9.
- Mailand N, Diffley JFX. 2005.** CDKs promote DNA replication origin licensing in human cells by protecting Cdc6 from APC/C-dependent proteolysis. *Cell* **122**: 915-26.
- Malumbres M, Barbacid M. 2005.** Mammalian cyclin-dependent kinases. *Trends in biochemical sciences* **30**: 630-41.
- Malumbres M, Barbacid M. 2007.** Cell cycle kinases in cancer. *Current opinion in genetics & development* **17**: 60-5.
- Malumbres M, Barbacid M. 2009.** Cell cycle, CDKs and cancer: a changing paradigm. *Nature reviews cancer* **9**: 153-66.
- Malumbres M, Harlow E, Hunt T, Hunter T, Lahti JM, Manning G, Morgan DO, Tsai LH, Wolgemuth DJ. 2009.** Cyclin-dependent kinases: a family portrait. *Nature Cell Biology* **11**: 1275-6.
- Manning G, Whyte DB, Martinez R, Hunter T, Sudarsanam S. 2002.** The protein kinase complement of the human genome. *Science* **298**: 1912-34.
- Mardin BR, Lange C, Baxter JE, Hardy T, Scholz SR, Fry AM, Schiebel E. 2010.** Components of the Hippo pathway cooperate with Nek2 kinase to regulate centrosome disjunction. *Nature cell biology* **12**: 1166-76.
- Matsumura S, Toyoshima F, Nishida E. 2007.** Polo-like kinase 1 facilitates chromosome alignment during prometaphase through BubR1. *The Journal of biological chemistry* **282**: 15217-27.
- McGuinness BE, Hirota T, Kudo NR, Peters JM, Nasmyth K. 2005.** Shugoshin prevents dissociation of cohesin from centromeres during mitosis in vertebrate cells. *PLoS biology* **3**: e86.
- Melixetian M, Klein DK, Sørensen CS, Helin K. 2009.** NEK11 regulates CDC25A degradation and the IR-induced G2/M checkpoint. *Nature cell biology* **11**: 1247-53.
- Mi J, Guo C, Brautigan DL, Larner JM. 2007.** Protein phosphatase-1alpha regulates centrosome splitting through Nek2. *Cancer research* **67**: 1082-9.

- Mikule K, Delaval B, Kaldis P, Jurczyk A, Hergert P, Doxsey S. 2007.** Loss of centrosome integrity induces p38-p53-p21-dependent G1-S arrest. *Nature cell biology* **9**: 160-70.
- Miller SL, Antico G, Raghunath PN, Tomaszewski JE, Clevenger CV. 2007.** Nek3 kinase regulates prolactin-mediated cytoskeletal reorganization and motility of breast cancer cells. *Oncogene* **26**: 4668-78.
- Miller SL, DeMaria JE, Freier DO, Riegel AM, Clevenger CV. 2005.** Novel association of Vav2 and Nek3 modulates signaling through the human prolactin receptor. *Molecular endocrinology* **19**: 939-49.
- Minoguchi S, Minoguchi M, Yoshimura A. 2003.** Differential control of the NIMA-related kinases, Nek6 and Nek7, by serum stimulation. *Biochemical and biophysical research communications* **301**: 899-906.
- Moniz LS, Stambolic V. 2011.** Nek10 mediates G<sub>2</sub>/M cell cycle arrest and MEK autoactivation in response to UV irradiation. *Molecular and cellular biology* **31**: 30-42.
- Morgan DO. 1995.** Principles of CDK regulation. *Nature* **374**: 131-4.
- Morgan DO. 1997.** Cyclin-dependent kinases: engines, clocks, and microprocessors. *Annual review of cell and developmental biology* **13**: 261-91.
- Morris NR. 1975.** Mitotic mutants of *Aspergillus nidulans*. *Genetical research* **26**: 237-54.
- Musacchio A, Salmon ED. 2007.** The spindle-assembly checkpoint in space and time. *Nature reviews molecular cell biology* **8**: 379-93.
- Myer DL, Bahassi el M, Stambrook PJ. 2005.** The Plk3-Cdc25 circuit. *Oncogene* **24**: 299-305.
- Nakayama KI, Nakayama K. 2006.** Ubiquitin ligases: cell-cycle control and cancer. *Nature reviews cancer* **6**: 369-81.
- Nassirpour R, Shao L, Flanagan P, Abrams T, Jallal B, Smeal T, Yin MJ. 2010.** Nek6 mediates human cancer cell transformation and is a potential cancer therapeutic target. *Molecular cancer research* **8**: 717-28.
- Neef R, Gruneberg U, Kopajtich R, Li X, Nigg EA, Sillje H, Barr FA. 2007.** Choice of Plk1 docking partners during mitosis and cytokinesis is controlled by the activation state of Cdk1. *Nature cell biology* **9**: 436-44.
- Neef R, Preisinger C, Sutcliffe J, Kopajtich R, Nigg EA, Mayer TU, Barr FA. 2003.** Phosphorylation of mitotic kinesin-like protein 2 by polo-like kinase 1 is required for cytokinesis. *The Journal of cell biology* **162**: 863-75.

- Nigg EA. 1995.** Cyclin-dependent protein kinases: key regulators of the eukaryotic cell cycle. *BioEssays* **17**: 471-80.
- Nigg EA. 2001.** Mitotic kinases as regulators of cell division and its checkpoints. *Nature reviews molecular cell biology* **2**: 21-32.
- Nigg EA, Raff JW. 2009.** Centrioles, centrosomes, and cilia in health and disease. *Cell* **139**: 663-78.
- Nishino M, Kurasawa Y, Evans R, Lin SH, Brinkley BR, Yu-Lee LY. 2006.** NudC is required for Plk1 targeting to the kinetochore and chromosome congression. *Current biology* **16**: 1414-21.
- Noguchi K, Fukazawa H, Murakami Y, Uehara Y. 2002.** Nek11, a new member of the NIMA family of kinases, involved in DNA replication and genotoxic stress responses. *The Journal of biological chemistry* **277**: 39655-65.
- Noguchi K, Fukazawa H, Murakami Y, Uehara Y. 2004.** Nucleolar Nek11 is a novel target of Nek2A in G<sub>1</sub>/S-arrested cells. *The Journal of biological chemistry* **279**: 32716-27.
- Novak B, Sible JC, Tyson JJ. 2001.** Checkpoints in the Cell Cycle. *Encyclopedia of Life Sciences*.
- O'Connell MJ, Krien MJE, Hunter T. 2003.** Never say never. The NIMA-related protein kinases in mitotic control. *Trends in Cell Biology* **13**: 221-8.
- O'Connell MJ, Norbury C, Nurse P. 1994.** Premature chromatin condensation upon accumulation of NIMA. *The EMBO journal* **13**: 4926-37.
- O'Regan L, Fry AM. 2009.** The Nek6 and Nek7 protein kinases are required for robust mitotic spindle formation and cytokinesis. *Molecular and cellular biology* **29**: 3975-90.
- O'Regan L, Blot J, Fry AM. 2007.** Mitotic regulation by NIMA-related kinases. *Cell division* **2**: 25.
- Oakley BR, Morris NR. 1983.** A mutation in aspergillus nidulans that blocks the transition from interphase to prophase. *Journal of Cell Biology* **96**: 1155-8.
- Ohkura H, Hagan IM, Glover DM. 1995.** The conserved Schizosaccharomyces pombe kinase plo1, required to form a bipolar spindle, the actin ring, and septum, can drive septum formation in G<sub>1</sub> and G<sub>2</sub> cells. *Genes & development* **9**: 1059-73.
- Oshimori N, Ohsugi M, Yamamoto T. 2006.** The Plk1 target Kizuna stabilizes mitotic centrosomes to ensure spindle bipolarity. *Nature cell biology* **8**: 1095-101.

- Osmani SA, Ye XS. 1996.** Cell cycle regulation in *Aspergillus* by two protein kinases. *The Biochemical journal* **317**: 633-41.
- Osmani SA, May GS, Morris NR. 1987.** Regulation of the mRNA levels of *nimA*, a gene required for the G2-M transition in *Aspergillus nidulans*. *The Journal of cell biology* **104**: 1495-504.
- Osmani AH, O'Donnell K, Pu RT, Osmani SA. 1991.** Activation of the *nimA* protein kinase plays a unique role during mitosis that cannot be bypassed by absence of the *bimE* checkpoint. *The EMBO journal* **10**: 2669-79.
- Osmani SA, Pu RT, Morris NR. 1988.** Mitotic induction and maintenance by overexpression of a G2-specific gene that encodes a potential protein kinase. *Cell* **53**: 237-44.
- Otto EA, Trapp ML, Schultheiss UT, Helou J, Quarmby LM, Hildebrandt F. 2008.** NEK8 mutations affect ciliary and centrosomal localization and may cause nephronophthisis. *Journal of the American society of nephrology* **19**: 587-92.
- Pardee AB. 1974.** A restriction point for control of normal animal cell proliferation. *Proceedings of the national academy of sciences of the United States of America* **71**: 1286-90.
- Pardee AB. 1989.** G<sub>1</sub> events and regulation of cell proliferation. *Science* **246**: 603-8.
- Pavletich NP. 1999.** Mechanisms of cyclin-dependent kinase regulation: structures of Cdks, their cyclin activators, and Cip and INK4 inhibitors. *Journal of molecular biology* **287**: 821-8.
- Pelegri AL, Moura DJ, Brenner BL, Ledur PF, Maques GP, Henriques JA, Saffi J, Lenz G. 2010.** Nek1 silencing slows down DNA repair and blocks DNA damage-induced cell cycle arrest. *Mutagenesis* **25**: 447-54.
- Pelka P, Scimè A, Mandalfino C, Joch M, Abdulla P, Whyte P. 2007.** Adenovirus E1A proteins direct subcellular redistribution of Nek9, a NimA-related kinase. *Journal of cellular physiology* **212**: 13-25.
- Petronczki M, Glotzer M, Kraut N, Peters JM. 2007.** Polo-like kinase 1 triggers the initiation of cytokinesis in human cells by promoting recruitment of the RhoGEF Ect2 to the central spindle. *Developmental cell* **12**: 713-25.
- Petronczki M, Lénárt P, Peters J. 2008.** Polo on the rise—from mitotic entry to cytokinesis with Plk1. *Developmental cell* **14**: 646-59.
- Piel M, Nordberg J, Euteneuer U, Bornens M. 2001.** Centrosome-dependent exit of cytokinesis in animal cells. *Science* **291**: 1550-3.

- Pines J, Rieder CL. 2001.** Re-staging mitosis: a contemporary view of mitotic progression. *Nature cell biology* **3**: E3-6.
- Polci R, Peng A, Chen PL, Riley DJ, Chen Y. 2004.** NIMA-related protein kinase 1 is involved early in the ionizing radiation-induced DNA damage response. *Cancer research* **64**: 8800-3.
- Pu RT, Osmani SA. 1995.** Mitotic destruction of the cell cycle regulated NIMA protein kinase of *Aspergillus nidulans* is required for mitotic exit. *The EMBO journal* **14**: 995-1003.
- Pu RT, Xu G, Wu L, Vierula J, O'Donnell K, Ye XS, Osmani SA. 1995.** Isolation of a functional homolog of the cell cycle-specific NIMA protein kinase of *Aspergillus nidulans* and functional analysis of conserved residues. *The Journal of biological chemistry* **270**: 18110-6.
- Pugacheva EN, Jablonski SA, Hartman TR, Henske EP, Golemis EA. 2007.** HEF1-dependent Aurora A activation induces disassembly of the primary cilium. *Cell* **129**: 1351-63.
- Qi W, Tang Z, Yu H. 2006.** Phosphorylation- and polo-box-dependent binding of Plk1 to Bub1 is required for the kinetochore localization of Plk1. *Molecular biology of the cell* **17**: 3705-16.
- Quarmby LM, Mahjoub MR. 2005.** Caught Nek-ing: cilia and centrioles. *Journal of cell science* **118**: 5161-9.
- Quarmby LM, Parker JDK. 2005.** Cilia and the cell cycle? *The Journal of cell biology* **169**: 707-10.
- Rapley J, Baxter JE, Blot J, Wattam SL, Casenghi M, Meraldi P, Nigg EA, Fry AM. 2005.** Coordinate regulation of the mother centriole component Nlp by Nek2 and Plk1 protein kinases. *Molecular and cellular biology* **25**: 1309-24.
- Rellos P, Ivins FJ, Baxter JE, Pike A, Nott TJ, Parkinson D, Das S, Howell S, Fedorov O, Shen QY, Fry AM, Knapp S, Smerdon SJ. 2007.** Structure and regulation of the human Nek2 centrosomal kinase. *The Journal of biological chemistry* **282**: 6833-42.
- Richards MW, O'Regan L, Mas-Droux C, Blot JM, Cheung J, Hoelder S, Fry AM, Bayliss R. 2009.** An autoinhibitory tyrosine motif in the cell-cycle-regulated Nek7 kinase is released through binding of Nek9. *Molecular cell* **36**: 560-70.
- Rieder CL, Faruki S, Khodjakov A. 2001.** The centrosome in vertebrates: more than a microtubule-organizing center. *Trends in cell biology* **11**: 413-9.
- Roig J, Groen A, Caldwell J, Avruch J. 2005.** Active Nercc1 protein kinase concentrates at centrosomes early in mitosis and is necessary for proper spindle assembly. *Molecular Biology of the Cell* **16**: 4827-40.

- Roig J, Mikhailov A, Belham C, Avruch J. 2002.** Nercc1, a mammalian NIMA-family kinase, binds the Ran GTPase and regulates mitotic progression. *Genes & development* **16**: 1640-58.
- Roshak AK, Capper EA, Imburgia C, Fornwald J, Scott G, Marshall LA. 2000.** The human polo-like kinase, PLK, regulates cdc2/cyclin B through phosphorylation and activation of the cdc25C phosphatase. *Cellular signalling* **12**: 405-11.
- Russell P, Nurse P. 1986.** Schizosaccharomyces pombe and saccharomyces cerevisiae: A look at yeasts divided. *Cell* **45**: 781-2.
- Sagona AP, Stenmark H. 2010.** Cytokinesis and cancer. *FEBS letters* **584**: 2652-61.
- Salaun P, Rannou Y, Prigent C. 2008.** Cdk1, Plks, Auroras, and Neks: the mitotic bodyguards. *Advances in experimental medicine and biology* **617**: 41-56.
- Sankaran S, Parvin JD. 2006.** Centrosome function in normal and tumor cells. *Journal of cellular biochemistry* **99**: 1240-50.
- Santamaría D, Barrière C, Cerqueira A, Hunt S, Tardy C, Newton K, Cáceres JF, Dubus P, Malumbres M, Barbacid M. 2007.** Cdk1 is sufficient to drive the mammalian cell cycle. *Nature* **448**: 811-5.
- Sasai K, Katayama H, Stenoien DL, Fujii S, Honda R, Kimura M, Okano Y, Tatsuka M, Suzuki F, Nigg EA, Earnshaw WC, Brinkley WR, Sen S. 2004.** Aurora-C kinase is a novel chromosomal passenger protein that can complement Aurora-B kinase function in mitotic cells. *Cell motility and the cytoskeleton* **59**: 249-63.
- Schatten H. 2008.** The mammalian centrosome and its functional significance. *Histochemistry and cell biology* **129**: 667-86.
- Schmit TL, Ahmad N. 2007.** Regulation of mitosis via mitotic kinases: new opportunities for cancer management. *Molecular cancer therapeutics* **6**: 1920-31.
- Schultz SJ, Fry AM, Sütterlin C, Ried T, Nigg EA. 1994.** Cell cycle-dependent expression of Nek2, a novel human protein kinase related to the NIMA mitotic regulator of Aspergillus nidulans. *Cell growth & differentiation* **5**: 625-35.
- Schöffski P. 2009.** Polo-like kinase (PLK) inhibitors in preclinical and early clinical development in oncology. *The oncologist* **14**: 559-70.
- Seki A, Coppinger JA, Du H, Jang CY, Yates JR 3rd, Fang G. 2008a.** Plk1- and beta-TrCP-dependent degradation of Bora controls mitotic progression. *The Journal of cell biology* **181**: 65-78.

- Seki A, Coppinger JA, Jang CY, Yates JR, Fang G. 2008b.** Bora and the kinase Aurora a cooperatively activate the kinase Plk1 and control mitotic entry. *Science* **320**: 1655-8.
- Shalom O, Shalva N, Altschuler Y, Motro B. 2008.** The mammalian Nek1 kinase is involved in primary cilium formation. *FEBS letters* **582**: 1465-70.
- Sherr CJ. 2000.** The Pezcoller lecture: cancer cell cycles revisited. *Cancer research* **60**: 3689-95.
- Sherr CJ, Roberts JM. 1999.** CDK inhibitors: positive and negative regulators of G1-phase progression. *Genes & development* **13**: 1501-12.
- Sherr CJ, Roberts JM. 2004.** Living with or without cyclins and cyclin-dependent kinases. *Genes & development* **18**: 2699-711.
- Shiba D, Manning DK, Koga H, Beier DR, Yokoyama T. 2010.** Inv acts as a molecular anchor for Nphp3 and Nek8 in the proximal segment of primary cilia. *Cytoskeleton* **67**: 112-9.
- Shimizu-Yoshida Y, Sugiyama K, Rogounovitch T, Ohtsuru A, Namba H, Saenko V, Yamashita S. 2001.** Radiation-inducible hSNK gene is transcriptionally regulated by p53 binding homology element in human thyroid cells. *Biochemical and biophysical research communications* **289**: 491-8.
- Shintomi K, Hirano T. 2010.** Sister chromatid resolution: a cohesin releasing network and beyond. *Chromosoma* **119**: 459-67.
- Sillibourne JE, Tack F, Vloemans N, Boeckx A, Thambirajah S, Bonnet P, Ramaekers FC, Bornens M, Grand-Perret T. 2010.** Autophosphorylation of polo-like kinase 4 and its role in centriole duplication. *Molecular biology of the cell* **21**: 547-61.
- Simmons DL, Neel BG, Stevens R, Evett G, Erikson RL. 1992.** Identification of an early-growth-response gene encoding a novel putative protein kinase. *Molecular and cellular biology* **12**: 4164-9.
- Slattery SD, Mancini MA, Brinkley BR, Hall RM. 2009.** Aurora-C kinase supports mitotic progression in the absence of Aurora-B. *Cell cycle* **8**: 2984-94.
- Sohara E, Luo Y, Zhang J, Manning DK, Beier DR, Zhou J. 2008.** Nek8 regulates the expression and localization of polycystin-1 and polycystin-2. *Journal of the American society of nephrology* **19**: 469-76.
- Sørensen CS, Melixetian M, Klein DK, Helin K. 2010.** NEK11: linking CHK1 and CDC25A in DNA damage checkpoint signaling. *Cell cycle* **9**: 450-5.
- Sorokin S. 1962.** Centrioles and the formation of rudimentary cilia by fibroblasts and smooth muscle cells. *The Journal of cell biology* **15**: 363-77.

- Sumara I, Giménez-Abián JF, Gerlich D, Hirota T, Kraft C, de la Torre C, Ellenberg J, Peters JM. 2004.** Roles of Polo-like kinase 1 in the assembly of functional mitotic spindles. *Current biology* **14**: 1712-22.
- Sumara I, Vorlaufer E, Stukenberg PT, Kelm O, Redemann N, Nigg EA, Peters JM. 2002.** The dissociation of cohesin from chromosomes in prophase is regulated by Polo-like kinase. *Molecular cell* **9**: 515-25.
- Sunkel CE, Glover DM. 1988.** *polo*, a mitotic mutant of *Drosophila* displaying abnormal spindle poles. *Journal of cell science* **89**: 25-38.
- Surpili MJ, Delben TM, Kobarg J. 2003.** Identification of proteins that interact with the central coiled-coil region of the human protein kinase NEK1. *Biochemistry* **42**: 15369-76.
- Suzuki K, Kokuryo T, Senga T, Yokoyama Y, Nagino M, Hamaguchi M. 2010.** Novel combination treatment for colorectal cancer using Nek2 siRNA and cisplatin. *Cancer science* **101**: 1163-9.
- Tanaka TU. 2010.** Kinetochore-microtubule interactions: steps towards bi-orientation. *The EMBO journal* **29**: 4070-82.
- Tanaka K, Nigg EA. 1999.** Cloning and characterization of the murine Nek3 protein kinase, a novel member of the NIMA family of putative cell cycle regulators. *The Journal of biological chemistry* **274**: 13491-7.
- Tanaka TU, Rachidi N, Janke C, Pereira G, Galova M, Schiebel E, Stark MJ, Nasmyth K. 2002.** Evidence that the Ipl1-Sli15 (Aurora kinase-INCENP) complex promotes chromosome bi-orientation by altering kinetochore-spindle pole connections. *Cell* **108**: 317-29.
- Thomas J, Morlé L, Soulavie F, Laurençon A, Sagnol S, Durand B. 2010.** Transcriptional control of genes involved in ciliogenesis: a first step in making cilia. *Biology of the cell* **102**: 499-513.
- Toyoshima-Morimoto F, Taniguchi E, Nishida E. 2002.** Plk1 promotes nuclear translocation of human Cdc25C during prophase. *EMBO reports* **3**: 341-8.
- Trapp ML, Galtseva A, Manning DK, Beier DR, Rosenblum ND, Quarmby LM. 2008.** Defects in ciliary localization of Nek8 is associated with cystogenesis. *Pediatric nephrology* **23**: 377-87.
- Tsai MY, Zheng Y. 2005.** Aurora A kinase-coated beads function as microtubule-organizing centers and enhance RanGTP-induced spindle assembly. *Current biology* **15**: 2156-63.
- Tsai MY, Wiese C, Cao K, Martin O, Donovan P, Ruderman J, Prigent C, Zheng Y. 2003.** A Ran signalling pathway mediated by the mitotic kinase Aurora A in spindle assembly. *Nature cell biology* **5**: 242-8.

- Tseng TC, Chen SH, Hsu YP, Tang TK. 1998.** Protein kinase profile of sperm and eggs: cloning and characterization of two novel testis-specific protein kinases (AIE1, AIE2) related to yeast and fly chromosome segregation regulators. *DNA and cell biology* **17**: 823-33.
- Tsunoda N, Kokuryo T, Oda K, Senga T, Yokoyama Y, Nagino M, Nimura Y, Hamaguchi M. 2009.** Nek2 as a novel molecular target for the treatment of breast carcinoma. *Cancer science* **100**: 111-6.
- Uhlmann F, Lottspeich F, Nasmyth K. 1999.** Sister-chromatid separation at anaphase onset is promoted by cleavage of the cohesin subunit Scc1. *Nature* **400**: 37-42.
- Upadhy P, Birkenmeier EH, Birkenmeier CS, Barker JE. 2000.** Mutations in a NIMA-related kinase gene, Nek1, cause pleiotropic effects including a progressive polycystic kidney disease in mice. *Proceedings of the national academy of sciences of the United States of America* **97**: 217-21.
- Urbani L, Stearns T. 1999.** The centrosome. *Current biology* **9**: R315-7.
- Vader G, Lens SMA. 2008.** The Aurora kinase family in cell division and cancer. *Biochimica et biophysica acta* **1786**: 60-72.
- Virchow R. 1858.** Die Cellularpathologie in ihrer Begründung auf physiologische und pathologische Gewebelehre. *August Hirschwald, Berlin*.
- Vérollet C, Colombié N, Daubon T, Bourbon HM, Wright M, Raynaud-Messina B. 2006.** Drosophila melanogaster gamma-TuRC is dispensable for targeting gamma-tubulin to the centrosome and microtubule nucleation. *The Journal of cell biology* **172**: 517-28.
- Wai DH, Schaefer KL, Schramm A, Korsching E, Van Valen F, Ozaki T, Boecker W, Schweigerer L, Dockhorn-Dworniczak B, Poremba C. 2002.** Expression analysis of pediatric solid tumor cell lines using oligonucleotide microarrays. *International journal of oncology* **20**: 441-51.
- Walczak CE, Vernos I, Mitchison TJ, Karsenti E, Heald R. 1998.** A model for the proposed roles of different microtubule-based motor proteins in establishing spindle bipolarity. *Current biology* **8**: 903-13.
- Wang X, Yang Y, Duan Q, Jiang N, Huang Y, Darzynkiewicz Z, Dai W. 2008.** sSgo1, a major splice variant of Sgo1, functions in centriole cohesion where it is regulated by Plk1. *Developmental cell* **14**: 331-41.
- Warnke S, Kemmler S, Hames RS, Tsai HL, Hoffmann-Rohrer U, Fry AM, Hoffmann I. 2004.** Polo-like kinase-2 is required for centriole duplication in mammalian cells. *Current biology* **14**: 1200-7.
- Waters AM, Beales, PL. 2010.** Bardet-biedl syndrome. *GeneReviews* PMID: 20301537.

- Weinberg RA. 1995.** The retinoblastoma protein and cell cycle control. *Cell* **81**: 323-30.
- Wheatley DN, Wang AM, Strugnell GE. 1996.** Expression of primary cilia in mammalian cells. *Cell biology international* **20**: 73-81.
- White MC, Quarmby LM. 2008.** The NIMA-family kinase, Nek1 affects the stability of centrosomes and ciliogenesis. *BMC cell biology* **9**: 29.
- Wloga D, Camba A, Rogowski K, Manning G, Jerka-Dziadosz M, Gaertig J. 2006.** Members of the NIMA-related kinase family promote disassembly of cilia by multiple mechanisms. *Molecular biology of the cell* **17**: 2799-810.
- Wu W, Baxter JE, Wattam SL, Hayward DG, Fardilha M, Knebel A, Ford EM, da Cruz E Silva EF, Fry AM. 2007.** Alternative splicing controls nuclear translocation of the cell cycle-regulated Nek2 kinase. *The Journal of biological chemistry* **282**: 26431-40.
- Wu L, Osmani SA, Mirabito PM. 1998.** A role for NIMA in the nuclear localization of cyclin B in *Aspergillus nidulans*. *The Journal of cell biology* **141**: 1575-87.
- Ye XS, Xu G, Pu RT, Fincher RR, McGuire SL, Osmani AH, Osmani SA. 1995.** The NIMA protein kinase is hyperphosphorylated and activated downstream of p34<sup>cdc2</sup>/cyclin B: coordination of two mitosis promoting kinases. *The EMBO journal* **14**: 986-94.
- Yin MJ, Shao L, Voehringer D, Smeal T, Jallal B. 2003.** The serine/threonine kinase Nek6 is required for cell cycle progression through mitosis. *The Journal of biological chemistry* **278**: 52454-60.
- Yissachar N, Salem H, Tennenbaum T, Motro B. 2006.** Nek7 kinase is enriched at the centrosome, and is required for proper spindle assembly and mitotic progression. *FEBS letters* **580**: 6489-95.
- Yuan K, Li N, Huo Y, Yan F, Yang Y, Ward T, Jin C, Yao X. 2009.** Recruitment of separase to mitotic chromosomes is regulated by Aurora B. *Cell cycle* **8**: 1433-43.
- Zimmerman WC, Erikson RL. 2007.** Polo-like kinase 3 is required for entry into S phase. *Proceedings of the national academy of sciences of the United States of America* **104**: 1847-52.
- de Vos S, Hofmann WK, Grogan TM, Krug U, Schrage M, Miller TP, Braun JG, Wachsmann W, Koeffler HP, Said JW. 2003.** Gene expression profile of serial samples of transformed B-cell lymphomas. *Laboratory investigation* **83**: 271-85.

**el-Deiry WS, Harper JW, O'Connor PM, Velculescu VE, Canman CE, Jackman J, Pietenpol JA, Burrell M, Hill DE, Wang Y, Wiman KG, Mercer WE, Kastan MB, Kohn KW, Elledge SJ, Kinzler KW, Vogelstein B. 1994.** WAF1/CIP1 is induced in p53-mediated G1 arrest and apoptosis. *Cancer research* **54**: 1169-74.